

Particle size analysis, Quantification and  
Identification of Microplastics in Selected  
Consumer Products: A Critical Comparison of  
Methods and Analytical Techniques

A thesis submitted for the degree of Doctor of  
Philosophy

By

Kofi Omare Renner

Institute of Environment, Health and Societies,

Brunel University

London

2018

# Abstract

Microplastics are particles that are < 5 mm in size and come from a wide range of sources. The global distribution in terrestrial and aquatic environments indicates they are likely to cause harm to living organisms. They are used in a variety of personal care products and kitchen scourers. To advance further studies, different approaches have been developed in recent years. In this research, a comparison of methods and analytical techniques were applied to characterise microplastics in two toothpastes and two facial scrubs. The analysis of microplastics was determined using light microscopy, laser diffraction, Fourier-transform infrared spectroscopy. This research reports for the first time, the application of Imaging flow cytometry to characterise microplastics, and was explored to characterise smaller sized particles in each product. The methods developed were validated by characterising particles abraded from kitchen scourers. Two market leading and three chain store brands of kitchen scourers were utilised for the characterisation of microplastics. The application of the different techniques indicated differences in the size, number and morphological characteristics of the particles analysed. The different approaches developed for particle extraction, and the analytical techniques had an apparent influence on the results produced. Currently, there are no universally accepted laboratory protocol and analytical techniques to characterise microplastics. However, this research can serve as a reference point to promote more studies on laboratory methods and analytical techniques to characterise microplastics, with the hope of understanding better these complex particles.

Abstract.....	1
DECLARATION.....	6
List of Figures.....	7
List of Tables.....	12
Acknowledgments.....	14
CHAPTER 1. INTRODUCTION.....	15
1.1. Entry, fate and transport of plastics in the Environment.....	19
1.2 Impact of plastics in the marine environment.....	21
1.3 Impact of plastics in freshwater environments.....	23
1.4 Impact of plastics in the terrestrial environment.....	24
1.5 Chemicals and additives associated with plastics.....	25
1.6. Aims and objectives.....	28
CHAPTER 2. LITERATURE REVIEW: Microplastics.....	29
2.1 Types of microplastics.....	30
2.1.1 <i>Primary microplastic</i> .....	30
2.1.2 <i>Secondary Microplastics</i> .....	32
2.2 Sources of Microplastics.....	33
2.3. Occurrence and abundance of microplastics in the environment.....	36
2.3.1. <i>Marine environment</i> .....	36
2.3.2. <i>Freshwater Environments</i> .....	39
2.3.3. <i>Terrestrial Environment</i> .....	43
2.4. Impact of microplastics on the environment.....	44
2.4.1. <i>The effects of microplastics in the marine environment</i> .....	44
2.4.2 <i>Impact of microplastics in freshwater environments</i> .....	47
2.4.3. <i>The Impact of Microplastics in Terrestrial Environments</i> .....	48
2.5. Challenges associated with the characterisation of microplastics.....	49
2.5.1. Laboratory Analysis: Density Separation.....	51
2.5.2. Filtration of particles separated from matrix.....	54
2.5.3. Characterisation of Microplastics.....	55
2.5.4. <i>Characterisation of particles using microscopy technique</i> .....	56
2.5.5. <i>Determining the size of particles using laser diffraction technique</i> .....	58
2.5.6. <i>Particle analysis by imaging flow cytometry</i> .....	59
2.6. Comparing Techniques for Microplastics Characterisation.....	61
2.7. Identification of Particles using Spectroscopy.....	61

CHAPTER 3: METHODS AND MATERIALS USED FOR THE CHARACTERISATION OF MICROPLASTIC PARTICLES. ....	63
3.1. Particles selected as the focus of study.....	63
3.2. Personal care products selected for the characterisation of particles.....	63
3.3. Separation of particles from personal care products .....	64
3.4. Characterisation of microplastic particles .....	65
3.4.1 Characterisation by direct imaging using light microscopy.....	65
3.4.2 Particle size analysis by laser diffraction.....	66
3.4.3 Imaging flow cytometry.....	67
3.4.4 Polymer identification. ....	68
3.5. Choice of kitchen scourers to be used for the analysis of particles.....	68
3.6. Abrasion of particles from kitchen scourers .....	69
3.7. Characterisation of particles abraded from kitchen scourers .....	70
3.7.1 Analysis of particles abraded from kitchen scourers by light microscopy. ....	70
3.7.2 Analysis of particle size distribution using laser diffraction.....	71
3.7.3 <i>Particle analysis by imaging flow cytometry</i> .....	71
3.8 Quality control to avoid contamination and loss of samples. ....	72
3.8.1 Sample preparation.....	72
3.8.2. <i>Analysis of particles</i> .....	73
CHAPTER 4. RESULTS: Challenges encountered in method development and final approaches for the characterisation of particles. ....	74
4.1. <i>Density separation of particles from personal care products.</i> .....	74
4.2. Assessment of the size of particles using different techniques.....	76
4.2.1 <i>Analysis of particle size distribution by laser diffraction.</i> .....	76
4.2.2 <i>Analysis of particle size and the limitations of the microscopy technique.</i> .....	82
4.3 <i>Evaluation of the number of particles determined using different counting protocols by microscopy.</i> .....	91
4.4. Challenges encountered for the analysis of particle size using the imaging flow cytometry technique.....	94
4.4.1. <i>Evaluation of template applied to differentiate calibration speed beads from particles in all products.</i> .....	94
4.4.2. <i>The development of a template to estimate the number of particles recovered from PCPs after disabling the calibration speed beads.</i> .....	97
4.5. Characterisation of microplastics separated from Personal care products.....	101
4.5.1 <i>Assessing the size of particles in personal care products by Microscopy</i> .....	101
4.5.2. <i>Assessing particle size distribution by Laser Diffraction</i> .....	105

4.5.3. Size analysis of particles in personal care products by Imaging flow cytometry.....	107
4.5.3.1 Development of a Gating strategy to identify single particle population.....	108
4.5.3.2. Application of the developed template for the analysis of particle size.....	109
4.5.3.5. Assessment of particle size using the diameter size feature.....	112
4.6. Analysis of the number of particles in personal care products using microscopy and imaging flow cytometry.....	116
4.6.1. Evaluation of the number of particles in personal care products by microscopy.....	116
4.6.2. Evaluation of the number of particles in personal care products by Imaging flow cytometry.....	118
4.7. An assessment of particle morphology using light microscopy.....	121
4.8. Evaluation of particle morphology as determined by Imaging flow cytometry.....	123
4.9. Assessing particle morphology in products using micro-FT-IR.....	125
4.1.0. Application of infrared spectroscopy for the identification of polymer particles in personal care products.....	126
4.1.1. Determining the Polymer identity of particles in PCPs using micro-FT-IR.....	127
4.1.2. Determining the particle identity using ATR-FT-IR.....	130
4.2. Multi-technique comparison to characterise particles in personal care products.....	131
4.2.1. Comparison of applied techniques used to determine particle size.....	132
4.2.2. Evaluation of the particle number as determined by the application of different techniques.....	135
4.2.3. Comparison of particle morphology applying different techniques.....	136
4.3. Challenges encountered in method development for the characterisation of particles from kitchen scourers.....	138
4.4. Final results for the characterisation of particles abraded from kitchen scourers.....	140
4.4.1. Assessing the size of particles from kitchen scourers using Microscopy.....	141
4.5 Assessment of the size distribution of particles abraded from kitchen scourers by Laser Diffraction.....	147
4.6. Application of the imaging flow cytometry technique to determine the size of particles abraded from kitchen scourers.....	149
4.6.1. Determination of the size of particles using the area feature.....	150
4.6.2. Analysis of particle size based on the length feature.....	151
4.6.3. Assessment of particle size based on the diameter feature.....	152
4.7. Estimation of the number of particles abraded from kitchen scourers.....	155
4.7.1. Evaluation of the number of particles abraded from kitchen scourers by microscopy.....	156
4.7.2. Evaluating the number of particles abraded from kitchen scourers using Imaging flow cytometry.....	158

4.8.0. Assessment of the morphology of particles abraded from kitchen scourers as determined by different techniques .....	162
4.8.1. <i>Morphology of particles by Microscopy</i> .....	163
4.8.2. <i>Evaluation of particle morphology as determined by Imaging flow cytometry</i> .....	164
4.8.3. <i>Assessing particle morphology in products using micro-FT-IR</i> .....	168
4.8.4. Polymer identification of particles abraded from kitchen scourers using micro Fourier transform infrared spectroscopy micro-FT-IR.....	171
4.8.4.1. <i>Determining polymer identity using reflectance micro-FT-IR technique</i> .....	171
4.8.4.2. <i>Polymer identification of particles abraded from kitchen scourers using attenuated total reflectance infrared spectroscopy ATR-FT-IR</i> .....	175
4.9. Multi-technique comparison to characterise particles abraded from kitchen scourers..	177
4.9.1. <i>Comparison of applied techniques used to determine particle size</i> .....	178
4.9.2. <i>Evaluation of the number of particles using microscopy and imaging flow cytometry techniques</i> .....	180
4.9.3. <i>Comparison of particle morphology applying different techniques</i> .....	181
CHAPTER 5: DISCUSSION .....	185
5.1 Density separation of particles from matrix .....	185
5.2 Filtration of particles separated from matrix .....	186
5.3. Characterisation of all particles using different techniques.....	188
5.3.1. <i>Particle analysis using the microscopy technique</i> .....	189
5.3.2. Laser diffraction analysis of microplastics.....	192
5.3.3. <i>Particle analysis using imaging flow cytometry</i> .....	194
5.4. <i>Particle polymer identification using FT-IR</i> .....	198
5.5. Assessment of the fate and transport of particles characterised by different techniques .....	200
5.6. Impact of microplastics on living organisms in the environment .....	203
CHAPTER 6: CONCLUSION .....	206
<b>FUTURE WORK</b> .....	209
<b>Glossary of terms</b> .....	210
<b>REFERENCES</b> .....	211
APPENDIX .....	246

## DECLARATION

The work submitted in this thesis was conducted between 2014 and 2017 at Brunel University West London. This research was conducted independently and has not been submitted for any other degree.

## List of Figures

Figure 1.1 Global plastics production for from 1950 to 2015. Plastics production has more than doubled between 1989 and 2015 Figure adapted from (Law 2017b; Zhao et al. 2017) .....	16
Figure 1.2. Pie chart showing the occurrence of plastics in surface waters in oceans globally. The oceans represented are; 1, Mediterranean Sea; 2, South Atlantic; 3, South Pacific; 4, North Atlantic; 5, Indian Ocean and 6, North Pacific Ocean. ....	21
Figure 2.1. Resin pellets shown in the image shows differences in shape, size and colour Shapes include circular, elongated and irregular. Figure copied from Tanya Cox 2017. ....	31
Figure 2.2. An illustration of the formation of secondary microplastics in the aquatic environment. ....	33
Figure 2.3. Conceptual diagram of the entry of microplastics from primary and secondary sources to freshwater environments. ....	40
Figure 2.4. Schematic diagram of a wastewater treatment plant, showing different stages of the wastewater treatment process. The image shows the different screens and separation of particles in the WWTP and final discharge to the environment. ...	41
Figure 2.5. The different possible measurements that can determine size of a particle. ....	56
Figure 2.6 Measurement features used to determine particle size using the microscopy technique. (Source: (Sympatec GmbH 2017)).....	57
Figure 2.7. FT-IR spectrum of Polyethylene showing the absorbance peaks indicative of the polymer .....	62
.....	62
Figure 3.1. Schematic diagram of the approach used to characterise microplastics in personal care products. The diagram shows the two pathways used for particle characterisation.....	64
Figure 4.1. Particle size distribution of microplastic particles extracted from personal care products analysed using a CILAS 1180 particle size analyser. Cumulative graph showing microplastics size distribution in each brand of personal care product.....	77
Figure 4.2. Size distribution of particles in four products analysed by laser diffraction and the addition of methanol as the carrier liquid for the instrument. All products analysed show multimodal peaks, indicating multiple peak populations for particles in the personal care products.....	81
Figure 4.3. Tukeys multiple comparisons of means at the 95 % family-wise confidence level. The confidence intervals that do not cut through the zero mark show a difference in the size of particles in the products. Confidence intervals that cut through the zero mark indicate similarities in the size of particles .....	84
Figure 4.4. The confidence intervals do not cut through the zero mark, indicating a significant difference in the size of particles for all paired products.....	86
Figure 4.5. Particle size distribution for TP1, determined by a selection of 2 and 6 transects in a Sedgewick-rafter cell. The measurements determined at 100X indicated	



differences in size distribution with measurements conducted at the magnification of 200X. In an SRC, one transect contains 50 individual counting chambers. .... 88

Figure 4.6. The size distribution for particles in FS1 based on measurements conducted in 2 and 6 transects in a Sedgewick-rafter cell. The differences in size distribution are demonstrated by the different selected transects and measurements determined at 100X and 200X..... 89

Figure 4.7. Pie chart showing the estimated number of particles per 100 g counted in selected personal care products at the magnification of 100X. .... 92

Figure 4.8. Histogram for the estimated number of particles per 100 g counted in all four personal care products at the magnification of 100X. .... 93

Figure 4.9. Image of a particle indicating the aspect ratio and the area of the particle. .... 95

Figure 4.9.1. Scatter plot for the estimated number of particles per mL determined in all four personal care products at the magnification of 100X..... 95

Figure 4.9.2. Template developed to distinguish calibration speed beads from particles in the selected products, based on the SSC profile. Template consists of five sub-templates to identify particles in focus (A); identify speed beads based on side scatter profile SSC (B). .... 96

Figure 4.9.3. Histogram for the number of speed beads and the number of particles separated from the selected products ..... 97

Figure 4.9.4. Templates developed to identify single particles in the sample (left) and particles that were in focus (right). .... 98

Figure 4.9.5. Template developed showing distinctions between elongated and circular-like particles..... 99

Figure 4.9.6. Descriptive image of the elongatedness and circularity shape features used to determine particle size..... 99

Figure 4.9.7. Histogram showing estimates for the number of particles separated from TP1 and FS1. The length and diameter size features demonstrated the same number of particles for the products analysed..... 100

Figure 4.9.9. Tukeys multiple comparisons of means at the 95 % family-wise confidence level. Confidence intervals that do not cut through the zero mark show differences in the size of particles in the products. Confidence intervals that cut through the zero mark indicate no difference in the size of particles. Particle size denoted by \* indicate measurements determined at the magnification of 200X. .... 104

Figure 4.9.9.1. Particle size distribution of microplastic particles extracted from personal care products analysed using a CILAS 1180 particle size analyser. Cumulative graph showing microplastics size distribution in each brand of personal care product. All products analysed show multimodal peaks, indicating multiple peak populations for particles in the personal care products. .... 106

Figure 4.9.9.2. Step 1 of the development of the particle analysis template. Scatter plot of the area vs the aspect ratio to identify single particles. .... 108

Figure 4.9.9.3. Template developed to identify particles that were in focus by plotting the histogram of gradient RMS. The images on the right show a description of the elongatedness and circularity of a particle. .... 109

Figure 4.9.9.5. Area, length and diameter size features used to analyse particle size .....	110
Figure 4.9.9.6. Box plot showing the number of particles per 100 g counted in personal care products at 100X (white box) and 200X (grey box). The box plot shows differences in number of particles between all products.....	118
Figure 4.9.9.8. Time size analysis for the number of particles estimated in all products. ....	121
Figure 4.9.9.9. The different shapes and colours of particles analysed under a microscope at 100X (A) and 200X magnification (B).....	123
Figure 4.9.9.9.1. Analysis of microplastics in personal care products using the Amnis ImageStream®X MkII at 20x magnification. Particles observed in blank samples (left image) and microplastics seen in FS2. Scale bar for all images is 20 µm.....	124
Figure 4.9.9.9.2. Image shows particles in PCPs and blank water samples that exhibited side-scatter properties. ....	125
Figure 4.9.9.9.3. Analysis of particles in personal care products using the micro-FT-IR technique.....	126
Figure 4.1.0. Reflectance micro-FT-IR spectra of polyethylene scanned in absorbance mode using the micro-FT-IR. The absorption peaks were based on reflectance in imaging mode with 2 co-added scans per pixel, an aperture size of 25 µm <sup>2</sup> and at a spectral resolution of 16 cm <sup>-1</sup> . ....	128
Figure 4.1.1. ATR-FT-IR spectra of polyethylene particles identified in all personal care products. The peaks were based on reflectance in imaging mode with 2 co-added scans per pixel, an aperture size of 25 µm <sup>2</sup> and at a spectral resolution of 16 cm <sup>-1</sup> . ....	131
Figure 4.2. Bar chart showing the mean size of particles as determined by the different techniques used. The chart shows the size of particles determined by microscopy at different magnifications (A), laser diffraction (B) and imaging flow cytometry (C) techniques.....	133
Figure 4.3. Bar chart showing the number of particles determined by the different techniques used. The larger number of particles as determined in FS2, by the imaging flow cytometry technique and the smaller number of particles as determined in FS2 by microscopy is also highlighted in the chart. ....	136
Figure 4.4. The images of particles in the personal care products are shown in the image above. The microscopy (A), indicate different shapes and colours of particles. The imaging flow cytometry (B) highlights different classifications for shape and shapes for artefacts. The micro-FT-IR (C) indicates the details and contours of particles in all products.....	137
Figure 4.5. Photomicrograph of particles abraded from all kitchen scourers and determined at the magnification of 100X.The image shows a high number of fibre particles in KS1, KS3 and KS5. ....	139
Figure 4.6. Photomicrograph of diluted sample of particles abraded from all kitchen scourers and determined at the magnification of 100X. ....	140
Figure 4.7. Tukeys multiple comparisons of means at the 95 % family-wise confidence level for particles measured at the magnification of 100X.The confidence intervals that	

do not cut through the zero mark show a difference in the size of particles in the products. Confidence intervals that cut through the zero mark indicate no difference in the size of particles..... 144

Figure 4.7.1. Tukeys multiple comparisons of means at the 95 % family-wise confidence level for particles measured at the magnification of 200X. The confidence intervals that do not cut through the zero mark show a difference in the size of particles in the products. Confidence intervals that cut through the zero mark indicate no difference in the size of particles. .... 145

Figure 4.7.2. Tukeys multiple comparisons of means at the 95 % family-wise confidence level for particles measured at the magnification of 100X and 200X. The confidence intervals that do not cut through the zero mark show a difference in the size of particles in the products. Confidence intervals that cut through the zero mark indicate no difference in the size of particles. Particle size denoted by \* indicate measurements determined at the magnification of 200X. .... 146

Figure 4.7.3. Particle size distribution of particles abraded from five kitchen scourers. The graph shows multimodal peaks indicating multiple peak populations for particles in the kitchen scourers. .... 148

Figure 4.7.4. Bar chart showing the number of particles released from kitchen scourers per wash. Values based on counts in six transects of a Sedgewick-Rafter cell at 200X. Particles categorised into all, fragments and fibre. .... 157

Figure 4.7.5. Pie chart indicating the proportion of particle fragments to fibre particles abraded from kitchen scourers, as determined at the magnification of 100X and 200X. .... 158

Figure 4.7.6. Bar chart showing the number of particles abraded from kitchen scourers using the Amnis ImageStream Mark II imaging flow cytometer. Three populations of particles were analysed based on the shape features from the template created. . 160

Figure 4.7.7. Pie chart indicating the proportion of elongated and circular particles abraded from five kitchen scourers, and determined by imaging flow cytometry. .. 160

Figure 4.7.8. Pie chart for the proportion of particles in the blank water samples to the particles abraded from all five kitchen scourers. .... 161

Figure 4.7.9. Histograms for the number of particles estimated using the imaging flow cytometry technique (Imagestream); and the microscopy technique determined at the magnifications of 100X and 200X..... 162

Figure 4.8.0 Images of particles abraded from five kitchen scourers and analysed at magnifications of 100X (left image) and 200X (right image). The different products showed differences in shape and colour for particles analysed in all five products. 164

Figure 4.8.1. Types of particles abraded from the five kitchen scourers analysed. 166

Figure 4.8.2. The elongated and circular particles abraded from five kitchen scourers determined by the imaging flow cytometer. The particles exhibited differences in fluorescence and side scatter properties. KS1 indicated particles demonstrated fluorescence and side scatter properties. Scale bar for all images is 20  $\mu\text{m}$ . .... 167

Figure 4.8.3. Morphology of particles abraded from KS1 and KS2 using the micro-FT-IR technique. The products were characterised by irregular and circular-like particles and a green colour. .... 169

Figure 4.8.4. Morphology and colour of particles abraded from KS5 using the micro-FT-IR technique. The particles from KS5 exhibited a black colour that was unique to this product. Particles appeared more irregular than elongated or circular-like.....	169
Figure 4.8.5. Colour of particles abraded from KS3 using the micro-FT-IR technique. The particles abraded from KS3 exhibited a white colour that was the same with the surface of the filter paper.....	170
Figure 4.8.6. micro-FT-IR spectra of polyethylene as determined in KS1 and KS4, and the IR spectra for polyester determined in KS2, KS3 and KS5. The red arrows point to the functional groups in the IR spectrum, indicative of polyethylene. ....	174
Figure 4.8.7. ATR-FT-IR spectra of polyethylene as determined in KS1 and KS4. The red arrows point to the functional groups in the IR spectrum, indicative of polyethylene. The spectra are presented as a function of 16 co-added scans carried out for each product at a spectral resolution of $4\text{cm}^{-1}$ and a wavenumber ranging from $4000\text{cm}^{-1}$ to $500\text{cm}^{-1}$ .....	176
Figure 4.8.8. ATR-FT-IR spectra of polyester as determined in KS2, KS3 and KS5. The functional groups in the IR spectrum that are indicative of polyester are shown with red arrows. The spectra are presented as a function of 16 co-added scans carried out for each product at a spectral resolution of $4\text{cm}^{-1}$ and a wavenumber ranging from $4000\text{cm}^{-1}$ to $500\text{cm}^{-1}$ . ....	177
Figure 4.8.9. Bar chart showing the mean size range for particles abraded from kitchen scourers. Mean particle size determined by microscopy at magnifications of 100X and 200X (A), imaging flow cytometry using area, length and diameter (B), and laser diffraction technique (C). ....	179
Figure 4.9.0. Bar chart showing the number of all particles abraded from kitchen scourers and analysed by the different techniques used. The larger number of particles as determined by imaging flow cytometry (bars in grey colour), and the smaller particle number as determined by microscopy (bars in white) are indicated in the chart. ...	181
Figure 4.9.1. Morphology of particles abraded from kitchen scourers and analysed by microscopy. The analysis of particle shape and colour was determined at magnifications of 100X and 200X.....	183
Figure 4.9.2. The images of particles abraded from kitchen scourers using Imaging flow cytometry and FT-IR techniques.....	184

## List of Tables

Table 2.1. Densities of polymers commonly identified in the environment as microplastics, units are in g/cm <sup>3</sup> .....	37
Table 2.2. Density separation solutions and corresponding densities .....	53
Table 4.1. Diameter values of particles in personal care products. ....	79
Table 4.2. Diameter values of particles in personal care products. ....	82
Table 4.3. Size of the particles measured in personal care products. ....	83
Table 4.4. Size of the particles measured in personal care products. ....	85
Table 4.5. Size analysis of particles in TP1 and FS1 based on sample volume reduction .....	91
Table 4.6. Size of the particles measured in personal care products. ....	102
Table 4.7. Diameter values of particles in personal care products. ....	107
Table 4.8. Area of particles in personal care products measured using Amnis ImageStream Mark II imaging flow cytometry. ....	111
Table 4.9. Size of all particles in personal care products measured using Amnis ImageStream Mark II imaging flow cytometry Populations of particles were analysed based on the length feature using the template created.....	112
Table 4.9.1. Particle size determined using the Amnis ImageStream Mark II imaging flow cytometry.. ....	114
Table 4.9.2. The average size for all artefacts analysed using the different size features for the imaging flow cytometry technique. ....	115
Table 4.9.3. Comparison of the average size of artefacts and particles in personal care products. ....	116
Table 4.9.4. Number of particles estimated in personal care products based on the length feature. ....	120
Table 5.1. IR absorptions of the functional groups for the identification of polymers of polyethylene and polyester.....	129
Table 6.1. Size of particles from kitchen scourers based on the size categories, measured at the magnification of 100X. ....	142
Table 6.2. Size of particles from kitchen scourers based on the size categories and determined at the magnification of 200X. ....	143
Table 6.3. Table shows size of microplastics based on D-Values (D10, D50 and D90) .....	149
Table 6.4. Area of particles abraded from kitchen scourers measured using Amnis ImageStream Mark II imaging flow cytometry. ....	151
Table 6.5. Table showing the length of particles abraded from kitchen scourers measured using Amnis ImageStream Mark II imaging flow cytometry. ....	152
Table 6.6. Table showing the diameter of particles abraded from kitchen scourers measured using Amnis ImageStream Mark II imaging flow cytometry. ....	153
Table 6.7. Evaluation of the differences between particle size measurements using the area and length features by the imaging flow cytometry. ....	154

Table 6.8. Determining the differences between the mean lengths for 'all' particles measured using the microscopy and imaging flow cytometry techniques. ....	155
Table 7.1. IR absorptions of the functional groups for the identification of polymers of polyethylene and polyester.....	173
Table 7.2. The different final volumes of samples prepared correspond to the different techniques used for the characterisation of particles.....	188
Table 7.3. Comparison of the different results for the size of fibre particles determined using laser diffraction and light microscopy. ....	193

## Acknowledgments

I would like to thank God for bringing me this far. Dr. Mark Scrimshaw for his unrelenting support and constructive criticism and for guiding me through my PhD and also his belief in what I was doing. I would also like to thank Dr. Edwin Routledge who always supported and encouraged me to enjoy the science.

To Dr. Helen Foster who was very supportive and encouraged me every step of the way, without her, achievements in this research would not have been possible.

To Nita Verma and Dr. Nico Nelson for being ready hands at every point it was required.

To my family Professor J.K. Renner, Mrs Emi Renner, Dr. Ekow Renner, Dr. Ayodele Renner and Adekunle Renner, blessings. For your love, prayers and support.

For my mum Mrs M.U. Renner, I wish you were here.....

“It is the labour of love, as in life, veiled in allegory and illustrated by symbols”

## CHAPTER 1. INTRODUCTION.

The word plastic is derived from the Greek word “plastikos”, meaning mouldable and capable of being shaped (Kamboj 2016). Plastics are the general name for synthetic organic materials made from polymers that form chains of molecules that are linked together to form plastics. As such, it is not a coincidence that many plastic materials commonly used start with the suffix “poly”. Plastics are made from polymers of polyester, aliphatic polyamides such as nylons, polyethylene (PE), polypropylene (PP), polyethylene-terephthalate (PET) and polyvinyl chloride (PVC) (Andrady 2017; Andrady 2015). Therefore, because plastics are made from polymers, both terms “plastic” and “polymers” are used interchangeably. When plastics are manufactured, organic polymers referred to as resins, are commonly used as a base (Geyer et al. 2017a). It is clear that when resins are made into plastics, additives such as colouring agents and dyes, plasticizers, ultra violet UV and thermal stabilisers and flame retardants are commonly added to the resin to improve the durability and aesthetics of the plastic (Geyer et al. 2017a; Law 2017a). Plastics are made from organic and inorganic materials and are characterised by their durability, versatility, weight and relative affordability. The malleable nature of plastics allows it to be cast and turned into different shapes and sizes, characteristics which have resulted in their varied domestic and industrial use ( Andrady 2017; Law 2017a; Geyer et al. 2017b; Kamboj 2016a). ).

Plastics are used in a myriad of applications including food packaging, as fabric in clothing, carrier bags, shower curtains, refrigerator liners, compact discs, plumbing pipes and in some instances, personal care products (Geyer et al. 2017b; PlasticsEurope 2016). In addition, polymers are light weight yet have high tensile strength, and so they are used in fabrics and clothing material, and they can be easily shaped into any form, as applied in toys, bottles and car parts ( Napper & Thompson 2016; Eriksen et al. 2014a). ). Materials such as glass and metals which were used more frequently in the past have been gradually replaced by plastics today (Huang et al. 2017). These polymers are important components of plastic materials because the structure of polymers confers a characteristic resistance to chemicals, they serve as good thermal and electrical insulators with applications in plastic coverings in home appliances (Andrady 2017; GESAMP 2015).



The wide use of plastics is reflected in the global increase in production (Law 2017b; GESAMP 2015). ). Since the 1950s, the annual global production of plastics has increased, with manufacturers capitalising on the dependence on plastics. Consequently, plastic production has increased from 1.5 million tonnes per year in the early 1950s to 245 million tonnes per year in the 21<sup>st</sup> century (Figure 1.1). It is apparent that the production of plastic has experienced a 99% increase since the early 1950s (Figure 1). .

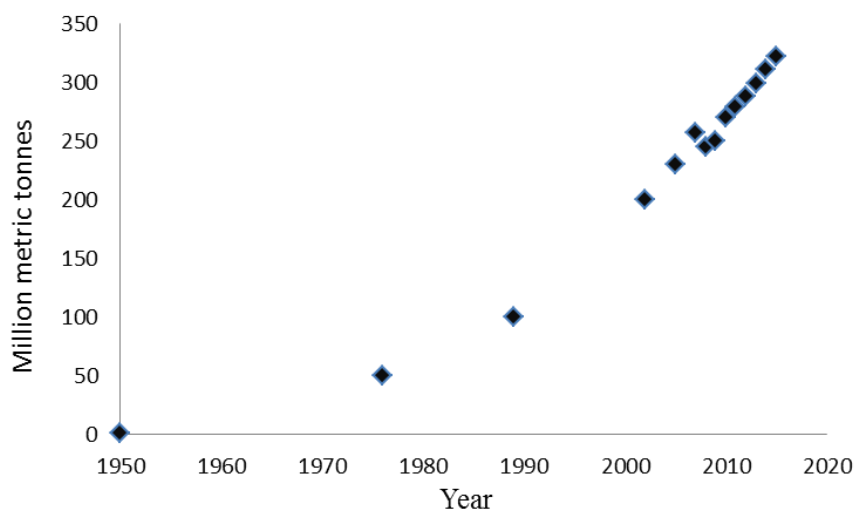


Figure 1.1 *Global plastics production for from 1950 to 2015. Plastics production has more than doubled between 1989 and 2015 Figure adapted from (Law 2017b; Zhao et al. 2017)*

It is clear that the plastics industry has become a global production platform with different countries producing large quantities of this so called wonder material. Documented reports suggests China; the European Union (EU) and North America, produced an estimated 161 million tonnes of plastics in 2013 (Geyer et al. 2017b; PlasticsEurope 2016). However, there is information to suggest that China alone accounts for about 28% of the total global plastic production and by contrast the commonwealth of independent states (CIS) produces about 3% (Geyer et al. 2017b; PlasticsEurope 2016). There is evidence to suggest that plastic production is also likely to increase with population growth (Geyer et al. 2017b; Ryan 2015). Therefore, with the current dependence on plastic for everyday use, it is apparent that consumers will use more plastic products in the future to meet daily needs.

The plastic industry and its growth has brought some benefits to the society. For example, it is apparent that the industry employs about 1.5 million people in Europe and recorded a turnover of over 340 billion euros (PlasticsEurope 2016). In addition, the income generated from plastic production has contributed about 27 billion Euros to welfare and public finance (PlasticsEurope 2016). As such, it is apparent that the plastic industry has provided jobs and benefited the society in one way or another. The industry is vast to the extent that it has also encouraged trade between countries, which has helped trading relationships and partnerships between countries. In addition, the larger plastic production countries supply and meet the demands of trade partner nations for them to meet their societal need. In particular, there is evidence to suggest that Germany, Italy, France, Spain, UK and Poland in that order, make up 70% of the plastic demand in Europe and Cyprus and Malta represent the least demand (PlasticsEurope 2016; PlasticsEurope 2015). What is apparent is that countries today depend on plastic for applications in industrial and domestic uses. In particular, there is evidence to suggest that in Europe, plastic is used mainly in the packaging industry and in 2015 accounted for almost 40% of plastic use (PlasticsEurope 2016). By contrast however, plastics were least used in the agricultural sector in Europe (PlasticsEurope 2016). It is likely that the dependence and demand of plastic from society served as a boost for more plastics packaging commonly used in groceries, and home appliances. As such foreign exchange from the sale of plastic have more than likely boosted the economies of trading countries, and met the demands of the society.

Although the benefits of plastics to the society are apparent, it is not without its problems to the society. This wonder material has been suggested to be the main culprit in a world that is continuously contaminated by plastics globally. This is largely because of an ever growing population that is increasingly dependent on the material (Geyer et al. 2017b). In addition, evidence suggests that the frequent use and disposal of single use plastic, especially plastic packaging is a major contributor to global contamination (GESAMP 2015; Law 2017a). Furthermore, evidence suggests that this is likely to increase with in parallel with population growth by 2050 (Geyer et al. 2017b; Ryan 2015). This increase in production is evidenced by the frequent use and disposal of plastic, the affordable price of the material as well as its flexible and improved design quality (Law 2017a; Geyer et al. 2017b).

There has been a drive by countries globally, to mitigate the plastic contamination (Geyer et al. 2017a). In particular, many countries have adopted recycling strategies which have had measureable impacts on the amount of plastics that are thrown away or find their way to the environment (PlasticsEurope 2016). Evidence suggests that over 7.5 million tonnes of plastic was recycled across Europe in 2014 (PlasticsEurope 2016). In the UK, plastic packaging commonly used for wrapping toys, food and some house hold appliances, makes up the largest source of plastic demand (Wrap 2016). In particular, out of the estimated 3.7 million tonnes of plastics per year in demand, it is apparent that rigid plastics commonly used in plastics bottles and trays, make up about 1.5 million tonnes. In addition, it is apparent that an estimated 0.77 million tonnes of the plastic in demand are used as films in plastics bags and labels for products (BPF 2018; Wrap 2016). In a drive to reduce the amount of plastics that enter the environment in the UK, it is estimated that about 59% of the 3.7 million tonnes of plastic is recovered and used as raw material for the manufacture of other products and 29% is recycled (BPF 2018). In a bid to boost recycling efforts, the UK currently exports almost twice as much plastic packaging for recycling (largely to China), than it is currently recycling domestically (Wrap 2016). However it is apparent that UK plastic exports for recycling will reduce because of the proposed ban of plastic importations by China (Laville, 2018). It is apparent that if this ban goes ahead, the UK will be required to find workable alternatives for recycling.

On a global scale, an estimated 14% of the plastic packaging is currently recycled (MacArthur 2017; Carey 2017). This is largely because of government policies that do not go a long way to ensure recycling is carried out as a matter of urgency (Carey 2017; PlasticsEurope 2016). It is apparent that limitations for the recycling of plastic material will result in the contamination of the environment (Law 2017a; Andrady 2015). It is estimated that out of the 6300 Mt plastic waste generated, 9% have been recycled, 12% have been incinerated and 79% accumulated in the environment or landfill sites (Geyer et al. 2017a). Plastics that have been recycled and used as material for other products, are called secondary plastics. It has been reported that only a small proportion (10%) of the 9% recycled plastics have been recycled more than once (Geyer et al. 2017a). Therefore, it is apparent that a large proportion, about 60% of plastics that have not been recycled or incinerated end up in landfills and the environment (Carey 2017; PlasticsEurope 2016).

## 1.1. Entry, fate and transport of plastics in the Environment

Although there have been wide benefits to using plastics, there is a general consensus that the frequency of their use and inappropriate disposal are a source of these contaminants in the environment (Geyer et al. 2017b; Gall & Thompson 2015). The characteristics of plastics namely, their durability, which makes them such a useful material, by contrast, also ensures their resistance to degradation. Therefore, plastics slowly degrade and persist in the environment, depending on the type and morphology, however, the length of time they remain in the environment is unknown (Syakti et al. 2017; Lebreton et al. 2017) .

The entry of plastics in the terrestrial environment is commonly through the disposal of plastic material. In some countries it is common to see plastic litter on the streets and sometimes they are transported by wind to other locations. However, in other instances, plastic waste is collected and disposed of in landfill sites where they remain for an unknown length of time. By contrast, it is apparent that plastics sent to landfills that are not properly managed end up being blown away and transported by wind to other locations, thus contaminating the environment.

Plastics are also used as mulch in agriculture to conserve soil moisture and to grow crops in countries like China and some countries in North America, Middle East and Europe (Saglam et al. 2017; Liu et al. 2014). Currently, plastic mulch used globally is made from polyethylene that is non-biodegradable. It is common practice to remove and dispose of the plastic mulch usually after harvest. However, it is apparent that this process is costly and time consuming. It has been reported that not all farmers properly dispose of the mulch, rather they either burn, or illegally dispose of the plastic (Saglam et al. 2017; Liu et al. 2014). Furthermore, it is apparent that the removal of plastic mulches from soil is not always complete. When farmers remove the plastic from the soil, part of it is torn off and remains in the soil. Therefore this suggests that the use of plastic mulch in agriculture acts as an entry point for plastics to the terrestrial environment.

In the terrestrial environment, it is apparent that the disposal of single use and throw away plastics (bags, wrappings, packaging) has gained notoriety, with some countries placing extra charges for their continued use (DEFRA 2018; Hodson et al. 2017). This

is in an attempt to reduce the incidence of plastic pollution in the environment. For example in England, it is apparent that the introduction of the 5p charge on plastic bags in major supermarkets has resulted in a reduction of the number of plastics sent to landfills (DEFRA 2018). In 2014, 7.6 billion plastic bags were issued to customers after shopping. Currently because of the introduction of the 5p charge, the use of plastic bags issued by supermarkets has reduced by 80% (DEFRA 2018). Over the next 10 years, it has been predicted that clean-up of plastic litter will save the government about £60million (DEFRA 2018). Although this approach has reduced the use and therefore entry of plastic bags used for shopping into the environment, other types of plastic material have not been subjected to this policy. Therefore, it is apparent that plastic materials that do not have charges placed on them will continue to be in use more frequently, and with the potential to enter the terrestrial environment.

The entry of plastics from the terrestrial environment to the aquatic environment has been widely reported (Law 2017b; Avio, Gorbi, et al. 2017). However, it is apparent that there are more reports of the entry of plastics to the marine environment than freshwater environments (Lebreton et al. 2017). It is not clear why this is so, but it is clear that plastics from terrestrial environments are more likely to be transported to the marine environment through freshwater environments. The entry of plastics into freshwater environments is commonly as a result of improper disposal, through drainage, transport by wind, and in some cases, direct dumping of plastic material into freshwater environments (Hennig et al. 2017; Hansen 2016). A study reported on the occurrence of persistent buoyant litter made up of plastics, polystyrene and wood litter at riversides because of the influence of human activity (Rech et al. 2014). In addition, the study indicated that plastic litter was transported to coastal beaches, thus suggesting entry of plastics to freshwater environments and transport to the marine environment (Rech et al. 2014).

It is widely acknowledged that an estimated 80% of plastics in the marine environment comes from land-based sources (Law 2017b; Galgani et al. 2017). This is evidenced by litter on beaches, surface waters and the sea floor (Andrady 2017; Cozar et al. 2014; Rech et al. 2014). Generally plastics that have not been properly disposed end up in the marine environment (Law 2017a; Kamboj 2016b). An estimated 8 million tonnes of plastic per year enter the marine environment globally, with the north pacific ocean having the largest number of surface plastics (Figure 1.2) (Law

2017b; Laurent C M Lebreton et al. 2017). However, it is clear that there is also a high occurrence of plastics in the Indian Ocean and the Mediterranean demonstrates the least plastic occurrence in all the oceans (Figure 1.2). It is apparent that there is a higher accumulation of plastics in the North Pacific Ocean because of the North Pacific Gyre, which has been described as a large rotating ocean current. The North Pacific Gyre is characterised by vortex of ocean water that rotates and transports plastic particles towards still waters where they accumulate in the much discussed pacific garbage patch (Karl & Church 2017; Bryant et al. 2016). In addition, another study reported that currently, estimates of at least 5.25 trillion plastic particles are floating at sea, and largely comprising of water bottles and single use packaging plastics. However, it is apparent that the particles also included microplastics (Eriksen et al. 2014b).

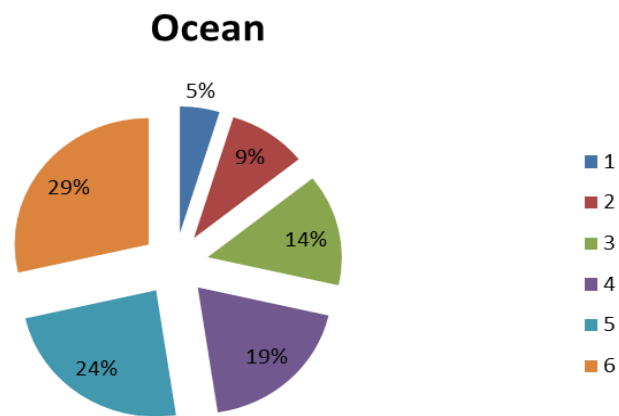


Figure 1.2. Pie chart showing the occurrence of plastics in surface waters in oceans globally. The oceans represented are; 1, Mediterranean Sea; 2, South Atlantic; 3, South Pacific; 4, North Atlantic; 5, Indian Ocean and 6, North Pacific Ocean.

## 1.2 Impact of plastics in the marine environment.

The occurrence of macroplastics has been a subject of concern because it affects the aesthetics of an environment, tourism, health and safety of beach goers, the fishing industry and the health status of terrestrial and aquatic organisms (Law 2017b; Romeo et al. 2015; Rochman et al. 2016; GESAMP 2015). Although there is wide evidence of the impact of macroplastics in the marine environment, information regarding their

impact on freshwater and terrestrial environments is more limited (Law 2017b; Rochman et al. 2013; Hodson et al. 2017; Barnes et al. 2009). The consensus on the harmful effect of macroplastics in the aquatic environment is based on the physical characteristics of plastics which have resulted in their ubiquitous distribution and transport by water currents and wind action to remote regions such as the Pacific Ocean (Gall & Thompson 2015; Rocha-Santos & Duarte 2015). Currently it is estimated that about 600 species, including seabirds, marine mammals, turtles and fish have been affected by plastic material in the marine environment (Gall & Thompson 2015; Rochman et al. 2015; Wilcox, Van Sebille, et al. 2015).

Investigations into the impacts of plastics on marine life have reported mortality in fish, turtles, whales and sea birds, due to the ingestion of plastics and/or entanglement with plastic materials (Gall & Thompson 2015; LI et al. 2016; Law 2017b). It is generally accepted that the ingestion of plastics blocks the feeding passage of the organisms and preventing any further ingestion and resulting in starvation (Lusher et al. 2013; Gall & Thompson 2015; Law 2017b). Although plastic ingestion does not always result in immediate mortality of the organism, there are potentially long-term consequences of sub-lethal effects from the ingestion of plastics (Wright et al. 2013a).

A study on plastic ingestion by demersal and pelagic fish species revealed that out of 290 gastrointestinal tracts analysed, 5.5% of the fish had plastics in them (Rummel et al. 2016). In addition, 31 % more plastics were ingested by pelagic fish than demersal fish (Rummel et al. 2016). This would indicate that there are more bioavailable plastics in the water column than in the benthic environment. Plastics have also been reported in the stomachs of whales, where a total of 59 plastics were ingested (De Stephanis et al. 2013). The report indicated that plastic sheets which are frequently used as covers in greenhouses, hosepipe, dishwater plastics and plastic burlap were ingested by the whale (De Stephanis et al. 2013). The study reported that greenhouse cultivation was a common occurrence in the region close to the sampling location and is a possible source of plastic entry to the environment. However, floating debris were not observed in the region where the study was conducted, therefore, it is not clear where the whales ingested the plastics. Whales feed at the surface through to the bottom of the marine environment and as such are exposed to plastic waste that is distributed in the different compartments of the marine environment.

In addition to adult organisms, the early life stage juvenile organisms are also exposed to plastics in the marine environment (Kühn et al. 2015; Law 2017b). One of many examples are juvenile sea turtles which are vulnerable to the high number of plastics entering the marine environment (Pham et al. 2017). Out of the gastrointestinal tracts of 24 loggerheads *Caretta caretta* from the North Atlantic subtropical gyre, 20 had ingested different particles, all of which were made from plastic (Pham et al. 2017). This study suggests that plastics in the marine environment can harm juvenile stage turtles, resulting in mortality and reducing population growth (Pham et al. 2017).

In order to understand the impact of plastics in the environment, indicator organisms have been suggested to be used in monitoring programmes (Karlsson et al. 2017; Provencher et al. 2015). In addition, international authorities have developed policies and directives to monitor and assess the impact of plastics in the environment (García-Rivera et al. 2017; Galgani et al. 2013). For example, the marine safety framework directive (MSFD), has as part of its priorities, included marine litter which plastics are a part of, as one of the eleven descriptors that demonstrates good environmental status in seas in Europe (García-Rivera et al. 2017; Galgani et al. 2013). One species frequently used to assess the level of plastic contamination in the marine environment are seabirds. Due to their travelling over long distances in search of food, it is not unusual they ingest or bring back plastics to their nests (Provencher et al. 2015). Documented reports show that out of 121 birds (16 different species), 27% (12 different species) had plastic particles in their gastrointestinal tract (Acampora et al. 2016). In particular, plastics were identified in 93% of the Northern Fulmars analysed. The mean mass of plastics reportedly ingested was 0.141 g, which was over the 0.1 g marine safety framework directive environmental quality threshold (Acampora et al. 2016).

### 1.3 Impact of plastics in freshwater environments

By contrast to the marine environment, information on plastic contamination and their impact in freshwater environments is limited (Rochman et al. 2013; Eerkes-Medrano et al. 2015a). To date, only a few studies have documented the



contamination of freshwater environments by plastics, and as a consequence it is difficult to assess the impact of these contaminants to these environments (Wagner et al. 2014). It has been suggested that freshwater environments act as a pathway for the entry of plastics to the marine environment. With the increasing population and dependence on plastics for various uses, it is likely that if not properly disposed, more plastics will enter freshwater environments. Currently it is estimated that between 1.2 to 2.4 million tonnes of plastic enters the sea every year from rivers globally (Laurent C. M. Lebreton et al. 2017). This influx is more than likely to have an impact on the environment in general and living organisms in particular, but what that impact is, is still unknown. Furthermore, it is difficult to fully assess the impact when the occurrence, distribution and residency time of plastics in freshwater environments is poorly understood (Rochman et al. 2013; Laurent C. M. Lebreton et al. 2017). However, it is likely that plastics are ingested by invertebrates, fish, and birds in freshwater environments. A survey of water bird species in the wetlands of central Spain reported that plastics were detected in the faeces of 43.8%, 60% and 45% of the European coot, mallard and shelduck (Gil-Delgado et al. 2017). This study demonstrated that plastics can be ingested and removed via excretion in this species. This suggests plastics can be removed from the systems of some species, but the degree of removal is unknown. Furthermore, the long-term impact of the ingestion is still unknown (Gil-Delgado et al. 2017).

#### 1.4 Impact of plastics in the terrestrial environment

Similar to freshwater environments, little is known about the impact of plastic on the terrestrial environment and living organisms in particular. In general, plastic bags, toys and in some cases, plastic water sachets inappropriately disposed, clog drains and often result in flooding with damaging consequences (Ojolowo & Wahab 2017; Butu & Mshelia 2014). With regards to living organisms, a study on Turkey Vultures (*Cathartes aura*) showed that 78% and 83% from coastal and inland sites respectively, contained plastic material in regurgitated pellets (Torres-Mura et al. 2015). Based on a scavenging diet, it is likely that turkey vultures fed on disposed plastic materials such as bags. An investigation on reintroduced population of California Condors *Gymnogyps californianus*, revealed 60% of nestlings ingested anthropogenic

materials referred to as junk, resulted in mortality 2 individuals (Mee et al., 2007). However, the report did not identify the composition of junk material, but from other studies that have detailed feeding habits of birds it is possible these included plastic material (Provencher et al. 2015).

Plastics in the environment can have other impacts on living organisms as has been reported (Townsend & Barker 2014). A study on the effects of anthropogenic nest material on American Crow *Corvus brachyrhynchos*, reported crow nests contained a high percentage (85.2%) of man-made material (Townsend and Barker, 2014). In addition, 5.6% of nestlings were entangled in man-made material including synthetic string, balloon string and nets, which resulted in a significantly lower fledging success than untangled nestlings (Townsend and Barker, 2014). It is apparent that reduced fledging affects the growth and survival of the bird, with the potential to impact population numbers. It is clear that anthropogenic plastic litter picked up by birds from locations where they search for food, suggests these contaminants have a wide distribution in the environment (Provencher et al. 2015; Torres-Mura Juan C et al. 2015). Historically, studies on the impact of macroplastics on wildlife in the terrestrial environments have been limited, the link between urbanisation and the occurrence of anthropogenic litter especially macroplastics is still a subject for investigation. However, it is clear that reports on plastic pollution in the environment have also focused on the chemical additives commonly added in the manufacture of the material.

### 1.5 Chemicals and additives associated with plastics

In the last decade, there have been investigations into the impact of toxic chemicals associated with plastic (Rochman et al. 2016). These chemicals can be classified into additives used in the manufacture of the plastic material, the by-products from the manufacturing process and other chemicals adsorbed from the environment (Rochman 2015). An overview of current documented reports widely suggests that the impact of plastics in the environment can be because of these toxic chemicals (Andrady 2017; Guerranti et al. 2016). Commonly referred to as priority pollutants in many countries globally, they are regulated by many government agencies because

of their level of toxicity and effect on living organisms (Rochman et al. 2013; Ivar Do Sul & Costa 2014).

Chemicals commonly incorporated into plastics with the potential to leach into the environment include, bisphenol A (BPA), commonly found in plastic water bottles, food storage containers and flasks (Rochman et al. 2013; Ivar Do Sul & Costa 2014). This chemical is often referred to as a synthetic estrogen and is frequently associated with endocrine disruption in living organisms (Rochman et al. 2016; Law 2017a; Vandenberg et al. 2017; Rochman et al. 2014). BPA has been increasingly associated with endocrine disruption in human beings especially because of the large dependence on plastic products (Rochman et al. 2014; Vandenberg et al. 2017). Another common chemical associated with plastics are phthalates, which are added to plastics such as polyvinyl chloride, to make them more flexible for use in a wide variety of products. Documented reports have suggested that BPA and phthalates can leach from the plastic products into the body, with the potential to cause harm in the endocrine system (Rochman 2015).

There have been reports that widely suggest plastics adsorb persistent organic pollutants (POPs) from the environment ( Bakir et al. 2014; Andrady 2017). The most common of these POPs include polycyclic aromatic hydrocarbons (PAH) and polychlorinated biphenyls (PCBs), and have been listed as persistent, bioaccumulative and toxic (PBTs) by some government agencies, some include the US environmental protection agency (EPA) and the Organisation for Economic Co-operation and Development (OECD) (Rochman 2015). Many of these chemicals are hydrophobic in nature and have been widely associated with plastic debris. Due to their hydrophobicity, they are readily sorbed onto organic matter and plastics (Antunes et al. 2013; Hodson et al. 2017). The impact of these chemicals have been reported in lug-worms, amphipods, fish, and seabirds upon ingestion of plastics environment (Hodgson et al. 2018; Koelmans et al. 2014; Rochman et al. 2013). It is not clear whether the impact was because of the ingestion of plastics alone, or the chemicals associated with the plastics. However, another report indicated that polybrominated diphenyl ethers (PBDE) were detected in adipose tissues of 25% of short-tailed shearwaters analysed. In addition, higher brominated congeners were detected in the stomachs of 3 birds, but were not present in pelagic fish that are their natural prey

(Tanaka et al. 2013). This suggests that a transfer chemical additives in plastic to marine organisms.

However, it is apparent that the reports on the impact of chemical additives in plastics have been largely laboratory based studies. It has been argued that the concentration of plastics and chemical additives organisms are exposed to in the laboratory, are orders of magnitude higher than environmental concentration (Koelmans et al. 2014). Therefore, it is not clear whether the impact on living organisms is because of the plastic alone or the effect of a plastic/chemical additive combination.

The types and size of plastics in the environment has an apparent impact on the absorption of chemicals from the environment (Rochman 2015). In particular, the physical and chemical properties; surface area, crystallinity, diffusivity, of the plastic allow for chemicals from the environment to accumulate on them (Rochman 2015). It has been reported that higher concentrations of organic chemicals are sorbed by polyethylene, polystyrene and polypropylene, than are sorbed by polyethylene terephthalate (PET) and polyvinyl chloride (PVC) (Rochman 2015).

As the environment is increasingly contaminated with plastic debris it is plausible that the combination of plastic contamination and toxic chemicals leached to the environment can have an apparent impact on living organisms (Hodson et al. 2017; Avio, Cardelli, et al. 2017; Doyle et al. 2011). However, to date, no study has demonstrated that mortality in aquatic and terrestrial organisms was directly linked to chemical additives in plastics. In addition, there is no strong evidence to suggest plastic additives have affected marine organisms at the population level (Galgani et al. 2017; Chris Wilcox et al. 2016).

The occurrence of macroplastics, more so in the aquatic than the terrestrial environment, has been widely acknowledged to be responsible for strangulation, drowning and starvation of living organisms (Ryan et al. 2009; Rochman et al. 2013; Law 2017a). However, a growing concern on the occurrence of smaller plastic particles has gained global interest (Law 2017a). In recent years there has been a shift in research from studies on the more visible macroplastics to smaller particles referred to as microplastics. Microplastics are plastic particles that are < 5 mm in size (Duis & Coors 2016a). Larger plastic particles in the environment fragment into smaller pieces

which are commonly referred to as microplastics and have gained global attention because of their potential to cause harm (GESAMP 2015; Auta et al. 2017a). In addition, the inclusion of micron sized plastics used intentionally as ingredients in some cosmetics such as personal care products PCPs have also gained global attention (Duis & Coors 2016b; Chang 2015). However, it is apparent that other potential sources of microplastics to the environment have not been reported.

## 1.6. Aims and objectives

The aim of this present study was to characterise microplastics in consumer products using a number of different methods. The results from each approach are compared to highlight the challenges involved in quantifying and determining the size of microplastics. This was applied to particles originating from selected PCPs and kitchen scourers. A range of techniques available (microscopy, laser diffraction, imaging flow cytometry and FT-IR) were to be used. The hypothesis was that they would give similar results in assessing characteristics of particles from relatively simple (in terms of complexity of environmental samples) matrices with a high number of particles per unit volume.

The key objectives were:

- To review extraction and separation techniques and use the PCPs to develop standardised approaches that would allow samples to be in a form for assessment by the range of techniques available.
- To optimise the methods available for characterisation and quantification of particles.
- To apply the techniques to particles extracted from PCPs and develop a flow stream of assessment that would give reproducible outcomes.
- To characterise and quantify the particles present in the PCPs
- To apply the methodology developed to particles from an alternative source, kitchen scourers, which have not previously been identified as a source of microplastics.
- To characterise and quantify the particles released from kitchen scourers.

## CHAPTER 2. LITERATURE REVIEW: Microplastics

During the early 1970s, the findings of a research survey reported observing an average of 3500 pieces and 290 g/m<sup>2</sup> of small plastic floating in the ocean (Carpenter & Smith 1972). Many of these pieces were shaped like pellets and weathering processes had rendered the particles brittle, therefore breaking into smaller pieces (Carpenter & Smith 1972). In addition, hydroids and diatoms attached to the surface of these particles, that were about 0.25 to 0.5 mm in diameter (Carpenter & Smith 1972). Over time, further studies revealed the presence of plastic fragments in birds (Thompson 2015a; GESAMP 2015; Horton et al. 2017). Since identifying these small particles in the environment, there has been an on-going debate as to the most accurate definition of a microplastic with regards to size limits. Although there is uncertainty about the formal acceptance of this definition, there is evidence in reports to show different size classifications for the definition of microplastics (Teresa Rocha-Santos & Duarte 2015; Sutton et al. 2016; Song et al. 2015). The different size definitions make data comparison of microplastics difficult and contribute to the challenges of trying to understand its occurrence and impact in the environment. However, following a workshop in 2009, participants' categorised microplastics as plastic fragments ranging between 333 µm and 5,000 µm (5mm) (Browne et al. 2011; T Rocha-Santos & Duarte 2015; Ryan 2015). Although convenient, this size range description of microplastics has not been fully embraced and other scientists have considered a broader classification into micro, meso and macro particles (Teresa Rocha-Santos & Duarte 2015; Sutton et al. 2016). Currently, the consensus is that microplastics are particles that are < 5 mm in size (Thompson 2015a). Microplastics come from various sources, they have a global distribution in terrestrial and aquatic environments and are likely to cause harm to the environment and living organisms (Auta et al. 2017a; Bosker et al. 2017a). There are different types of microplastics which exhibit differences based on their density. For example, polyethylene is a polymer particle commonly reported in studies. Small particles of polyethylene are described as low density particles, and are usually buoyant and float at the surface of the aquatic environment.

## 2.1 Types of microplastics

Microplastics are released from a myriad of sources, and it is apparent that these sources have an impact on the two categories of microplastics that have been reported.

### 2.1.1 *Primary microplastic*

These are plastics that have been manufactured intentionally to be microscopic in size (GESAMP 2015; Peng et al. 2017). Primary microplastics are intentionally added to some cosmetics such as lipsticks and personal care products PCPs which include some brands of toothpastes and facial scrubs ( Gregory 1996a; Duis & Coors 2016b; Hernandez et al. 2017; Saskia Honcoop 2018). In addition, primary microplastics include polymers of acrylic and polyester commonly used as scrubbers by blasting on the hull of ships and their engines to remove rust and worn out paint ( Gregory 1996a; Desforges et al. 2014; Sharma & Chatterjee 2017). Plastics used in this technology are generally sub-angular and come in different sizes (Graco, 2017). According to industry sources, the abrasive properties of a particle is dependent on its size, shape, hardness and density (Graco 2017). Scrubbers are used several times before they are disposed of. In addition, the particles breakdown into further smaller sizes, therefore releasing more particles (Gregory 1996a). However, it is not clear how many particles are released from blasting of ships and engines.

Another common example of primary microplastics are resin pellets which are produced in different shapes and colours, and are the raw materials from which plastics moulds are made (Figure 2.1) (Acosta-Coley & Olivero-Verbel 2015; Ziccardi et al. 2016). Resin pellets are typically < 5 mm, but a size range of 1-5 mm is the general size range (Figure 2.1) (Acosta-Coley & Olivero-Verbel 2015; Eerkes-Medrano et al. 2015a). The circular-like shapes of the particles are indicative of their origin (Hidalgo-Ruz & Gutow 2012; Duis & Coors 2016b; Acosta-Coley & Olivero-Verbel 2015). In addition, the particle size demonstrates the size category associated with microplastics (Antunes et al. 2013; Cole et al. 2016). Resin pellets are made from polyethylene and polypropylene resin pellets and are introduced to the environment

as a result of accidental spills from shipping vessels and from industrial sources (Castillo et al. 2016; Sutton et al. 2016). Their light weight, buoyancy and conditions in the oceans ensure they are transported over wide distances (Castillo et al. 2016; Sutton et al. 2016; Ivar Do Sul & Costa 2014). Accidental spills of resin pellets is a significant source of primary microplastics, and have the potential to enter the environment to cause harm (Acosta-Coley & Olivero-Verbel 2015; Yeo et al. 2017).

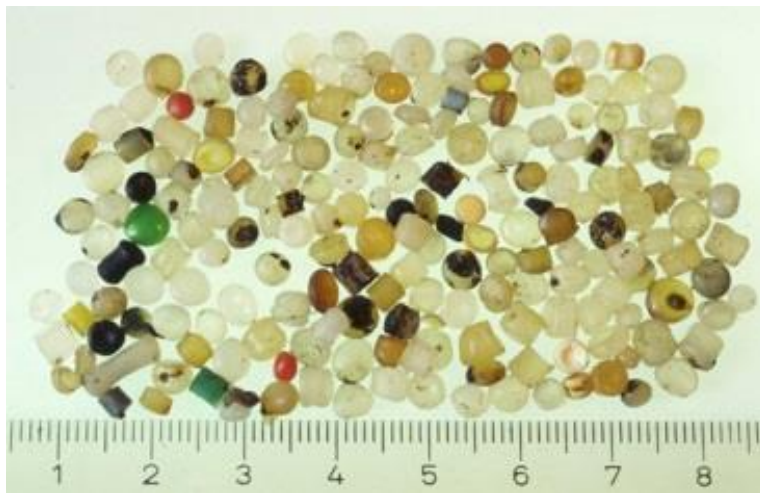


*Figure 2.1. Resin pellets shown in the image shows differences in shape, size and colour. Shapes include circular, elongated and irregular. Figure copied from Tanya Cox 2017.*

Since the early 1980s, microplastics have been used in personal care products (PCPs), because of their suggested exfoliating and scrubbing properties (Thompson et al., 2004; Fendall and Sewell, 2009). PCPs including some brands of toothpastes, facial scrubs and hand cleansers, contain particles polyethylene and polystyrene as part of their ingredient (Chang 2015; T Rocha-Santos & Duarte 2015; L. M. Hernandez et al. 2017). Previously however, apricot and oatmeal were used as scrubbers in PCPs such as facial scrubs (Chang 2015; T Rocha-Santos & Duarte 2015; Hernandez et al. 2017). The particles in many of these PCPs are advertised as microbeads which are produced in different colours, sizes and polymer composition, depending on the manufacturer and possibly target consumer (Cole et al. 2011; Hintersteiner 2015; Duis & Coors 2016a). However, it has been reported that the frequent use of these PCPs contribute to the microplastics load in the environment (Duis & Coors 2016b; Mason et al. 2016). It is apparent that primary microplastics used in PCPs are a significant



source of particles to the environment (Fendall & Sewell 2009; Chang 2015; Duis & Coors 2016a).

### *2.1.2 Secondary Microplastics*

Secondary microplastics are formed from the fragmentation of larger plastics (macroplastics), which occurs by a combination of physical, chemical and biological processes that reduce the structural integrity of the particles (Andrady 2017; Auta et al. 2017a). In addition, exposure to sunlight, temperature and the density and size of the particles has an apparent impact on the fragmentation of macroplastics. On exposure to ultraviolet radiation, the oxidation of the plastics matrix, results in bond cleavage and breakage (Figure 2.2) (Andrady 2011a; Andrady 2015; Sharma & Chatterjee 2017). In the aquatic environment only particles that exhibit a lower density to the water will float and therefore will be exposed to ultraviolet light. Therefore, particles exhibiting low density are susceptible to fragmentation. In addition, the size of the particle suggests the likelihood of fragmentation into smaller sizes, because of the large surface area that is exposed to ultraviolet light. In the coastal marine environment and in beaches in particular, secondary microplastics are readily formed. This is because of exposure to ultraviolet light and the crashing of waves on the shore, turbulence and the availability of oxygen (Andrady 2017; Barnes et al. 2009; Matthew Cole et al. 2011). Over time the particles become brittle and break into smaller pieces due to physical abrasion of the waves and change colour on exposure to sunlight. Particles are transported by tide and waves to surface waters, where they remain exposed and eventually fragment further. . In addition, organisms can feed on macroplastics, resulting in the production of secondary microplastics in the marine environment (Rocha-Santos & Duarte 2015; Andrady 2017; Auta et al. 2017). It is possible that fragmentation of macroplastics can occur when fed upon by large marine organisms such as sharks and whales (Lusher 2015; Lusher et al. 2015). However, it is not clear if this is a significant source of secondary microplastics to the environment.

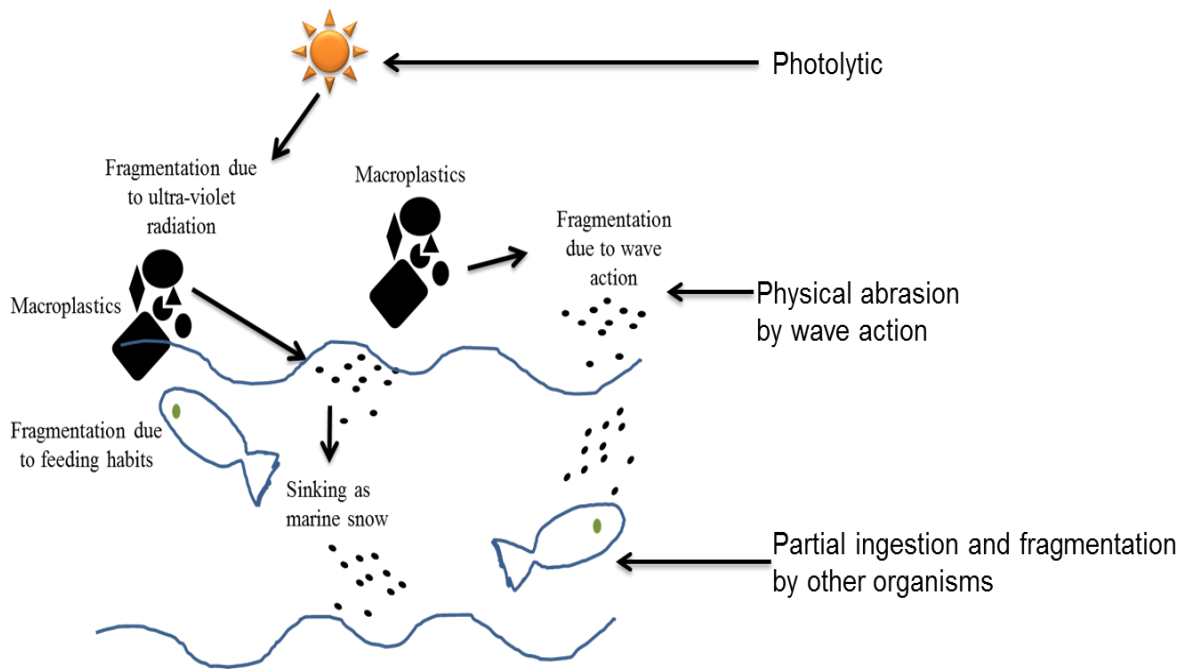


*Figure 2.2. An illustration of the formation of secondary microplastics in the aquatic environment.*

## 2.2 Sources of Microplastics

Microplastics typically originate from land-based and marine-based sources (Duis & Coors 2016b; Auta et al. 2017b). Land-based sources have been reported to be the largest source (80%), of microplastics to the environment, this is largely because of the global dependence on plastic based materials, such as plastic bags; the improper disposal of plastic based materials (Auta et al. 2017; Lebreton et al. 2017). In addition, it is widely acknowledged that waste water treatment plants WWTPs are a significant source of particle entry to the environment (Mintenig et al. 2017; Ziajahromi et al. 2017a; Carr et al. 2016a). In particular, the frequent use of PCPs that contain microplastics, and the washing of garments with synthetic particles (nylon, polyester) are transported through WWTPs (Auta et al. 2017; Lebreton et al. 2017). WWTPs are equipped with different treatment technologies designed to capture particles. WWTPs have screens ranging from fine screens (1.5 – 6 mm), coarse screens >6 mm and some are equipped with a membrane bioreactor (MBR), which screens particles using microfiltration or ultrafiltration (Talvitie et al. 2017; Leslie et al. 2017; Karlsson et al. 2017). However, it is clear that WWTPs cannot efficiently capture all particles in the

flow. Current reports on microplastics in treated waste water suggest the number of particles that were  $<500 \mu\text{m}$ , ranged from  $1 \times 10^1 \text{ m}^{-3}$  –  $9 \times 10^3 \text{ m}^{-3}$  particles (Mintenig et al. 2017). By contrast, a smaller number of particles ( $> 500 \mu\text{m}$ ), were detected in the treated waste water and ranged from 0 to  $5 \times 10^1 \text{ m}^{-3}$  particles (Mintenig et al. 2017). In addition, the report suggests that there were more particles of fibre detected than fragment particles. The particles of fibre were identified as polyester, and the fragment particles mostly comprised of polyethylene (Mintenig et al. 2017). However, other studies have reported different estimates for particles in WWTPs ranging from  $2 \times 10^3$ ,  $7 \times 10^{-3}$  –  $35 \times 10^{-2}$  and  $2 \times 10^{-3}$  and  $1.5 \times 10^{-2}$  (Ziajahromi et al. 2017a; Leslie et al. 2013). Particles captured by the treatment process in WWTPs are transferred to sludge and applied on farmlands (Nizzetto et al. 2016; Leslie et al. 2017). During run-off, particles in sludge may eventually enter the environment suggesting WWTPs could be an important source of microplastics.

The freshwater environment has been suggested as the link between land-based sources of microplastics and the marine environment (Eerkes-Medrano et al. 2015b). Microplastics particles from land-based sources enter freshwater environments directly from disposal of plastic waste, transport by wind (something that is less studied), and by contributions from WWTPs (Eerkes-Medrano et al. 2015a; Scherer et al. 2017). Therefore, this suggests that freshwater environments are a significant link and not necessarily a source of particles to the larger marine environment (Horton et al. 2017; Eerkes-Medrano et al. 2015a). Marine-based sources of microplastics to the environment have been described in reports and include but are not limited to, marine based - fishing and shipping activities (Duis & Coors 2016a; Oluniyi Solomon & Palanisami 2016).

Nets and hook lines largely made from synthetic or semi-synthetic plastic materials are commonly used in the aquaculture and fisheries industry (Fao 2017; Magnusson et al. 2016; Heathcote, et al. 2015). Plastics are used as part of construction of boats, fishing gears which include but are not limited to trawls, traps and dredges (Fao 2017). Plastic material used in fisheries and aquaculture industry is made from a wide variety of polymers some of which include polyethylene, polyvinylchloride and polypropylene (Kerstin Magnusson et al. 2016; GESAMP 2015). Plastic materials used in the fisheries and aquaculture can be a source of microplastics entry to the environment, because equipment made from plastics is sometimes deliberately discarded, lost, or

abandoned at sea (Fao 2017; Wilcox, Heathcote, et al. 2015). It has been reported that an estimate of 9000 nets have been detected in the northern coast of Australia (Wilcox, Van Sebille, et al. 2015). Abandoned fishing equipment exposed to physical, chemical and biological conditions in the environment will fragment to form secondary microplastics. .

The marine environment is also characterised by shipping activities, including transport of goods and services, which often results in the contamination of the marine environment with microplastics (GESAMP 2015; Oluniyi Solomon & Palanisami 2016; Auta et al. 2017a). Plastic pellets which are  $\leq 5$  mm are accidentally spilled by ships have been detected in the marine environment (PlasticsEurope 2017; Acosta-Coley & Olivero-Verbel 2015; Kerstin Magnusson et al. 2016). In addition, it has been suggested that spilled pellets from shipping activity accounts for about 10% of the plastic pellets on beaches (Patil & Raghvendra 2017). In addition, it was reported that 165 tonnes of plastic pellets were accidentally spilled across the shores of Lamma Island, Hong Kong, in 2012. The pellets were released from shipping containers that were knocked off because of a typhoon (Reuters 2012). Currently, there are reports on the accidental spill of pellets in beaches in the UK and in the marine environment in South Africa, from shipping activity (Guy 2017; Willimans 2015). Improved safety during the transport of pellets at sea will reduce plastic spills in the environment. However, shipping activity remains an important source of microplastics (Antunes et al. 2013; Acosta-Coley & Olivero-Verbel 2015).

A less researched aspect of marine-based pollution is from dumping of garbage by luxury cruises, merchant vessels and military vessels. There are reports which indicate that plastic materials have been dumped at sea by shipping activities. There are international conventions such as the International maritime organisation (IMO), established to protect the marine environment from human activities and especially pollution. However, it is clear that not all shipping activity can be monitored, and the incidences of illegal dumping of plastic materials still occurs (IMO 2018). The IMO has recognised that shipping activities are a major source of pollution to the environment. In particular, it aims to reduce the amount of garbage that is thrown overboard from shipping activity (Jim Walker 2017; IMO International Maritime Organisation 2018b). Although throwing away garbage at sea is not common, not all shipping activities can be monitored and so it is possible that garbage from ships will still continue. In the last

three years, there have been reports of dumping of garbage overboard ships (WVEC 2017; Jim Walker 2017).

### 2.3. Occurrence and abundance of microplastics in the environment.

Microplastics are distributed into different parts of the environment. They have been detected in the marine, freshwater and terrestrial environment. However, more studies have been conducted in the marine environment and less in freshwater and terrestrial environment (Wagner et al. 2014; Eerkes-Medrano et al. 2015a).

#### 2.3.1. *Marine environment*

An overview of the many anthropogenic pressures on the marine environment indicates a growing concern for the accumulation of microplastics which is reflected in the increase in studies on microplastics in the marine environment over the last decade (Peng et al. 2017; Van Cauwenberghe, Devriese, et al. 2015a). The distribution of these particles on sea surfaces, water column and in sediment is determined in part by the different densities of polymers which tend to sink or float (Andrady 2011b; Woodall et al. 2014; Thompson et al. 2004). The densities of commonly identified microplastics range from 0.89 g/cm<sup>3</sup> for low-density polyethylene PE, to 1.58 g/cm<sup>3</sup> for polyvinylchloride PVC (Table 2.1) (Hidalgo-Ruz & Gutow 2012; Stolte et al. 2015; Law 2017a).

In the marine environment particles with a density lower than sea water will readily float on the surface of the water. For example HDPE and LDPE with low densities (Table 2.1) will readily float on the surface of sea water which has a density of 1.20 g/cm<sup>3</sup> (Crichton et al. 2017; Karlsson et al. 2017).

*Table 2.1. Densities of polymers commonly identified in the environment as microplastics, units are in g/cm<sup>3</sup>*

Polymer name	Abbreviation	Density
High-density polyethylene	HDPE	0.94–0.97
Low-density polyethylene	LDPE	0.89–0.94
Polypropylene	PP	0.89–0.91
Polyvinylchloride	PVC	1.3–1.58
Polyethylene terephthalate	PET	1.29–1.40
Polystyrene	PS	1.04–1.08
Polyamide	PA	1.07–1.08
Polycarbonate	PC	1.20
Polymethyl-methacrylate	PMMA (acrylic)	1.17–1.20

Currently the distribution of particles in the marine environment has been well documented and widely acknowledged (Thompson 2015b; Auta et al. 2017b). There is evidence to show the presence of these particles in the marine and coastal environment (Auta et al. 2017a; Kanhai et al. 2017). Surface waters of the marine environment, the water column and benthic environments have been contaminated with microplastics from different sources (Auta et al. 2017b; Yeo et al. 2017; K Magnusson et al. 2016). Different studies have reported the distribution of particles on the surface waters in the marine environment range from 0.022 – 8,654 particles m<sup>3</sup>, 1.15 particles m<sup>3</sup>, 8654 m<sup>3</sup> and 9180 particles m<sup>3</sup> (Kanhai et al. 2017; Nuelle et al. 2014; Desforges et al. 2014; Eriksen et al. 2014a). However, particles are transported to lower depths of the marine environment where they persist (Auta et al. 2017b; Nor & Obbard 2014).

It has been reported that processes like biofouling which is the accumulation of microorganisms, algae, plants or animals on microplastics has the potential to alter the density of the particles (Kowalski et al. 2016). Therefore the aggregation of living organisms on the particle, may cause the particles to sink to the bottom of the marine environment (Courtene-Jones et al. 2017; Avio, Cardelli, et al. 2017). The process of biofouling could have an impact on the transport of smaller particles at a faster rate,

because of the larger surface area to volume ratio. Therefore, the smaller the particle, the more likely it will sink to the bottom of the marine environment because of biofouling (Kowalski et al. 2016). A laboratory based study reported sinking rates were increased with increased aggregation of phytoplankton on 2  $\mu\text{m}$  polystyrene microbeads (Long et al. 2015). Another study reported the relationship between size and rate of sinking due to biofouling. The report suggested that smaller particles sank faster than larger particles (GESAMP 2015). Therefore it is apparent that biofouling has an impact on the transport of particles from water surfaces to lower compartments of the marine environment. . Therefore, particles no longer bioavailable to pelagic organisms will become bioavailable to organisms in the water column and the benthic environment (Woodall et al. 2015; Van Cauwenberghe, Claessens, et al. 2015). Generally, particles denser than water tend to sink to the bottom as marine snow, likewise microorganisms acting upon the surface of the particles will increase the density, allowing them to sink to the bottom of the water body (Zhao et al. 2017; Avio, Gorbi, et al. 2017).

Currently there is limited information on the occurrence of microplastics in terrestrial and freshwater environment. It is conceivable that the close proximity of freshwater and terrestrial environments to the source(s) of plastic pollution, will add to the secondary microplastics load in these environments (Eerkes-Medrano et al. 2015a). Secondary microplastics are widely associated with areas of high human population because of the frequent use of and inappropriate disposal of products made from plastics (Eerkes-Medrano et al. 2015a). One area of emerging concern in recent years, has been the production of secondary microplastics arising from washing of garments (Eerkes-Medrano et al. 2015a; Napper & Thompson 2016). Clothing materials which previously made mainly from natural materials such as cotton, linen and wool, have now been substituted with synthetic polymers including polyester, nylon and acrylic (Browne et al. 2011; Napper & Thompson 2016). Notably, garments such as fleeces commonly made from polyester and nylon undergo abrasion during the laundry process, resulting in the shedding microfibers.

### 2.3.2. *Freshwater Environments.*

Although acknowledged by scientists, international bodies and government institutions that microplastics are an emerging environmental threat, it is widely known that most studies have focused more in the marine environment than freshwater environments (Qiu et al. 2016; Wagner et al. 2014; Matthew Cole et al. 2011). It has been argued that freshwater environments serve as a pathway for the transport of microplastics from land based sources to the marine environment (Auta, Emenike, & Fauziah, 2017; Magnusson et al., 2016; Cauwenberghe et al., 2015). For example, PCPs and other products which contain polymers of polyethylene particles are transported through the sewer system to WWTPs (Figure 2.3) (Horton et al. 2017; Chang 2015).

Secondary sources of particle entry to freshwater environments include wear and tear from car tyres (Kole et al. 2017), polymers used in clothing and textiles such as including nylon and acrylic may be washed through to city mains from homes and offices during laundry with washing machines (Figure 2.3) (Napper & Thompson 2016). Currently, there is no information to determine if the brand of the washing machine, the age of the clothing material and/or the detergent used has any effect on the shedding of these particles. What is certain however is that these particles are transported to through WWTPs and eventually enter freshwater environments (Eerkes-Medrano et al. 2015b; Wagner et al. 2014). Furthermore, in the event of heavy rainfall, there is increased certainty that these particles would be washed back onto land surfaces via floods, resulting in repeated contamination of the terrestrial environment. This suggests a feedback-contamination loop between the freshwater and terrestrial habitats.



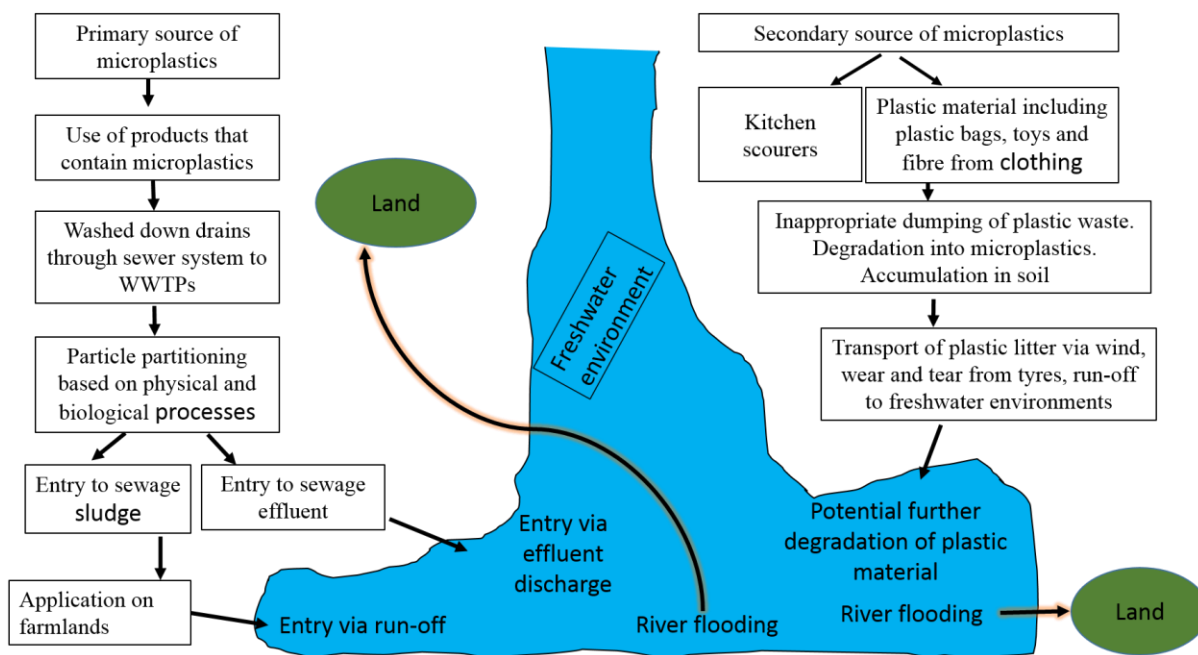


Figure 2.3. Conceptual diagram of the entry of microplastics from primary and secondary sources to freshwater environments.

The basis for the entry of particles to the freshwater environment has been ascribed to the screening processes in WWTPs, especially the screens that would normally trap small particles (Figure 2.4). . It is likely that partitioning of particles in WWTPs based on particle density will occur (Figure 2.4). As such, particles with a high density like polyester and acrylic will likely sink in sludge and settle; by contrast, low density particles like polyethylene will float in sewage effluents (Kowalski et al. 2016). In addition, it is likely that the rates of settling and buoyancy will be affected by clumping of these particles with other microplastics and/or clump with organic matter in the WWTPs to form highly dense aggregates that will aid sinking in sludge. Likewise, in the presence of organic matter, the surface of these particles can become colonised by microorganisms (biofilm), increasing the particle density, thereby increasing the likelihood of sinking in sludge (Kowalski et al. 2016). The consequence of the entry of primary and secondary particles to WWTPs and the effects of particle partitioning results in both the entry of particles to freshwater environments via effluent discharge and/or the addition of other highly dense or agglomerated particles to sludge, which is applied to agricultural land (Fendall & Sewell 2009; Chang 2015; Kowalski et al. 2016). Particles in sludge and applied to agricultural land eventually enter freshwater

environments via run-off, thereby adding to the micropalstic content in these environments (Eerkes-Medrano et al. 2015a; Horton et al. 2017).

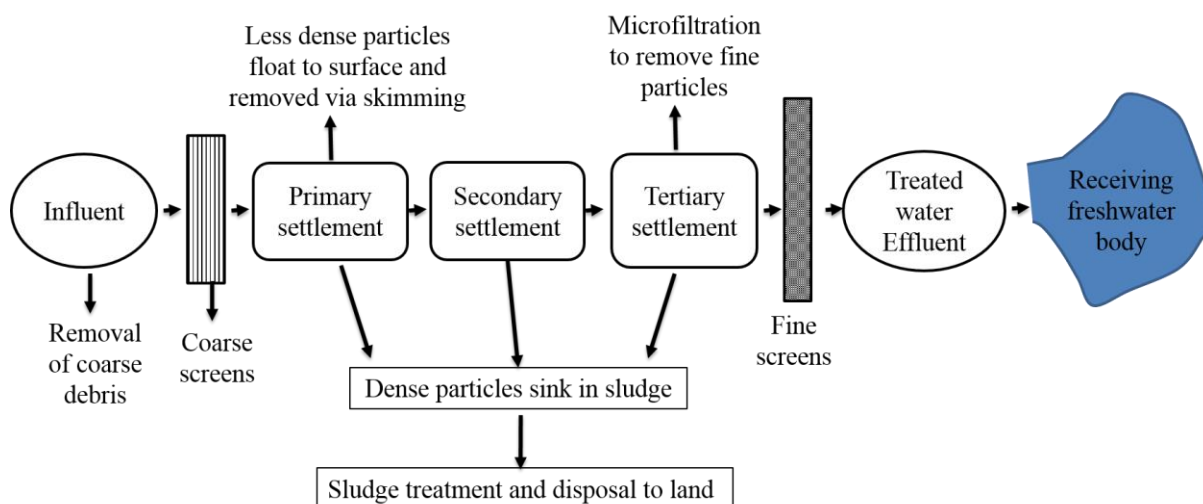


Figure 2.4. Schematic diagram of a wastewater treatment plant, showing different stages of the wastewater treatment process. The image shows the different screens and separation of particles in the WWTP and final discharge to the environment.

A report on the occurrence of particles in three freshwater bodies which receive treated wastewater effluents in Texas indicated reported two particle size classes of between 53–105  $\mu\text{m}$  and 106–179  $\mu\text{m}$ . The mean mass of particles counted ranged from  $0.79 \pm 0.88$  mg/L to  $1.56 \pm 1.64$  mg/L for the 53–105  $\mu\text{m}$  class size, and  $0.31 \pm 0.72$  mg/L to  $1.25 \pm 1.98$  mg/L for the 106–179  $\mu\text{m}$  class size. In addition, the analysis of water samples in the surrounding wetlands revealed the occurrence of particles with similar size classes mentioned above. Consequently, the mean particles for the 53–105  $\mu\text{m}$  size class ranged from  $0.64 \pm 0.92$  mg/L to  $5.51 \pm 9.09$  mg/L, and from non-detects to  $1.79 \pm 3.04$  mg/L for the 106–179  $\mu\text{m}$  size class (Lasee et al. 2017). This report suggests that effluents from WWTPs contribute directly to particle load in freshwater environments and indirectly via urban run-off.

Other documented reports on fresh water environments reveal an average abundance of approximately 43,000 microplastics particles  $\text{km}^{-2}$  in surface waters of the Laurentian Great Lakes. These particles consisted of multi-coloured spherical particles similar to micro-beads found in personal care products (Eriksen et al. 2013). Furthermore, 466,000 particles  $\text{km}^{-2}$  particles on surface water were counted

downstream from the point of sampling. Although the size, texture and composition of the microplastics reported appear similar to microbeads found in personal care products, the results were inconclusive (Eriksen et al. 2013). The study reported similarities in the polymeric elemental characteristics of microplastics collected with microbeads separated from PCPs. However, this is not enough evidence of the polymer identity. The appropriate technique was not used to determine the polymer identity of the microplastics.

By comparison with the marine environment, freshwater environments have less areas of convergent currents, it is likely that the particle count and distribution will be low (Gordon 2017). Although information is limited for freshwater environments and fragmented for backwaters (part of a water body not reached by current, relatively stagnant), there is evidence to support the occurrence of a high number of particles. A study on the backwaters of the Xiangxi River which is a tributary for the Three Gorges Reservoir, number of particles ranged from  $0.55 \times 10^5$  to  $342 \times 10^5$  microplastics  $\text{km}^{-2}$  and 80 to 864 microplastics  $\text{m}^{-2}$  in surface water and sediment samples respectively. Furthermore, in surface waters, microplastics were identified as polyethylene, polystyrene and polypropylene while polyethylene terephthalate, polypropylene and polyethylene were identified in sediment samples (Zhang et al. 2017).

The transfer of microplastics to the bottom of freshwater bodies has been documented (Lebreton et al. 2017). A report that documented the distribution of these particles in sediment samples in freshwater environments, reveal that 34 – 64 microplastics  $\text{kg}^{-1}$  dry weight were identified (Wagner et al. 2014). In addition, based on the survey of four rivers, River Rhine accounted for the highest number of particles (Wagner et al. 2014). A breakdown of the particles showed that 60% of the particles identified were fragments and 40 % were fibre (Wagner et al. 2014). Fragments could have been from primary and/or microplastics that have undergone further fragmentation and introduced directly via effluent discharge or urban run-off. In addition, the particles of fibre would have been more likely to be secondary microplastics, notably fibre from clothing material.

### 2.3.3. *Terrestrial Environment*

There is limited information and less documented reports on the distribution of particles in the terrestrial environment, compared to the aquatic environment (Duis & Coors 2016a; Eerkes-Medrano et al. 2015a). However it is likely that particles from primary and secondary microplastics enter the terrestrial environment due to inappropriate disposal of litter which is likely to fragment over time and the application of sewage sludge to agricultural land (Horton et al. 2017; Duis & Coors 2016c). As such terrestrial environments act as a sink for the deposition of particles from different sources.

The application of sewage sludge which contains dense particles, typically fibres, adds to the microplastic load on agricultural lands and other areas of the terrestrial environment (Nizzetto et al. 2016; Auta et al. 2017a). Fibres have been used in monitoring studies as an environmental indicator to determine the level of contamination resulting from sewage sludge applications (Duis & Coors 2016a). However, what is uncertain is differentiating between fibre deposits from sludge, atmospheric deposits, wind driven sources and from freshwater environments via flooding. What is certain however is that particles in the terrestrial environment will be deposited and distributed on soil surfaces, with the potential to sink over time to different depths (Rillig 2012; Duis & Coors 2016b). In addition, the rate of particle degradation on the soil surface is likely to be higher compared to the aquatic environment, notably because of the higher availability of oxygen in the soil and the potential for direct exposure to ultra-violet light (Andrady 2011a; Peng et al. 2017).

A common source of particles to land is the application of plastic mulches frequently used in agricultural practices to control weed growth, moisture and temperature (Steinmetz et al. 2016). Plastic mulches improve crop yields, improve the efficient use of water, earlier harvests are recorded and the quality of crops are improved, giving significant benefits (Steinmetz et al. 2016). However, it is apparent that the incomplete removal of mulches from soil as described in section 1.1, will likely contribute to the plastic load in the soil (Steinmetz et al. 2016). The problem is that frequent exposure to sunlight, will degrade the physical integrity of the plastic over time, forming fragments that will further breakdown into smaller sized particles (Duis & Coors 2016d). In addition, toxic additives commonly associated with some polymers will

eventually leach out into the soil, causing further contamination (Steinmetz et al. 2016) It is hypothesised that organisms in soil will use these particles as substrates for feeding and transport, thus causing a migration pattern for the particles on land (Rillig et al. 2017; Huerta Lwanga et al. 2017).

In the terrestrial environment, it is possible that particles can be transported over distances by wind currents (Laurent C M Lebreton et al. 2017). The movement of winds over soil surfaces has the potential to transport particles over long distances, depositing these particles in land masses far from the particle origin (Provencher et al. 2015; Laurent C M Lebreton et al. 2017). However, little is known about the role wind plays in the distribution of microplastics because it is a less studied aspect of microplastics research.

#### 2.4. Impact of microplastics on the environment

It has been generally acknowledged that the occurrence of microplastics in the environment has the potential to cause harm to living resources (Duis & Coors 2016a; Ivar Do Sul & Costa 2014). However in field studies, information is limited on the known effects of these particles alone on living organisms with uncertainty about any direct effects of the particle exposure to living organisms. At best and by contrast, laboratory controlled experiments however, have been able to detect microplastics in tissues of organisms (Taylor et al. 2016; Phuong et al. 2016). Furthermore it has been suggested that the concentration of microplastics used in laboratory experiments far exceed concentrations of particles observed in field surveys ( Burton 2017; Phuong et al. 2016). There is increasing awareness that the aquatic and terrestrial environments are frequently contaminated by microplastics and is likely to increase because of the dependence on plastic based products (Duis & Coors 2016b; Desforges et al. 2014).

##### *2.4.1. The effects of microplastics in the marine environment*

In the marine environment, the potential effect of these particles can be attributed to a number of factors; the different densities of particles allow for distribution in

different compartments of the marine environment. Documented reports suggest that ingestion of microplastics can result in lower energy levels and reduced feeding in living organisms (Courtene-Jones et al. 2017; Ivar Do Sul & Costa 2014). The size of the particle also has an effect on the feeding and ingestion processes of marine organisms (Eerkes-Medrano et al. 2015a; Courtene-Jones et al. 2017). For example, particles that are in the larger size category (1–5 mm), are more likely to be ingested by organisms that have the digestive capacity to, such as sea turtles, sea birds and fish (Ivar Do Sul & Costa 2014; Lusher et al. 2013; Hammer & VanBrocklin 2016). Conversely, particles in the smaller size class (< 20 µm) are more likely to be ingested by small invertebrates and zooplankton (Cole et al. 2013; Lusher 2015; Cole et al. 2016).

After the Costa Concordia wreck, environmental sampling was conducted to assess the particle number, size and type in surrounding waters of Giglio Island (Cardelli, et al. 2017). The report showed that 85% of the fish sampled contained microplastics, notably, all the benthic-pelagic fish analysed contained particles (, Cardelli, et al. 2017). In addition, the common particle size classes identified were; 0.5 – 1 mm, 37%; 0.1 – 0.5 mm, 35%, 1 – 5 mm, 20% and 0.1 mm, 8%. Furthermore for all the particles analysed, polyethylene was the most common polymer (35 – 40%), however, higher density particles such as PVC, PA, and Nylon were identified (, Cardelli, et al. 2017).

Documented reports on the ingestion of microplastics in the western English channel by fish larvae show that particle sizes recorded were 100 x50 µm for the European eel and 270 µm for the Thickback sole respectively (Steer et al. 2017a). Particles analysed were identified as polyamide-polypropylene and rayon respectively for the species mentioned above. The report went on to add that only one blue fragment and one red fibre were observed in the larvae of the European eel and the Thickback sole respectively (Steer et al. 2017a).

A study which compared particles in surface water, sediment samples and mussels in the marine environment, detected an average of 27 microplastics L<sup>-1</sup> in surface water and a mean of 48 particles kg d.w.<sup>-1</sup> microplastics in the sediment samples (Karlsson et al. 2017). However, the concentration of particles in mussels analysed revealed a significantly higher number of particles than in surface waters and sediment samples combined (Karlsson et al. 2017). They recorded a mean of 37,000

microplastics kg d.w.<sup>-1</sup>, and an analysis of a subsample of mussel tissue revealed 5 to 19 particles were found, ranging from 30 to 2000 µm (Karlsson et al. 2017). It is apparent that mussels can store microplastics in their bodies and therefore can be used in monitoring studies to assess their impact (Karlsson et al. 2017).

It has been reported that in some instances, organisms cannot tell the difference between prey and man-made particles such as microplastics. This is most likely because the particles have colours that attract the organism, and the organisms feeding mechanism cannot discriminate between the particles and its prey (Cole et al. 2016; GESAMP 2015). Furthermore, in an area with a high particle count, plankton which act as prey for many organisms will become mixed with these particles, making differentiation difficult and ingestion possible (Moore 2008; Ivar Do Sul & Costa 2014)

In the manufacturing process of some polymers, additives such as phthalates and alkylphenols, are incorporated to improve their physical, chemical and mechanical properties, with the aim of keeping the integrity of the plastic intact and reducing degradation on exposure to the environment (Andrady 2011b; Syakti et al. 2017; Steinmetz et al. 2016). There are suggestions that under the right conditions these additives can be released to the environment with the potential to cause harm to living organisms (Law 2017a; Avio et al. 2016; Andrady 2015). In particular, phthalates have been considered as endocrine disrupting chemicals because of their ability to alter the hormonal system in a living organism (Wagner et al. 2014). There is evidence to show the occurrence of phthalates associated with in the marine environment. Out of 23 surface plankton and neuston samples collected, 13 ingested contained microplastics (Fossi et al. 2012). Furthermore, mono-(2-ethylhexyl)-phthalate MEHP was detected in the blubber of fin whales, as a result of bio-concentration of particles from ingestion of plankton and water filtration (Fossi et al. 2012). This suggests that phthalates can be transferred from the particles to the fin whale, because of their feeding habit and by ingestion of microplastics, thus making an argument for the transfer of toxic chemicals to living organisms. By contrast, another study reported detectable concentrations of the plastic softener and its metabolite Di(2-ethylhexyl)phthalate (DEHP) and mono-(2-ethylhexyl)-phthalate (MEHP), in Tuna which did not have any microplastics (Guerranti et al. 2016). However, it is apparent that phthalates occur in the environment there is currently no established link between the detection of particles/chemicals and an effect on living organisms.

As a response, a laboratory controlled experiment was conducted to test the pathway of entry for chemical additives by leaching and not ingestion (Nobre et al. 2015). The sea urchin *Lytechinus variegatus* was exposed to raw virgin pellets and pellets collected from the beach in two assays. The comparison of both assays showed that virgin pellets had a more significant effect on embryo development than the beached pellets (Nobre et al. 2015). This suggests microplastic pellets can act as a vector of chemical additives and highlights different pathways (in this instance, leaching) through which living organisms can be affected by particles in the environment (Nobre et al. 2015).

In addition to containing chemicals from manufacture, plastics may also attract hydrophobic contaminants. There is still the argument that particles readily adsorb and transport persistent bio-accumulative toxic chemicals (PBT) including polycyclic aromatic hydrocarbons (PAH), organochlorine pesticides and polychlorinated biphenyls (PCBs) at different concentrations ranging from ng/g to µg/g (Claessens & Meester, 2011; GESAMP, 2015). The ingestion of these particles by aquatic organisms may increase the chance of toxic exposure through leaching of these toxic substances in the digestive system (Cole et al., 2013; Wright et al., 2013). Currently, there is still limited information on the release of toxic chemicals from particles to the environment and their bio-magnification in the food chain (Andrady, 2011; Ziccardi et al., 2016). There is currently no established relationship between the occurrence of chemicals associated with particles and an effect on living organisms (Burton 2017).

#### 2.4.2 Impact of microplastics in freshwater environments

A wide range of organisms in freshwater environments are exposed to microplastics, however, the impacts remain unknown (Horton et al. 2017; Eerkes-Medrano et al. 2015a). One report showed that from 11 streams sampled in France, 12 % of the fish *Gobio gobio* had microplastics in their digestive tract (Sanchez et al. 2014). A similar study under laboratory conditions demonstrated uptake of particles by annelids *Lumbriculus variegatus*, gastropods *Potamopyrgus antipodorum*, crustaceans *Daphnia magna* and *Gammarus pulex* and ostracods *Notodromas monacha* (Hannes et al. 2013) In a more recent study, an analysis of the stomach



content of the bluegill *Lepomis macrochirus*, longear *Lepomis megalotis* and sunfish *Centrarchidae*, showed that out of a total of 436 fish samples collected, 45 % had microplastics in their stomach content. In addition, 96 % of the total debris in the stomach content was made up of microplastics. This study not only highlighted the scale at which these particles were ingested but also the importance of some fish species as indicator organisms in the environment (Peters & Bratton 2016). In laboratory conditions, one study showed that the water flea *Daphnia magna* ingested particles with size of 0.02 and 1 mm particles rapidly (Rosenkranz et al. 2009). The report suggested particles accumulated in the lipid storage droplets of the organism by crossing the epithelium of the gut and were likely therefore to cause more harm (Rosenkranz et al. 2009).

#### 2.4.3. *The Impact of Microplastics in Terrestrial Environments*

It is widely acknowledged that particles enter the terrestrial environment via fragmentation of larger plastics that have been inappropriately discarded and by application of sewage sludge. In addition, it is likely that soils in terrestrial environments can act as a sink for wide range of microplastics, suggesting that successive generations of organisms will be exposed to microplastics with the potential to cause harm (Zubris & Richards 2005; Duis & Coors 2016a). However, little is known about the impact of particles on terrestrial organisms (Rillig 2012; Duis & Coors 2016b; Rillig et al. 2017). Although there is currently no available information on the impact of particles on living organisms in field studies, laboratory controlled experiments have suggested *Lumbricus terrestris* some organisms act as a means of transport for the distribution of particles (Huerta Lwanga et al. 2017). Notably, a greater number of particles were transported in the formation of burrows at higher concentrations of microplastic exposure (Lwanga et al. 2017). There is the potential for additives in the particles to leach into the soil and to also sorb toxic chemicals (Huerta Lwanga et al. 2017). In addition, the effect of particles (250 -1000  $\mu\text{m}$ ) on earthworms *Eisenia andrei* Bouche was conducted, and demonstrated no significant effects on the number and survival of juveniles and the growth of adults. However, further tests revealed evidence of damage to the gut and molecular changes in the

body of *Eisenia Andrei* Bouche suggestive of an induced immune system response (Rodriguez-Seijo et al. 2017).

## 2.5. Challenges associated with the characterisation of microplastics

The significance of microplastics and the potential impact to the environment and living organisms has been widely acknowledged (Wright et al. 2013a; Oluniyi Solomon & Palanisami 2016). However, the challenge in evaluating these effects has been largely because of a lack of a uniform and standardised studies (Hidalgo-Ruz & Gutow 2012; Van Cauwenberghe, Devriese, et al. 2015b). Likewise has been suggested that a lack of a universally accepted sampling and laboratory protocol, to effectively characterise; determining particle size, number, shape, identity and morphology, microplastics in the environment and laboratory controlled studies (Van Cauwenberghe, Devriese, et al. 2015b; Hidalgo-Ruz & Gutow 2012). There is currently no universally accepted standard protocol for the extraction of microplastics from environmental or laboratory controlled samples (Hidalgo-Ruz & Gutow 2012). However, there are general steps that have been widely adopted to characterise microplastics (Qiu et al. 2016; Besley et al. 2017; Shim et al. 2017). These include all of but not limited to the following steps; density separation, filtration and particle characterisation using different techniques. The characterisation of particles generally covers particle size, number, morphology and the particle identity.

Sample preparation forms the basis for an accurate particle characterisation. Sample preparation forms the basis of this process and is based on the extraction of microplastics from a matrix by combinations of density separation using a range of concentrated solutions that are dependent on the polymer identity. Once extracted, microplastics size can be characterised by applying techniques suited to determine particle size distribution; quantifying microplastics by determining the number of microplastics based on the units of measure for the study; and resolving the polymer identity of the microplastic (Hidalgo-Ruz & Gutow 2012; Van Cauwenberghe, Devriese, et al. 2015b).

The characterisation of microplastics in personal care products, even of a similar nature and function, undertaken by a number of researchers has given a wide range

of values (Napper et al. 2015; Chang 2015; Fendall & Sewell 2009). This range may be real or may be a function of methods used, from laboratory protocol for sample preparation to the characterisation of microplastics with analytical techniques. The lack of any reference materials gives no baseline from which to assess the method performed.

Personal care products have been identified as containing microplastics, commonly containing polyethylene (L. M. Hernandez et al. 2017; Rochman et al. 2015; Napper et al. 2015). Concern about their possible effects of such use have led to restrictions on their use (Rochman et al. 2015; Kramm & Völker 2018), debate in parliaments (Bennet 2016; Girard et al. 2106; Morden 2016) and voluntary withdrawals (Kramm & Völker 2018; Vaughan 2016). However, the uses of microplastics are not under review and the degradation of macroplastics will still continue to produce microplastic fragments.

Another important secondary microplastic that has not been widely looked into are particles from hard scourers (HS); and kitchen scourers (KS). Kitchen scourers are commonly used in domestic and industrial applications to clean surfaces and kitchenware (Academic Mintel 2014). These KS are usually made from polyester, acrylic resin and according to some manufacturers, recycled plastics. Kitchen scourers are characterised by different shapes, sizes and colours, and the frequent use causes shedding of fibres and particles off its surface, due to abrasion from the process of washing. Information on synthetic fibres from shed from KS is scarce, however, we suspect that like microbeads from PCPs, these contaminants have the potential to pass through kitchen drains to city mains and out to the environment, with an effect on the biota likely but uncertain. What is certain however is the frequency of use supported by a marketing survey. The survey showed that hard scourers HS and KS were the most popular cleaning equipment from an online survey and accounted for 99 and 91% of UK household usage in 2014. This means at least nine out of ten homes make use of these products and a 70 % increase in use has been forecast for 2019 (Academic Mintel 2014). It is plausible that based on frequency of use, almost every home in the UK could be contributing secondary microplastics to the environment through use of KS.

There is therefore a continuing need for monitoring of microplastics in the environment. There is already a significant amount of data on microplastics with focus on the marine and environment (Auta et al. 2017a; Lusher 2015; Hidalgo-Ruz & Gutow 2012).

### 2.5.1. Laboratory Analysis: Density Separation

The density separation of particles in matrices is based on the fact that particles have different densities. In general, particles with a higher density than the matrices will sink, but lighter density particles tend to float in matrices. Therefore, the differences in particle density is utilised to separate particles from matrices which could be water or sediment samples. Depending on the density of the particles, a density separation solution with a higher or lower density to the particles is commonly used. For example, a particle with a low density will readily float in a density solution that has a higher density to the particle. Conversely, a particle with a higher density than the density separation solution will not float but will sink to the bottom of the solution. Typically, in the marine environment, low density polymers such as polyethylene will readily float in sea water which has a higher density than the particle. However, if the microplastic is acted upon by fouling with living organisms or by microbial colonisation, the particle becomes heavier than it originally is, and will increase in density. Consequently, the particle will sink and remain in the water column, the residency time is widely unknown, and eventually sinks to the bottom of the sea (Duis & Coors 2016c; Huang et al. 2017).

The importance of the right density separation solution cannot be overemphasised; it is a process that will determine in part, the success of particle extraction of particles from matrices. In general, microplastics have a wide range of densities (Table 2.1) and a knowledge of which, is important in identifying the right density separation solution to use for the extraction of the particles (Hidalgo-Ruz & Gutow 2012; Stolte et al. 2015; Duis & Coors 2016c). For example polyethylene with a density of  $0.92 - 0.97 \text{ g cm}^{-3}$  will readily float in a solution with a density that is equal to or greater than the density of the particle (Syakti et al. 2017; Zhang et al. 2017). Conversely, polyester with a density of  $1.24 - 2.3 \text{ g/cm}^3$  will require a solution with a higher density than the particle for it to be separated from the matrices (Hidalgo-Ruz & Gutow 2012) (Thompson et al.

2004). Density separation has been widely applied in the extraction of microplastics from matrices, with a wide range of solutions used over time, the choice of solutions for this process has evolved over time (Weinstein et al. 2016; Eerkes-Medrano et al. 2015a).

Generally, a range of solutions with densities ranging from 0.9 – 2.3 g/cm<sup>3</sup> have been useful for the separation of particles from matrices (Table 3.1) (Hidalgo-Ruz & Gutow 2012; Eerkes-Medrano et al. 2015; Karlsson et al. 2017). However, one solution commonly used and reported by authors in micropalstics studies is NaCl solution, with a density of 1.2 g/cm<sup>3</sup> (Table 2.2) (Hidalgo-Ruz & Gutow 2012; Stolte et al. 2015; Duis & Coors 2016c). However NaCl solution is only useful in separating plastic polymers with lower specific densities such as polyethylene, and cannot be applied to particles like polyester, polyvinylchloride which have a higher specific density (Claessens 2013; Weinstein et al. 2016; Crichton et al. 2017). Furthermore, particles in sediment samples are difficult to separate from the matrix using NaCl, because they are covered with organic matter which has a higher density of 1.7 g/cm<sup>3</sup> (Hidalgo-Ruz & Gutow 2012; Tenzer & Gladkikh 2014; Van Cauwenberghe et al. 2015). To overcome the limitations of density separation solutions in extracting high density particles from matrices, a range of solutions and approaches have been explored to recover particles of interest (Table 2.2) (Eerkes-Medrano et al. 2015a; Karlsson et al. 2017; Hidalgo-Ruz & Gutow 2012).

For example, one study applied a two-step approach, employing an elutriation technique where lighter particles are separated from heavier ones by passing an upward stream of liquid through the system (Claessens 2013). Consequently, a fluidised sand bath was used and liquid was passed through, after which lighter particles floated to the top of the system, flowed over and collected on 35 µm sieve (Claessens 2013). After this first cleaning step, the particles collected were further extracted by adding sodium iodide (NaI) and the solution was centrifuged. In addition, the NaI step was repeated three times to ensure all the particles of interest were effectively extracted (Claessens 2013). Consequently, the density separation process adopted had a 100 % efficiency in recovering all polyvinylchloride particles (Claessens 2013). Although the application of NaI in the density separation process, suggests it is useful in the extraction of high density particles, it is relatively expensive as 1 kg costs about \$366 while 1 kg of NaCl costs about \$55 (Fisherscientific 2017a;

Fisherscientific 2017b). Consequently, further steps have been explored to reduce costs when using density separation solutions and to improve the separation of particles from matrices. One is volume reduction, with the aim of reducing the volume of a sample to cut the amount of density solution to be used. In one study, air-induced (AIO) process based on fluidisation in NaCl solution was used as a first step to pre-extract particles from sediment samples. This achieved a volume reduction of up to 80 %, allowing for a reduced volume of NaI solution to be used for further density separation. The recovery for particles including polyethylene and polyvinyl chloride was between 91 and 99 % (Nuelle et al. 2014).

Further exploration of novel techniques and solutions for the density separation of particles from matrices has led to the use of canola oil which was cost-effective and had a 96 % recovery for microplastics, and a recovery rate of 92 % and 99 % for fibre and fragment particles respectively (Crichton et al. 2017). A review of other reports shows that zinc chloride ( $ZnCl_2$ ), Zinc bromide ( $ZnBr_2$ ), calcium chloride ( $CaCl_2$ ) and sodium polytungstate have been used in density separation processes (Maes et al. 2017; Stolte et al. 2015). However, in addition to the limitations of NaCl solution, the applications of other solutions also have their limitations. Notably, higher density solutions such as sodium polytungstate, suggested to have a high efficiency in separating particles from matrices; despite its high density and cost, was not entirely useful in successfully separating particles of polyvinyl chloride from matrix (Ivleva et al. 2017). Likewise  $ZnCl_2$  with a higher specific density than NaCl, and has been used in a number of studies, and although cheaper than sodium polytungstate, is more environmentally hazardous than other density separation solutions used in the extraction of microplastics from matrices (Ivleva et al. 2017; Imhof et al. 2016).

*Table 2.2. Density separation solutions and corresponding densities.*

Density separation solutions	Density
Sodium chloride NaCl	1.2
Sodium Iodide	1.8
Sodium Polytungstate	3.1
Zinc Chloride	2.91
Sea Water	1.0

### 2.5.2. Filtration of particles separated from matrix

There is variability in the methods applied for the filtration of microplastics samples (Hidalgo-Ruz & Gutow 2012). Filtration of samples can be conducted either under normal pressure determined by gravity, or with the assistance of a vacuum pump (Rocha-Santos & Duarte 2015; Hidalgo-Ruz & Gutow 2012). Reports on filtration of particles indicate that approaches range from using a microsyringe filter holder that contains an 8 filter paper (Fendall & Sewell 2009), coffee filter papers (Chang 2015) and vacuum filtration (Karlsson et al. 2017; Kanhai et al. 2017; Hidalgo-Ruz & Gutow 2012). Research on the filtration of microplastics suggests that the different approaches used have their advantages and limitations. Vacuum filtration allows for a faster and more efficient filtration of samples (Zhang et al. 2016; Zhilin & Kjonaas 2013). In addition, the pressure from the pump can be adjusted to prevent the filter paper from ripping. However filter paper can get blocked largely because of the viscous characteristics of the matrix. It is hypothesised that particles separated from PCPs will block filter paper because of the viscous nature of the matrix. Toothpastes and facial scrubs are characterised by a viscous solution that will not flow through the filter paper. Therefore, an approach to remove the viscosity of the sample will be required, to allow for vacuum filtration of the particles. By contrast the conventional filtration method is rarely used in microplastics studies. This is because this approach is slower than vacuum filtration. This filtration method depends on the force of gravity to filter out samples, but filter papers can get blocked, because of the nature of the sample matrix. It is hypothesised that the viscous particles separated from PCPs will block filter paper.

Filter paper of different pore sizes (0.2 to 5  $\mu\text{m}$ ) and diameters (25 to 125 mm) have been explored for the filtration of microplastics (Maes et al. 2017; Crichton et al. 2017; Claessens et al., 2013; Hidalgo-Ruz & Gutow 2012; Frias et al., 2010).

Further sample preparation is required for particles that are difficult to filter. Centrifugation and digestion (acid, alkaline and enzymatic), have been used in microplastics studies (Karlsson et al. 2017; Cole et al. 2014). Centrifugation allows for the separation of particles from matrix, after which the top layer of the solution containing the particles can then filtered under vacuum (Rocha-Santos & Duarte 2015). Enzymatic digestion is carried out commonly on environment samples that

have a matrix characterised by organic matter. However, it is apparent that the application of this method is inconsistent and the application of some acids ( $H_2SO_4$ ) can damage the structural integrity of the particle (Cole et al. 2014).

The different approaches for sample preparation of microplastics are important and are the basis for further particle analysis. The analysis of particles is important to assess the characteristics of the particle and implication for risk assessment. However, it is apparent that the limitations and the challenges encountered with their application have not been discussed. In addition, it is hypothesised that the application of different techniques to characterise microplastics will produce the same results.

### 2.5.3. Characterisation of Microplastics

A fundamental concept which is generally misunderstood when it comes to measurements in particle size analysis and how it influences data from different particle size analysis techniques is that of what a particle is. Particles are characterised by differences in shapes, size and mode of dispersal in a matrix. This makes particle size analysis a complex science, but is made simple by understanding data derived and the interpretation of such data. What is the size of a particle? What single and unique number can describe a particle? The measurements that can be determined on a particle are endless (Figure 2.5) and are only restricted by the technique used.

The analysis of particles allows for the determination of size, number, morphology and polymer identity. It is reported that different techniques have been used for the characterisation of microplastics (Courtene-Jones et al. 2017; Shim et al. 2017; Hidalgo-Ruz & Gutow 2012). The analytical techniques commonly used for particle analysis are described in this section. With developments in technology, other techniques that are not currently in use can be applied for the analysis of microplastics. Therefore, some of the novel techniques will be described in this section.



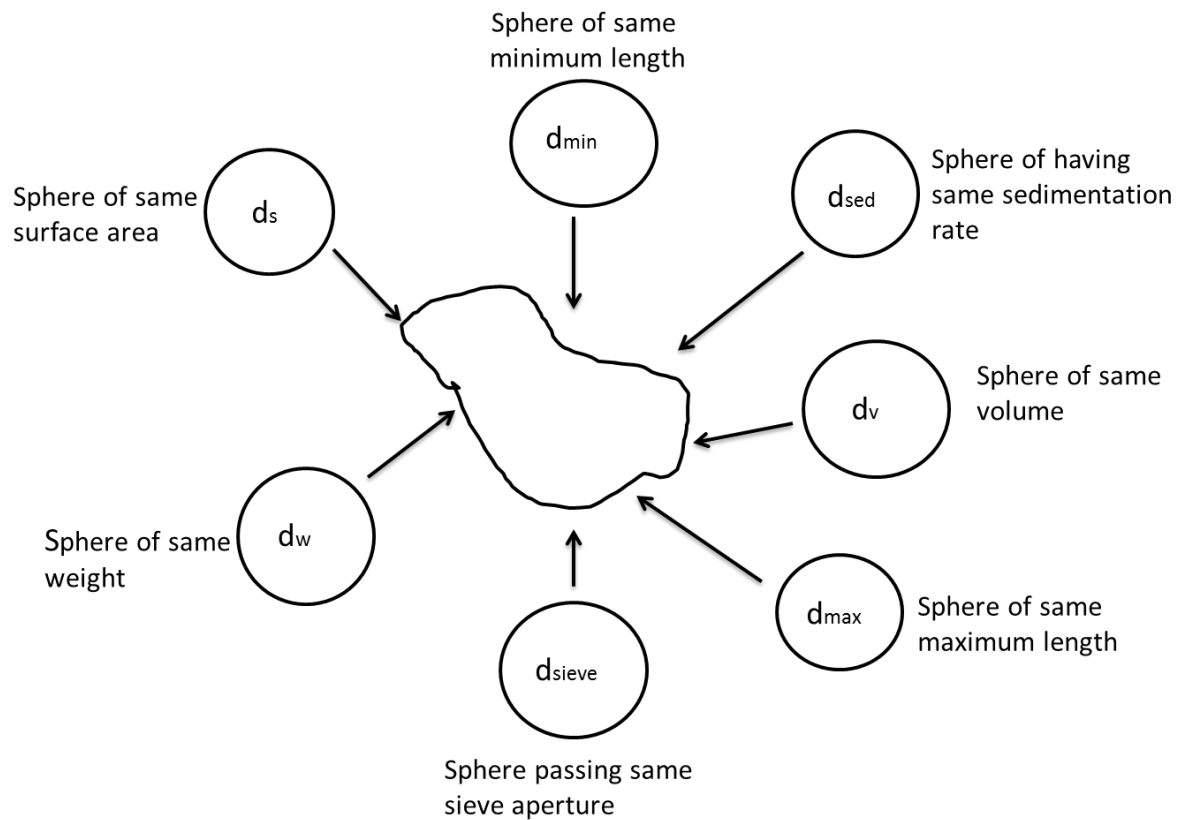


Figure 2.5. The different possible measurements that can determine size of a particle.

#### 2.5.4. Characterisation of particles using microscopy technique

The size, colour and physical identification of microplastics has been carried out by visual sorting with the aid of a microscope (Beaton-Green et al. 2016; Chang 2015; Hidalgo-Ruz & Gutow 2012; Fendall & Sewell 2009). With the microscopy technique, it is possible to view each particle and is relatively easy to detect particle aggregation (Rawle et al. 2003). The microscopy technique enables a 2D image of the particle to be viewed. Therefore for the analysis of particles, different physical properties of the particle can be measured (Malvern 2015). For example the Feret's diameter (**F**) which is the distance between two tangents on opposite sides a particle and parallel to a fixed dimension. In addition, the Martin diameter (**M**), is a size feature based on a line that cuts through the image of a particle (Sympatec GmbH 2017; Rawle et al. 2003). Drawn in any direction, lines drawn must be constant for all the measurements of the image (Figure 2.6). Furthermore, the longest dimension is a measured diameter equivalent to the maximum value of the Feret's diameter (Figure 2.6). The number of measurements that can be carried out with microscopy to determine particle size

highlights the difficulty in ascribing one unique number to describe particle size and distribution. Reports suggest different approaches to determine the size of microplastics using microscopy. In one report, the length of particles were measured (Fendall & Sewell 2009) and in another the diameter of the particles were determined (Chang 2015). It is not clear from the methods which of the physical properties of the particle were measured and why. In addition, different magnifications were used to determine particle size. Therefore, this suggests that particle size measurements will be different based on the physical properties of the particles measured and the magnifications used (Chang 2015; Fendall & Sewell 2009).

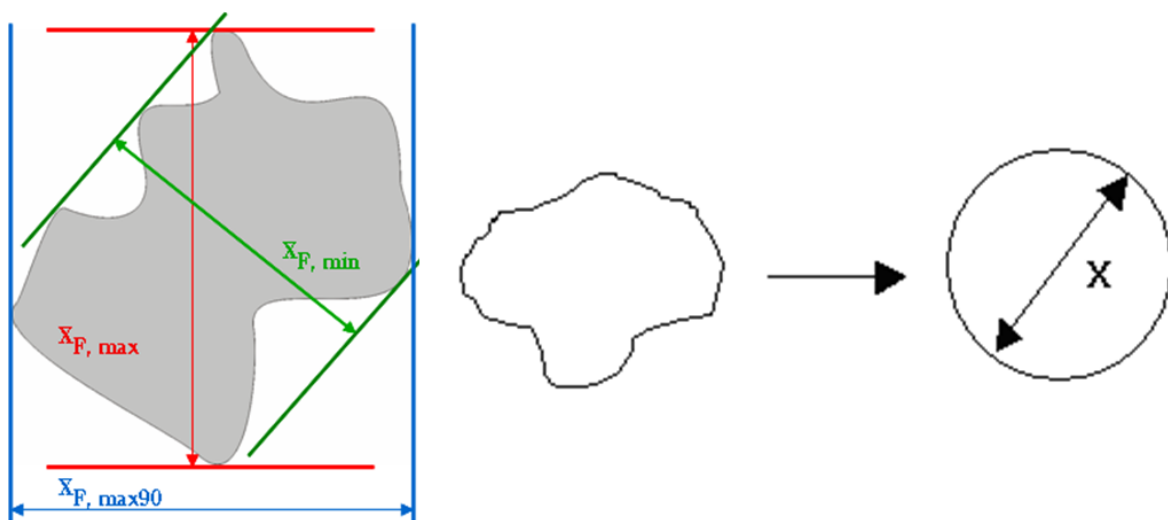


Figure 2.6 Measurement features used to determine particle size using the microscopy technique. (Source: (Sympatec GmbH 2017))

Direct imaging with microscopy is useful for the analysis of particles in a sample. The microscopy technique determines a number-weighted distribution based on equal weightings that are independent of the particle size (Rawle et al. 2003). Although microscopy is a simple technique to characterise microplastics, it is not possible to analyse a large number of samples because of the time it would take. Furthermore the question of “which dimension to measure?” arises because of the different measurement dimensions that are possible with a particle.

### *2.5.5. Determining the size of particles using laser diffraction technique*

Laser diffraction as an operational technology commonly used to determine particle size has been used widely in industry and has become the standard for quality control for where particle size is important (Baosupee et al. 2014). Laser diffraction is based on the premise that the angle of diffraction of a particle is inversely proportional to the size of the particle. Therefore as the angle of the laser beam increases, there is a decrease in particle size. The basis for laser diffraction technique is the interaction between light and particles. When a particle is struck by light, the light is either absorbed, reflected, refracted or diffracted (Malvern 2015). Diffracted and refracted light is useful for determining the size of a particle based on the intensity and angle of light that is scattered. The diffraction pattern can be measured and mapped to the distribution of particle size based on the Fraunhofer theory (Slotwinski et al. 2014). The theory assumes that particles are larger than the wavelength of light used; opaque, and do not transmit light, and, the different sizes of particles scatter light with the same efficiency (Malvern 2015). The advantage of the Fraunhofer theory is that knowledge of the optical property of the particle to be measured is not required (Rawle et al. 2003). Therefore the theory can be applied to samples that exhibit differences in particle type and shape. This suggests that microplastics that demonstrate different shapes and optical properties can be analysed by laser diffraction. Typically using the laser diffraction technique, the size of the particle is determined based on a volume of equivalent spherical diameter. Therefore, the particles analysed are assumed to have the same size as a sphere. This suggest that particles with different shapes and sizes can be measured using the laser diffraction technique.

Depending on the manufacturer, particles are circulated through the instrument by a carrier liquid, usually water. It is not clear whether microplastics that exhibit different densities will float or sink in the sample collection chamber. Particles such as polyethylene that exhibit a lower density to water will float at the surface of the sample collection chamber. Therefore, it would be difficult to determine the particle size of polyethylene. Measurements with laser diffraction require that particles are dispersed

in the instrument. However, it is possible that particles can form aggregates and therefore the results produced may be an artefact of particle agglomeration. This suggests that the results could be skewed towards larger sized particles.

In practice, laser diffraction technique has a wide measurement range, some of which cover 0.03 – 2500  $\mu\text{m}$  (CILAS 1180), it offers the ability to measure samples in both dry and liquid mode, and is a highly repeatable technique which ensures a high level of reliability. It is also a non-destructive and non-intrusive technique which maintains the integrity of the sample and allows for sample recovery. Particle size analysis is useful in determining size distributions of particles and can be explored in microplastics studies. Currently its application in microplastics studies is limited (Napper et al., 2015) and detailed information on the method used is unavailable (Napper et al., 2015). Particle size analysis offers an avenue to determine size distributions of microplastics in the environment and assess changes in size patterns over time, especially as more microplastics are introduced to the environment.

#### *2.5.6. Particle analysis by imaging flow cytometry*

In many biological and clinical science related research, flow cytometry has been explored to characterise cells (Lannigan & Erdbruegger 2017; Headland et al. 2014a). Flow cytometry provides a high magnitude quantitative measurement of scattered light including the emission properties assessed by fluorescence of a huge number at a rate of thousands of cells in a sample. The application of flow cytometry has been explored in science to examine differences in cell function, structure and abnormality, which aids diagnosis of human diseases (Grimwade et al. 2016; Pugsley & Kong 2013). Currently improvement in technology have resulted in the developments of advanced flow cytometry applications. One of such is the Amnis Imaging flow cytometer. The ImageStream is an advanced second generation imaging system, based on the same operating principles of a flow cytometer (Probst et al. 2017; Headland et al. 2014b). The ImageStream can produce up to 12 high resolution images of each particle in a sample, at the rate of about 1000 cells in a second, thus providing data in the shortest possible time (Basiji 2016; Headland et al. 2014a). Therefore the ImageStream is capable of differentiating particles in heterogeneous

samples which would be difficult using a conventional flow cytometer. This suggests that microplastics which exhibit differences in shape, size and number can be characterised using imaging flow cytometry.

The ImageStream boasts of an image gallery display area, where images of samples running through the instrument can be visualised (Lannigan & Erdbruegger 2017; Basiji 2016). This helps to monitor the flow of the samples through the instrument and to adjust parameters to suit the purpose of a study. Therefore, microplastics can be detected and differences in size and shape can be observed in the image gallery display area. The smallest particle that can be detected by the ImageStream is basically a function of side scatter profile of the particle. The limit of detection of particles is below 300 nm diameter through side scatter and 50 nm resolution for mixed populations (Amnis EMD Millipore 2018). The standard of the ImageStream is maintained by SpeedBeads in suspension, which is run constantly through the machine and is essential for the calibration of the instrument. The detailed calibration process that uses images of the SpeedBeads to safeguard accurate functioning of the system, based on factory settings (Amnis Cooperation, 2016). The ability of the ImageStream to quantitate morphology, its high sensitivity the high information content produced for each cell, are some of the characteristics that makes it novel (Headland et al., 2014; Amnis Cooperation, 2016; Basiji, 2016).

In the light of microplastics research, the advancement of basic flow cytometry can be explored for characterisation. The high speed of the ImageStream allows for the imaging and analysis of large heterogeneous populations of particles for a statistically valid data. However, the Amnis ImageStream has a cut-off restriction at 70  $\mu\text{m}$ . It is apparent that the Imagestream exhibits the narrowest pathway of 250  $\mu\text{m}$ , therefore to prevent the syringe pumps in the instrument from clogging, samples are filtered through a 70  $\mu\text{m}$  filter (Amnis 2018). This suggests that microplastics <250  $\mu\text{m}$  can be characterised using the Imagestream. It is apparent that particles which have potential environmental impacts due to the large surface area to volume ratio, can be studied in detail. Currently there is no report on the application of imaging flow cytometry technique for the analysis of microplastics. Therefore this is the first report on the analysis of microplastics with the imaging flow cytometry technique.

## 2.6. Comparing Techniques for Microplastics Characterisation

Characterisation of microplastics with different techniques raises questions about the differences and similarities of data produced. It is apparent that each technique will produce a different result because of the different measurement principles of the techniques. For example, direct imaging with the conventional light microscopy technique, the size of the particle is based on the physical property of the particle that is measured. In addition, the microscopy allows for the analysis of the particles at different magnifications. This allows for the analysis of smaller sized particles that cannot be detected at a lower magnification. However, at a higher magnification it is apparent that larger particles may not be detected. This suggests that the size, number and morphology of microplastics can be determined by microscopy. Furthermore, depending on the field of view of the magnification, smaller sized microplastics can be analysed. By comparison, the laser diffraction technique determines particle size based on the assumption that all particles have an equivalent volume to a sphere. This technique uses the volume of the particles to determine the size distribution. Depending on the instrument, the laser diffraction technique can detect particles between 0.04 – 2500  $\mu\text{m}$  (CILAS 2016). Therefore the laser diffraction technique measures a wider particle size range than the microscopy technique. This suggests that microplastics at the lower and upper micron size class that cannot be analysed with microscopy can be analysed by the laser diffraction technique. However, it is apparent that the imaging flow cytometry technique analyses particles based on a <70  $\mu\text{m}$  cut-off. Therefore compared with the other analytical techniques, it is clear that imaging flow cytometry can determine the smallest particle size range. In addition, the technique is equipped with an automated software that allows for the analysis of particles in the sample.

## 2.7. Identification of Particles using Spectroscopy.

The application of techniques for the identification of microplastics should further improve our understanding of microplastics in the environment. One of such methods is the application of infrared spectroscopy (IR). This method has been applied in the identification of different types of organic and inorganic matter; determining the

functional groups in compounds and has been applied in the identification of polymers and plastics (Crichton et al. 2017; Tagg et al. 2015). In infrared spectroscopy, the identification of compounds is based on the principle of absorption of infrared radiation by the molecules of the compound. This absorption causes vibrations of the molecules and is expressed as an infrared spectrum, unique to the compound (Ng and Obbard, 2006; Harrison et al. 2012; Lusher et al., 2013; Tagg et al. 2015).

Most organic molecules absorb infrared light at particular frequencies as a result of their covalent bonds. This unique property confers the characteristic of that molecule. When more molecules of a sample form a bond and absorb infrared light, it gives an indication of the structure and thus identity of the sample. This is made evident by the functional groups present in the molecule (Figure 2.7) (Tagg et al. 2015; Harrison et al. 2012). When infrared light is passed through a sample, covalent bonds absorb the light and are indicated as peaks on the infrared spectrum. The polyethylene reference shows the stretching, bending and rocking of the CH<sub>2</sub> functional group at 2914, 2846, 1474 and 720 cm<sup>-1</sup> (Figure 9).

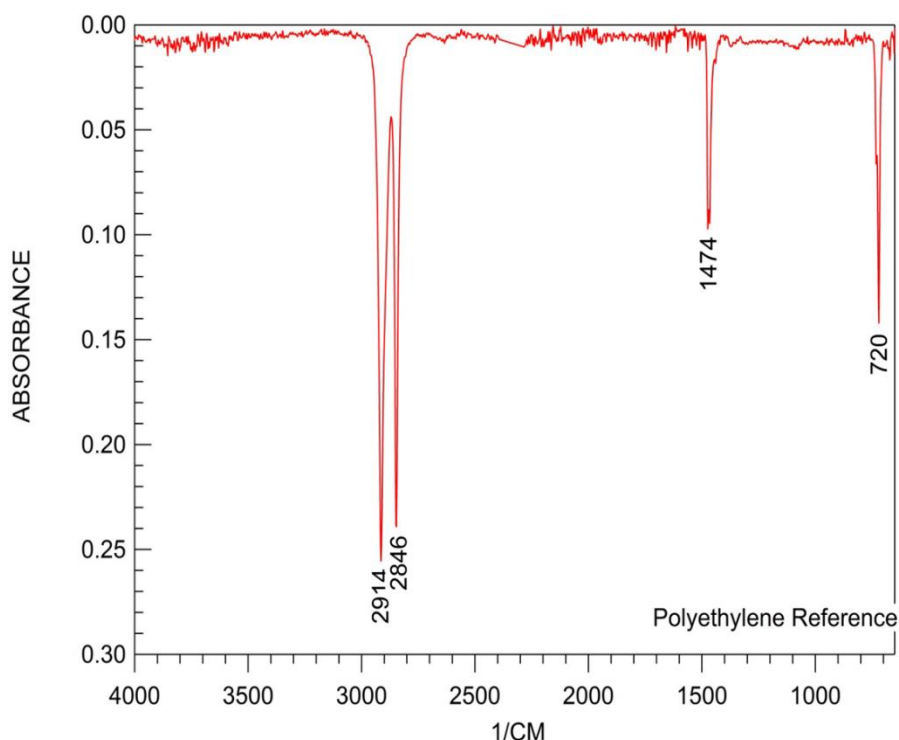


*Figure 2.7. FT-IR spectrum of Polyethylene showing the absorbance peaks indicative of the polymer*

The Fourier transform infrared spectroscopy (FT-IR) technique has been used in studies on polymer identification and characterisation (Tagg et al. 2015), and in the field of medicine as a mapping tool in cancer research (Minnes et al. 2017; Thumanu et al. 2014) and bone structure studies (Koletsi et al. 2016; Sroka-Bartnicka et al. 2015). FT-IR has been used in laboratory analysis for the detection of microplastics in water and sediment samples (Ziajahromi et al. 2017b; Karlsson et al. 2017; Tagg et al. 2015).

## CHAPTER 3: METHODS AND MATERIALS USED FOR THE CHARACTERISATION OF MICROPLASTIC PARTICLES.

### 3.1. Particles selected as the focus of study

Particles of polyethylene were selected as the focus for this thesis because they are used as ingredients in toothpastes and facial scrubs commonly sold in stores nationwide. In addition, particles abraded from kitchen scourers were also selected for this study. This is because the abrasion of kitchen scourers during use may be a source of secondary microplastics. The packaging on the kitchen scourers did not make reference to the composition of the product as was the case with the personal care products.

### 3.2. Personal care products selected for the characterisation of particles

Two types of PCPs were chosen for this study, toothpastes and facial scrubs. According to the labelling all products contained polyethylene. The toothpastes selected were Colgate “Max White One Luminous” (TP1) and “Advanced White Go Pure” (TP2). The two facial scrubs were Palmolive, “Clean and Clear Morning Energy Skin Energising Daily” (FS1) and “Blackhead Clearing Oil Free Daily” (FS2). The size distribution of the polyethylene microplastics in personal care products was characterised using the two pathways outlined in Figure 3.1. In pathway 1, particle size distribution was determined by laser diffraction using a CILAS 1180 particle size



analyser; direct imaging, particle size and quantification was determined by microscopy with each sample analysed in triplicate, at each stage. In the independent second pathway, imaging flow cytometry with an Amnis ImageStream Mark II (Merck Millipore) was used, which generated a size distribution and number of particles, but incorporated a 70 µm filter, eliminating larger particles from the analysis. For this pathway, each sample was analysed in duplicate.

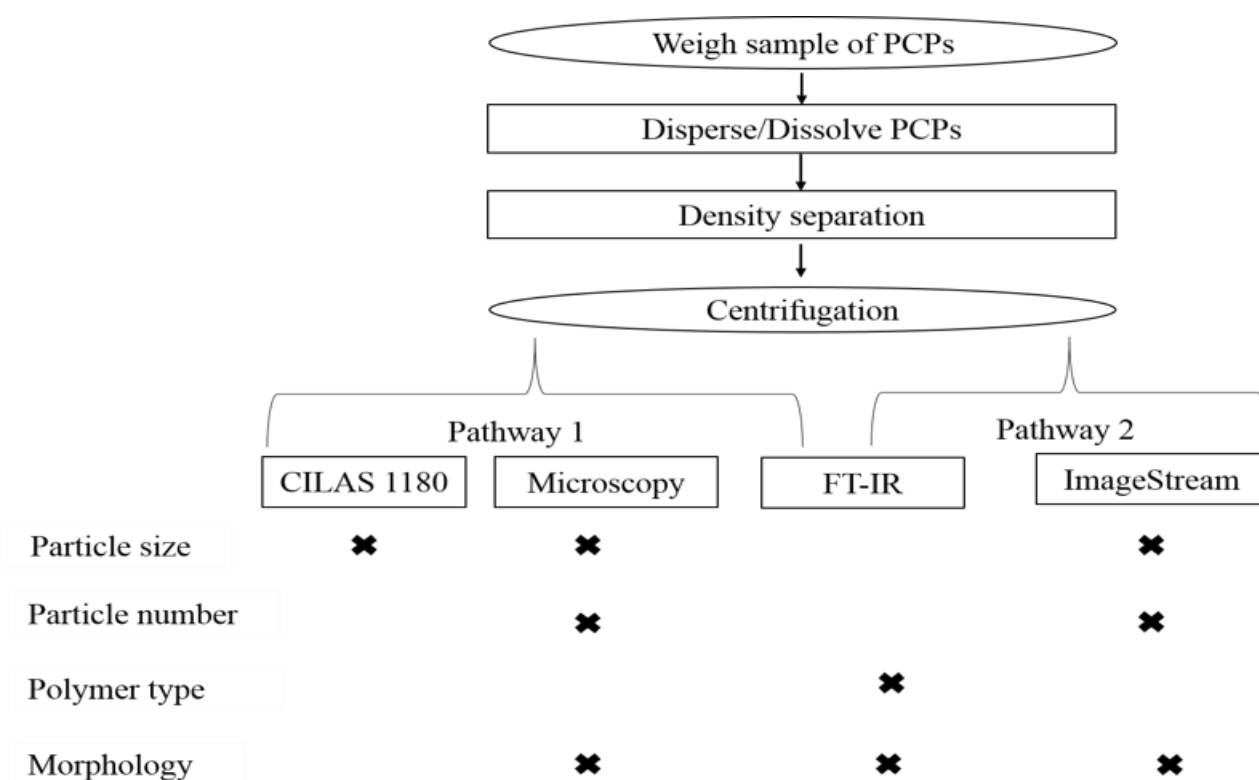


Figure 3.1. Schematic diagram of the approach used to characterise microplastics in personal care products. The diagram shows the two pathways used for particle characterisation.

### 3.3. Separation of particles from personal care products

The approach to density separation described here was based on previous studies, with minor modifications. For all samples, 0.5 g wet weight of each product was accurately weighed on an analytical balance (Sartorius 1702), and was subsequently dispersed in 1 ml of water at 50-60°C. To achieve density separation, 50 ml of sodium chloride solution (140g/ L<sup>-1</sup>) at 50-60°C was then added to the dispersion in a 200 mL

glass beaker. The resulting solution was mixed for 7 min with a glass rod, and left to settle for 5 min. The microplastic (polyethylene) particles (now floating on the surface) were collected by decanting 15 ml into a clean glass beaker. Not all particles floated to the surface, possibly due to the matrix characterised by a viscous solution. Therefore, the density separation process was repeated by adding another 50 ml of salt solution to the residual ~35 ml to ensure complete extraction of the microplastics. Another 15 mL was decanted from the second solution. This density separation resulted in an approximate volume of 30 ml sodium chloride solution with the suspended microplastics on the surface. The volume of this solution was then reduced by pipetting 15 ml of sodium chloride solution from the bottom of the beaker (Harrison et al. 2012). At this stage, the extract was cloudy, due to the viscous nature of the sample solution. To facilitate removal of plastics from the remaining matrix components, a centrifugation step was introduced.

The residual 15 ml volume was completely transferred to a 50 ml centrifuge tube, and the after which 30 ml of the hot sodium chloride solution and 5 ml of sodium pyrophosphate solution (10%, room temperature) were added. The sodium pyrophosphate was used as a dispersant to prevent the microplastics from clumping together. Centrifugation was carried out at 1700 × g, after which the top layer of the solution (around 10 ml) containing microplastics was decanted into a clean 50 ml beaker.

### 3.4. Characterisation of microplastic particles

#### 3.4.1 Characterisation by direct imaging using light microscopy.

Samples were first analysed with the laser diffraction technique using the CILAS 1180, to have a general idea of the particle size distribution. Following this, the particles were flushed out of the instrument and samples were collected in four 1 L beakers. The four 1 L samples collected from the CILAS 1180 were transferred onto a 1.2 µm GF/C filter (Whatman, UK) under vacuum and then washed off with 30 mL of ultrapure water into a 50 mL beaker. Pipetting from the bottom, the water containing microplastics was then reduced to a volume of 10 mL on the line of the beaker. The

suspension was then agitated, and a 1 ml aliquot was transferred to a Sedgewick Rafter cell (SRC) etched with a 50 column by 20 row grid. Size and particle count measurements were determined at 100X and 200X magnifications with an Olympus BX 51 calibrated eyepiece binocular microscope with QCapture Pro 5.1 imaging software. For each product, three replicates of 0.5 g wet weight were used and the longest length of the first 100 particles in 6 randomly selected transects were measured. To determine particle size distribution, 300 particles from each sample were measured. The lengths were manually determined with an ocular calibrated micrometer and then the values were converted to microns. Statistical analysis was conducted using R programming language. An analysis of variance (two-sample assuming unequal variance) and a post-hoc t-Test was used to establish whether statistical differences in size occurred between the PCPs. An estimate of the mean number of particles in each product was determined by counting all particles in 6 randomly selected transects of the SRC, using a mechanical counter (VWR Mechanical counter, four figures, 0 - 9999). A rough estimate of 900 particles were counted in 6 transects of the SRC.

#### 3.4.2 Particle size analysis by laser diffraction.

Following centrifugation, particle size analysis was undertaken using a CILAS 1180 (Quantachrome, UK), with an operational range of 0.04 to 2,500  $\mu\text{m}$ . This involved running background scans to ensure a consistent low count level was reached between sample runs. The extracted microplastics were transferred from the 50 ml beaker and washed into the sample holding tank of the CILAS 1180 with high purity, 18M $\Omega$ , water (MilliQ, Millipore, UK). Subsequently, a further 30 ml of 10% sodium pyrophosphate solution was added to further aid particle dispersion after which measurements for size distribution of the microplastics in each product were conducted. Results were collated by the Size Expert software and the retrieved data were subsequently analysed using Microsoft Excel.

Initial work with particle size analysis showed that particles were retained in the feeder tank, resulting in a smaller particle size range than anticipated from parallel microscopy work. In order to investigate this issue, methanol was added to the tank

(10% in high purity water) to lower the density of the carrier liquid. Dispersants are widely used in geology and particle-size science for separation of particles. Agents such as anionic dyes, sodium dodecyl sulphate and sodium pyrophosphate act to overcome attractive forces by strengthening the repulsive forces to achieve particle separation and dispersal (Silva et al. 2015; Fedotova et al. 2015; Tinke et al. 2009). It has been suggested that sodium pyrophosphate inhibits bond formations between particles and does not damage the integrity of the particle (Silva et al. 2015; Sehly et al. 2015). Therefore sodium pyrophosphate was added before centrifugation and to the tank of the CILAS particle size analyser to aid dispersal of particles. This allowed for the analysis of a larger particle size range which was not previously possible.

### 3.4.3 Imaging flow cytometry.

For the second pathway, following density separation and centrifugation, 10 mL of the microplastic extract was transferred to a 50 ml beaker and agitated. Using a micropipette 1 mL of the agitated sample was transferred to a 1.5 mL microcentrifuge tube and data was acquired with the Amnis ImageStream®<sup>x</sup> Mark II (Merck Millipore) using Inspire™ software. For all samples, particles were filtered with a 70 µm sterile cell strainer (Fisherbrand™). For each sample, microplastics were determined with a 70 µm cut-off filter and image capture was conducted with a 20x objective with a 120 µm field of view using brightfield and 488nm laser set at 100 mW. To ensure only particles in the sample were captured, the calibration speedbeads were turned off (based on manufacturers' advice). Image acquisition was defined using the brightfield channel with data collection parameters of either 10,000 particles in focus or a 10 minute maximum acquisition time, whichever occurred first.

IDEAS® version 6.2.65.0 software was used to analyse the microplastics data. The initial step gated for single particles which defined via brightfield area versus aspect ratio (minor axis divided by major axis). In addition, particles that were in focus were analysed using the gradient root mean square (RMS) function. Using the gated single event in the "in focus" population, a histogram of aspect ratio vs normalised frequency was plotted to identify elongated and circular particles. Finally, the diameter feature;

which provides the diameter of the circle that has the same area of the object, was used to determine the size distribution for all particles.

#### 3.4.4 Polymer identification.

Following microscopy, microplastics were washed from the Sedgewick rafter cell with Milli-Q water into 50 mL glass beakers and again vacuum filtered (1.2  $\mu\text{m}$  GF/C). Polymer identification was conducted using molecular mapping through reflectance  $\mu$ -FTIR with a Perkin Elmer Spotlight Imaging FTIR microscope Model (Perkin-Elmer, UK) analyses at the mid-IR range of between 700 and 4,000  $\text{cm}^{-1}$ . Utilising the focal plane array (FPA) method, the spectral results were based on reflectance in imaging mode with 2 co-added scans per pixel, an aperture size of 25  $\mu\text{m}^2$  and at a spectral resolution of 16  $\text{cm}^{-1}$ . This method of spectra acquisition provided information about the identification of a polymer within minutes (Ojeda et al. 2015; Claessens 2013). Spectra of polyethylene was confirmed using a spectrum search in a customised polymer library that contained the spectra of polymers commonly associated with microplastics. In addition, the functional groups detected in the regions of absorbance were cross referenced with a table showing the FT-IR peaks characteristic for the polymer type.

### 3.5. Choice of kitchen scourers to be used for the analysis of particles

For this thesis, five kitchen scourers were selected for the study. These included “two market leading” and three chain store brands. The brands were “Spontex heavy duty” (KS1), “Tesco Everyday Value” (KS2), “Tesco non scratch sponge scourer” (KS3), “Spontex strong and long lasting” (KS4) and “Tesco sponge scourer” (KS5). The same analysis pathways used for the characterisation of particles from personal care products was adopted for the analysis of particles abraded from kitchen scourers. Particles abraded from the kitchen scourers were characterised in triplicates at each stage and were based on size distribution, number of particles produced, particle morphology and identity. In summary the number and morphology of particles were determined by direct imaging using a light microscope; particle size distribution was

determined by laser diffraction using a CILAS 1180 particle size analyser. Particles in the sub-70 $\mu\text{m}$  fraction were characterised and their size, number and morphology by imaging flow cytometry; and particle polymer identity was determined using micro-Fourier Transform infrared spectroscopy  $\mu\text{-FTIR}$ .

### 3.6. Abrasion of particles from kitchen scourers

An 800 mL glass tank was washed thoroughly and rinsed with Milli-Q water before being filled with 500 mL of Milli-Q. A 300 mL ceramic bowl was wet by dipping in the 800 mL tank. Particles were abraded from each kitchen scourer by wetting with water provided in the 800 mL glass tank. Water from the scourers was squeezed into the ceramic bowl. The ceramic bowl was washed for 20 seconds, and the scourer was squeezed again and placed on foil paper provided. The “wet, squeeze, wash and squeeze” process was equivalent to one wash cycle. The entire ceramic bowl was rinsed with 200 mL of Milli-Q water and collected in a 1 L glass tank. The ceramic bowl was placed on aluminium foil. This procedure was repeated with all types of kitchen scourers. The 200 mL of Milli-Q water used to rinse the ceramic bowl was vacuum filtered through a glass microfiber filter (Whatman GFC 1.2  $\mu\text{m}$ ). The filter was then flushed with Milli-Q water into a 50 mL glass beaker. After allowing settling for 5 minutes, the solution was volume reduced to 40 mL using a pipette. Particles in some scourers floated to the surface and particles in other products sank to the bottom of the 50 mL glass beaker. Therefore, the solution with floating particles was volume reduced by pipetting from the bottom of the 50 mL beaker. By contrast, the sample with particles at the bottom of the 50 mL beaker was volume reduced by pipetting from the surface of the solution. This final solution was mixed with a 5 mL pipette, from which 5 mL was used for microscopy. However, because of the concentration of particles, 1 mL from the 5 mL microscopy solution was diluted with 9 mL of Milli-Q water. For the laser diffraction analysis, 10 mL of the sample was used, 5 mL for imaging flow cytometry and the final 10 mL was vacuum filtered again for  $\mu\text{-FTIR}$  analysis.

### 3.7. Characterisation of particles abraded from kitchen scourers

The techniques that were used for the characterisation of particles separated from personal care products were applied for the analysis of particles abraded from kitchen scourers with some modifications. Therefore, characterisation of all particles was determined using microscopy, laser diffraction, imaging flow cytometry and Fourier transform infrared spectroscopy.

#### 3.7.1 Analysis of particles abraded from kitchen scourers by light microscopy.

The suspension of particles was agitated, and an aliquot (1 mL) was transferred to a Sedgewick Rafter cell (SRC) etched with a 50 column by 20 row grid. Size and particle count measurements were determined at magnifications of 100X and 200X, with an Olympus BX 51 calibrated eyepiece binocular microscope with QCapture Pro 5.1 imaging software. For each product, the longest length of the first 100 particles in 6 randomly selected transects were measured and conducted in three replicates. The lengths were determined in ocular units and then converted to microns. A statistical analysis of the results was conducted using the programming language R, and the statistical component of Microsoft excel. The descriptive statistics for particle measurements was determined for all products using Microsoft excel. An analysis of variance (two-sample assuming unequal variance) and a post-hoc t-Test was determined using the R programming language, to establish statistical differences in size and number existed between the kitchen scourers.

To determine the estimate for the number of particles abraded from kitchen scourers, a mechanical counter (VWR Mechanical counter, four figures, 0 - 9999) was used to count all particles in 6 randomly selected transects of the SRC were counted and the value was multiplied by the total number of transects to attain the microplastics count in 1 mL of the kitchen scourer solution. Furthermore this value was multiplied by the dilution factor to get the original number of particles and scaled up to determine the number of particles in one wash cycle.

### 3.7.2 Analysis of particle size distribution using laser diffraction.

The analysis of particles did not require a centrifugation step because unlike the personal care products, these products did not exhibit any viscous components. Therefore, particle size analysis was conducted using a CILAS 1180 (Quantachrome, UK), characterised with a measurement range of 0.04 to 2,500  $\mu\text{m}$ .

After background scans for the particle size analyser (CILAS 1180) were taken, particles abraded from kitchen scourers were transferred from the 50 mL beaker into the CILAS 1180 sample collection tank containing high purity 18M $\Omega$  water (MilliQ, Millipore, UK). Following this 30 ml of sodium pyrophosphate (10%) solution was added to the CILAS 1180 sample collection tank, to aid dispersion. Methanol (10% in high purity water) was added to the tank to lower the density of the carrier liquid. Particles with a lower or similar density to water floated to the surface of the sample holding tank, and therefore methanol was added to the carrier liquid. But by contrast, methanol was not added to the carrier liquid for particles that exhibited a higher density to the carrier liquid. Subsequently, measurements for size distribution of particles abraded from the kitchen scourers were conducted. The results for the analysis of particles were collated by the Size Expert software and subsequently analysed using the statistical component of the Microsoft excel software. A cumulative frequency distribution for the size of particles abraded from kitchen scourers was determined using Microsoft excel software. After each analysis, samples were flushed out and collected as described in section 4.4.

### 3.7.3 Particle analysis by imaging flow cytometry.

The second pathway for the characterisation of particles abraded from kitchen scourers was determined using the imaging flow cytometry technique. 1 mL from the 5 mL solution was agitated and transferred to a 1.5 mL micro centrifuge tube and analysed with the Amnis FlowSight Imaging Flow Cytometer. The instrument settings used for the analysis of particles separated from personal care products were adopted for the characterisation of particles abraded from kitchen scourers. In addition the



results were analysed as described in section 4.4, using the IDEAS software version 6.2.65.0.

#### *3.7.4 Polymer identification of particles abraded from kitchen scourers.*

The analysis of all particles abraded was determined using the methods developed for the polymer identification of particles separated from personal care products.

### 3.8 Quality control to avoid contamination and loss of samples.

Steps were taken during the sample preparation process and during the analysis of particles separated and abraded from the selected products.

#### 3.8.1 Sample preparation

- For all experiments, cotton lab coats and laboratory gloves were worn at all times.
- For the abrasion of particles from kitchen scourers, a timer was used to monitor wash times.
- A control run was set up by extracting 1.5 L of Milli-Q water onto a filter paper to ensure non contamination in the study.
- During sample preparation and analysis, two blank 25 mm GFC filter papers with a 1.2  $\mu\text{m}$  pore were placed close to the set-up. The filter papers were viewed under the microscope and checked for particles of Debris.
- During vacuum filtration, a laboratory bottle with Milli-Q water was be used to wash the walls of all glass reservoirs onto the filter paper, to remove remnant particles. All containers were rinsed this way.
- To prevent cross contamination between each wash, the vacuum funnel and filter membrane was washed with 500 ml of Milli-Q water and reassembled for the next wash. In addition, the ceramic roaster and soup bowl was thoroughly

washed with 500 ml of Milli-Q water and placed on clean aluminium foil that will be provided.

### 3.8.2. Analysis of particles

- For the techniques used for the analysis of particles, different approaches were taken for quality control. Therefore for the microscopy technique blank water samples (laboratory grade water run alongside samples) were analysed to detect particles of debris.
- Using the laser diffraction technique, after each analysis, the sample was discharged from the particle size analyser and collected into four 1 L glass beakers during the washing cycle. To ensure complete recovery of microplastics from the instrument, three background scans were run (after four repeated flushes of the instrument) and were compared to the initial background scans, based on manufacturer's recommendations.
- For the imaging flow cytometry, filter sterilised water was run on the system between samples to prevent cross-contamination.
- Using the micro-FT-IR, to avoid contamination, filter papers were placed in glass Petri dishes with a pair of forceps and stored in a desiccator at room temperature until fully dry (Harrison et al. 2012).

## CHAPTER 4. RESULTS: Challenges encountered in method development and final approaches for the characterisation of particles.

In this section the challenges encountered in sample preparation and analysis of particles in all products is presented. In addition, the analysis of the particles is categorised according to the size, number, morphology and polymer identity. Furthermore the difficulties encountered in the application of the different characterisation techniques are also presented in this section.

### *4.1. Density separation of particles from personal care products.*

An initial approach to extract microplastics from the facial scrubs and toothpastes, three replicates of 0.5g of each product was added to 25 ml of hot water (70°C) in the barrel of a 30 ml glass syringe with Luer lock fitting. The syringe was attached to a polycarbonate 25 mm microsyringe filter holder containing a 25 mm nitrocellulose membrane filter with a pore size of 1.2  $\mu\text{m}$ . Thereafter, to achieve a homogenous solution, the syringe was shaken for about 2 mins. However, it was difficult to separate particles from the products using the glass syringe attached to the membrane filter. This is because the solution flooded the microsyringe filter holder chamber. Furthermore, there was a back flow of the solution, likely due to the clogging of the nitrocellulose membrane filter because of the formation of particle aggregates. Therefore further characterisation of the particles in all the products could not be conducted. Consequently, an alternative method to separate particles from the products was explored.

Using another approach to separate particles from the products, 1 mL of laboratory grade water (MilliQ) was added to the 0.5g of each product to get the particles into solution. Following this, density separation using a saline solution was explored to separate particles from all products. This was achieved by adding 50 mL of sodium chloride solution (140g L<sup>-1</sup>) at 50 - 60 °C, to each weighed product. The solution was mixed for 7 min, left to settle for 5 min and the resulting microplastic particles floating on the surface were poured into a 50 mL beaker. The density separation process was repeated one more time to ensure the separation of all particles from the products. Although the density separation of particles was achieved, it was difficult to collect the

particles during the filtration process. In this study, a vacuum filtration process was explored to filter out the solution and collect the particles separated. However, filtration of the particles was difficult to achieve, because the particles clogged the surface of the 47 mm glass microfiber filter paper with a pore size of 1.2  $\mu\text{m}$  (GFC). It is likely that the products contained other additives which made the solution sticky and viscous, therefore reducing the flow and increasing the likelihood of clogging. To increase the flow of the solution, small volumes of the solution were introduced slowly and at intervals, to the filter cup. Consequently, between 1 – 5 mL of the solution were introduced to the filter cup at intervals of between 10 – 20 seconds. However, this procedure was still not efficient because the glass microfiber filter paper became clogged and the filtration of the particles was not successful. It is likely that the sticky and viscous additives in the solution did not allow for the successful filtration of the particles in all products.

To overcome the clogging of the glass microfiber, the sticky viscous additives had to be removed. Therefore a further separation procedure was introduced after the density separation step. As such, after the separation of the particles from all products, the solutions were left to stand for 5 minutes after which the particles floating on the surface were carefully poured into a 50 mL beaker. The density separation process was repeated one more time to ensure all particles of interest were separated from the solution. Subsequently, a sterile cell strainer (Fisherbrand 40  $\mu\text{m}$  pore size) was introduced as an additional step for the filtration of particles. To filter the particles and reduce the sticky and viscous additives, a pair of forceps was used to hold the sterile cell strainer and placed it under the running ultra-pure Milli-Q water for 1 minute. There were differences in the viscosity across all the products analysed. In particular, the toothpastes were more viscous than the facial scrubs. Although this filtration procedure allowed for the reduction of the viscous additive in the solution, it was not completely removed. This was apparent because when the sample was viewed under a microscope, a cloudy image was observed, and this was likely because of the viscous additives. Furthermore, it was observed that when the particles in the sterile cell strainer were washed with running ultra-pure Milli-Q water for longer than 1 minute, the particles formed aggregates, therefore making particle characterisation difficult.

Therefore the filtration approach was abandoned and centrifugation was attempted to separate the particles from the viscous solution. The centrifugation process was carried out at 4000 rpm/4 min, after which the top layer of the solution containing microplastics was decanted into a clean 50 ml beaker. The centrifugation process ensured complete separation of the target particles from the viscous solution, and reduced the agglomeration of the particles.

#### 4.2. Assessment of the size of particles using different techniques.

Challenges were encountered in the preliminary work undertaken to determine particle size distribution. This was true for all the particle sizing methods however, the challenges encountered were unique to each technique. As such the preliminary results indicated that although size measurements were determined, the application of the different techniques could be improved. Therefore technique specific solutions were applied to resolve the challenges encountered.

##### *4.2.1 Analysis of particle size distribution by laser diffraction.*

In this section the challenges encountered during the analysis of particles using laser diffraction are presented. It was clear that two challenges encountered limited the measurements of the size of particles in all four products. .

The first challenge was the agglomeration of particles, as observed in the sample collection chamber. Particles in TP1, TP2 and FS1 formed aggregates more readily than the particles in FS2. As such, these aggregates observed in the sample collection chamber were not evenly dispersed and reliable particle size measurements could not be determined. The cumulative distribution graph shows that there were differences in the particle size range across all products analysed. The particle size distribution in TP1, TP2 and FS1, was relatively narrow, whereas FS2 had a wider distribution (Figure 4.1). In particular, TP1 indicated particle size distribution ranged from 1 – 120  $\mu\text{m}$ , and TP2 and FS1 exhibited a particle size distribution from 1 – 100  $\mu\text{m}$ . By contrast, particles in FS2 exhibited a distribution of 1 – 600  $\mu\text{m}$  (Figure 4.1).

Observations of all the particles indicated that FS2 exhibited particles that were different from particles in other products. In particular, the particles in FS2 appeared more spherical and were more than the particles in the other products (something proved by the microscopy and imaging flow cytometry techniques). Therefore the wider particle size distribution exhibited by particles in FS2 is likely because of the higher number of particles, which were readily detected by the instrument's lasers.

Although the smallest particle size distribution for all products was not obvious from the cumulative size distribution graph, data from the instrument indicated that the smallest particles were exhibited in TP2 with a size of 0.04  $\mu\text{m}$ . In addition, the smallest particles in the other products were 0.4, 0.1 and 0.4  $\mu\text{m}$ , as demonstrated in TP1, FS1 and FS2 (Table 4.1). Furthermore, the distribution exhibited cut-offs that were different in all products, but the first cut-offs were between 10 and 40  $\mu\text{m}$  in TP1 and TP2, and between 10 and 70  $\mu\text{m}$  in FS1 and FS2 respectively (Figure 10).

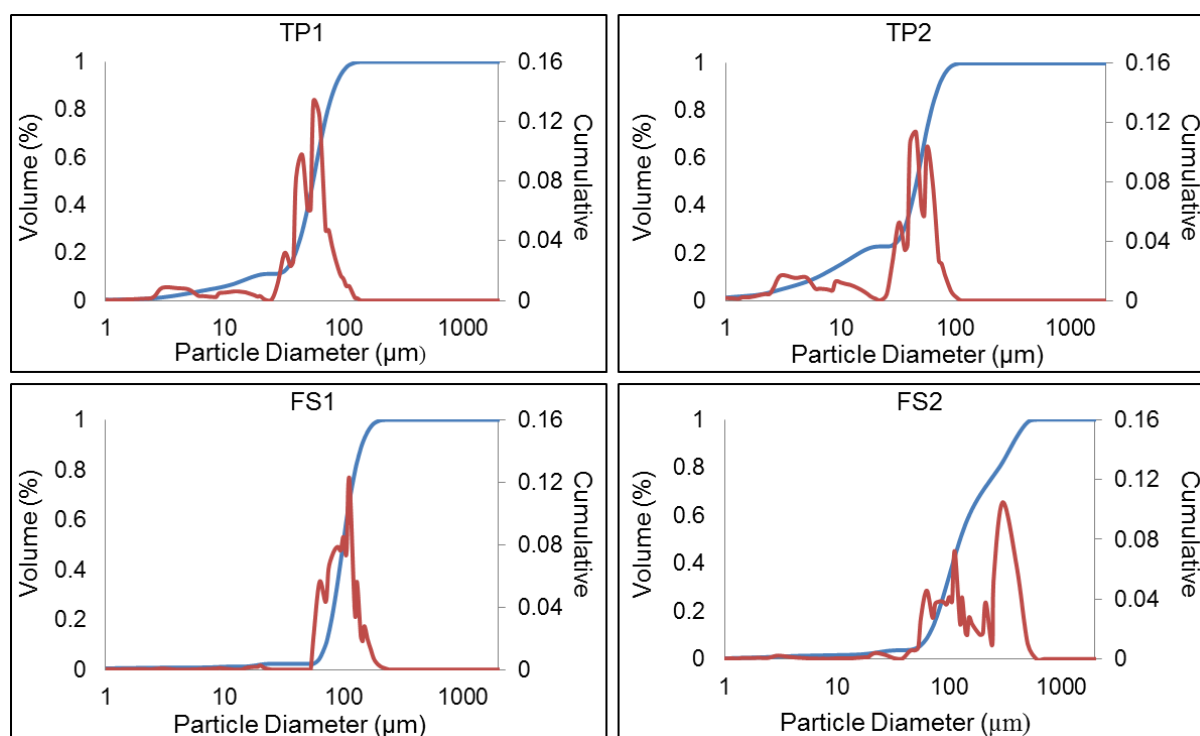


*Figure 4.1. Particle size distribution of microplastic particles extracted from personal care products analysed using a CILAS 1180 particle size analyser. Cumulative graph showing microplastics size distribution in each brand of personal care product.*

Generally D10, D50 and D90 are commonly used to describe the 10, 50 and 90% intercepts of the cumulative mass. Typically, D10 and D90 describe the range of the

particle size distribution whilst D50 describes the value where half of the particle population exists above and below this value. The analysis of diameter 'D' values indicated differences in the sizes across all four products analysed. For easier understanding of the texture of the particles based on the different sizes, a soil classification system which categorises particles and predicts their likely behaviour in the environment has been used as a reference. The texture of the particles ranged from silt like to medium particles (Table 4.1). However, there were differences in the texture of particles measured at the same D value. For example, TP1, TP2 and FS2 exhibited silt-like particles but by contrast the D10 value in FS1 indicated a larger size and exhibited very fine-like particles (Table 3). The analysis of D50 values also indicated differences in the size of particles across all the products analysed. For example, the D50 measurements indicated that particles in TP1 and FS1 exhibited very fine like particles. However, the D50 measurements values in TP2 indicated the smallest values for all the products, and exhibited very fine-like particles. By contrast the D50 values in FS2 exhibited the largest particles and indicated the occurrence of fine-like particles (Table 4.1). Measurements to determine D90 values also showed differences for all the products analysed and demonstrated differences in the particle texture. For example TP1 and TP2 showed that the D90 values were characterised by very fine-like particles. By contrast however, the particles in FS1 and FS2 exhibited larger D90 values that indicated fine and medium-like particle textures respectively (Table 4.1). The differences in the size of particles were not only observed in the D value measurements. The mean size of particles was different across all the products analysed. For example, TP1 and TP2 exhibited mean particle sizes characterised by very fine and silt-like particles. By contrast however, the mean particle size for the facial scrubs exhibited similar particle texture and were characterised by fine-like particles (Table 4.1).

*Table 4.1. Diameter values of particles in personal care products.*

Product	D10 % ( $\mu\text{m}$ )	D50% ( $\mu\text{m}$ )	D90% ( $\mu\text{m}$ )	Mean ( $\mu\text{m}$ )
TP1	17.5	55.6	85.8	55.7
TP2	6.4	45.5	70.5	42.7
FS1	71.0	99.2	143.4	102.7
FS2	26.4	171.5	391.0	195.4

*D values at intercepts at 10, 50 and 90 % of the cumulative mass of particles in personal care products.*

Although particle size distribution was determined, the results were not as accurate as they could have been. This is likely because of the agglomeration of particles which were invariably not detected by the instrument's lasers. Therefore a dispersing agent was required to reduce the surface tension between particles and to ensure particle dispersal. Because this was a first experiment to determine particle sizes of microplastics from personal care products by laser diffraction, the manufacturer was consulted on likely dispersing agents to use in the experiment. , Based on the manufacturers advice Tetrasodium pyrophosphate was used to disperse the particles in the instrument. After applying the dispersant, there was a wider particle size distribution in all products, as compared to the first laser diffraction experiment (Figure 4.2). As such the results showed a wider size distribution to the initial results, but this distribution was still relatively narrow.

Although particle dispersal had been achieved, the lasers were still not detecting all the particles. This is because of a second challenge encountered in the analysis of particle size by laser diffraction. Particles were clearly observed floating at the surface of the sample collection chamber and were not drawn into the laser detection range of the instrument. This was likely because of the differences in the density of particles from all four products and the carrier liquid (water from the mains supply) for the instrument. Polyethylene with a density of between  $0.90 - 0.92 \text{ g/cm}^3$  will float on water, which has a density of  $1 \text{ g/cm}^3$ . After consultations with the manufacturer, the density of the carrier liquid for the instrument had to be reduced, to aid the sinking of particles so that they could be detected by the lasers. Ethanol and methanol with densities of  $0.789$  and  $0.792 \text{ g/cm}^3$  respectively were explored to assess the better



solution to alter the density of the carrier liquid. However, due to time constraints, a solution of methanol as described in the methods was used for the experiment because it was cheaper and available for use. Consequently, size analysis of particles in all products was determined, but with the addition of Tetrasodium pyrophosphate as a dispersing agent and methanol as a carrier liquid.

The particle size distribution was characterised by multiple peak populations for all the products analysed. In particular, the particles in TP2 exhibited two distinct peak populations, which were unique to this product (Figure 4.2). Differences in the particle size range across all products analysed was observed. Generally the particle size ranged from 1 – 600  $\mu\text{m}$ . Although the smallest particle size distribution measured in the four products was not obvious from the graph, the data from the instrument indicated data that the smallest particles were exhibited in TP1 with a size of 0.07  $\mu\text{m}$  (Table 4.2 Appendix).

In addition, the smallest particles in the other products were 0.3, 0.07 and 0.5  $\mu\text{m}$ , as demonstrated in TP2, FS1 and FS2. Furthermore, the distribution exhibited cut-offs that were different in all products. For example the first cut-offs were between 10 and 200  $\mu\text{m}$  in TP1, FS1 and FS2, but in TP2 the first cut-off was between 50 and 100  $\mu\text{m}$  (Figure 4.2).

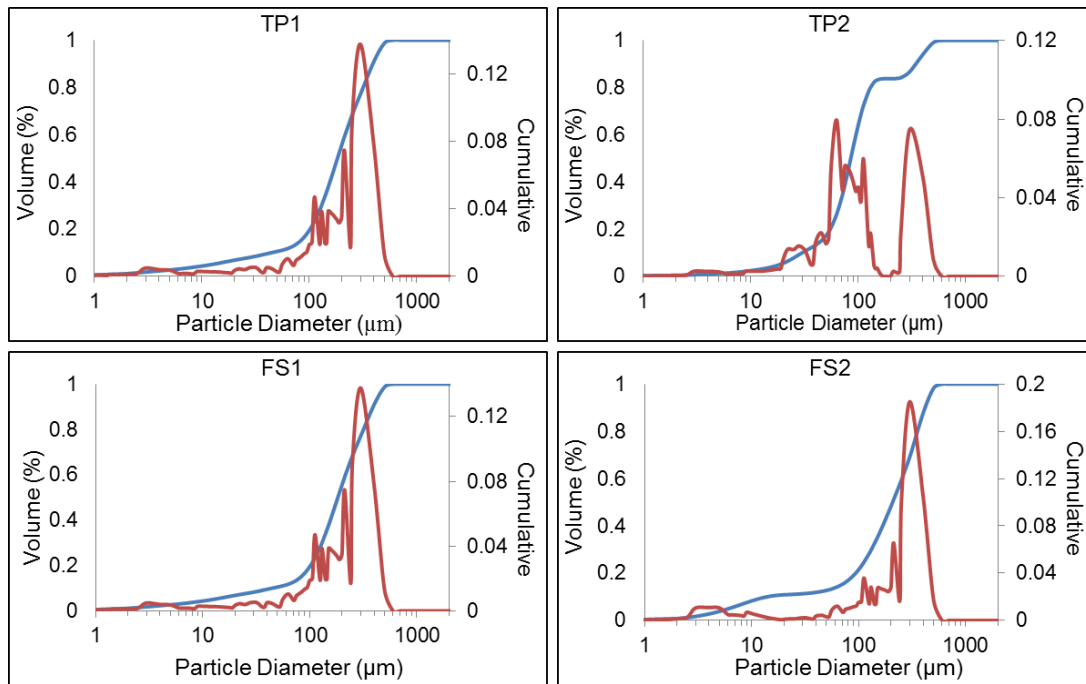


*Figure 4.2. Size distribution of particles in four products analysed by laser diffraction and the addition of methanol as the carrier liquid for the instrument. All products analysed show multimodal peaks, indicating multiple peak populations for particles in the personal care products.*

The texture of the particles ranged from silt like to medium particles (Table 4.2). However, there were also differences in the texture of particles measured at the same D value. For example for the D10 values, TP2 and FS2 exhibited silt-like particles, but TP1 and FS1 exhibited larger particles that were very fine-like particles (Table 4.2). The analysis of D50 values also indicated differences in the size of particles across all the products analysed. For example, the D50 measurements indicated that particles in TP2 were very fine, but the particles in TP1, FS1 and FS2 exhibited fine like particles (Table 4.2). Measurements to determine particle size at D90 also showed differences in size for all the products analysed. The particle size at D90 ranged from 342.1 to 452.9  $\mu\text{m}$  and indicated that the products were characterised by medium-like particles (Table 4.2).

The differences in the size of particles were not only observed in the D value measurements. The mean size of particles was different across all the products analysed. For example, TP1, TP2 and FS2 exhibited mean particle sizes characterised by fine particles. By contrast the mean particle size for FS1 was characterised by medium-like particles (Table 4).

*Table 4.2. Diameter values of particles in personal care products.*

Product	D10 % ( $\mu\text{m}$ )	D50% ( $\mu\text{m}$ )	D90% ( $\mu\text{m}$ )	Mean ( $\mu\text{m}$ )
TP1	69.2	204.3	426.0	225.8
TP2	14.5	48.9	342.2	119
FS1	76.9	290.5	452.9	274.8
FS2	44.2	182.9	391.6	206.0

*D values at intercepts at 10, 50 and 90 % of the cumulative mass of particles in personal care products.*

The analysis of particle size by laser diffraction revealed differences in the distribution of particles in all four products analysed. However, there were limitations in determination of particle size which were overcome by the addition of solutions of Tetrasodium pyrophosphate and methanol used for particle dispersion and as a carrier liquid. A comparison of cumulative distribution graphs, indicated differences in the particle size distributions. In particular, the results determined from experiments where Tetrasodium pyrophosphate and methanol were used was characterised by a wider particle size distribution in most of the products, than when none of these solutions was used. Furthermore, there was improved particle dispersion, indicated by multiple peak populations in the particle size distribution graph.

#### *4.2.2 Analysis of particle size and the limitations of the microscopy technique.*

Although the microscopy technique allowed for the analysis of particle size, there were challenges in determining particle size. Firstly, measurements conducted at the magnification of 100X indicated that particles below 80  $\mu\text{m}$  could not be measured because they were not visible at this magnification. This was different from the laser diffraction results which detected particles in the smaller sized micron range were detected. Secondly measurements based on the number of transects in the Sedgewick-rafter cell SRC, indicated differences in particle size distribution. Lower number of transects revealed a different particle size distribution than when a larger number of transects was selected for size measurements. Thirdly, the approach adopted for the transfer of samples from the 50 mL beaker to the Sedgewick Rafter cell (SRC) limited the number of particles introduced to the SRC. This was because

the 40 mL volume of the sample in the 50 mL beaker was diluted and so it was difficult to measure out the 1 mL volume required for transfer to the SRC. Therefore, in this section, the results for particle size and highlighting the challenges are presented.

#### 4.2.2.1. Determining particle size measurements at the magnification of 100X.

Size measurements were conducted by measuring particles in 14 out of 20 transects of the SRC. The particles in all four products exhibited differences in size, as measured at the magnification of 100X. In particular, the particles in FS1 exhibited the widest particle size range, and TP1 had the smallest size range. In addition, the results indicated that out of the four products analysed, the facial scrubs demonstrated the occurrence of the smallest particles with particles sizes of 80  $\mu\text{m}$  (Table 4.3). The results further showed that the mean size of particles in all products analysed ranged from 165.3 – 298.3  $\mu\text{m}$ , as demonstrated by TP2 and TP1 respectively.

*Table 4.3. Size of the particles measured in personal care products.*

Product	Minimum	Maximum	Mean	Median
TP1	170	495	298.3	298.3
TP2	91.6	253.3	165.3	165
FS1	80	433.3	195.2	88.3
FS2	80	431.7	207.3	197.5

*The table shows the size range of the particles in all products, measured at the magnification of 100X.*

A comparison of the mean size of the particles indicated clear differences as determined in all four products. In particular, this difference was statistically significantly different ( $p < 0.01$ ) in size between microplastics for the four personal care products [ $F(3, 1596) = 494.93, p = 2.5736E-227$ ]. A post-hoc Tukeys multiple comparison of means test at the 95% family-wise confidence level indicated a significant between-group difference for the size of particles in all the products analysed. (Figure 4.3).

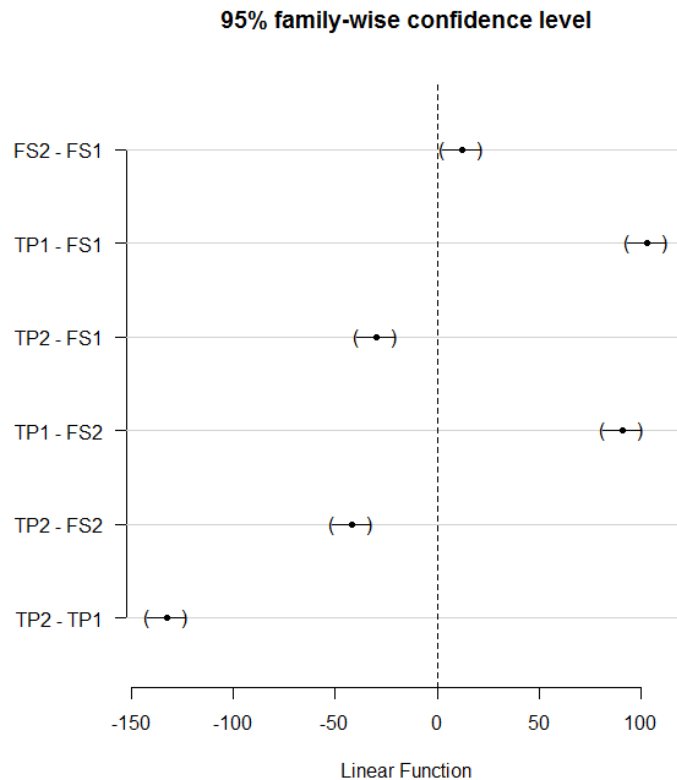


*Figure 4.3. Tukeys multiple comparisons of means at the 95 % family-wise confidence level. The confidence intervals that do not cut through the zero mark show a difference in the size of particles in the products. Confidence intervals that cut through the zero mark indicate similarities in the size of particles*

The results indicated that applying the microscopy technique for the analysis of particle size allowed for the measurement of particles  $\geq 80 \mu\text{m}$  in size. Therefore measurements conducted at the magnification of 100X had apparent effect on the minimum size of particles that could be determined. Consequently the measurements of particles in all products was analysed at a higher magnification.

*4.2.2.2. Analysis of the size of particles in personal care products determined at the magnification of 200X.*

At a higher magnification of 200X, smaller particles were identified than at the magnification of 100X (Table 4.4). Consequently, the results indicated that the smallest particles measured in all products ranged from 5 to 35  $\mu\text{m}$  (Table 4.4). In addition, the smallest particle measured at the magnification of 100X was larger than

the smallest particle determined at the magnification of 200X by a factor of 16. The results indicated that there were similarities and differences in the size of the largest particles for all products. In particular, particles in TP1 and TP2 exhibited a similar maximum size. However, the results indicated that the particles in FS1 and FS2 demonstrated differences in the maximum particle size.

*Table 4.4. Size of the particles measured in personal care products.*

Product	Minimum	Maximum	Mean	Median
TP1	5	500	135	113
TP2	5	200	15	10
FS1	35	250	106	100
FS2	15	220	72	70

*The table shows the descriptive statistics and size range for particles measured in all four personal care products, determined at the magnification of 200X.*

A comparison of the mean size of the particles indicated clear differences as determined in all four products. In particular, this difference was statistically significantly different ( $p < 0.01$ ) in size between microplastics for the four personal care products [ $F(3, 361) = 57.18814$ ,  $p = 2.87074E-30$ ]. A post-hoc Tukeys multiple comparison of means test at the 95% family-wise confidence level indicated a significant between-group difference for the size of particles in all the products analysed (Figure 4.4).

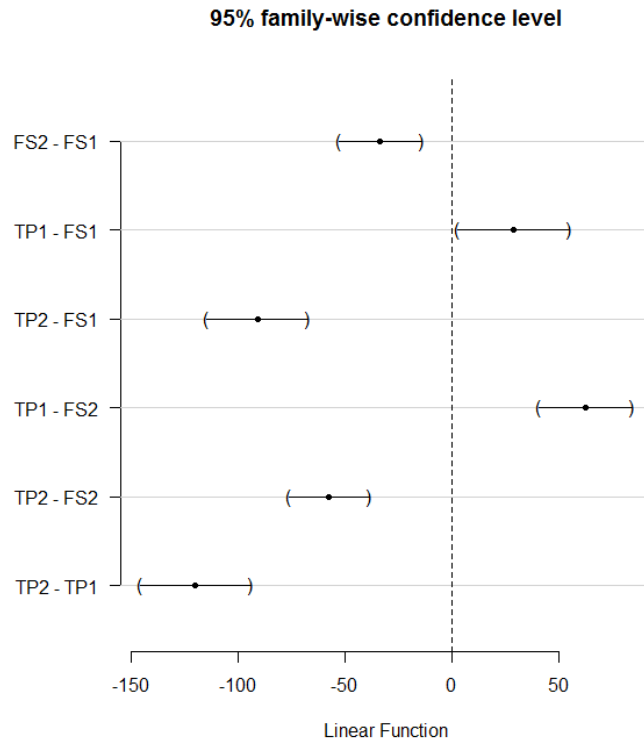


*Figure 4.4. The confidence intervals do not cut through the zero mark, indicating a significant difference in the size of particles for all paired products.*

The measurement of particles at the magnification of 200X had an apparent effect on the size analysis of smaller particles. As such measurements conducted at the magnification of 200X revealed smaller particles than what was determined at the magnification of 100X. It was therefore apparent that size measurements at different magnifications demonstrated differences in particle size. Although the lower limit for particle size measurement was improved by using the higher magnification, it was uncertain whether differences in particle size would be observed based on the number of transects selected for size measurements.

#### *4.2.2.3. Evaluation of particle size analysis based on the number of transects used in a Sedgewick-rafter cell (SRC).*

One toothpaste and facial scrub were selected to determine differences in particle size based on different transect measurements. At the magnification of 100X, the results indicated that particles in TP1 exhibited differences in particle size distribution, based on the number of transects selected. As such particle size based on 6 transects

demonstrated a wider particle size distribution by comparison with 2 transect measurements (Figure 4.5). The particle size ranged from 75 to 400  $\mu\text{m}$  in 2 transect measurements and 80 to 500  $\mu\text{m}$  for measurements in 6 transects (Figure 4.5). The results showed that when more transects were selected, more particles were observed and available for particle size measurements. For example, between 150 and 400  $\mu\text{m}$ , the 6 transect measurements exhibited a higher number of particles by comparison with the 2 transect measurements. Consequently, it was possible to measure more particles based on the 6 transect measurements, which allowed for a more robust analysis of particle size. However, measurements conducted at the magnification of 100X indicated particle size distributions that varied with measurements determined at the magnification of 200X.

There were differences in particle size distribution between the transect measurements. For 2 transect measurements, the particle size distribution determined at the magnification of 200X ranged from 5 to 350  $\mu\text{m}$ . By comparison, the 6 transect measurements demonstrated a wider particle size distribution and ranged from 5 to 500  $\mu\text{m}$  (Figure 4.5). As such size measurements conducted at the magnification of 200X proved useful for observing smaller particles that could not be detected at the magnification of 100X. However size distributions were characterised by multiple peaks, based on the different transect measurements. In particular, below the 100  $\mu\text{m}$  size, particle size analysis determined in 6 transects was characterised by a higher number of particles than measurements determined in 2 transects (Figure 4.5).

A comparison of the results for particle size measurements determined at the magnification of 200X demonstrated a wider size distribution than measurements conducted at the magnification of 100X. For example, a comparison of the smallest particles indicated that for 2 transect measurements, particles in TP1 analysed at the magnification of 100X were 15 times larger than those measured at the magnification of 200X (Figure 4.5). A similar trend was observed for the smallest particles in TP1 determined in 6 transects. As such the smallest particles determined at the magnification of 100X was 16 times larger than those determined at the magnification of 200X (Figure 4.5). However there was a marginal difference for the largest particles between magnifications, but this was not true in all cases. For example, the measurements determined using 2 transects indicated a larger particle size as



determined at the magnification of 100X. However, the measurements determined in 6 transects exhibited particles with the same maximum size (Figure 4.5). Therefore, the number of transects selected for size analysis had an influence on the size distribution of particles in TP1.

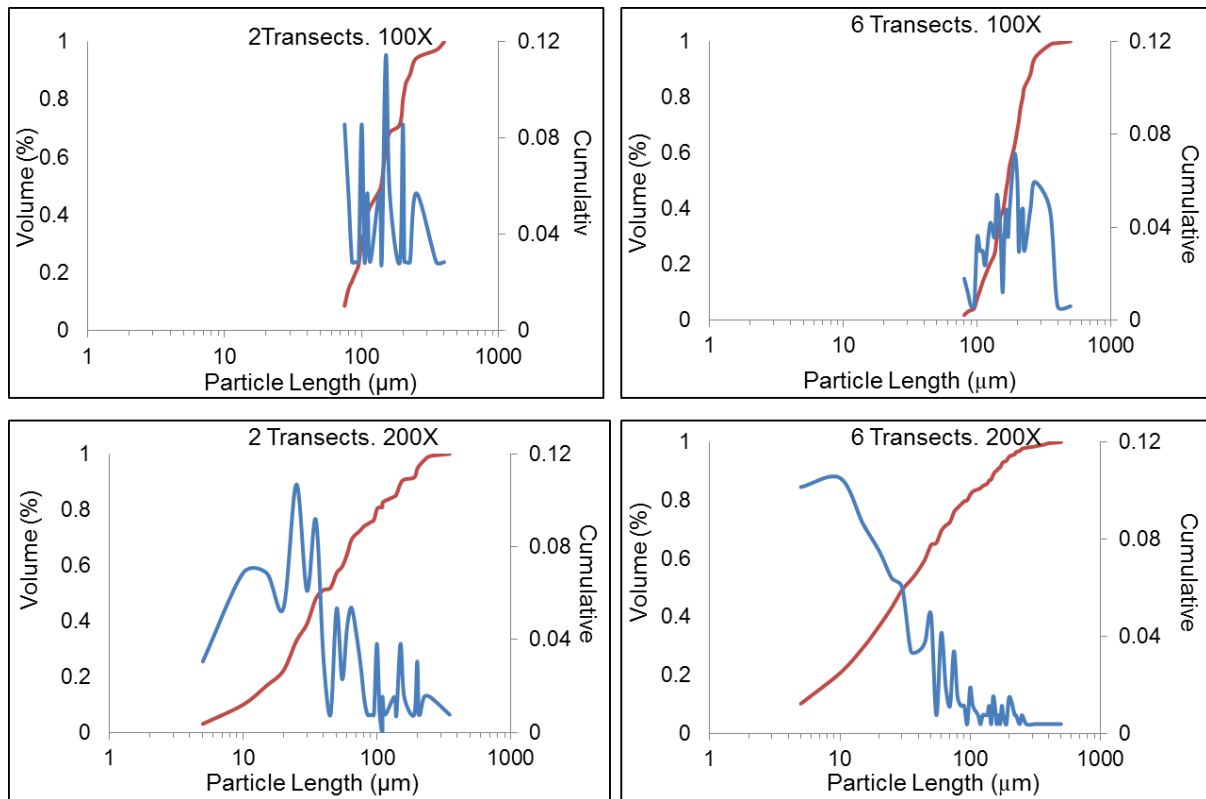


*Figure 4.5. Particle size distribution for TP1, determined by a selection of 2 and 6 transects in a Sedgewick-rafter cell. The measurements determined at 100X indicated differences in size distribution with measurements conducted at the magnification of 200X. In an SRC, one transect contains 50 individual counting chambers.*

In an equivalent experiment using a facial scrub, the particle size distribution for FS1 indicated differences in the size distribution between transect measurements and magnifications. The measurements conducted in 2 transects exhibited a smaller particle size distribution by comparison with the 6 transect measurements. The particle size ranged from 70 to 350  $\mu\text{m}$  for the 2 transect measurements and 70 to 400  $\mu\text{m}$  for the 6 transect measurements (Figure 4.6). By comparison, the measurements determined at the magnification of 200X indicated size distribution ranged from 35 to 250  $\mu\text{m}$  for the 2 transect measurements and 25 to 225  $\mu\text{m}$  for the 6 transect measurements (Figure 4.6). In addition at the magnification of 200X, smaller particles

that were not detected at the magnification of 100X were clearly seen and measured. The smallest particles determined at the magnification of 100X and in 2 transects measurements, was larger than the smallest particles determined at the magnification of 200X, by a factor of 2. The same trend was indicated for particles measured in 6 transects and between the magnifications used (Figure 4.6). The measurements conducted at the magnification of 200X revealed the presence of smaller particles that were not detected before now. However comparison with measurements at the lower magnification, showed that measurements using a higher number of transects at the higher magnification, demonstrated a smaller particle size range for the distribution.

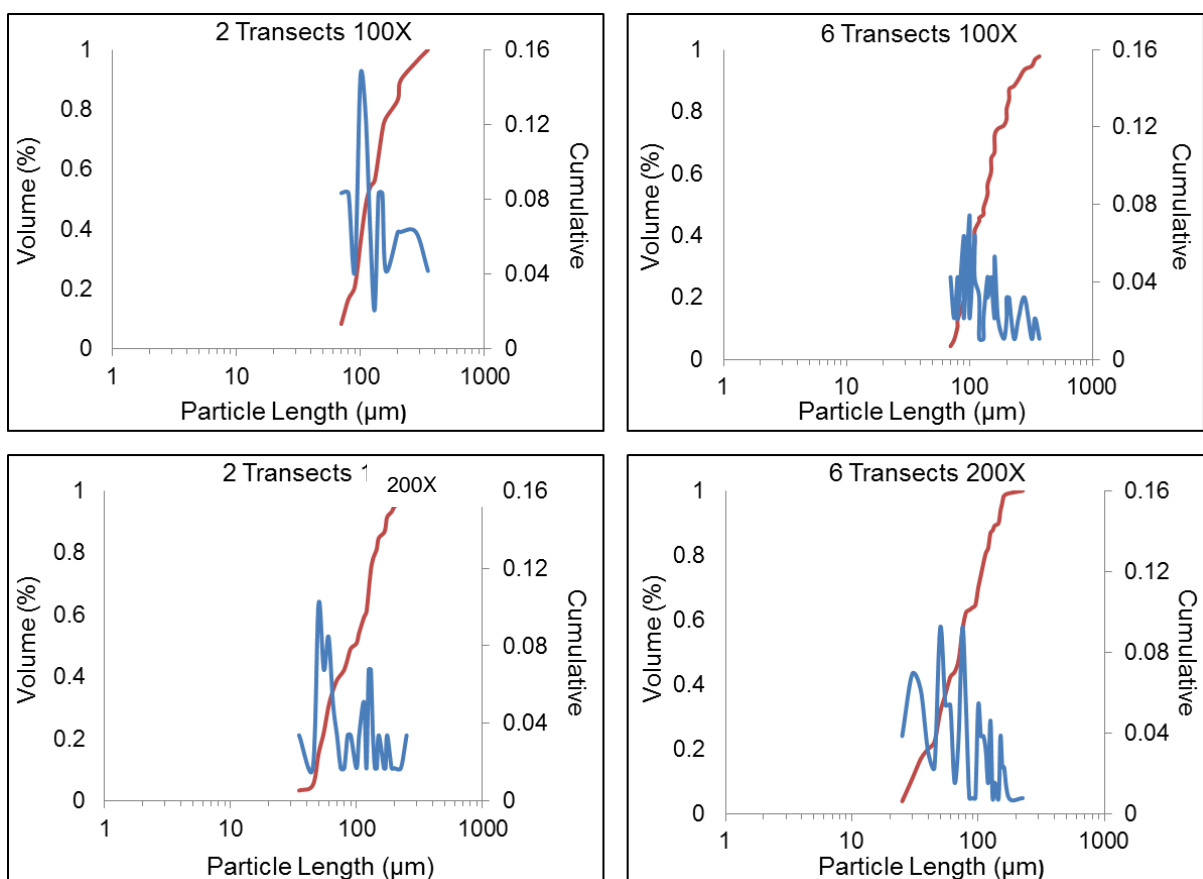


*Figure 4.6. The size distribution for particles in FS1 based on measurements conducted in 2 and 6 transects in a Sedgewick-rafter cell. The differences in size distribution are demonstrated by the different selected transects and measurements determined at 100X and 200X.*

The analysis of microplastics using this method showed that particle size measurements based on 14 selected transects (Section 4.2.2.1) was labour intensive and time consuming.

#### *4.2.2.4. The volume reduction of particle samples to evaluate the effect on size measurements.*

The reduction of the sample volume had an effect on the size of particles measured in the selected products. The results demonstrated a wider size range of particles than the size range determined in Section 4.2.1.3, for TP1 but not in FS1. The largest size of particles exhibited in FS1 was smaller than what was previously determined by 80  $\mu\text{m}$ . As such, at the magnification of 100X, the size of the particles ranged from 50 to 500  $\mu\text{m}$  and 50 to 320  $\mu\text{m}$ , in TP1 and FS1, respectively (Table 7). By comparison with the analysis at the 100X magnification, measurements determined at the magnification of 200X indicated a wider size range, with particles ranged from 5 to 500  $\mu\text{m}$  and 35 to 450  $\mu\text{m}$ , respectively (Table 4.5).

Results indicated differences in the size of particles in comparison to the particle sizes described in section 4.2.2.1. For example, the smallest particles exhibited in TP1 and measured at the magnification of 100X was 50  $\mu\text{m}$ . This was 35  $\mu\text{m}$  smaller than the minimum particle size exhibited by TP1 and measured at the magnification of 100X in section 4.2.2.1. It was clear from the results that the sample volume reduction had an effect on the smallest and largest particles because of the increased concentration of particles and, therefore the transfer and analysis of more particles than in section 4.2.2.1. Consequently the reduction of the volume for the particle samples was adopted in all further experiments.

*Table 4.5. Size analysis of particles in TP1 and FS1 based on sample volume reduction*

Product	Minimum	Maximum	Mean	Median
TP1 100X	50	500	171.2	165
FS1	50	320	119.5	100
TP1 200X	5	500	77.7	40
FS1	35	450	146.9	127.5

*The descriptive statistics and size range of particles determined in TP1 and FS1, measured at the magnifications of 100X and 200X. The particle sizes are based on the reduction of sample volume which allowed for the analysis of more particles.*

After resolving the challenges encountered for the analysis of particle size using the laser diffraction and microscopy techniques, it was clear there were also challenges associated with estimating the number of particles in the products analysed. This was particularly true for the estimation of the number of particles using the imaging flow cytometry technique.

#### *4.3 Evaluation of the number of particles determined using different counting protocols by microscopy.*

To estimate the number of particles in the products selected, isolated particles were introduced onto a Petri dish. It was observed that the particles introduced on the petri dish were not stable and were displaced every time the dish was moved during the counting process. Therefore at the magnification of 100X, the results indicated that the number of particles ranged from 107,800 (TP1) to 166,400 (FS1), accounting for 39% and 61% of microplastics in the products (Figure 4.7). It is likely that the displacement of the particles during counting would have resulted in a biased count and not given a true estimate for the number of particles. Therefore it was not possible to give an accurate estimate of the number of particles in all products analysed.

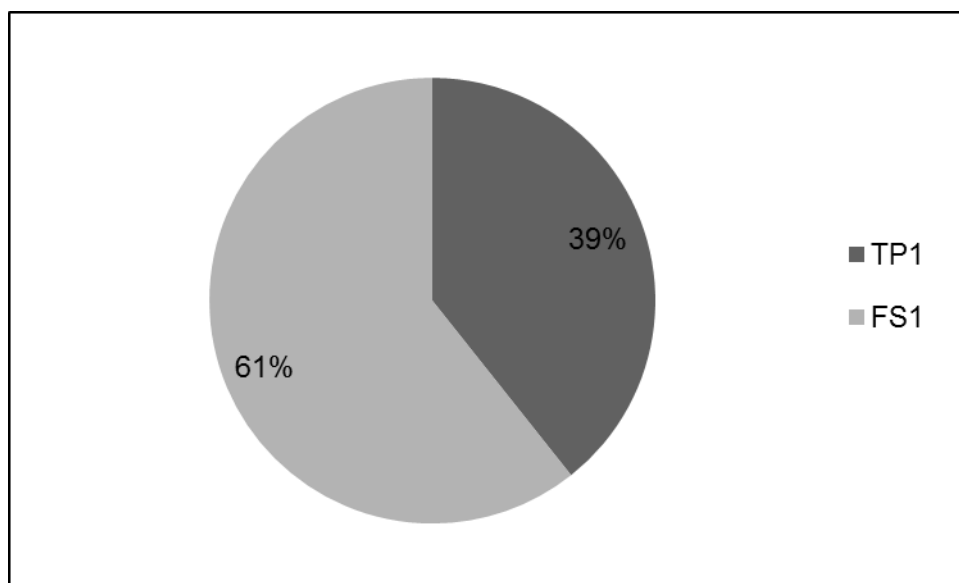


*Figure 4.7. Pie chart showing the estimated number of particles per 100 g counted in selected personal care products at the magnification of 100X.*

A more standardised method for the quantification of particles was adopted using the Sedgewick-rafter cell. The Sedgewick-rafter cell proved useful for estimating the number of particles based on a pre-determined number of counting cells within transects. It was possible to estimate the number of particles in all transects of the SRC, but this would have been time consuming, labour intensive and would have resulted in errors. However, counting a smaller or larger number of transects demonstrated differences in the total number of particles, based on the number of transects used. For example, the number of particles determined in 6 transects of the SRC indicated the number of particles ranged from 8,240,000 to 8,430,000 particles, in FS1 and TP1 respectively (Figure 4.8). However, an estimation of the number of particles based on two transect counts revealed the number of particles ranged from 2,746,667 to 5,920,000 in FS1 and TP1 respectively (Figure 4.8). Therefore the application of different estimation methods revealed differences in the estimated number of particles.

The difference in the number of particles was also indicated when particle estimates were determined at different magnifications. As such at the number of particles determined at the magnification of 200X indicated there were more particles than the estimates determined at the magnification of 100X. Therefore, the number of particles estimated in two transects at the magnification of 200X, ranged from 5,493,333 to

6,480,000 particles, as demonstrated by FS1 and TP1 respectively. By contrast the number of particles estimated in six transects ranged from 12,000,000 to 14,860,000 particles, as demonstrated by FS1 and TP1 respectively (Figure 4.8).

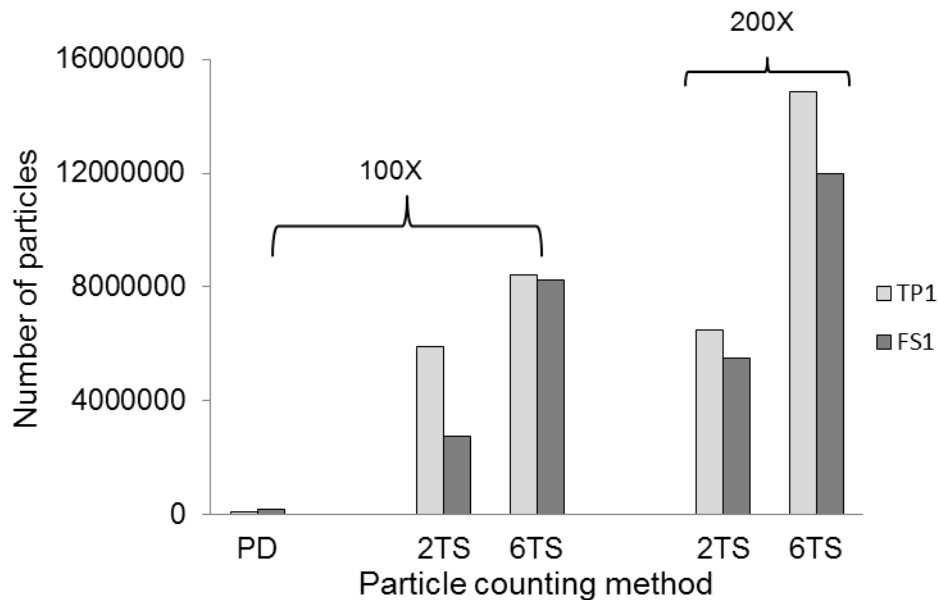


Figure 4.8. Histogram for the estimated number of particles per 100 g counted in all four personal care products at the magnification of 100X.

The results indicated that the Petri dish method revealed the smallest number of particles, and was prone to error because particles were not stationary. However, by applying the SRC, provided more stability for the particles, and there were differences in the number of particles based on the different transect counts. Although the general rule with a Sedgewick-rafter cell is to count at least 10% of the particles to get a statistically reliable number, the 6 transect counts indicated the largest number of particles in the products selected. In addition, the number of particles determined at the magnification of 200X revealed more particles than the smaller magnification of 100X. Therefore, all further particle estimation experiments were conducted by counting all the particles in 6 transects and at the magnification of 200X.

#### 4.4. Challenges encountered for the analysis of particle size using the imaging flow cytometry technique.

For the first time the imaging flow cytometry technique was used to characterise particles in personal care products. In particular, it is the first time this novel technique has been applied for the analysis in any microplastic study. Generally this technique is widely used to study biological cell processes, but has not been applied in any study of polymer particles. In addition, the capabilities of this technique as described in Chapter one, indicated its usefulness and application for the characterisation of particles separated from PCPs.

However, it was difficult to determine particle size and estimates for the number of particles in all the products. This was because of the occurrence of the calibration speedbeads which exhibited similar sizes to the particles separated from all four products. Therefore, it was a challenge applying the right template to differentiate speedbeads from particles separated from PCPs. Therefore, the challenges encountered and the results for the number of particles are presented in this section.

##### *4.4.1. Evaluation of template applied to differentiate calibration speed beads from particles in all products.*

The IDEAS software is equipped with a range of features that allowed for the development of templates to characterise particles in a sample. As a first step, the analysis of the size and shape of particles separated from PCPs was to be conducted. This was determined by area vs the aspect ratio scatter plots. The area feature which is the number of square microns in a particle which is equal to the area of that particle, was determined (Figure 4.9). Therefore, a particle exhibiting a smaller area suggests single particles, while particles with a larger area suggest doubling of particles otherwise called doublets. Furthermore, determining how long, short or round a particle is, was determined by the aspect ratio, which is the width divided by the height of the particle.

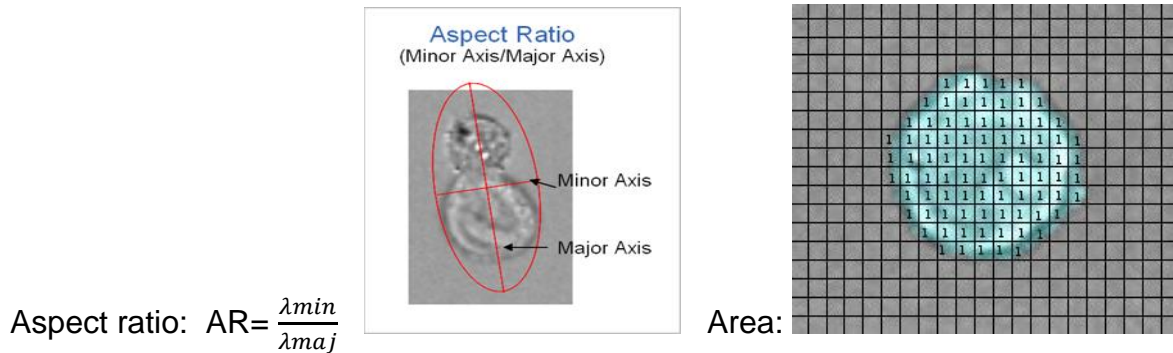


Figure 4.9. Image of a particle indicating the aspect ratio and the area of the particle.

the calibration speedbeads (which monitors and adjusts the flow of samples) that continuously run through the instrument were not distinct from particles separated from PCPs. Consequently, an estimate of the number of particles could not be determined (Figure 4.9.1).

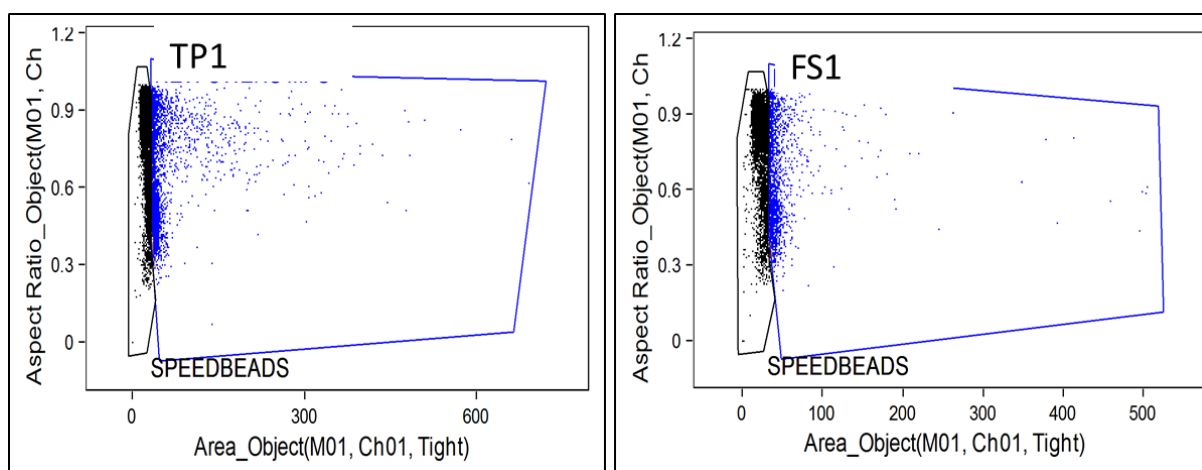


Figure 4.9.1. Scatter plot for the estimated number of particles per mL determined in all four personal care products at the magnification of 100X.

The next step was to develop a template that would distinguish speed beads from the particles. It is apparent that the calibration speeds exhibit a well-defined side scatter profile that can be used to tell them from other particles. Particles that pass through a beam of laser light scatter light. In addition, side scatter is proportional to the granularity of a particle. Therefore this characteristic exhibited by the calibration speedbeads was explored and applied to the development of a template (Figure 4.9.2).



The results indicated that there were still overlaps between the particles and the calibration speedbeads. This was apparent from interrogating the template and observing the size and shape of particles in the image display gallery. The interrogation revealed that the speedbeads and some of the particles exhibited similarities in shape and size. In addition, the similarities were apparent after plotting a scatter plot of area vs intensity (Figure 4.9.2).

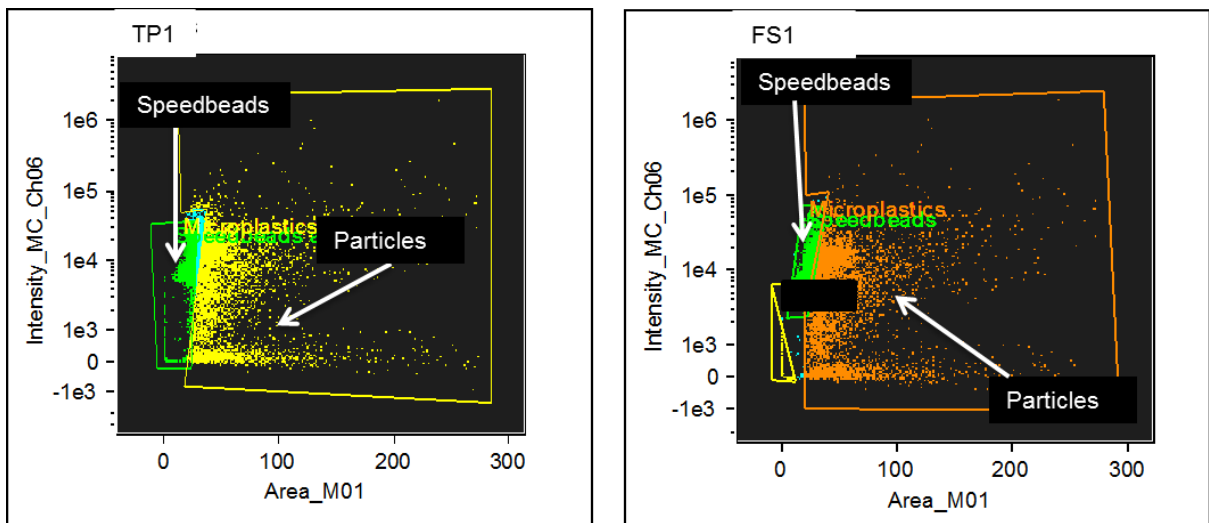
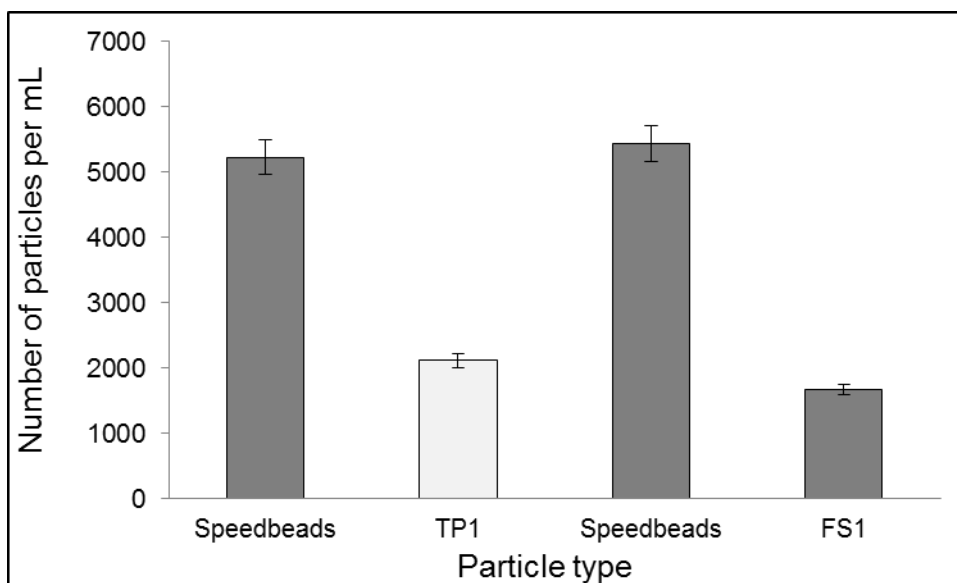


Figure 4.9.2. Template developed to distinguish calibration speed beads from particles in the selected products, based on the SSC profile. Template consists of five sub-templates to identify particles in focus (A); identify speed beads based on side scatter profile SSC (B).

Although observations of the scatter plot indicated that there were more particles than Speedbeads, a histogram plot to determine the number of particles showed differences. There were more speedbeads than the number of particles separated from the selected products. In particular, the speed beads were two times the number of particles in TP1 (Figure 4.9.3). It is not clear why this was so, but it could be because there were particles from the products that also exhibited a similar SSC profile to the calibration speed beads, and exhibited similarities in number.



*Figure 4.9.3. Histogram for the number of speed beads and the number of particles separated from the selected products*

The number of particles from the selected products was not estimated using the templates developed. Therefore the calibration speed beads which continuously run through the instrument were turned off. Following this, another template was developed and applied to estimate for the number of particles in all products.

*4.4.2. The development of a template to estimate the number of particles recovered from PCPs after disabling the calibration speed beads.*

The analysis of particles separated from PCPs, was based on modifications of the template described in section 4.4.1. Therefore, single particles that were in focus were analysed using the template. There were less particles running through the instrument when the speed beads were turned off. This was indicated by analysis template for single particles and observed in the scatter plot of area vs aspect ratio (Figure 4.9.4).

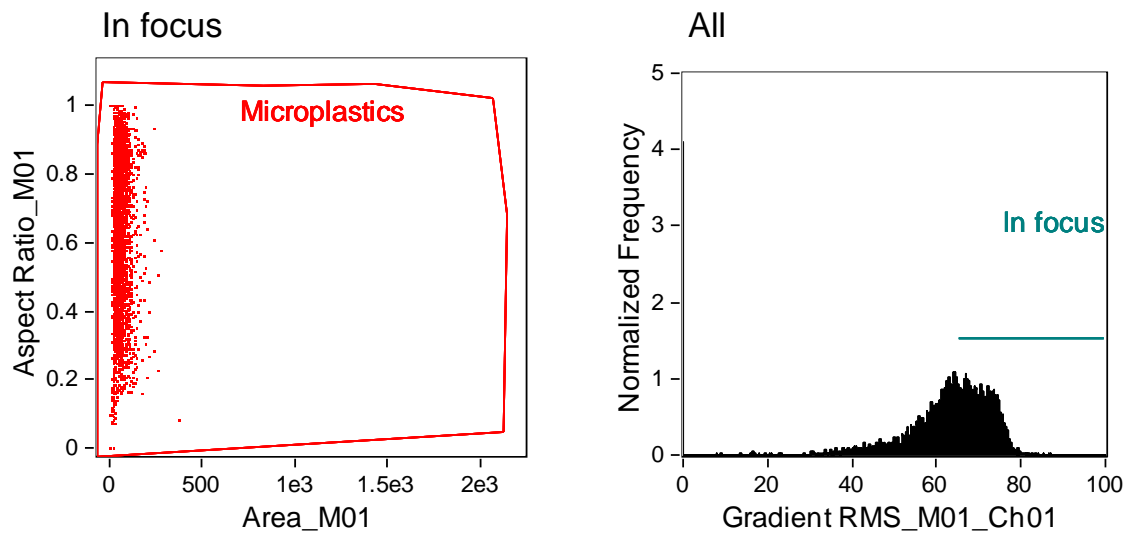


Figure 4.9.4. Templates developed to identify single particles in the sample (left) and particles that were in focus (right).

In addition, a template to distinguish between particles based on shape features was developed. This allowed for the analysis of two distinct populations of particles according to their shape. Therefore elongated and circular-like particles were determined by a plot of the aspect ratio vs normalised frequency (Figure 4.9.5). The separation of elongated from circular particles was based on values of the aspect ratio which follows that particles with aspect ratios of 1 represents a circle while values of 1 represent a thin and elongated particle. Consequently, particles with aspect ratio values ranging from 0 – 0.55 were gated as elongated particles, while aspect ratio values ranging 0.56 – 1.0 were gated as circular particles (Figure 4.9.5).

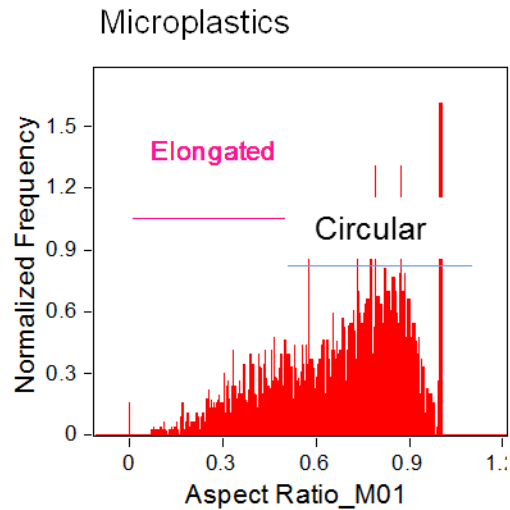


Figure 4.9.5. Template developed showing distinctions between elongated and circular-like particles.

The elongatedness feature is the width divided by the height of the particle was used to identify particles that were long or short. The circularity feature is the degree of similarity of a particle to a circle, and measures the average distance from a particles centre to its boundary, and is divided by the variation of the distance. Therefore, larger the variation, the further away the particle is from a perfect circle and vice versa (Figure 4.9.6).

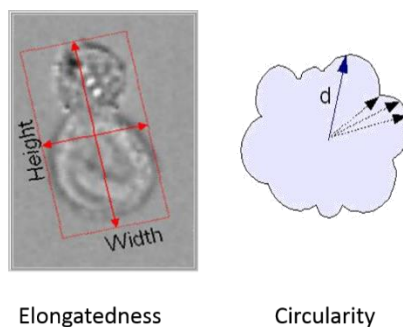


Figure 4.9.6. Descriptive image of the elongatedness and circularity shape features used to determine particle size.

To verify that the particles where either elongated or circular, random bins in the histogram were checked and images were successfully confirmed for both populations

(Figure 4.9.6.1 and 4.9.6.2. . A histogram plot was generated for particle size distribution to show elongated and circular particles.

The results indicated that there more particles estimated in TP1 than in FS1 (Figure 4.9.7). However, there were differences in the number of particles based on the analysis features applied. Therefore, using the size features (length and diameter) the results indicated that the number of particles estimated were the same. For example, using the length and diameter features 159,980,700 particles were estimated in TP1 (Figure 4.9.7). The results showed that the number of particles was the same for elongated and circular particles determined with the length and diameter features (Figure 4.9.7). It is apparent that the analysis for particle estimates was determined for the same population. Therefore, the number of particles determined would be the same.

However, the number of particles were different based on the shape features used. For example using the length feature, there were more circular-like particles (CIR) than elongated particles (ELG) in TP1 (Figure 4.9.7).

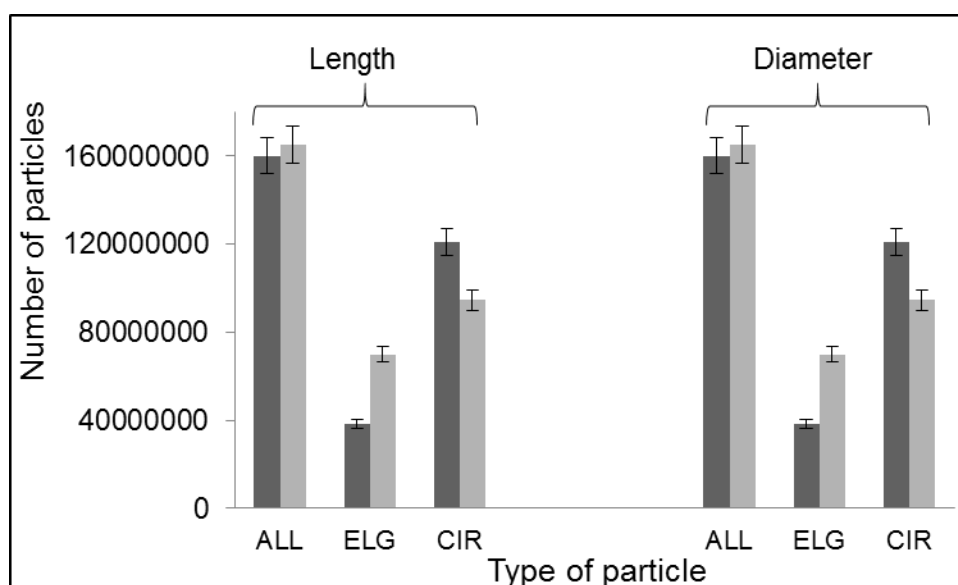


Figure 4.9.7. Histogram showing estimates for the number of particles separated from TP1 and FS1. The length and diameter size features demonstrated the same number of particles for the products analysed.

Sample preparation for the analysis of particles via imaging flow cytometry was carried out with filtered laboratory grade water. As such, the laboratory grade water

was run as blanks and as a part of quality control. However the analysis of the blank samples indicated high number of particles. Therefore debris was present in the blanks, and was different from the particles separated from the selected products. Therefore, the analysis to estimate the number of particles was blank corrected for all samples, and the results are presented in section 4.6.2.

#### 4.5. Characterisation of microplastics separated from Personal care products

The results in this chapter are based on the outputs of the methods developed and techniques applied for the characterisation of particles in personal care products. In addition, the results for the characterisation of particles have been categorised based on the size, number, morphology and polymer identity of the particles in all personal care products analysed. Furthermore, a comparison of the characterisation results based on the different techniques used is presented in this chapter.

The analysed data for particle size, number, morphology and polymer identity, have been presented as tables, graphs and figures, to describe the results and indicate significant differences where applicable.

##### *4.5.1 Assessing the size of particles in personal care products by Microscopy*

The size of particles measured at magnifications of 100X and 200X in all PCPs showed significant differences (Table 4.6). In addition, the differences exhibited between the measurements conducted at magnifications of 100X and 200X are highlighted in this section. The results showed that there was a wide size range of particles in all PCPs measured at magnifications of 100X and 200X. As such at 100X magnification, particles in FS2 and TP2 were recorded as having the smallest and largest particles in PCPs. By contrast, measurements conducted at magnifications of 200X, indicated that TP1 and TP2 exhibited the smallest particles, while TP1 had the largest particles. An analysis of particle size at the magnification of 200X was useful in observing smaller particles that were not observed at 100X magnification. Typically, the smallest particle size observed at 200X magnification was 10 times smaller than

the smallest particle viewed at 100X magnification (Table 4.6). In addition, there was a difference in the largest particle size viewed at 100X and 200X magnifications by margin of 50  $\mu\text{m}$ .

The results showed that the average size of particles exhibited differences between both magnifications. The mean size of particles at 100X magnification was recorded between 114 – 190  $\mu\text{m}$ , and at 200X magnification the mean size of particles was between 72 – 146  $\mu\text{m}$  (Table 4.6). Therefore, example, measurements conducted at the magnification of 100X indicated a larger mean size than what was measured at the magnification of 200X (Table 4.6).

*Table 4.6. Size of the particles measured in personal care products.*

Product	Minimum		Maximum		Mean		Median	
	100X	200X	100X	200X	100X	200X	100X	200X
TP1	50	5	433	483	157	72	155	38
TP2	70	5	420	403	190	97	180	50
FS1	50	40	317	407	120	143	105	125
FS2	47	20	320	423	114	146	100	115

*The table shows the differences in minimum, maximum and mean values of microplastics per 100 g of personal care products. The differences in size are based on measurements of 300 particles per brand.*

There was a statistically significant difference between the size of particles in all the products measured at 100X, [F(3, 396) =24.72, p = 1.11E-14] (p < 0.001). Likewise, at 200X magnification, there was a statistically significant difference between the sizes of particles in the personal care products analysed, [F(3, 396) =15.75, p = 1.08E-09] (p < 0.001). Furthermore, there was a statistically significant difference between measurements conducted at the different magnifications [F(7, 792) =20.5519, p = 1.8E-25] (p < 0.001). A post-hoc Tukeys multiple comparisons of means test at the 95% family-wise confidence level was determined between magnifications of 100X and 200X. The results indicated that half of the products contained particles with similar sizes. In addition a post-hoc Tukeys multiple comparisons of means test at the

95% family-wise confidence level was determined at 100X and 200X magnification. The results showed that at 100X magnification, the sizes of particles in all products were different except particles in FS2 and FS1 (Figure 4.9.8). By contrast however, at 200X magnification, the post-hoc Tukeys multiple comparisons of means at the 95 % family-wise confidence level, showed that there was no difference in the size of particles in FS2 and FS1 and between TP2 and TP1 (Figure 4.9.9). Furthermore the post-hoc test for measurements at both magnifications revealed similarities and differences in the size of particles determined in all products analysed (Figure 4.9.9).

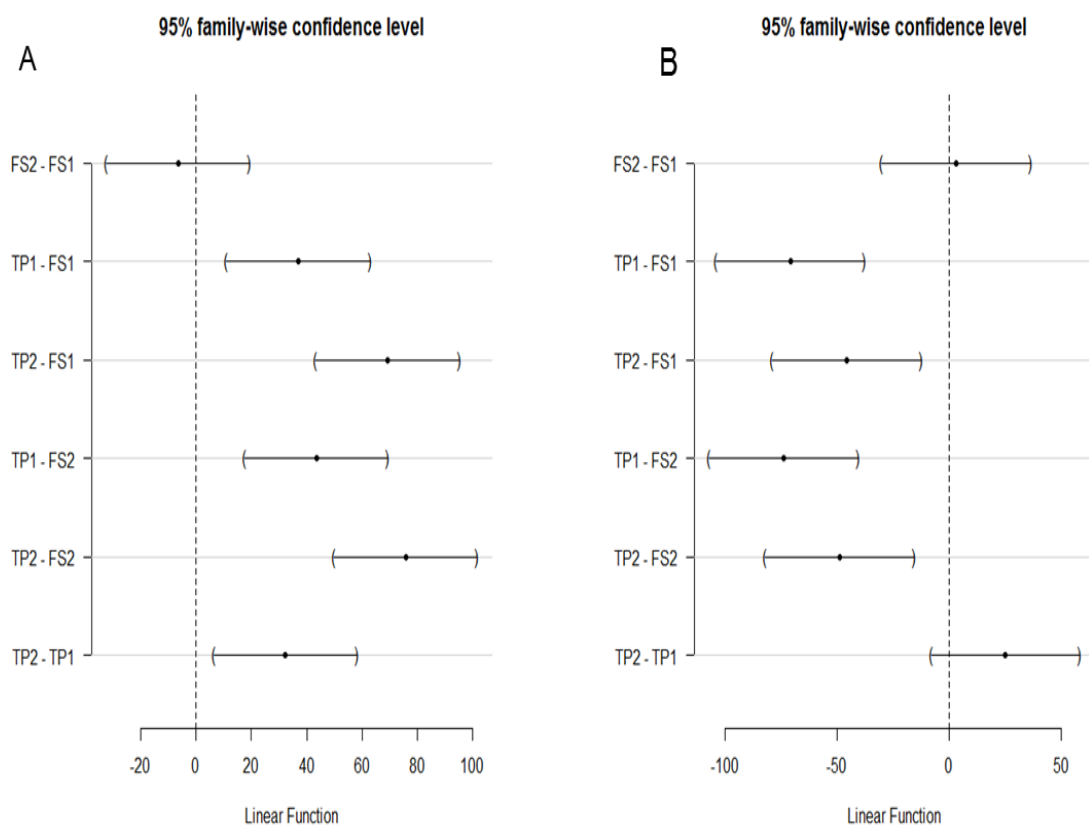


*Figure 4.9.8. Tukeys multiple comparisons of means at the 95 % family-wise confidence level. The confidence intervals that do not cut through the zero mark show a difference in the size of particles in the products. Confidence intervals that cut through the zero mark indicate similarities in the size of particles.*



### 95% family-wise confidence level

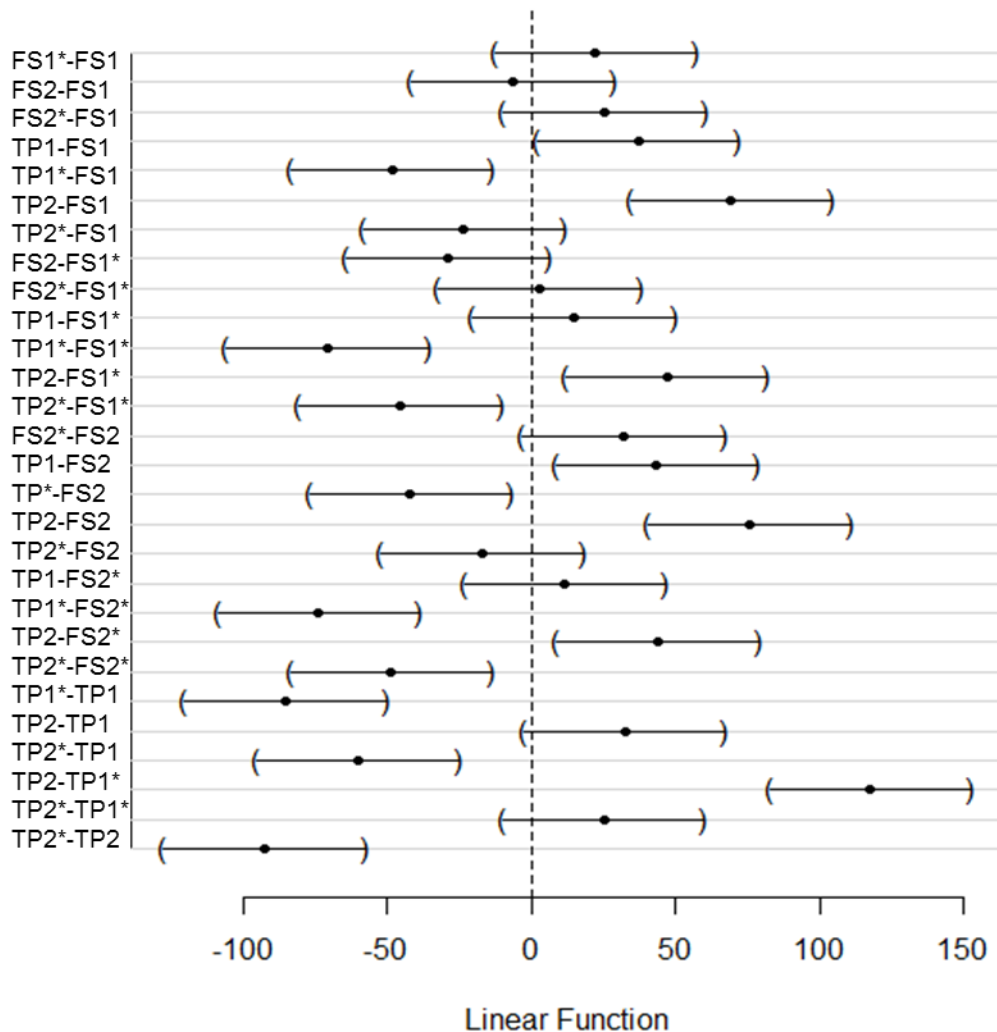


Figure 4.9.9. Tukeys multiple comparisons of means at the 95 % family-wise confidence level. Confidence intervals that do not cut through the zero mark show differences in the size of particles in the products. Confidence intervals that cut through the zero mark indicate no difference in the size of particles. Particle size denoted by \* indicate measurements determined at the magnification of 200X.

The results indicated that the different magnifications produced different results; particularly, there were also differences between particles in the products, measured at the same magnifications. Microscopy as a technique allows for the observation of particles, providing images which aid size measurements and observation of differences in size, as is the case of the particles in PCPs.

#### *4.5.2. Assessing particle size distribution by Laser Diffraction*

This section describes the particle size distribution by the laser diffraction technique. The results are displayed as a cumulative frequency distribution graph, showing the different peak populations of particles in all four products analysed. The results have also been presented as Diameter (D) values which describe the percentage of particles that are less or equal to the percentage cut-off. Particle size distribution allows for the estimation of D, which describe the diameter of a sphere which groups particles of a sample into a defined ascending order by mass. Laser diffraction analysis showed that all four products contained particles with sizes from the low micron range up to hundreds of microns, (Figure 4.9.9.1). Generally, particle size ranged from 10 – 900  $\mu\text{m}$ , however, the distribution showed a cut-off at the larger size range, which was steep in all cases, and occurred between 300 and 900  $\mu\text{m}$  (Figure 4.9.9.1). In addition, the results showed that there were specific differences in particle sizes across the personal care products analysed. Typically at the lower end of the measurement scale, the particle size distributions were more extended, which was more pronounced in the toothpastes. Although the number of small particles was low and was not visible in the cumulative frequency distribution graph, the raw data demonstrated their occurrence in the personal care products at 0.2 to 0.5  $\mu\text{m}$ . However what was clear was that TP1 exhibited the narrowest particle size distribution that ranged from 10 - 400  $\mu\text{m}$  (Figure 4.9.9.1). Likewise, the particle size distribution in TP2 demonstrated the occurrence of particles in the lower end, and although the peak was low, the raw data showed the occurrence of particles that ranged in size from 0.2 to 0.4  $\mu\text{m}$ . Furthermore, TP2 showed a particle size distribution that ranged from 10 - 600  $\mu\text{m}$  (Figure 4.9.9.1). In comparison, the facial scrub FS2, demonstrated the broadest particle size distribution for all the products analysed (Figure 4.9.9.1).

It was further observed that the tail of the particle size distribution demonstrated a left-skewed distribution showing that particle size distribution in all products was negatively skewed. To put it into context, the results based on laser diffractions showed that there were more particles  $\geq 200 \mu\text{m}$ .

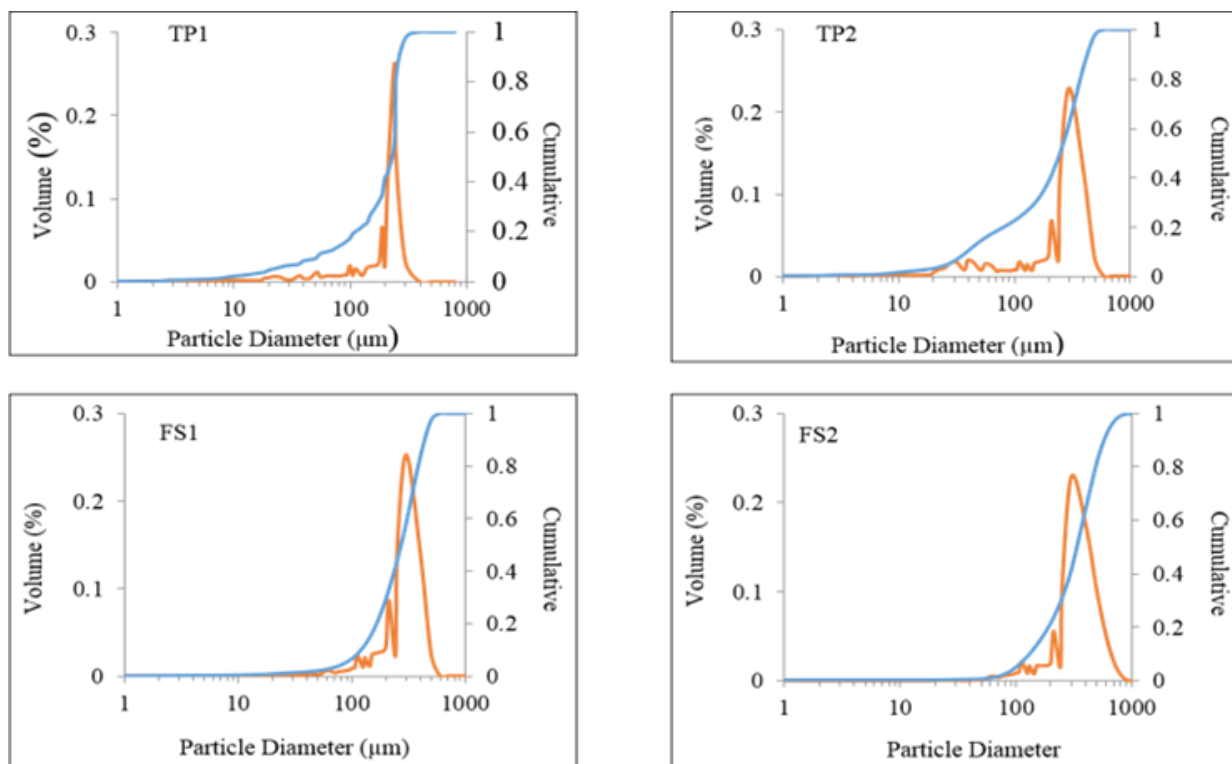


Figure 4.9.9.1. Particle size distribution of microplastic particles extracted from personal care products analysed using a CILAS 1180 particle size analyser. Cumulative graph showing microplastics size distribution in each brand of personal care product. All products analysed show multimodal peaks, indicating multiple peak populations for particles in the personal care products.

The particles in all personal care products, exhibited a wide size range for measured D values, therefore this indicated that the texture of particles ranged from very fine to coarse (Table 4.7). For example, D10 values indicated that 10% of particles in TP1 exhibited fine particles, but by comparison, FS1 with ~ 2 times the D10 value of TP1, exhibited fine particles (Table 4.7). The median size value described by the D50, showed different results for particles in the personal care products. As such the particles in all products analysed exhibited a medium texture, on the basis of the D50 values. In particular, TP1 exhibited the largest size, which was larger than the smallest particle in FS2, by a factor of 1. The medium to coarse particles in the personal care products, described by the D90 value, showed 90% of the particles in FS1 and by contrast, 90% of the particles in FS2 exhibited medium to coarse particles (Table 4.7).

The mean values for the particle size distribution was determined in all personal care products analysed. For example, the general mean size of particles in the

personal care products ranged from 276.7  $\mu\text{m}$  - 351.1  $\mu\text{m}$  (human hair is 40 – 300  $\mu\text{m}$ ). These values describe the central point of the particle size distribution and is less used in reporting particle size analysis results, but is useful for comparison with the output other techniques. Based on the mean values, the particles in the four products exhibited a medium texture.

*Table 4.7. Diameter values of particles in personal care products.*

Product	D10 % ( $\mu\text{m}$ )	D50% ( $\mu\text{m}$ )	D90% ( $\mu\text{m}$ )	Mean ( $\mu\text{m}$ )
TP1	220.7	340.5	502.8	351.1
TP2	102.2	307.8	513.5	310.8
FS1	91.9	276.4	443.9	276.7
FS2	113.8	271.1	461.1	279.3

*D values at intercepts at 10, 50 and 90 % of the cumulative mass of particles in personal care products.*

#### *4.5.3. Size analysis of particles in personal care products by Imaging flow cytometry*

In this section for the first time, analysis of microplastics ( $\leq 70 \mu\text{m}$ ), using imaging flow cytometry is reported. In addition, for the first time, the area of microplastics is also reported. The template that was developed for the analysis of particles in the four PCPs was applied for particle size measurements. The analysis of particles in the four products indicated differences in the size of particles in the four PCPs. In particular, it was observed that the size measurements determined using the area feature revealed the widest particle size distribution by comparison to size measurements determined by the length and diameter features.

#### 4.5.3.1 Development of a Gating strategy to identify single particle population

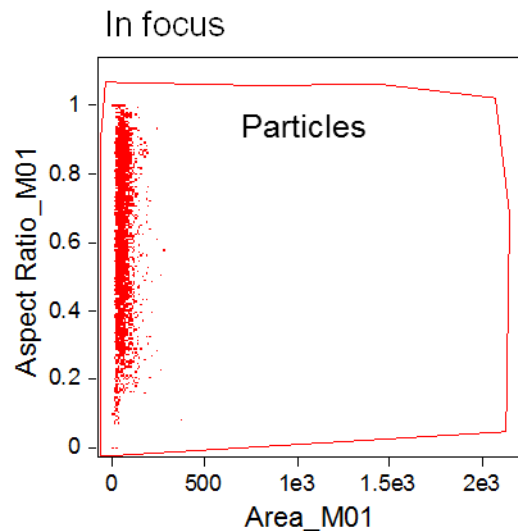


Figure 4.9.9.2. Step 1 of the development of the particle analysis template. Scatter plot of the area vs the aspect ratio to identify single particles.

Following the identification of single particles, a texture feature, the gradient RMS, which measured the overall contrast of a particle, was used to identify particles that were in focus. Consequently, a histogram of gradient RMS versus normalised frequency was plotted (Figure 4.9.9.3). Subsequently, the particles in focus were divided into elongated and circular populations, by plotting a histogram of aspect ratio versus normalised frequency. Having established particles in focus, shape features; elongatedness and circularity were used to identify elongated and circular particles.

The elongatedness feature is the proportion of the height over the width of the particle and was used to identify particles that were long or short. The circularity feature is the degree of similarity of a particle to a circle, and measures the average distance from a particles centre to its boundary, and is divided by the variation of the distance. Therefore, larger the variation, the further away the particle is from a perfect circle (Figure 4.9.9.3)

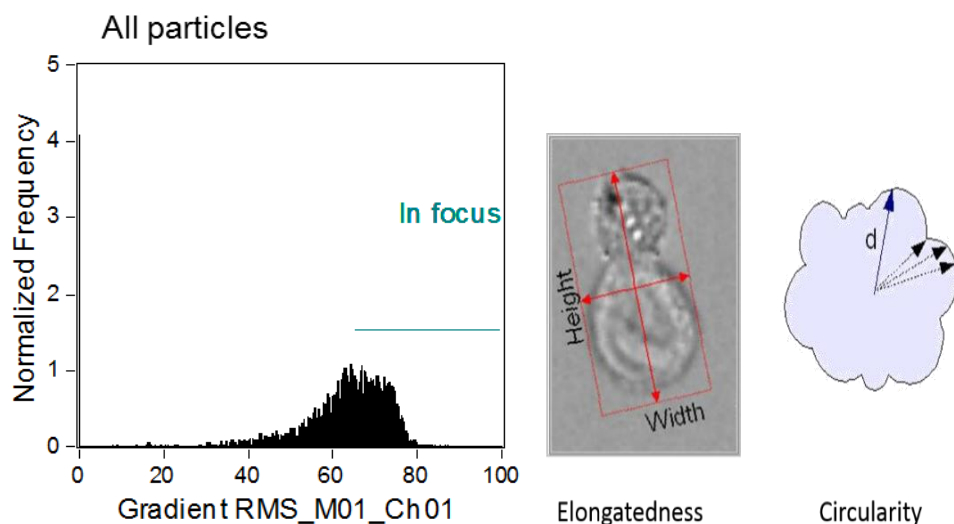


Figure 4.9.9.3. Template developed to identify particles that were in focus by plotting the histogram of gradient RMS. The images on the right show a description of the elongatedness and circularity of a particle.

The separation of elongated from circular particles was based on values of the aspect ratio which follows that particles with aspect ratios of close to 1 represents a circle while values of close to 0 represent a thin and elongated particle. As such, the interrogation of the aspect ratio histogram revealed that circular and elongated particles were easy to differentiate at the mid cut-off point. Consequently, particles with aspect ratio values ranging from 0 – 0.55 were gated as elongated particles, while aspect ratio values ranging 0.56 – 1.0 were gated as circular particles (Figure 4.9.5).

#### 4.5.3.2. Application of the developed template for the analysis of particle size

Having established a template for the analysis, the area, length and diameter size features were used to assess the size of particles in all four personal care products (Figure 4.9.9.5). The templates indicated that the area feature demonstrated the widest size distribution for the particles separated from all four products. In addition, the diameter feature exhibited the smallest particle size distribution (Figure 4.9.9.5).

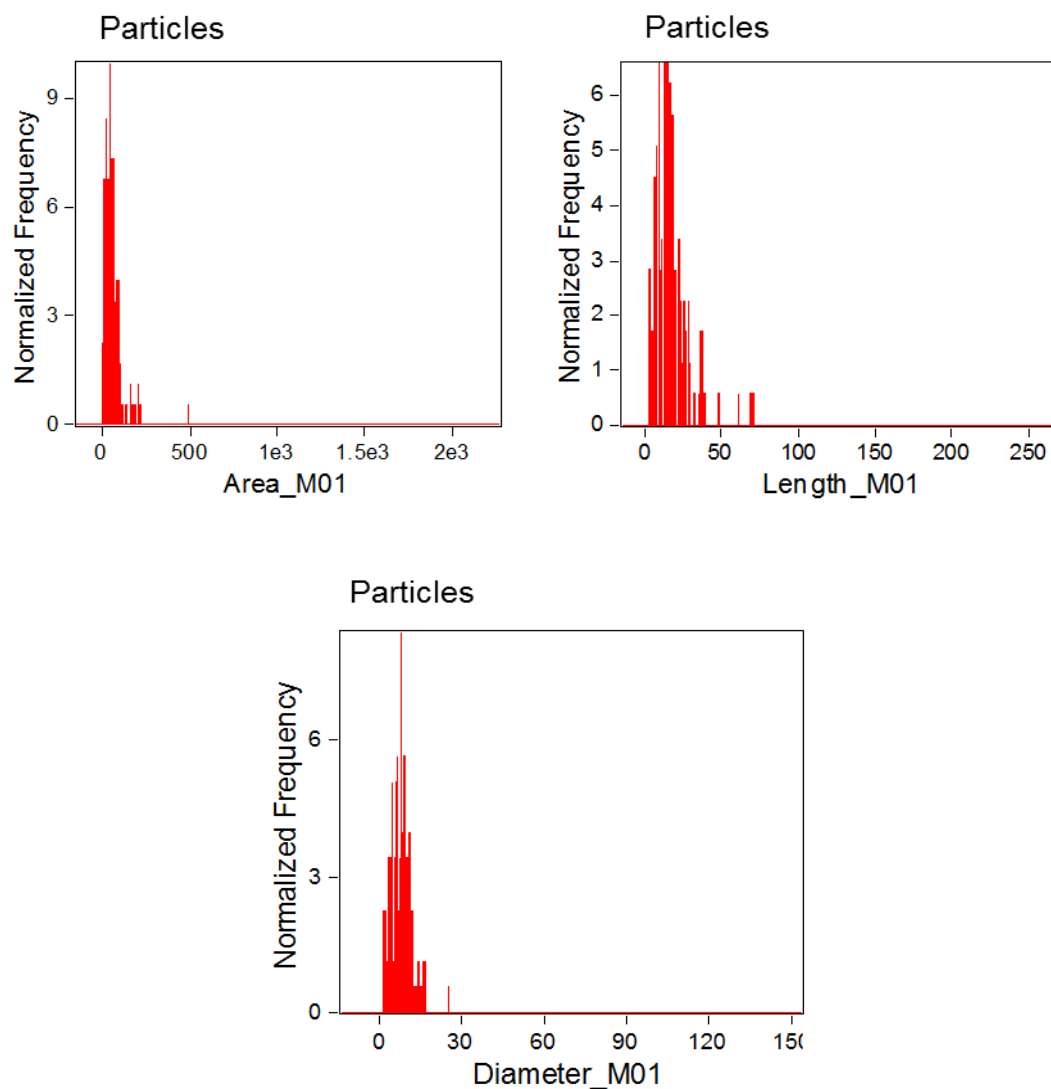


Figure 4.9.9.5. Area, length and diameter size features used to analyse particle size

#### 4.5.3.3. Analysis of particles separated from PCPs using the area size feature

In this section the template developed was used for the analysis of particles in the four products. In particular applying the area size feature demonstrated for the first time its application in microplastics research. To determine the area of particles based on the shape features, the elongated and circular shape features available in the template were applied determine particle area. In addition, the area for the elongated particles was generally larger than the circular particles, and this was true for the elongated particles analysed using the length and diameter features (Table 4.8).

The results of the area for ‘all’ particles indicated particle size ranged from 1 – 977.5  $\mu\text{m}^2$ , exhibited by particles in FS2 and FS1 (Tables 4.8). In addition, the mean particle size ranged from 37 to 63.1  $\mu\text{m}^2$ . However there were clear differences between the area of elongated and circular particles. For example, a comparison of the mean particle size indicated that the elongated particles exhibited the largest particle (Table 4.8). Furthermore, the results indicated that the elongated particles had the largest median particle size, by comparison to the circular and all particles (Table 4.8).

Following the evaluation of the particle size analysis by area, the analysis of particle size based on the length feature was also reported.

*Table 4.8. Area of particles in personal care products measured using Amnis ImageStream Mark II imaging flow cytometry. The area of particles is based on the ‘all’ particles, ‘elongated’ and ‘circular’ particles. The values for the area are in microns squared; all other values are in microns.*

All					Elongated				
Product	min	max	mean	median	Product	min	max	mean	median
TP1	2	312.5	48.5	43.5	TP1	5.5	265	49.3	43.5
TP2	2	492	54.2	47	TP2	7	492	55.0	48
FS1	3.5	977.5	63.1	44	FS1	5	822	88.8	57.5
FS2	1	768	37	32	FS2	3	435.5	32.8	28

Circular				
Product	min	max	mean	median
TP1	5	266.5	48.2	44
TP2	9	130	55.0	48
FS1	6	896	47	38.5
FS2	3	435.5	38.3	33

#### 4.5.3.4. Determination of the size of particles using the length size feature

The length for all particles generally ranged from 1 – 103  $\mu\text{m}$  demonstrating that FS2 and FS1 had the smallest and largest particles respectively (Tables 4.9). In particular, the size range was different for the elongated and circular particles. The elongated particles were generally larger than the circular particles (Table 4.9). By



comparison with the area size feature, the results indicated that the elongated particles determined using the length feature was larger by a factor of 3 (Table 4.9).

The results showed that the median particle size ranged from 7.5 – 17.5  $\mu\text{m}$  (Table 4.9). However the results indicated that the elongated particles exhibited larger median particle sizes by comparison to the circular particles (Table 4.9). In particular, the median size for elongated particles was larger than the circular and all particles (Table 4.9). However, the area feature indicated that the size of particles were generally larger than the particle size determined using the length feature (Table 4.9).

*Table 4.9. Size of all particles in personal care products measured using Amnis ImageStream Mark II imaging flow cytometry. Populations of particles were analysed based on the length feature using the template created. The size for all, elongated and circular particles are presented as minimum, maximum, mean and median, which are in microns.*

All					Elongated				
Product	min	max	mean	median	Product	Min	Max	Mean	Median
TP1	2	61	10.25	9.5	TP1	2.5	55.5	10.9	14
TP2	2	59	15.75	14	TP2	4.5	59	19.6	16.75
FS1	1.5	103	14.6	17.5	FS1	1.5	103	20.15	16.5
FS2	1	82.5	10.8	14.3	FS2	1	78	13.35	13.5

Circular				
Product	Min	Max	Mean	Median
TP1	2.5	48.5	10.3	8.5
TP2	3	32	13.1	11.25
FS1	3	62	11.215	9
FS2	2	76.5	10.05	7.5

#### **4.5.3.5. Assessment of particle size using the diameter size feature**

Generally, the diameter feature for the analysis of particles showed that particle size ranged from 1.1 – 33.7  $\mu\text{m}$  (Table 4.9.1). In addition the results indicated that there were larger elongated particles by comparison to the circular particles (Table 4.9.1). As such the diameter feature showed that elongated particle size ranged from 1.9 – 31.3  $\mu\text{m}$ , exhibited by particles in FS1 and FS2 respectively. Furthermore, particle size

determined by the diameter feature showed that particles were also smaller than particles determined by the area feature by a factor of 29 (Table 4.9.1).

The results indicated that there were differences in the mean particle size for the different shape features. For example, the range for the mean size for elongated particles ranged from 6.1 to 9.6  $\mu\text{m}$ , however, the circular particles exhibited a smaller mean size distribution that ranged from 6.6 to 7.8  $\mu\text{m}$  (Table 4.9.1). Therefore based on the mean particle sizes, the elongated particles were larger than the circular particles (Table 4.9.1).

However, a comparison of the largest mean particle sizes indicated differences for all the shape feature categories (all, elongated and circular), used for the analysis. Therefore, the mean particle size measured using the diameter feature was 7 times smaller than the area and approximately 2 times smaller than the length feature (Table 4.9.1).

The median particle size for the elongated particles indicated particle size ranged from 5.9 – 8.5  $\mu\text{m}$ , exhibited by particles in FS2 and FS1 respectively (Table 4.9.1). In addition, the results showed that the elongated particles exhibited larger particles by comparison to the circular particles (Table 4.9.1). However, the median sizes indicated that the diameter of the particles were 6 times smaller than the area and approximately 2 times smaller than the length feature measurements (Table 4.9.1).

*Table 4.9.1. Particle size determined using the Amnis ImageStream Mark II imaging flow cytometry. The diameter feature was used to analyse particle size and was categorised into all particles, elongated particles and circular particles. The values for the minimum, maximum, mean and median, and are in microns.*

All					Elongated				
Product	min	max	mean	median	Product	Min	Max	Mean	Median
TP1	1.55	19.8	7.5	7.4	TP1	2.5	17.95	7.55	7.35
TP2	1.5	20.7	7.7	7.7	TP2	3.55	20.7	7.65	6.95
FS1	2	33.7	8.2	7.45	FS1	2.5	31.3	9.65	8.5
FS2	1.1	31.15	6.55	6.3	FS2	1.9	28.65	6.15	5.9

Circular				
Product	Min	Max	Mean	Median
TP1	2.45	18.35	7.55	7.45
TP2	3.3	14	7.8	7.9
FS1	2.7	31.2	7.35	6.95
FS2	1.9	22.9	6.65	6.4

#### *4.5.3.6. Analysis of the particle size for artefacts of debris in blank samples*

As part of quality control, blank samples (filtered laboratory grade water processed alongside samples) were run and exhibited high particle counts. There were artefacts present in the samples that were different from the particles of interest. These artefacts had similar sizes to the particles in all products analysed. As such it was a challenge analysing particles in all products alone, because of the presence of the artefacts. Therefore the results for the analysis of the size of artefacts are presented in this section.

The size of the artefact particles detected in the blank water samples was determined using the area, length and diameter features. However, the size for 'all' artefact particles was determined for the analysis. Because a general assessment of the artefact sizes was required, the size for the elongated and circular artefacts was not determined. Typically, the largest size range was observed for the area of the particles and ranged from 6 – 614  $\mu\text{m}$ . In addition, the length of the particles ranged from 3 – 75  $\mu\text{m}$ , and the diameter of the particles ranged from 2.9 – 102  $\mu\text{m}$  (Table 4.9.2).

*Table 4.9.2. The average size for all artefacts analysed using the different size features for the imaging flow cytometry technique.*

Feature	min	max	mean	median
Area	6	614	40	33
Length	3	75	13.1	11
Diameter	2.9	102	8.7	7.2

#### *4.5.3.7. Comparison of the size of artefacts and particles in personal care products*

The area, length and diameter size features were applied to determine the size of artefacts and particles separated from four personal care products. From the results that the average size of artefacts in the blank water samples exhibited similarities and differences with the size of particles separated from all personal care products. For example, the average area for artefacts was smaller than the size of particles in TP1, TP2 and FS1. However, although the average area of artefacts was larger than the average area of particles in FS2, the values were similar (Table 4.9.3).

The similarities in the size of artefacts and particles in all products, made it increasingly difficult to separate the two distinct particle populations. The results indicated that the area and length of the particles in all products was generally wider than the artefacts seen in the blanks and samples. However, the diameter of the particles was smaller than the diameter of the artefacts (Table 4.9.3). An analysis of the average area, length and diameter of the artefacts and particles in all products indicated that there was no statistically significant difference [ $F(1,4) = 0.180417$ ,  $p = 0.692866$ ] ( $p < 0.05$ ).

Therefore, it is likely that the similarities in size would have made it difficult to successfully separate artefacts seen in the blanks and samples from the particles separated from the products.

*Table 4.9.3. Comparison of the average size of artefacts and particles in personal care products.*

Size feature	Artefacts	TP1	TP2	FS1	FS2
Area	39.9	48.5	54.2	63.1	37
Length	13.1	10.2	15.7	14.6	10.8
Diameter	8.7	7.5	7.7	8.2	6.5

The imaging flow cytometry demonstrated the ability to determine the size of particles in all four products. The results highlighted the differences in particle size based on the different size features used.

However, the ImageStream with its speed and sensitivity was able to detect artefacts that were seen in the blanks and sample of particles separated from the products. By comparison artefacts were not detected during the interrogation of blanks and particle samples by the microscopy and laser diffraction techniques. It is not clear why, but it is likely it is because the two techniques are not as sensitive as the imaging flow cytometry technique. In addition, because the application of the imaging flow cytometry technique is a novel application for the characterisation of particles in PCPs, it has provided baseline data upon which further studies can be conducted.

#### 4.6. Analysis of the number of particles in personal care products using microscopy and imaging flow cytometry

In this section the results for the estimation of the number of particles per 100 g in all the personal care products analysed are reported. The differences between each product and at the magnifications of 100X and 200X are presented here. In addition, the differences in the number of particles based on the shape features used for the flow cytometry technique are also reported. Furthermore, the differences between the estimates for the number of particles between the microscopy and imaging flow cytometry techniques are compared and reported in this section.

##### 4.6.1. Evaluation of the number of particles in personal care products by microscopy

This section shows the microscopy results to determine the number of particles in personal care products per 100 g. The quantification of the particles in the personal care products revealed differences in number, between all products analysed. In addition, there were marked differences in the number of particles counted between the 100X and 200X magnifications.

There were differences in the number of microplastic particles in the PCPs counted at the magnification of 100X. In addition, the difference between the smallest and largest number of particles in the products varied by a factor of 2. Therefore, the number of particles ranged from 6,234,000 to 13,190,667 particles per 100 g respectively, exhibited by particles in TP1 and FS1 respectively. In addition, TP2 and FS1 indicated a similar number of particles (Figure 4.9.9.6). Although there was an observed difference in the number of particles in all products, this difference was not statistically significant [ $F(2,9) = 0.001721$ ,  $p = 0.99828$ ] ( $p < 0.05$ ).

By comparison, the analysis of the number of particles determined at the magnification of 200X indicated differences with estimates determined at the magnification of 100X. The number of particles estimated at 200X magnification ranged from 12,642,667 (TP1) to 24,934,667 (FS2) particles, and varied by a factor of 2. In addition, TP2 and FS1 exhibited a similar number of particles and had 10,389,333 and 10,606,667 particles per 100 g respectively (Figure 4.9.9.6). However the difference in the number of particles determined at the magnification of 200X was not statistically [ $F(2,9) = 0.006008$ ,  $p = 0.994014$ ] ( $p < 0.05$ )

There was a clear difference for the number of particles counted at magnifications of 100X and 200X. For example, the number of particles in FS2 counted at magnifications of 100 X and 200X, varied by a factor of 2 (Figure 4.9.9.6). However, there was no statistically significant difference between the numbers of particles counted between both magnifications, [ $F(1,6) = 3.193781$ ,  $p = 0.124148$ ] ( $p < 0.05$ )

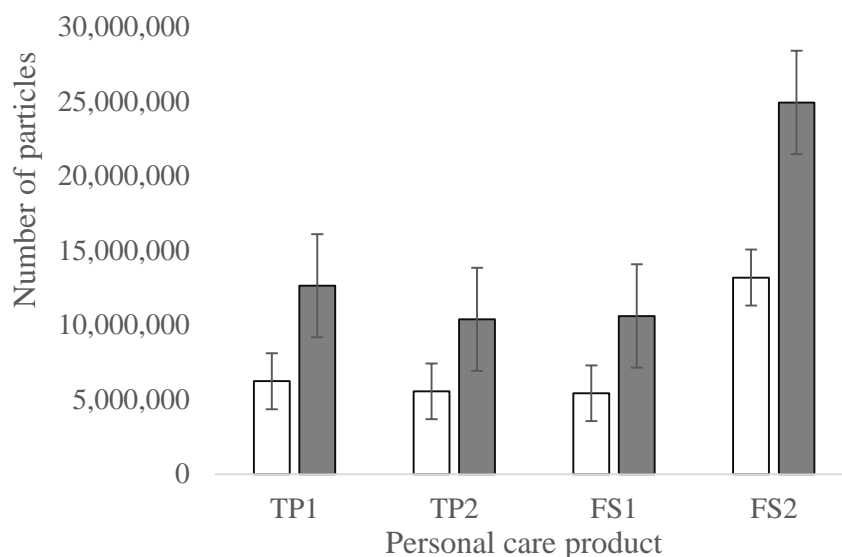


*Figure 4.9.9.6. Box plot showing the number of particles per 100 g counted in personal care products at 100X (white box) and 200X (grey box). The box plot shows differences in number of particles between all products.*

This study identified that particle count at different magnifications will indicate number of particles that would be largely different, thus supporting the hypothesis. Generally, the results showed the same trend with measurements to determine the size of particles in all four products. As such just as size measurements at 100X and 200X indicated differences in particle size within and between magnifications, the numbers of particles were also different within and between the magnifications used. Microscopy as a technique allows for the observation of particles, providing images which aid size measurements and observation of differences in size, as is the case of the particles in PCPs.

#### *4.6.2. Evaluation of the number of particles in personal care products by Imaging flow cytometry*

This section shows the results for the number of particles  $\leq 70 \mu\text{m}$ , in personal care products per 100 g. The number of particles in personal care products was not successfully determined in all products, by imaging flow cytometry. It was observed that the analysis of ultra-pure water samples revealed the occurrence of artefacts, which contained a high number of particles as background levels. Consequently only the number of particles in FS2 was determined. In addition, the results in this section

indicated a general decrease in the number of particles with time during analysis. Furthermore, there was no difference in the number of particles in each product counted, based on the size features (length and diameter). Likewise for the size features further categorised into all, elongated and circular particles, there was no difference in number for all products analysed.

As part of quality control, blank samples (filtered laboratory grade water processed alongside samples) were run and exhibited high particle counts. Consequently, the analysis of blank water samples revealed that 165,804 particles per unit mass were detected. Therefore the number of particles in each personal care product based on length and diameter features are blank corrected (Table 4.9.4). One sample, (FS2) exhibited particle numbers well above background count, with  $3,766 \times 10^6$  particles per 100 g. Furthermore, a comparison of the blanks with FS2 showed that the blanks accounted for 4 % (standardised to 100 g) of the total number of particles analysed by imaging flow cytometry (Figure 4.9.9.7). However the number of particles in other products could not be determined as they exhibited lower numbers to the blanks.

It was observed during the operation of the ImageStream that two factors could account for this, firstly in all samples except FS2, the recovered plastics rapidly separated (settled and/or floated in the tube) which, was compounded by a delay in data acquisition by the instrument. During this delay, although the instrument was not acquiring, images of larger plastic particles were visible on the real time image display, and the acquired data indicate a decline in both the size and number of particles with time, consistent, with uptake of a non-homogenous sample.



Table 4.9.4. Number of particles estimated in personal care products based on the length feature.

Product			Product		
		Number per 100 g			Number per 100 g
TP 1	All	ND	TP 1	Elongated	ND
TP 2		ND	TP 2		ND
FS 1		ND	FS 1		ND
FS 2		3766 × 10 <sup>6</sup>	FS 2		864 × 10 <sup>6</sup>

Product		
		Number per 100 g
TP 1	Circular	ID
TP 2		ND
FS 1		ND
FS 2		2878 × 10 <sup>6</sup>

Number of particles in personal care products using Amnis ImageStream Mark II imaging flow cytometry. Populations of particles were analysed based on all (A), elongated (B), and circular-like particles.

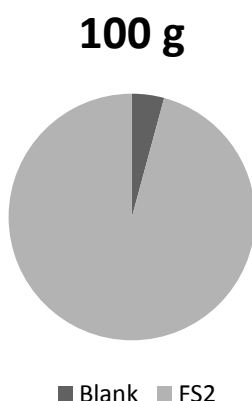


Figure 4.9.9.7. Pie chart indicating the proportion of artefacts in the blank samples to the particles in FS2.

There were observed changes in the number of particles estimated in all products over time. However, there were differences in time taken for the detection of larger particles across all the products. For example, based on the time series graph, there were larger particles indicated in TP1 and FS2 within 80 seconds of the analysis. However, by contrast, larger particles were still detected in TP2 and FS1, after 80 seconds of analysis (Figure 4.9.9.8). Furthermore, this time-particle size trend

indicating larger particles detected early in the analysis, was indicated more in FS2 than the other products (Figure 4.9.9.8).

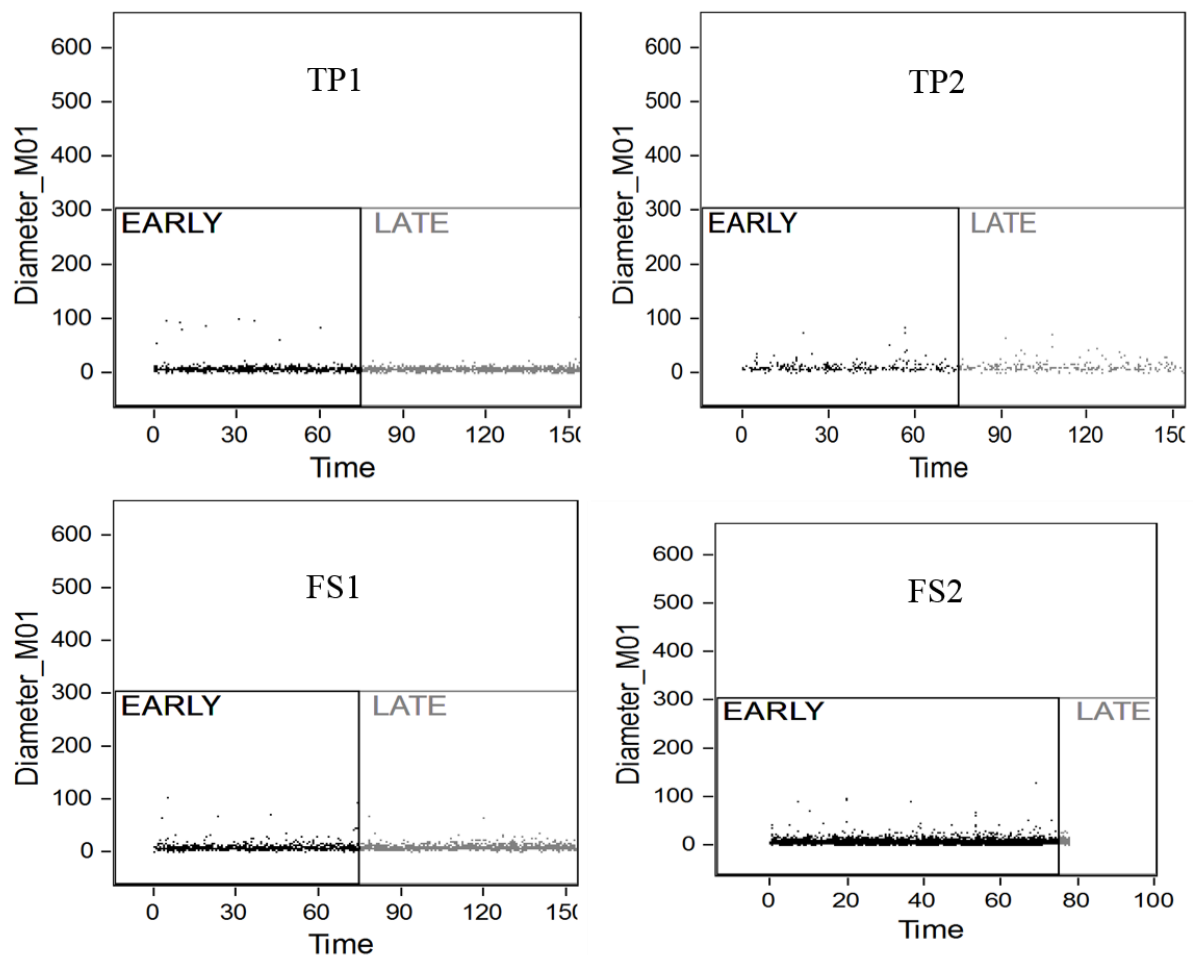


Figure 4.9.9.8. Time size analysis for the number of particles estimated in all products.

By comparison with microscopy, imaging flow cytometry indicated a higher number of particles by a factor of 151. Consequently, the application of the different techniques had an influence on the estimate of the number of particles.

#### 4.7. An assessment of particle morphology using light microscopy

In this section the results show that the morphology of particles was largely different across all the products analysed. In addition, this difference was obvious between particle assessments at magnifications of 100X and 200X. Particles observed at the

magnification of 200X were more detailed than those observed at a magnification of 100X.

Generally the particles observed in all four of the personal care products showed a variety of shapes within and between each product. These ranged from irregular, grain-like, elliptical, rods to threadlike shapes (Figure 4.9.9.9). However, there were only a few particles that appeared to be circular in shape, and it was observed that there were differences in the texture of the particles observed. In particular, the particles in FS2 appeared more grain-like, by comparison to the particles in TP2 that appeared threadlike and elongated (Figure 4.9.9.9).

.At 200X magnification, particles in all personal care products exhibited traces of smaller particles at some of the edges, especially in TP2 (Figure 4.9.9.9). It is likely that with a manual technique like microscopy, many of these particles will be missed or will take a long time to count.

The results also showed the different colours of the particles in the personal care products. The colours of particles in each product ranged from dark brown, grey, blue and black. In particular, TP1 exhibited particles that had a distinct blue colour, which was quite specific to this product.

For this study, the smallest particle that could be analysed was  $\geq 5 \mu\text{m}$ ; as such the morphology and colour of smaller particles could not be accurately determined (Figure 4.9.9.9). The different magnifications had an influence on the resolution of the particles in all products analysed. In particular, there were observed differences between particles from products at the same magnifications. In addition, seeing the particles can be used to decide if a good dispersion of the particles has been achieved.

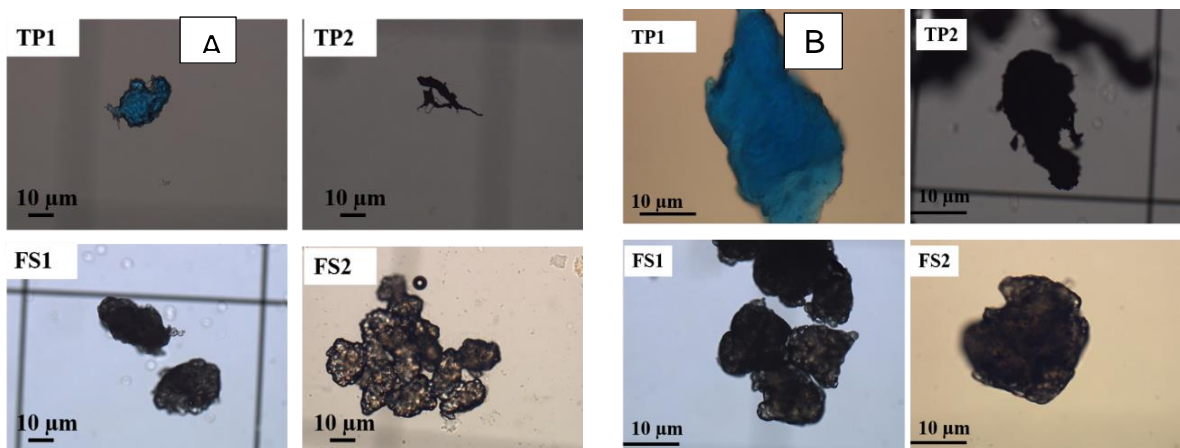


Figure 4.9.9.9. The different shapes and colours of particles analysed under a microscope at 100X (A) and 200X magnification (B).

#### 4.8. Evaluation of particle morphology as determined by Imaging flow cytometry

In this section, the morphology of particles in all products analysed show that particle shape in the  $\leq 70 \mu\text{m}$  fraction, ranged from elongated, irregular to circular-like shapes. The results also show the morphology of artefacts observed in the blank water sample. Therefore, the results of an assessment for the differences between particle shape and artefacts observed are reported.

During the analysis of particles, each individual object shown in the histogram or dot plots can be interrogated and viewed in the image display gallery. Therefore, this ensured accurate identification of the particles of interest. The morphology of particles in the personal care products was determined using shape features to show the distinct sub-populations of particles. Imaging flow cytometry recorded an image of each particle which facilitated post analysis observation of the shapes of the microplastics in each product analysed.

The particles observed ranged from elongated, irregular to circular-like shapes which were present in all samples including the blanks (Figure 4.9.9.9.1). However, particles in one product had a distinct morphology to particles in other products. Specifically, the particles in FS2 showed unique characteristics, notably a large number of perfectly circular objects. The fact that similar particles were not

observed in other samples maybe due to their true absence and/or an artefact of separation during introduction to the imaging flow cytometer.

An automated technique like the imaging flow cytometry did not fit with how a manual method like microscopy evaluates particles. Therefore the application of a different technique like imaging flow cytometry had an influence on the detail of the particle morphology. The ImageStream which combines the power of microscopy and flow cytometry is useful for the multi-spectral imaging of particles in flow. Furthermore, it creates a record of files and stores images automatically, that can be viewed later. This is unlike the microscopy technique where each image has to be acquired manually at the time of observation.

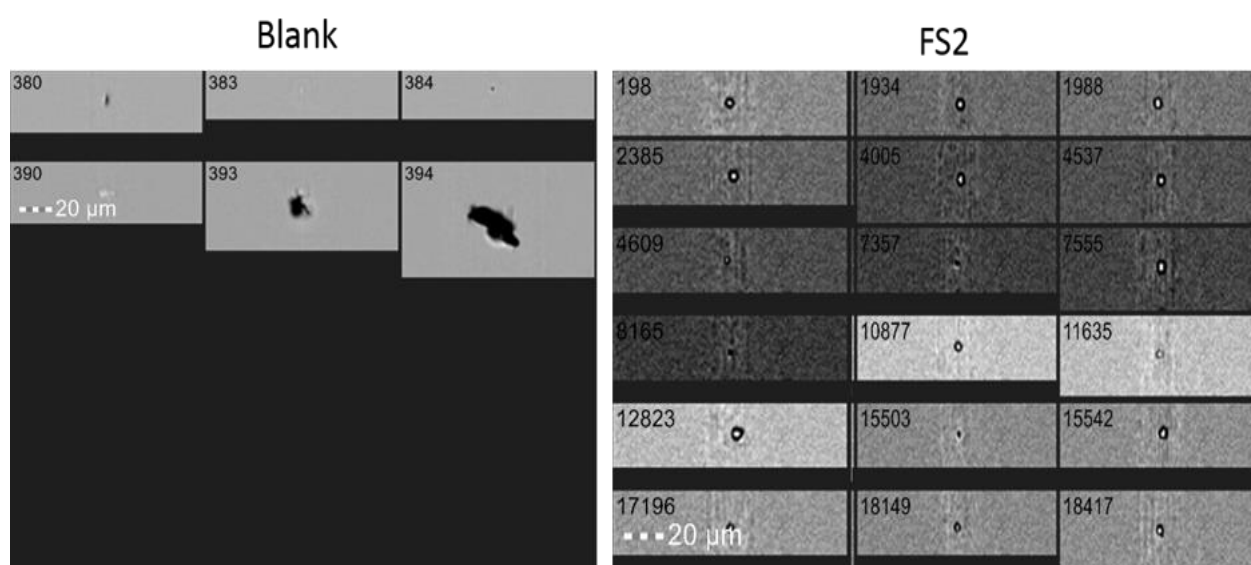


Figure 4.9.9.1. Analysis of microplastics in personal care products using the Amnis ImageStream@X MkII at 20x magnification. Particles observed in blank samples (left image) and microplastics seen in FS2. Scale bar for all images is 20  $\mu\text{m}$ .

The results indicated that in all PCPs, some particles exhibited side scatter properties, as indicated by their detection in channel 06 (Ch06), which is the designated channel that detects this property (Figure 4.9.9.2). The imaging flow cytometer allows for the detection of particles that demonstrate these properties, and can be used to detect microplastic particles. However, it could not be applied in this study, because some particles in the blanks also exhibited side-scatter properties.

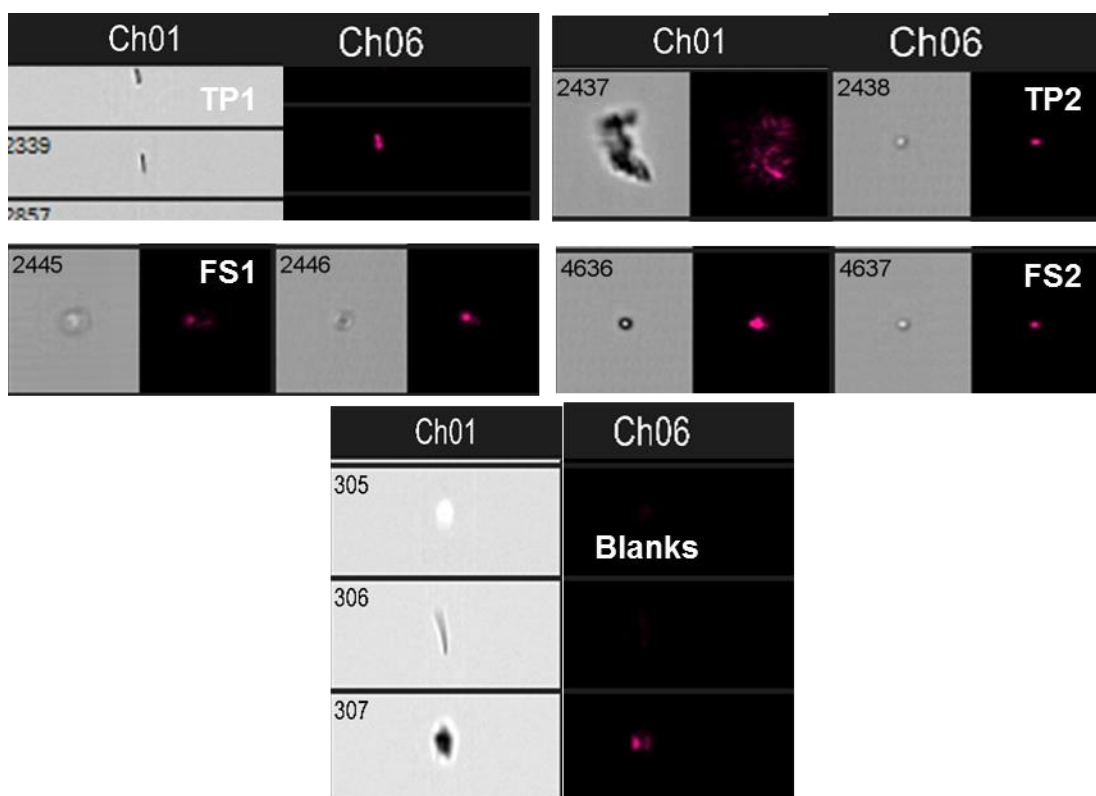
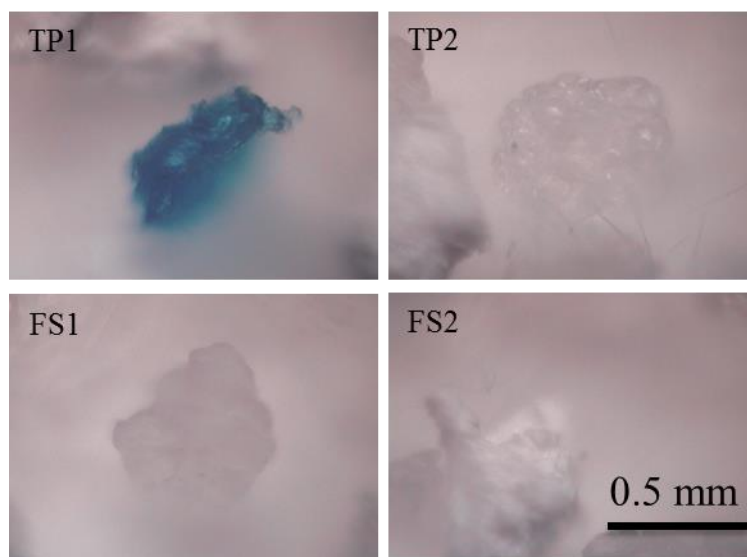


Figure 4.9.9.9.2. Image shows particles in PCPs and blank water samples that exhibited side-scatter properties.

#### 4.9. Assessing particle morphology in products using micro-FT-IR.

The morphology of particles separated from personal care products was determined using the micro-FT-IR technique. The particles exhibited differences in their colour and morphology for all the products analysed (Figure 4.9.9.9.3). It was also again observed that particles in TP1 had a blue colour that was unique to this product alone. Similar to the imaging flow cytometry technique, an automated technique like the micro-FT-IR did not fit with the evaluation of particle shape, like the manual microscopy technique. By comparison with the imaging flow cytometry, both techniques exhibited differences in particle shape and in the detail of the shapes. The micro-FT-IR technique only allowed for the direct observation of the particle morphology, but the imaging flow cytometry used templates for the analysis of particle morphology. Therefore the application of a different technique like imaging flow cytometry had an influence on the detail of the particle morphology.

Although the FT-IR technique is widely used for the identification of particles, it can also be applied to the assessment of particle morphology. In addition, because it is a relatively automated technique, it allows for the investigation of particles of interest and as such, can be used to analyse the shapes and colours of the particles. Similar to the microscopy and imaging flow cytometry techniques, the FT-IR demonstrates the ability to detect agglomeration of particles and assess the degree of dispersion of the particles of interest.



*Figure 4.9.9.3. Analysis of particles in personal care products using the micro-FT-IR technique.*

#### *4.1.0. Application of infrared spectroscopy for the identification of polymer particles in personal care products*

This section shows the results for works conducted for the identification of particles separated from the personal care products. Using the functional group region of the IR spectrum, all particles were successfully identified with the absorbance peaks corresponding to the wavenumber regions unique to the polymer. Therefore, the application of micro-FT-IR and ATR-FT-IR technique confirmed the polymer identity of the particles separated from personal care products. Furthermore, the chemical imaging of particles separated from personal care products is also presented in this section. The micro-FT-IR technique was useful for the chemical imaging of the particles, and was presented as false colour images. All particles in the personal care

products were successfully identified using the regions of absorbance to confirm polymer identity.

#### **4.1.1. Determining the Polymer identity of particles in PCPs using micro-FT-IR**

The results presented as absorbance spectra showed that generally, the analysis of the particles demonstrated infrared absorption over the entire region of absorption, from 4000 -750  $\text{cm}^{-1}$  (Figure 4.1.0). There were clear differences in the intensity of the absorbance peaks observed across the IR spectrum. In particular, there were noticeable high absorbance peaks, at the short wavelength (high wavenumber) end of the absorption spectra (Figure 4.1.0). The polymer identity of the particles was determined by assessing the absorbance peaks mainly in the functional group region of the IR spectrum (4000 – 1500  $\text{cm}^{-1}$ ) and in the finger print region (1500 – 500  $\text{cm}^{-1}$ ). Consequently, the results of the scans demonstrated the presence of absorbance peaks in each polymer at 1500-1450  $\text{cm}^{-1}$  and 3000-2770  $\text{cm}^{-1}$ , indicated by the bending and stretching of C-H bonds respectively. Therefore it was confirmed that the peaks identified in the absorbance spectra of the particles were unique to polyethylene. Consequently, all particles separated from the personal care products were polyethylene.

Generally, the particles showed weak to strong absorbance peaks across the IR spectrum. Typically, there were strong peaks of C-H bonds between 3000-2770  $\text{cm}^{-1}$ , compared to the relatively medium absorbance peaks between 1500-1450  $\text{cm}^{-1}$  and 750  $\text{cm}^{-1}$ . There were observed differences in the absorbance peaks in each product and across all the products analysed (Figure 4.1.0). For example, there was a relatively low absorbance in TP1, by comparison to particles in other products analysed. Typically in TP1, the absorbance peaks for the C-H bonds between 3000 – 2770  $\text{cm}^{-1}$  demonstrated an absorbance of ~ 0.26 and 0.27 Au (Figure 4.1.0). By contrast, particles in FS1 exhibited the highest absorbance peaks at 0.45 and 0.47 Au, corresponding to the C-H bonds between 3000 – 2770  $\text{cm}^{-1}$  (Figure 4.1.0). To confirm the polymer identity of the particles a table indicating the FT-IR peaks and functional groups indicative of the plastic polymers was consulted (Table 4.1.0). In addition, particles were also identified using a spectrum search in a customised



polymer library that contained the spectra of polymers commonly associated with microplastics.

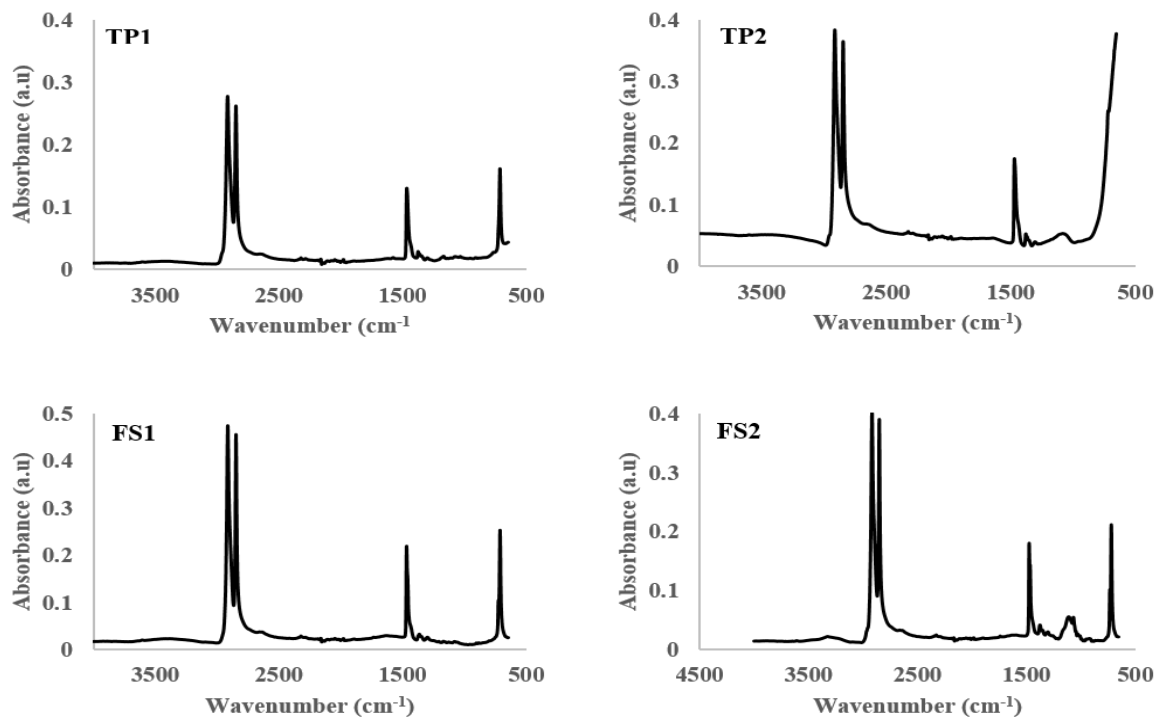


Figure 4.1.0. Reflectance micro-FT-IR spectra of polyethylene scanned in absorbance mode using the micro-FT-IR. The absorption peaks were based on reflectance in imaging mode with 2 co-added scans per pixel, an aperture size of 25  $\mu\text{m}^2$  and at a spectral resolution of 16  $\text{cm}^{-1}$ .

*Table 4.1.0. IR absorptions of the functional groups for the identification of polymers of polyethylene and polyester.*

IR Frequency (cm-1)	Functional Group
Polyethylene	
2914, 2846	CH <sub>2</sub> stretch
1474	CH <sub>2</sub> bend
720	CH <sub>2</sub> rock
Polyester	
2969, 2907	C-H stretching
1711	C=O stretching
1504	Aromatic ring C=C stretching
1472, 1405, 1340	C-H bending
1241	Ester's C-O stretching
1093	C-O stretching
871	Aromatic ring C-H bending
718	C-H bending

The micro- FT-IR technique combines the imaging capabilities of microscopy and FT-IR spectroscopy and requires relatively little simple preparation. In addition, the micro-FT-IR demonstrates the enhancement of spatial resolution, and allows for the identification of infrared bands and comparison with progressively smaller samples. Another advantage is that particles can be directly examined on membrane filters. This technique offers the user both reflectance and transmission mode options for the analysis of samples, both of which have their advantages and limitations. For this study, the reflectance mode was used which allowed for the analysis of opaque samples similar to the particles from the personal care products. A major advantage with micro-FT-IR is the application of focal plane array detectors (FPA), which allows for the simultaneous and rapid collection of large amounts of infrared spectra for

particles in a sample; without the need to select particles by eye before analysis, and also provides an independent infrared spectrum. However, depending on the settings of the instrument, for example, the number of co-added scans, the analysis can take between minutes to hours to conduct.

#### *4.1.2. Determining the particle identity using ATR-FT-IR*

To assess whether reflectance micro-FT-IR had an effect on the spectra of particles, especially with regards to the shape of the particles, the analysis was compared to spectra produced by the ATR-FT-IR analysis. Consequently, the ATR-FT-IR was explored as an alternative technique for the polymer identification of particles in all products. The polymer identity of the particles in all four products was determined by identifying peaks in the functional group region of the IR spectrum ( $4000 - 1500 \text{ cm}^{-1}$ ) and finger print region ( $1500 - 500 \text{ cm}^{-1}$ ) (Figure 4.1.1). Therefore, peaks were identified at  $3000-2770 \text{ cm}^{-1}$  and  $1500-1450 \text{ cm}^{-1}$ , which indicated stretching and bending of C-H bonds respectively, were unique to polyethylene (Figure 4.1.1). Consequently, all particles separated from all products and analysed by ATR-FT-IR were polyethylene.

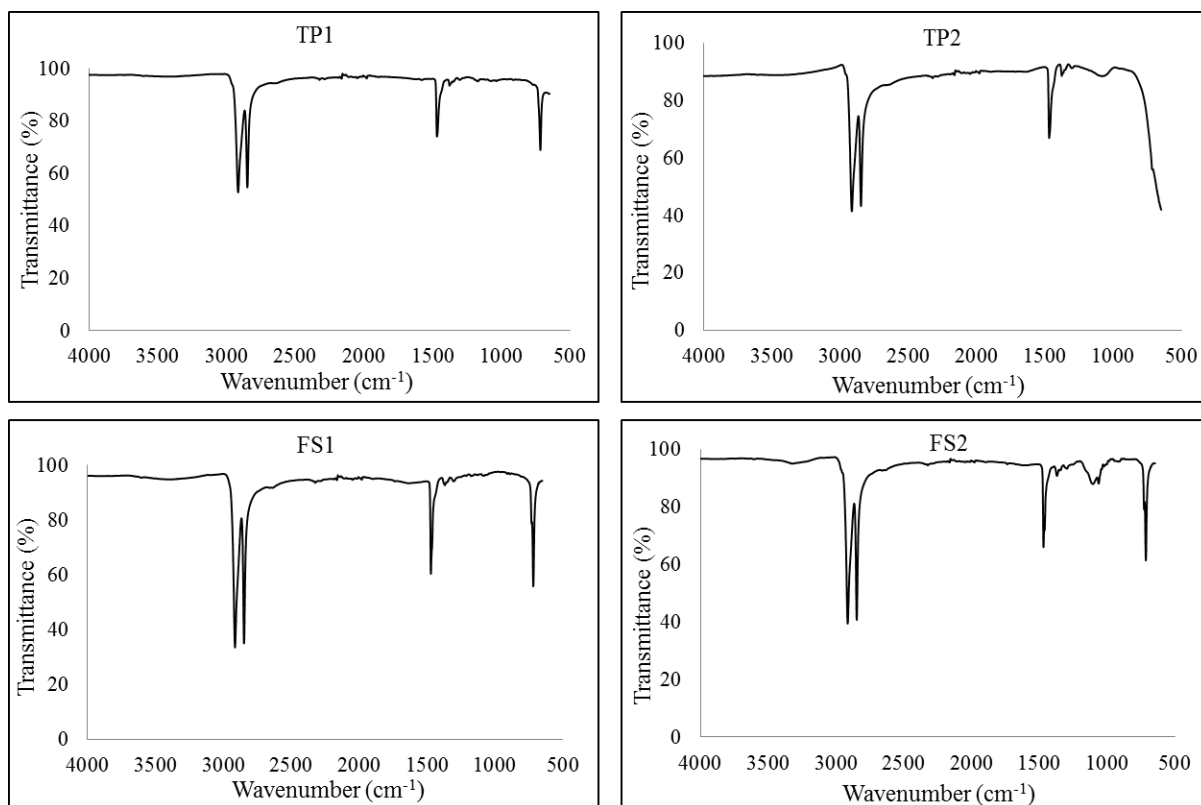


*Figure 4.1.1. ATR-FT-IR spectra of polyethylene particles identified in all personal care products. The peaks were based on reflectance in imaging mode with 2 co-added scans per pixel, an aperture size of  $25 \mu\text{m}^2$  and at a spectral resolution of  $16 \text{ cm}^{-1}$ .*

The ATR-FT-IR technique proved useful in the polymer identification of particles in all four products analysed. By comparison, the micro-FT-IR technique did not have an effect on the spectra of the particles. In addition, the shapes of particles in all four products had no effect on the spectra. The ATR-FT-IR technique allowed for the direct analysis of particles without the need to scan the surface of a filter paper. Therefore this technique is a rapid approach for the polymer identification of particles and can be used as a complementary technique with micro-FT-IR.

#### 4.2. Multi-technique comparison to characterise particles in personal care products

The following section describes the characterisation of particles separated from personal care products using different techniques. In particular it highlights the comparison for the results of the different techniques used in the study. Furthermore the section is classified based on the analysis of particle size, number and

morphology. In addition each of the techniques used demonstrated different uses and applications

#### *4.2.1. Comparison of applied techniques used to determine particle size*

There were observed differences in the size, number and morphology of the particles analysed based on the different techniques used. In particular, the imaging flow cytometry results indicated the widest particle size distribution, based on the application of the area measurement size feature. This was followed by the laser diffraction measurements that revealed a wide size distribution, but was smaller in comparison to the imaging flow cytometry analysis. However of all the techniques used; microscopy demonstrated the smallest particle size distribution. Likewise, it was clear from the results that there were differences in the number of particles determined by using the different techniques. Therefore, the analysis of the number of particles showed that imaging flow cytometry exhibited the largest number of particles compared to the microscopy analysis. In addition, the morphology of the particles demonstrated the presence of similar shapes and colours for microscopy, imaging flow cytometry and FT-IR.

Using the average size of particles, the laser diffraction technique indicated the largest particles in the four products analysed. This was followed by particles analysed by the microscopy technique and finally by the particles measured using the imaging flow cytometry technique which revealed the smallest particles because it measured particles in the  $\leq 70 \mu\text{m}$  fraction (Figure 4.2).

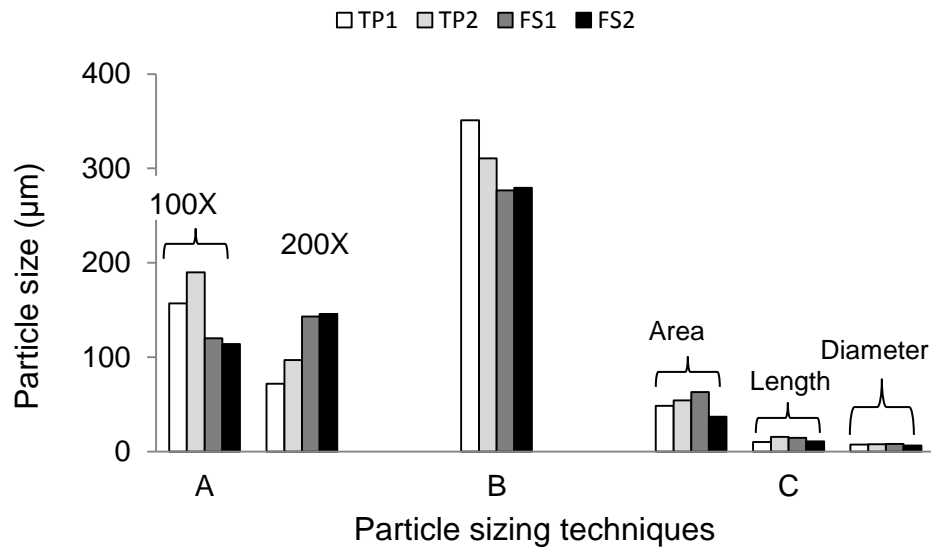


Figure 4.2. Bar chart showing the mean size of particles as determined by the different techniques used. The chart shows the size of particles determined by microscopy at different magnifications (A), laser diffraction (B) and imaging flow cytometry (C) techniques.

Apart from the differences in particle size, there were differences in the mode of analysis. For example, the laser diffraction technique, allowed the classification of particles size analysis based on the 'D' values, which indicated the differences based on particle texture. In addition, the classification of the size of particles was also based on the volume of the particles in the sample, otherwise called the volume distribution. Therefore it was possible to determine the size of particles at a particular percentage volume in the given sample.

By comparison, the imaging flow cytometry technique allowed for the automated analysis of particles and classification according to size features. In addition, it gives great detail of the  $\leq 70 \mu\text{m}$  fraction, showing wide size distribution within it. Therefore, apart from the area, the length and diameter of the particles were determined. Furthermore, it allowed for the classification of the particles based on the shape features. Therefore, particles were categorised into elongated, circular and 'all' particles. This was the only technique that demonstrated the ability to apply templates that automatically characterised particles based on set criteria.

This automated classification of particles was not possible with the microscopy technique. However, the microscopy technique allowed for the analysis of particle size at two different magnifications which revealed differences in particle size. This was useful in determining the observed differences in the size of particles between the magnifications. Although the option of different magnifications is possible with the imaging flow cytometry, the use of different magnifications is only limited by the field of view. For example at the magnification of 20X used for this study, the field of view was 120  $\mu\text{m}$  width, however, a larger magnification of 60X has a smaller field of view of 40  $\mu\text{m}$  width (Amnis EMD Millipore 2012).

Likewise, the laser diffraction technique did not allow for the analysis of particles at different magnifications, as such it was not possible to compare particle size on that basis. Although the microscopy technique was manual and labour intensive, it allowed for direct observations of particles in all products analysed. That way, it was clear to see single and aggregate particles and determine particle size. However, the classification of particle size was not automated as it was with the imaging flow cytometry and the laser diffraction techniques.

The techniques used for the measurements of particles demonstrated different modes of operation. It is likely that manual techniques are prone to bias, which is less likely in the automated techniques. A comparison of the sizing techniques showed that the differences exhibited in the size of particles is likely because of the different measurement operating principles of the individual techniques. The application of the different techniques showed that different results will be produced for the same particles in a given sample. This is important especially in the evaluation of particle size in microplastics research. Furthermore, it is apparent that results produced by applying different techniques should be described based on the respective techniques used.

It was hypothesised that measurements of particles size will produce results that would be similar, however, this has been disproved. Consequently, the application of the different techniques apparently had an influence on the size of particles in all four products analysed.

#### *4.2.2. Evaluation of the particle number as determined by the application of different techniques*

Given that different techniques were used, there were clear differences in the number of particles in all products analysed (Figure 4.3). Although this study did not quantify particles by laser diffraction, the application of the imaging flow cytometry exhibited higher number of particles in FS2, than the number particles determined by microscopy (Figure 4.3). The highest number of particles determined by imaging flow cytometry was more than highest number of particles as determined by the microscopy technique, by a factor of 151. However, although the number of particles was not successfully determined in all products using imaging flow cytometry, both techniques indicated FS2 exhibited the largest number of particles. It is likely that the difference in the number of particles was because of the different modes of operation for both techniques. Typically, the imaging flow cytometry technique demonstrated the ability to automatically quantify particles, including debris. By contrast, using microscopy which is a manual technique, it was easier to observe particles that were different from those separated from the personal care products and accounted for debris. Therefore with microscopy, it was easier to identify debris by direct observation on the SRC, and so avoided counting them.



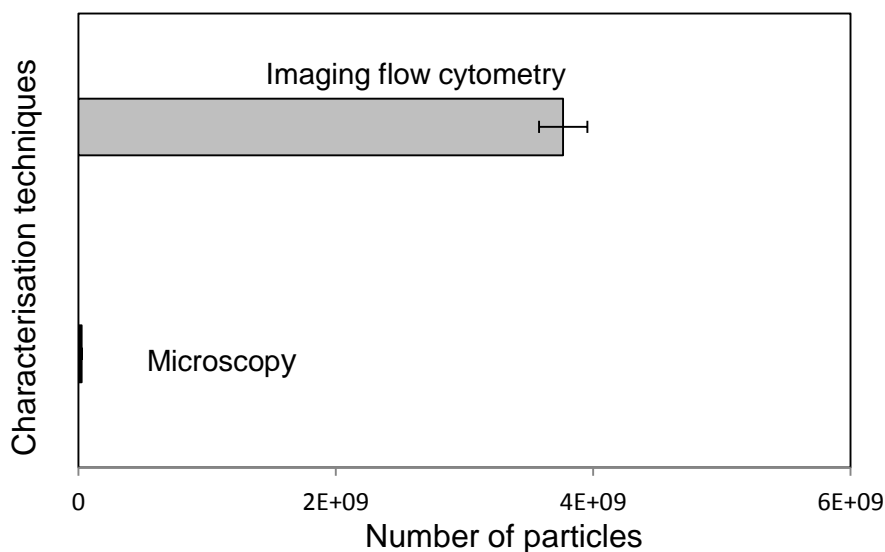


Figure 4.3. Bar chart showing the number of particles determined by the different techniques used. The larger number of particles as determined in FS2, by the imaging flow cytometry technique and the smaller number of particles as determined in FS2 by microscopy is also highlighted in the chart.

#### 4.2.3. Comparison of particle morphology applying different techniques

There was a wide range of particle shapes in all four products analysed. In addition, the different techniques demonstrated differences in the general shapes for the particles analysed. The shapes of the particles ranged from irregular, rods to grain-like shapes. The microscopy technique exhibited a more detailed shape description in comparison to the other techniques. Microscopy showed that there were irregular, grain-like, elliptical, rods to threadlike shapes (Figure 4.4). Similarly, the analysis of particle shape by the FT-IR technique revealed that particle shape ranged from elongated, irregular to circular-like particles and particles appeared more detailed. Using the microscopy and micro-FT-IR techniques, contours and particle shape characteristics were observed in more detail (Figure 4.4). By contrast, the imaging flow cytometry revealed less clearly defined shape descriptions, but it allowed for the classification of particles into elongated, irregular to circular-like shapes (Figure 4.4).

Some particles had a shape that was unique to one of the products analysed. As such a comparison of the shapes across the techniques demonstrated that the particles in FS2 appeared generally circular and this was true for all techniques except FT-IR, which showed artefacts around the edges of the particle. These artefacts were

also visible in the microscopy images but not obvious in the imaging flow cytometry images (Figure 4.4). The techniques also demonstrated differences in the colour of the particles in all products analysed.

The microscopy results showed a more realistic true colour description of the particles, followed by the FT-IR and the imaging flow cytometry. For example the unique blue colour of TP1 was observed using microscopy and the FT-IR, but was in grey colour with the application of the imaging flow cytometry (Figure 4.4). The difference in the colour output is likely due to the different modes of image capture unique to each technique. It is possible that manual and automated techniques will produce differences in the shape and colour of the particles observed. Generally, the different techniques demonstrated the ability to determine particle shape. The different techniques apparently had an influence on the shape and colour of the particles in all four products analysed.

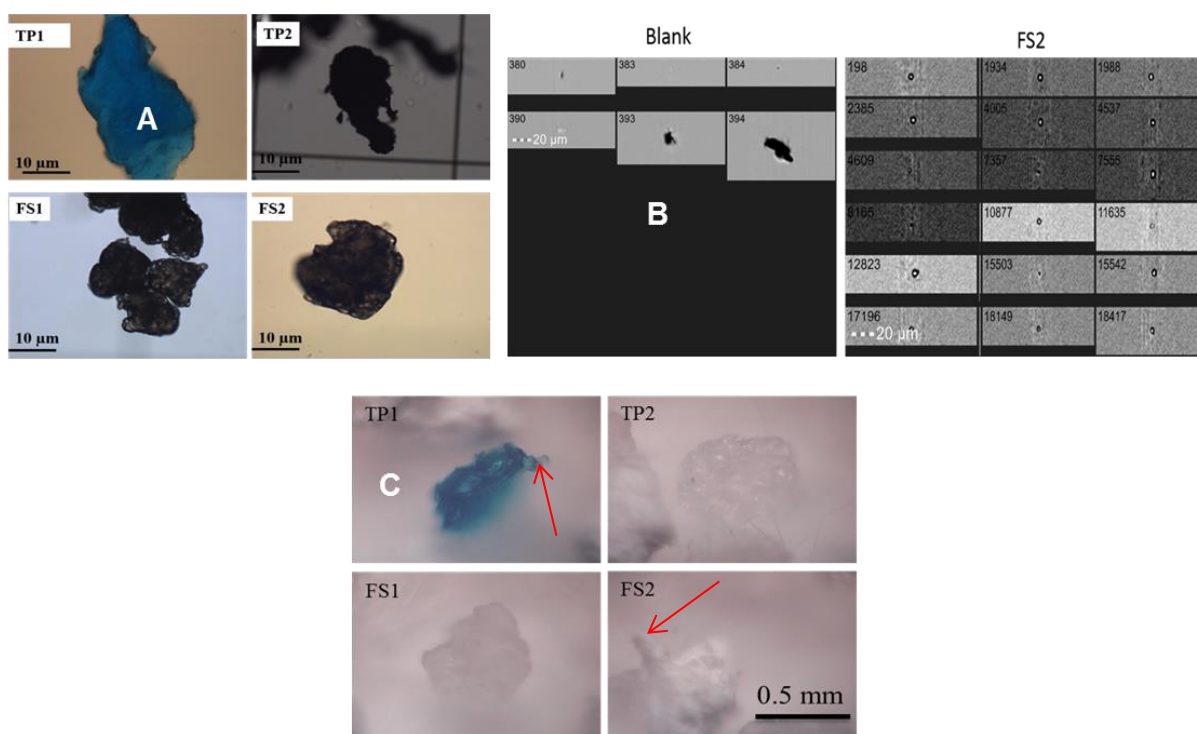
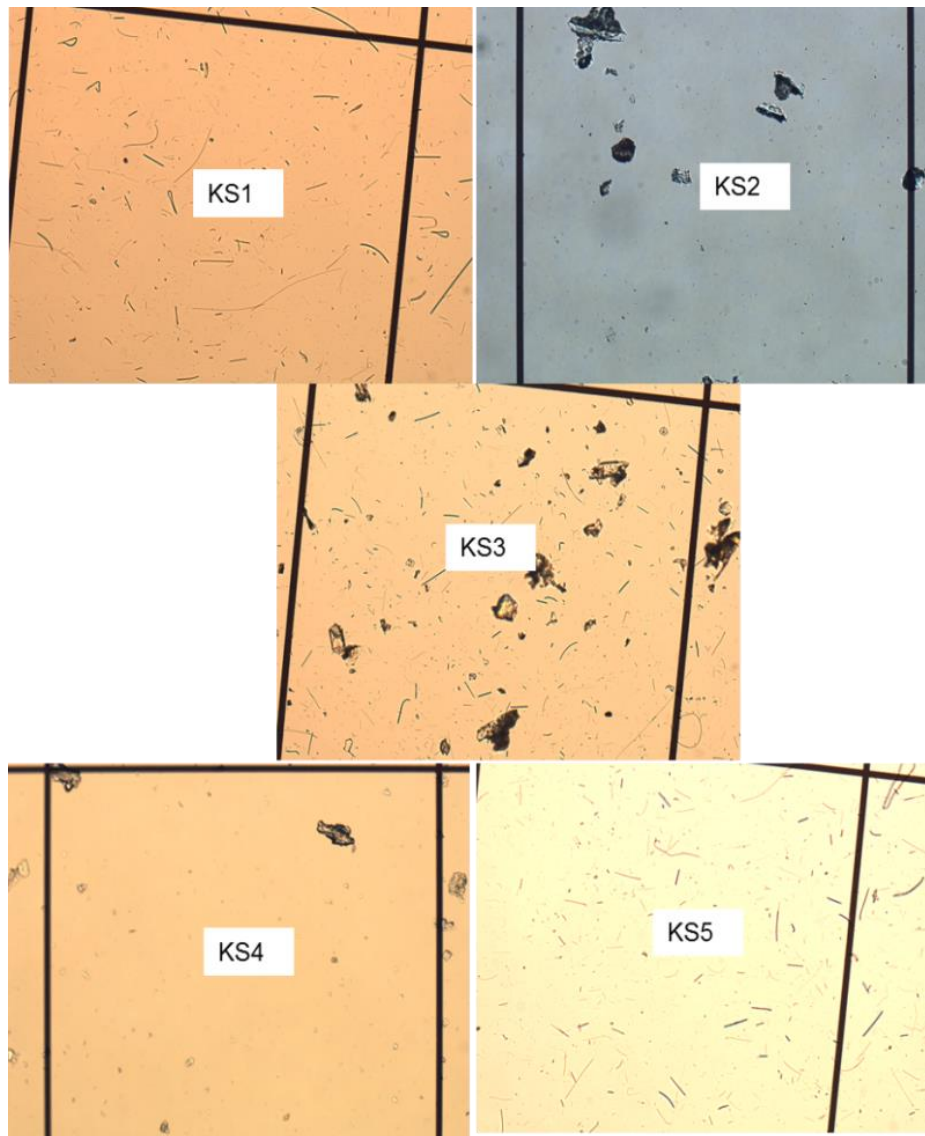


Figure 4.4. The images of particles in the personal care products are shown in the image above. The microscopy (A), indicate different shapes and colours of particles. The imaging flow cytometry (B) highlights different classifications for shape and shapes for artefacts. The micro-FT-IR (C) indicates the details and contours of particles in all products.

Similar to the analysis of microplastics separated from PCPs, challenges were encountered for the characterisation of particles abraded from KS. These challenges are detailed in the following section.

#### 4.3. Challenges encountered in method development for the characterisation of particles from kitchen scourers.

The methodology developed for the characterisation of particles separated from personal care products was applied to particles abraded from kitchen scourers. However, the type of material from which the particles in the kitchen scourers were made from, influenced the application of already developed methods and therefore the characterisation of the particles. In particular, the size and number of particles abraded from the kitchen scourers was difficult to estimate, particularly because of the high number of fibre particles present in the samples. The high number of fibre particles was more obvious for all kitchen scourers, except KS2 and KS4 that did not abrade fibre particles. Furthermore, these observations were apparent when the abraded particles were analysed under the microscope at the magnifications of 100X (Figure 4.5).



*Figure 4.5. Photomicrograph of particles abraded from all kitchen scourers and determined at the magnification of 100X. The image shows a high number of fibre particles in KS1, KS3 and KS5.*

Because of the high number of fibre particles, it was difficult to clearly distinguish between the different particles of fibre and to determine particle size. Consequently, to reduce the high number of particles and to ensure measurements for particle size were determined, the samples of abraded particles were diluted. After the dilution step, it was possible to determine the size of all particles and in particular, fibre particles abraded from all kitchen scourers. However fibres were not observed in KS2 and KS4 (Figure 4.6).

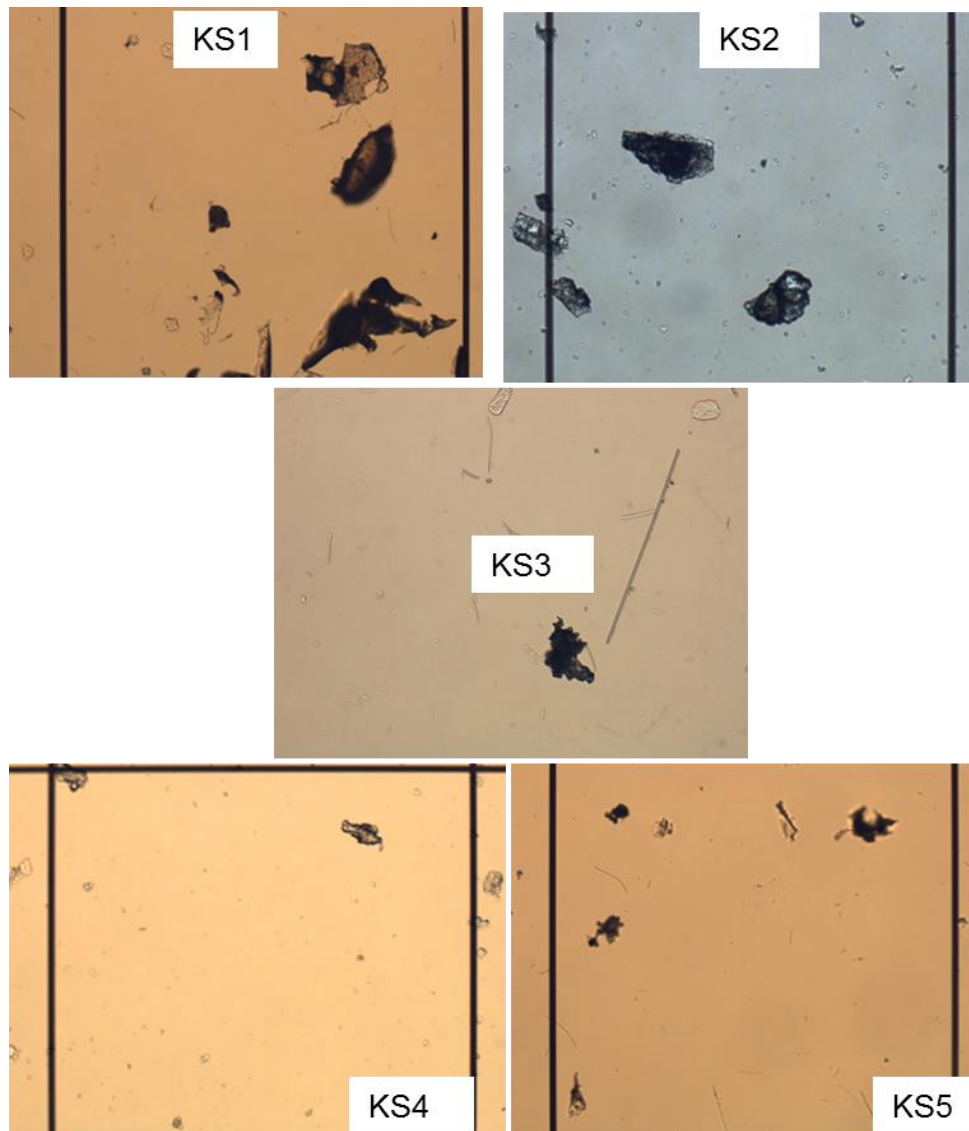


*Figure 4.6. Photomicrograph of diluted sample of particles abraded from all kitchen scourers and determined at the magnification of 100X.*

All samples to determine the size and number of particles abraded from kitchen scourers were diluted because this sample preparation step reduced the concentration of particles and allowed for the particle analysis to be conducted. Therefore this step was adopted in the final experiments, and the results are presented in the next section.

#### 4.4. Final results for the characterisation of particles abraded from kitchen scourers

In this section the results for the characterisation of particles abraded from kitchen scourers are presented. In addition, the results are based on the application of the methods and different techniques developed for the characterisation of particles in

personal care products. The techniques were useful for the characterisation of particles abraded from kitchen scourers. In this chapter, the results are sectioned according to the size, number morphology and polymer identity of the particles in all five kitchen scourers. Likewise, the results for the characterisation of particles, based on the shape and size features are also presented in this chapter. A comparison of the results for the characterisation of particles using different techniques is also reported. Consequently, particle size measurements by microscopy was reported based on the 100X and 200X magnifications, size distribution of particles was determined by laser diffraction, and the analysis of smaller size particles  $\leq 70 \mu\text{m}$  using the imaging flow cytometry was also reported. Furthermore, the polymer identity of particles abraded from kitchen scourers were confirmed using the micro-FT-IR, ATR-FT-IR. False colour images were also used to determine the intensity of absorbance as measured on the scale of absorbance.

#### 4.4.1. Assessing the size of particles from kitchen scourers using Microscopy

The microscopy study allowed for the observation of differences in the size of particles abraded from the kitchen scourers. In particular, to demonstrate differences in size, the particles were classified according to two observed and distinct shapes (fragments and fibre), and was applied in all the five kitchen scourers analysed. It was observed that these differences were also noticeable when particles were measured at magnifications of 100X and 200X (Table 4.1.1). Therefore, the overall average particle size range was from 5 – 390  $\mu\text{m}$ , measured at magnification of 100X. As such the smallest and largest particles were observed in KS4 and KS1 respectively (Table 4.1.1).

By contrast size measurements conducted at 200X magnification demonstrated an overall average particle size range from 2.5 – 1566.5  $\mu\text{m}$ . The largest particle measured at magnification of 200X was ~ 4 times the largest particle determined at a magnification of 100X (Table 4.1.2). By comparison, measurements conducted at the magnification of 200X allowed for the observation of smaller particles. For example, at the magnification of 100X, the smallest particle observed was larger than its equivalent determined at the magnification of 200X, by a factor of 2.

In this study, shape features were used to determine the different categories and sizes of particles abraded from kitchen scourers. For example, the particles were classified into fragments (circular like) and fibres (elongated particles). Using these shape features to classify the size of particles, revealed differences in particle size and type for all the kitchen scourers analysed. Consequently, the measurements conducted at 100X magnification revealed that the largest fragment particle was larger than the largest particle of fibre. However, particles of fibre were not observed in all the kitchen scourers, as demonstrated by KS2 and KS4. Likewise, conducting the measurements at the magnification of 200X did not reveal any particles of fibre in KS2 and KS4. Furthermore, measurements conducted at the higher magnification revealed larger particles.

The mean size of particles observed indicated differences in all the five kitchen scourers analysed. The measurements conducted at 200X magnification showed that for 'overall', the largest mean particle size was 3 times the mean particle size determined at the magnification of 100X. There were differences in the size proportion of particles based on the size categories within and between magnifications.

*Table 4.1.1. Size of particles from kitchen scourers based on the size categories, measured at the magnification of 100X. The results are based on the particle size for overall average particle size, fragment, and particles of fibre. N.S represents not seen*

Product	Minimum	Maximum	Mean	Median
KS1	5.0	433	41.0	30.0
KS2	5.0	220	36.0	23.0
KS3	10.0	331	55.0	40.0
KS4	5.0	566	67.0	40.0
KS5	15.0	281	57.0	40.0

Product	Minimum	Maximum	Mean	Median
KS1	10.0	433	41.0	30.0
KS2	10.0	220	36.0	23.0
KS3	10.0	306	57.0	40.0
KS4	10.0	566	67.0	40.0
KS5	16.0	226	53.0	40.0

Product	Minimum	Maximum	Mean	Median
KS1	10.0	346	59.1	40.0
KS2	N.S	N.S	N.S	N.S
KS3	10.0	356	54.0	40.0
KS4	N.S	N.S	N.S	N.S
KS5	13.0	336	60.0	41.0

Table 4.1.2. Size of particles from kitchen scourers based on the size categories and determined at the magnification of 200X. The results in the table describe the particle size for overall average particle size, fragments, and fibre particles. N.S represents not seen

Product	Minimum	Maximum	Mean	Median	
KS1	10.0	<b>Overall</b>	1566	194	120
KS2	5.0		753	134	106
KS3	10.0		1166	199	146
KS4	2.5		580	29.9	10.0
KS5	10.0		1016	213	155

Product	Minimum	Maximum	Mean	Median	
KS1	10.0	<b>Fragment</b>	1600	146.4	80.0
KS2	10.0		753.3	134.4	106.7
KS3	10.0		1000	195.7	146.7
KS4	5.0		580	30.0	10.0
KS5	10.0		700	184.2	160

Product	Minimum	Maximum	Mean	Median	
KS1	10.0	<b>Fibre</b>	1533	242	160
KS2	N.S		N.S	N.S	N.S
KS3	10.0		1333	203	146.7
KS4	N.S		N.S	N.S	N.S
KS5	10.0		1333	243	150

There was a statistically significant difference between the overall mean size of particles abraded from kitchen scourers, measured at 100X, [F(4, 495) =4.66, p = 0.00105] (p < 0.05). However, there was no statistically significant difference between the fragments and particles of fibre [F(1, 8) =2.03, p = 0.191846] (p < 0.05). Likewise, at 200X magnification, there was a statistically significant difference between the sizes of particles in the kitchen scourers analysed, [F(4, 495) =21.6767, p = 1.69452E-16] (p < 0.05). However, there was no statistically significant difference between fragments and particles of fibre measured at the magnification of 200X, [F(1, 8) =7.49707E-06,p=0.997882] (p < 0.05). Further analysis showed that there was a statistically significant difference in the overall particle size measurements conducted between magnifications of 100X and 200X.



A post-hoc test was conducted to determine where the differences in the particle size were. As such, for the measurements conducted at the magnification of 100X, the confidence levels indicate the only between-group significant difference was for KS4 - KS1, and KS4 - KS2 (Figure 4.7).

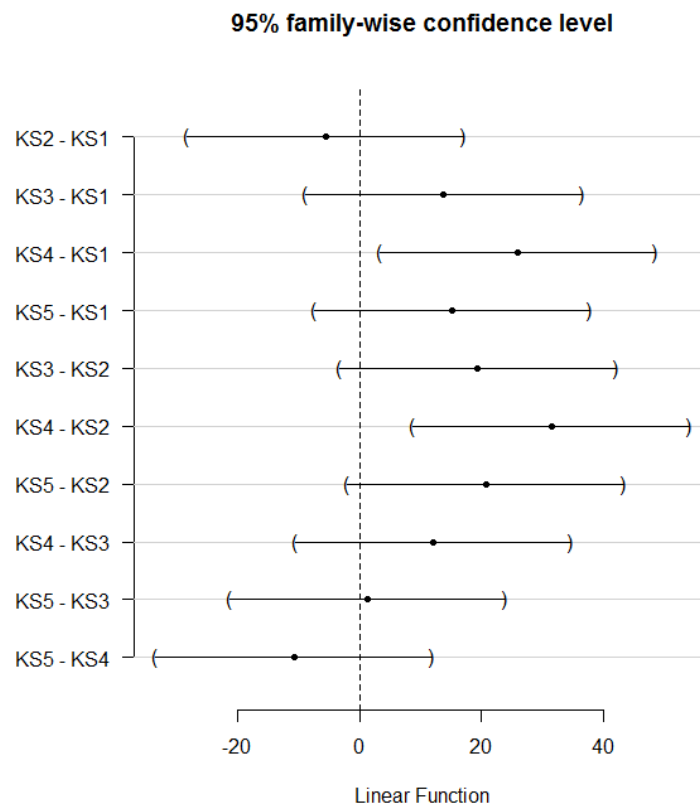


*Figure 4.7. Tukeys multiple comparisons of means at the 95 % family-wise confidence level for particles measured at the magnification of 100X. The confidence intervals that do not cut through the zero mark show a difference in the size of particles in the products. Confidence intervals that cut through the zero mark indicate no difference in the size of particles.*

By comparison, the post-hoc test for particle size conducted at the magnification of 200X was different from tests determined at the magnification of 100X. Therefore, at the magnification of 200X, the post-hoc test indicated significant differences, as indicated by particles in KS4 – KS1, KS3 – KS2, KS4 – KS2, KS5 – KS2, KS4 – KS3, and KS5 – KS4. All other between-group pairings did not indicate any significant difference (Figure 4.7.1).

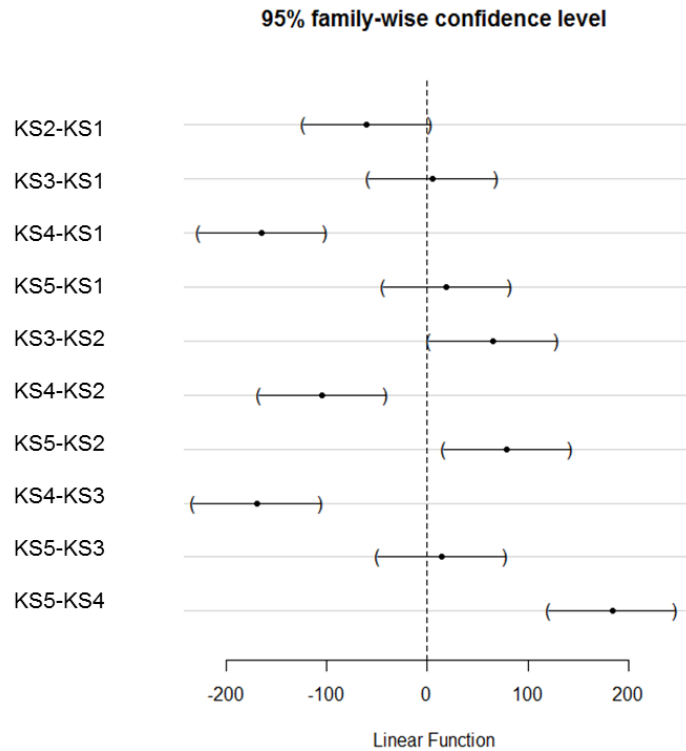


*Figure 4.7.1. Tukeys multiple comparisons of means at the 95 % family-wise confidence level for particles measured at the magnification of 200X. The confidence intervals that do not cut through the zero mark show a difference in the size of particles in the products. Confidence intervals that cut through the zero mark indicate no difference in the size of particles.*

The post-hoc test for particle size between the magnifications of 100X and 200X, indicated differences and similarities between particles. Therefore, out of the 45 between-group comparisons, 27 product pairs did not contain 0 in the confidence intervals; therefore, these pairings demonstrated significant differences in particle size (Figure 4.7.2).

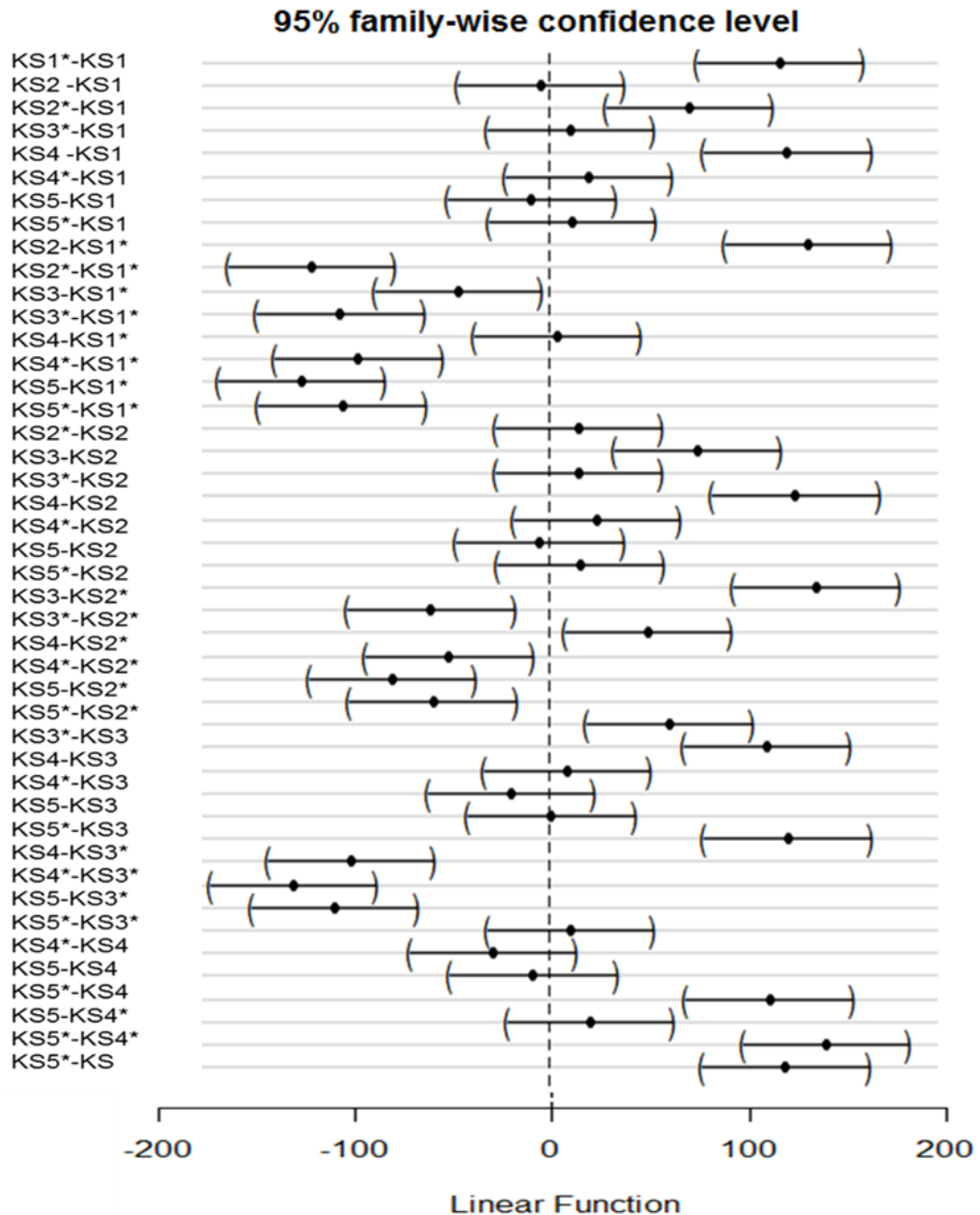


Figure 4.7.2. Tukeys multiple comparisons of means at the 95 % family-wise confidence level for particles measured at the magnification of 100X and 200X. The confidence intervals that do not cut through the zero mark show a difference in the size of particles in the products. Confidence intervals that cut through the zero mark indicate no difference in the size of particles. Particle size denoted by \* indicate measurements determined at the magnification of 200X.

#### 4.5 Assessment of the size distribution of particles abraded from kitchen scourers by Laser Diffraction

In this section particle size distribution results are described using a cumulative frequency distribution graph. The graph indicates the different peak populations for particles abraded from the five kitchen scourers and the D values describe the percentiles (10, 50 and 90). Particle size distribution allows for the estimation of diameter (D value), which describe the diameter of a sphere which groups particles of a sample into a defined ascending order by mass.

The laser diffraction analysis demonstrated that all five kitchen scourers contained particles with sizes from the low micron range up to hundreds of microns, (Figure 6.6). Although the lower and upper particle size limits detected by the instrument were not visible in the cumulative frequency distribution graph, the raw data indicated that there were particles as small as 0.04 to 0.4  $\mu\text{m}$ . Therefore, based on the raw data, the particle size ranged from 0.04 – 2400  $\mu\text{m}$ , with the distribution showing a rapid cut-off at the larger size range, which was steep in all cases, and occurred between 300 and 700  $\mu\text{m}$  (Figure 6.6). KS4 exhibited the narrowest particle size distribution and ranged from 30 - 600  $\mu\text{m}$ , and KS5 had the widest particle size distribution that ranged from 40 – 2000  $\mu\text{m}$  and was the only product with particles > 1000  $\mu\text{m}$  (Figure 4.7.3).

The results also showed that the particle size distribution was negatively skewed, indicated by the long left tail of the cumulative curve. Therefore there were larger particles in all the five kitchen scourers as indicated by the particle size distribution results. The results indicated specific differences in particle size across all five kitchen scourers analysed. This was apparent at the lower end of the measurement scale, where particle size distributions were more extended, and pronounced in KS4 and KS5 (Figure 4.7.3).

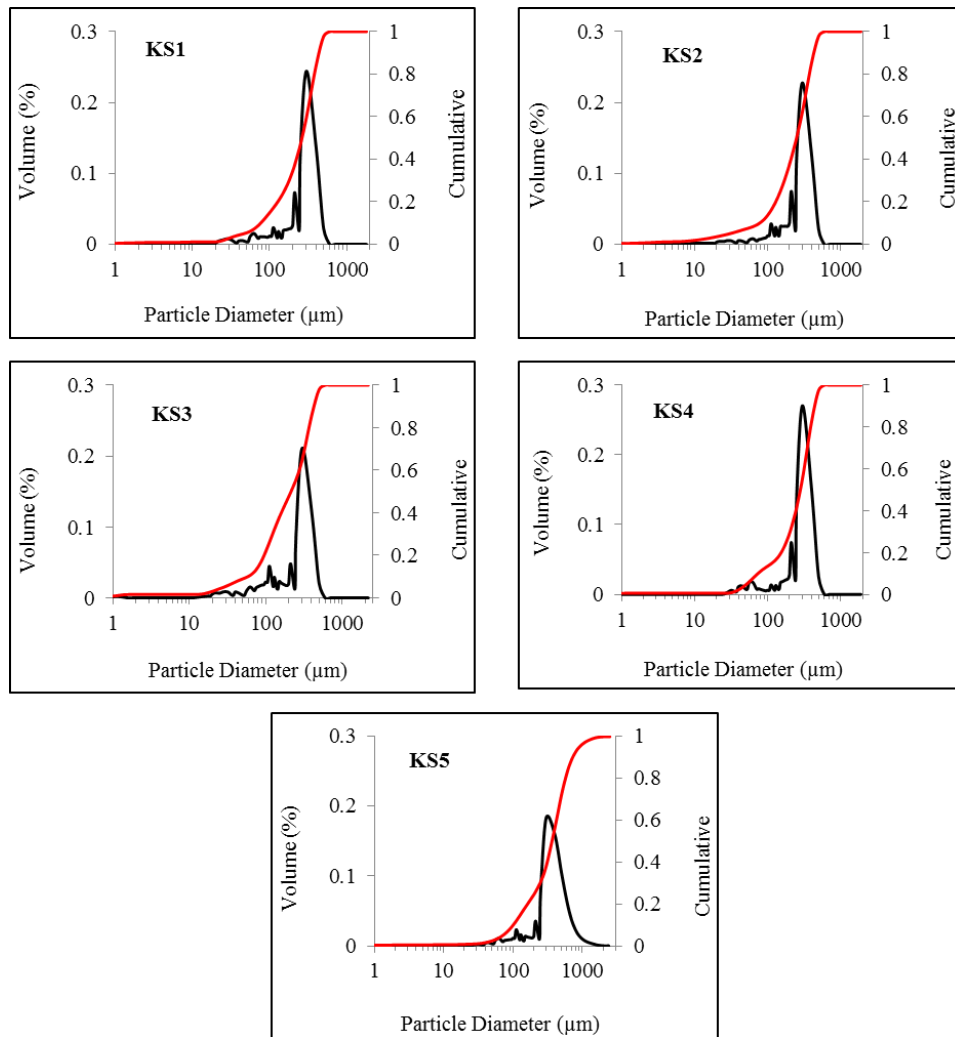


*Figure 4.7.3. Particle size distribution of particles abraded from five kitchen scourers. The graph shows multimodal peaks indicating multiple peak populations for particles in the kitchen scourers.*

It was clear from the results that laser diffraction demonstrated a wider particle size distribution when compared to the particles size as determined by microscopy. For example, the largest mean size of particles determined by the microscopy technique at the magnifications of 100X and 200X were 67.6 and 199  $\mu\text{m}$  respectively. By comparison, the largest mean particle size as determined by the laser diffraction technique, exhibited a particle size of 632  $\mu\text{m}$ . As such the laser diffraction result was 9 times larger than the size determined at the magnification of 100X and larger than particle size at the magnification of 200X, by a factor of 3.

The D10 values indicated that particles from KS4 exhibited the finest texture measured at 49.4  $\mu\text{m}$  however KS5 exhibited more medium texture particles (Table 4.1.3). The results also showed that the median size described by D50, was different

for all the particles from the kitchen scourers. For example, the largest median particle size indicated in KS5 was larger than the smallest median size in KS3. Furthermore, according to the classification for particles, the median size for all particles abraded from kitchen scourers ranged between fine and medium. By contrast the particles abraded from KS5 were coarse. The results further showed that based on the D90 values, which indicated medium to coarse particles, particles abraded from KS5 were the most coarse and were larger than the smallest D90 values in KS2, by a factor of 3.4 (Table 4.1.3).

Measurements of the mean particle size indicated that particles abraded from the kitchen scourers were generally coarse, and demonstrated that KS5 abraded the most coarse particles. .

*Table 4.1.3. Table shows size of microplastics based on D-Values (D10, D50 and D90), which describe the microplastics size distribution that are intercepts on a cumulative graph for 10 %, 50 % and 90 %. Mean particle diameter derived from a volume weighted distribution*

Product	D10 % (µm)	D50% (µm)	D90% (µm)	Mean (µm)
KS1	58.7	275	446	265
KS2	64.1	251	434	254
KS3	61.4	239	510	271
KS4	49.4	296	455	274
KS5	119	448	1484	632

#### 4.6. Application of the imaging flow cytometry technique to determine the size of particles abraded from kitchen scourers

In this section of the results, the size analysis for particles abraded from kitchen scourers is reported. The template developed for the analysis of the particles from personal care products was applied to the particles abraded from kitchen scourers. Therefore, the particle area, length and diameter are reported in this section. Generally, the analysis indicated differences in particle size for the five kitchen

scourers. In particular, it was observed that the particle size determined using the area feature exhibited the widest distribution, by comparison to particle size determined by the length and diameter features. In addition, the results presented in this section show the differences in the size of particles based on the elongated and circular shape features. Using the shape features, microplastics were categorised according to 'all', circular-like particles referred to as fragments and elongated microplastics called fibre particles.

#### *4.6.1. Determination of the size of particles using the area feature*

The area of particles abraded from kitchen scourers was different for all five products analysed. In particular, there was a difference in the area of particles based on the different shape features used. Therefore, the area based on all the total number of particles ranged from 1 – 1401.5  $\mu\text{m}^2$ . In particular, KS1<sub>all</sub>, KS2<sub>all</sub> and KS5<sub>all</sub> exhibited particles with the smallest area, and KS1<sub>all</sub> had the largest particle area (Table 4.1.4). Furthermore, the difference between the largest and smallest area of particles was a factor of 5. By comparison, there were differences in the area of particles based on the shape classifications. As such, the largest area for elongated particle had the same size with the largest particle area for the 'all' shape feature (Table 4.1.4). However the largest area for the circular particles was less than the largest particle area for 'all' and 'elongated' particles by a factor of 2 (Table 4.1.4). The results also indicated that the smallest particle area was exhibited by the 'all' particles category, and was smaller by a factor of 3, in comparison to the 'circular' particles category (Table 4.1.4).

Although the area of the particles between the shape feature categories looked different, the analysis of the mean values demonstrated that these differences were not statistically significant [ $F(2, 12) = 0.498743$ ,  $p = 0.619343$ ] ( $p < 0.05$ ).

Table 4.1.4. Area of particles abraded from kitchen scourers measured using Amnis ImageStream Mark II imaging flow cytometry. Area of particles is based on shape features for all particles, elongated and circular particles. The values for minimum, maximum, mean and median are in microns.

Product	Minimum	Maximum	Mean	Median
KS1	1.0	1401	67.0	48.5
KS2	1.0	577	55.4	47.0
KS3	1.5	728	70.1	57.0
KS4	9.0	1264	79.9	56.0
KS5	1.0	261	43.8	39.5

Product	Minimum	Maximum	Mean	Median
KS1	4.0	1401	73.3	53.0
KS2	4.0	553	52.5	45.0
KS3	7.5	728	72.8	58.0
KS4	10.0	1264	122	64.0
KS5	3.0	228	39.2	36.5

Product	Minimum	Maximum	Mean	Median
KS1	6.0	593	64.8	47.0
KS2	6.0	417	56.6	48.0
KS3	6.5	569	69.0	56.0
KS4	13.5	402	61.6	54.0
KS5	3.0	261	45.0	40.0

#### 4.6.2. Analysis of particle size based on the length feature.

The measurements of particle length showed a general particle size range from 1 – 181  $\mu\text{m}$  (Table 4.1.5). However, there were differences between the lengths of particles, based on the different shape features used. For example a comparison of the largest mean sizes indicated that particles in the ‘all’ category were smaller than the elongated particles. By contrast however, using the largest mean size, the circular particles were smaller than particles in ‘all’ (Table 4.1.5). The results also showed that the smallest particles were observed in ‘all’ and ‘elongated’ shape categories. In addition, multiple products exhibited the smallest particle across the different categories. Therefore, KS1<sub>all</sub>, KS2<sub>all</sub> and KS5<sub>all</sub> had indicated the smallest particles and KS5<sub>elongated</sub> exhibited the smallest particles in ‘elongated’ particles (Table 4.1.5).



There was a statistically significant difference in the length of particles between all, elongated and circular particles measured using imaging flow cytometry [F(2, 12) = 15.22423, p = 0.00051] (p < 0.05).

*Table 4.1.5. Table showing the length of particles abraded from kitchen scourers measured using Amnis ImageStream Mark II imaging flow cytometry. Area of particles is based on shape features for all particles, elongated and circular particles. The values for minimum, maximum, mean and median are in microns.*

Product	Minimum	Maximum	Mean	Median	
KS1	1.0	<b>All</b>	140	12.7	11.0
KS2	1.0		181	11.9	10.0
KS3	1.5		73.	13.0	11.0
KS4	4.0		110	14.1	11.0
KS5	1.0		55.5	10.7	9.0

Product	Minimum	Maximum	Mean	Median	
KS1	1.5	<b>Elongated</b>	140	17.1	15.0
KS2	2.0		165	15.6	15.0
KS3	3.5		70.5	17.2	16.0
KS4	4.5		110	21.3	17.0
KS5	1.0		44.5	13.7	13.5

Product	Minimum	Maximum	Mean	Median	
KS1	3	<b>Circular</b>	66.0	11.2	9.5
KS2	2.5		69.0	10.8	9.0
KS3	2.5		59.0	11.6	10.0
KS4	4.0		65.0	10.9	9.5
KS5	2.0		55.5	9.9	8.0

#### 4.6.3. Assessment of particle size based on the diameter feature.

Size analysis using the diameter feature for the analysis of particles abraded from kitchen scourers indicated that particle size ranged from 1.1 – 70 µm (Table 4.1.6). However, particle diameter was different based on the shape feature categories used. In particular, the results showed differences in the particle diameter, as determined by the different shape feature categories. Therefore, the elongated particles showed the

widest particle size distribution, (Table 4.1.6) and exhibited larger diameters than the circular particles by a factor of 2 (Table 4.1.6).

*Table 4.1.6. Table showing the diameter of particles abraded from kitchen scourers measured using Amnis ImageStream Mark II imaging flow cytometry. Area of particles is based on shape features for all particles, and circular particles. The values for minimum, maximum, mean and median are in microns.*

Product	Minimum		Maximum	Mean	Median
KS1	1.1	<b>All</b>	42.0	8.6	7.8
KS2	1.1		26.5	7.9	7.7
KS3	1.3		30.3	9.0	8.5
KS4	3.1		38.7	9.2	8.4
KS5	1.1		18.2	7.2	7.0

Product	Minimum		Maximum	Mean	Median
KS1	2.2	<b>Elongated</b>	42.0	8.0	8.2
KS2	2.2		25.8	7.7	7.5
KS3	3.0		70.0	17.2	16.0
KS4	3.4		38.7	10.4	8.7
KS5	1.9		17.0	6.8	6.8

Product	Minimum		Maximum	Mean	Median
KS1	2.7	<b>Circular</b>	27.2	8.5	7.7
KS2	2.7		22.9	8.0	7.8
KS3	2.8		26.6	8.9	8.4
KS4	3.8		21.2	8.5	8.2
KS5	1.9		18.2	7.3	7.1

There were differences in the mean particle diameter for all the five products analysed. Although the mean particle diameter ranged from 6.8 – 17.2 µm, there were differences in the mean size between the shape feature categories. As such, the elongated particles had a larger mean diameter than the circular particles, by a factor of 2 (Table 4.1.6). However, the difference in particle diameter between the three shape feature categories was not statistically significantly different [F(2, 12) = 0.93031, p = 0.421106] (p < 0.05).

Imaging flow cytometry was useful to determine the diameter of particles abraded from kitchen scourers. However, the results were not compared with microscopy because measurements of particle diameter was not determined using the technique. Differences in the size of particles when the different size features measurements were applied. As such the results showed that the particle area was larger than the length of the particles, and this was true in all particle shape categories. For example, for all particles, the largest particle area was larger than the particle with the longest length by a factor of 7 (Table 4.1.7).

*Table 4.1.7. Evaluation of the differences between particle size measurements using the area and length features by the imaging flow cytometry.*

Product	Area ( $\mu\text{m}^2$ )	Length ( $\mu\text{m}$ )
KS1	1401	140
KS2	577	181
KS3	728	73.0
KS4	1264	110
KS5	261	55.5

By comparison to length measurements determined with microscopy, the particles determined by imaging flow cytometry were generally smaller. This is because of the differences in maximum particle size each technique can determine. For example, using the mean particle length for 'all' particles, conducted at magnifications of 100X and 200X indicated larger particles than particles measured using imaging flow cytometry. As such the using the largest mean lengths, particles measured using microscopy at the magnification of 100X, were larger than imaging flow cytometry measurements by a factor of 4 (Table 4.1.8). However, measurements conducted at 200X were 15 times larger than the lengths for all particles as determined by imaging flow cytometry (Table 4.1.8).

*Table 4.1.8. Determining the differences between the mean lengths for ‘all’ particles measured using the microscopy and imaging flow cytometry techniques. The units for the measurements are in microns.*

Product	Microscopy		Imaging flow cytometry
	100X	200X	20X
KS1	41.0	194	12.7
KS2	36.0	134	11.9
KS3	55.0	199	13
KS4	67.0	29.9	14.1
KS5	57.0	213	10.7

The imaging flow cytometry demonstrated the ability to determine the size of particles abraded from the five kitchen scourers. The results highlighted the differences in particle size based on the different particle shape features applied. These differences were based on the maximum and mean particle sizes. Therefore measurements of area, length and diameter had an apparent influence on the size of particles in the products analysed. The ImageStream with its speed and sensitivity was used to determine the size distribution of particles in personal care products. This is the first time particles abraded from kitchen scourers is reported. In addition, no other study has reported particle size measurements of particles from kitchen scourers using imaging flow cytometry. Furthermore this technology is novel and represents advancement in particle size analysis of microplastics. However, it was not apparent which technique was better, in terms of consistency. The microscopy technique demonstrated measurements for larger particles and exhibited a larger size range however the imaging flow cytometry technique exhibited the lower size range.

#### 4.7. Estimation of the number of particles abraded from kitchen scourers

The results for the number of particles abraded from all five kitchen scourers per wash are reported. In addition, the results indicate the differences between each product, estimated at the magnifications of 100X and 200X. Furthermore, the

differences in the number of particles based on the shape categories. The results for the flow cytometry technique indicate the differences in the number of particles abraded from all kitchen scourers, based on the shape features applied. In this section, a comparison of the differences between the numbers of particles estimated using the microscopy and imaging flow cytometry techniques are presented in this section.

#### *4.7.1. Evaluation of the number of particles abraded from kitchen scourers by microscopy*

In this section, the number of particles abraded from kitchen scourers in one wash cycle, as determined by microscopy is presented. The results showed differences in the number of particles for all five kitchen scourers analysed. In addition, the difference in the number of particles was demonstrated by the shape feature classifications. Furthermore, there were clear differences in the number of particles determined at magnifications of 100X and 200X (Figure 4.7.4). However these differences were not statistically significantly different.

The total number of all particles (fragments and fibre) abraded from kitchen scourers determined at 100X magnification ranged from  $246,222 \pm 6711$  to  $1,234,222 \pm 30,101$  particles per wash (Figure 4.7.4). Therefore KS1 and KS5 exhibited the smallest and largest number of particles for the all particles. By contrast, the number of all particles determined at the magnification of 200X exhibited a wider range for the number of particles. Particle count conducted at the magnification of 200X indicated higher particle count than the number determined at the magnification of 100X, by a factor of  $\sim 1.3$  (Figure 4.7.4). This was consistent with the estimation of the number of particles in personal care products using the microscopy technique.

The results showed differences in the number of particles of fibre and fragments as determined within and between magnifications of 100X and 200X (Figure 4.7.4). In particular, the difference between the number of particles of fibre and fragments was product specific. For example, at the magnification of 100X KS1 indicated the highest number of fibre particles which accounted for 80% of the total number of particles abraded from KS1.

However, not all products exhibited particles of fibre as demonstrated by the particles in KS2 and KS4. Therefore, there were more particles of fragment in KS2 and KS4, which accounted for 100% of the total number of particles in those specific products (Figure 4.7.4). Some products indicated higher number of fibre particles than fragments, including KS1 and KS5 where fibres accounted for 80% and 69%, respectively of the total particle count at the magnification of 200X (Figure 4.7.4). A similar trend in the proportion of fibre particles to fragments was exhibited with counts conducted at both magnifications (Figure 4.7.4).

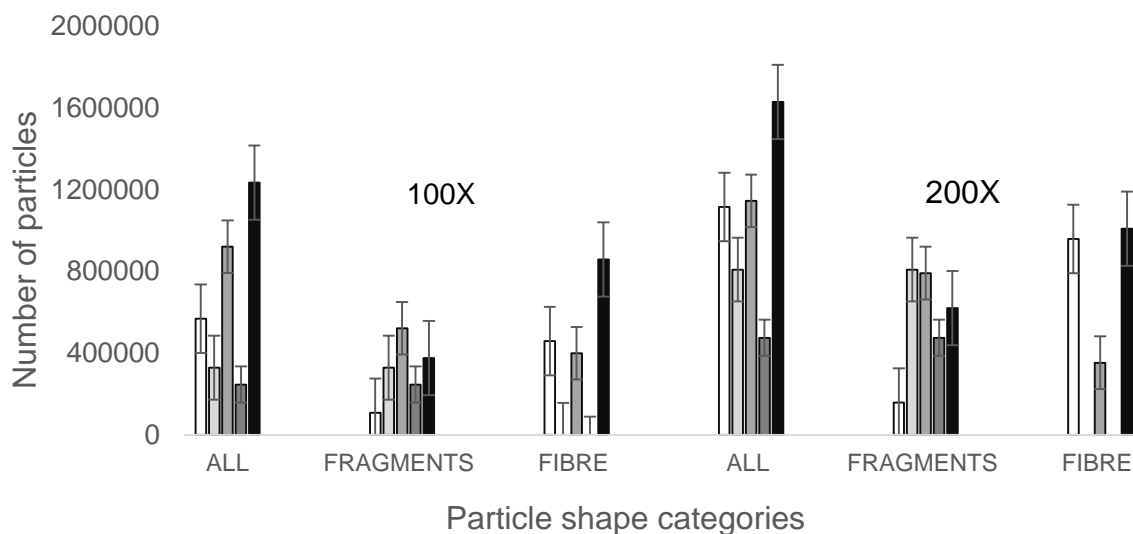
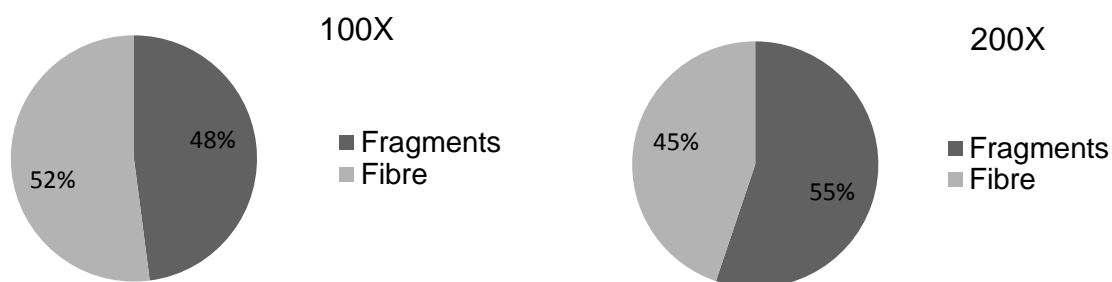


Figure 4.7.4. Bar chart showing the number of particles released from kitchen scourers per wash. Values based on counts in six transects of a Sedgewick-Rafter cell at 200X. Particles categorised into all, fragments and fibre.

The analysis of the proportion of fibre to fragment particles indicated overall differences in the five products analysed. At the magnification of 100X, the particles of fragments and fibre accounted for 48% and 52% of the total number of particles in the kitchen scourers (Figure 4.7.5). By contrast, the particles of fragments and fibre accounted for an average of 55% and 45% of the total number of particles, counted at the magnification of 200X (Figure 4.7.5). Although differences were indicated in the results, there was no statistically significant difference between the number of fragments and fibre particles. This was true for counts conducted at the magnification of 100X,  $[F(1, 8) = 0.024059, p = 0.880577]$  ( $p < 0.05$ ). Likewise there was no statistically significant difference between the number of fibre and fragments at the magnification of 200X  $[F(1, 8) = 0.180329, p = 0.682281]$  ( $p < 0.05$ ).



*Figure 4.7.5. Pie chart indicating the proportion of particle fragments to fibre particles abraded from kitchen scourers, as determined at the magnification of 100X and 200X.*

The microscopy technique demonstrated the ability to estimate the number of particles abraded from all five kitchen scourers. In addition, it was possible to determine particle number estimates at two different magnifications. This was consistent with the estimation of the number of particles from personal care products. Therefore, for the kitchen scourers and personal care products, the estimation for the number of particles at the higher magnification indicated a greater number of particles were counted. However, the estimation of the number of particles based on the shape feature classifications was demonstrated by the kitchen scourer particles but not the particles from the personal care products. This is apparently because particles abraded from the kitchen scourers exhibited more defined shapes than the personal care products particles that were largely varied. The microscopy technique has shown that the number of particles abraded from kitchen scourers at different magnifications had an apparent influence on the number of particles and so disproves the hypothesis.

#### *4.7.2. Evaluating the number of particles abraded from kitchen scourers using Imaging flow cytometry*

The number of particles ( $\leq 70 \mu\text{m}$ ) abraded from kitchen scourers and determined by imaging flow cytometry is presented in this section. In addition, the results indicate the difference in the number of particles abraded from all five scourers. Furthermore,

the difference in the number of particles based on the different shape features is reported in this section. The results for the blank water sample which revealed the presence of artefacts is presented in this section.

The analysis followed the same pattern with the particles from the personal care products. As such, all (total) particles were counted and then were divided into elongated and circular particles. To put these features into context, the fibre like particles are described as elongated particles, and the particles of fragments are described as circular particles. After applying the template created for the analysis, the number of particles was computed and standardised to particles per wash.

The total number of particles abraded from kitchen scourers ranged from 1,743,797 particles to 23,873,686 particles (KS4 and KS5 respectively) (Figure 4.7.6). The number of elongated particles ranged from 567,186 to 4,783,961 particles (KS4 and KS5 respectively). By contrast, the circular particles demonstrated a wider particle number distribution to elongated particles. As such, the number of circular particles ranged from 1,155,044 – 18,948,949 particles (KS4 and KS5 respectively) (Figure 4.7.6). There were therefore many more circular particles than elongated particles by a factor of 3 (Figure 4.7.6).

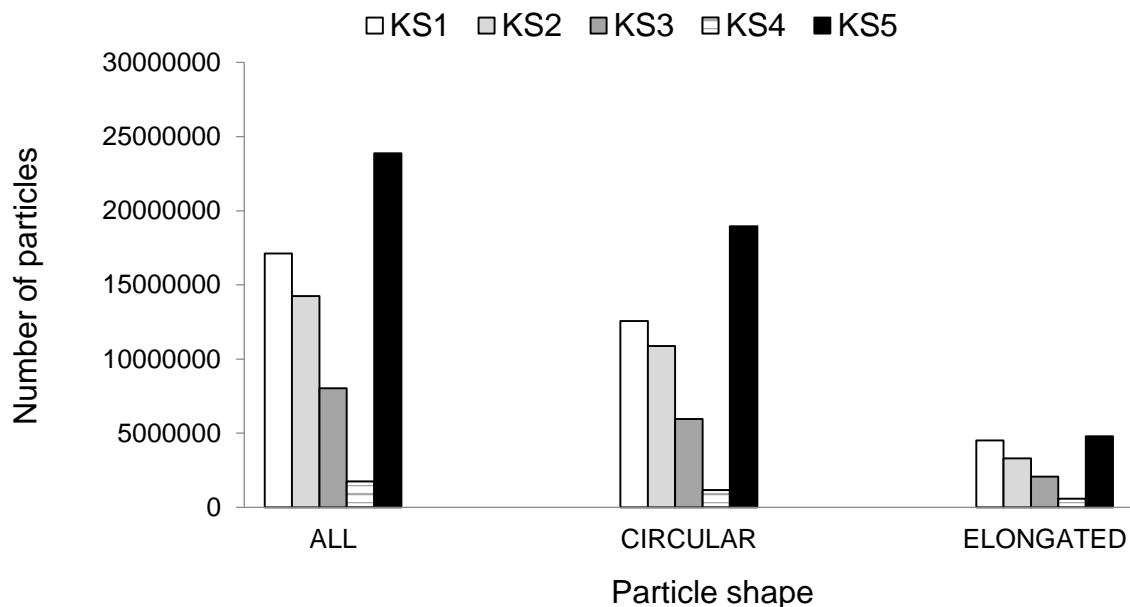




**Figure 4.7.6. Bar chart showing the number of particles abraded from kitchen scourers using the Amnis ImageStream Mark II imaging flow cytometer. Three populations of particles were analysed based on the shape features from the template created.**

There were differences in the number of elongated and circular particles abraded from the different scourers. As such the circular and elongated particles accounted for an average of 74% and 26% respectively, of the total number of particles abraded from the kitchen scourers (Figure 4.7.7). Although there was a clear difference between the number of circular and elongated particles, it was not statistically significant,  $[F(1, 8) = 4.837131, p = 0.059054]$  ( $p < 0.05$ ).

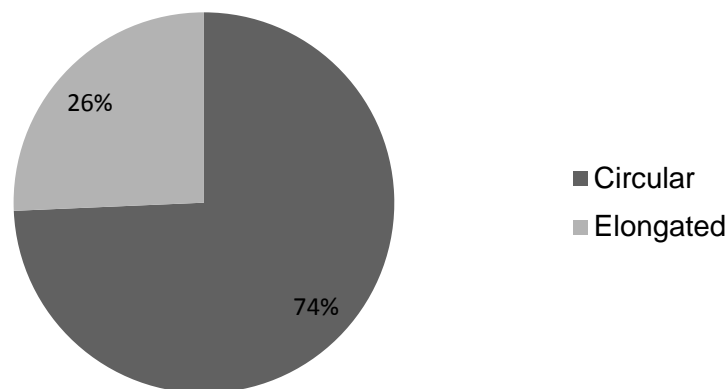


**Figure 4.7.7. Pie chart indicating the proportion of elongated and circular particles abraded from five kitchen scourers, and determined by imaging flow cytometry.**

The blank water samples (filtered laboratory grade water processed alongside samples) run as part of quality control exhibited a particle count of 15249. The number of particles in the blank water sample was subtracted from the number of particles from the kitchen scourers. The particles in the blank samples accounted for different proportions of particles for all samples analysed. For example, the blanks accounted for < 1% of the total number of particles in KS4 (Figure 4.7.8).

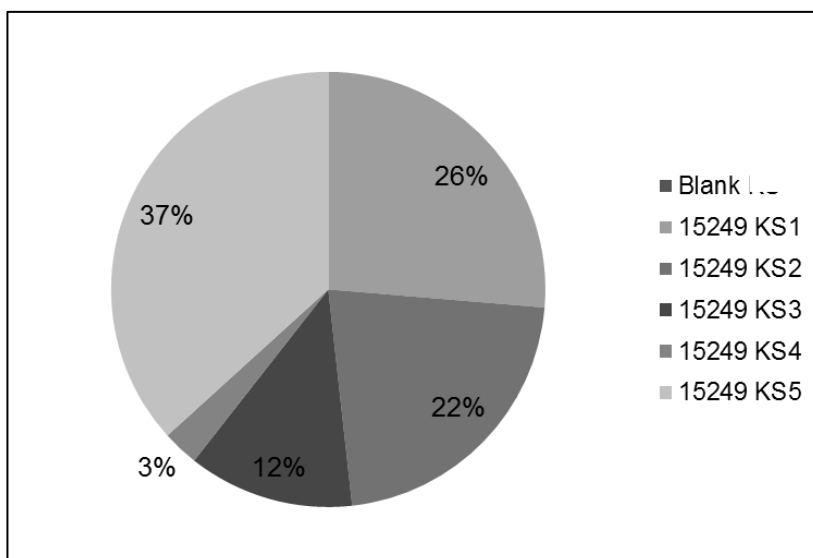


*Figure 4.7.8. Pie chart for the proportion of particles in the blank water samples to the particles abraded from all five kitchen scourers.*

In comparison to microscopy, imaging flow cytometry which analysed  $\leq 70 \mu\text{m}$  fractions, demonstrated a higher number of particles (Figure 4.7.9) up to 14 times higher than the numbers indicated by microscopy. Furthermore, the differences in the number of particles determined by using both techniques was a statistically significantly. In particular, there was a statistically significant difference between the number of particles determined by microscopy at the magnification of 100X and imaging flow cytometry [ $F(1, 8) = 10.55474$ ,  $p = 0.011722$ ] ( $p < 0.05$ ); and at 200X magnification [ $F(1, 8) = 9.921847$ ,  $p = 0.013601$ ] ( $p < 0.05$ ).

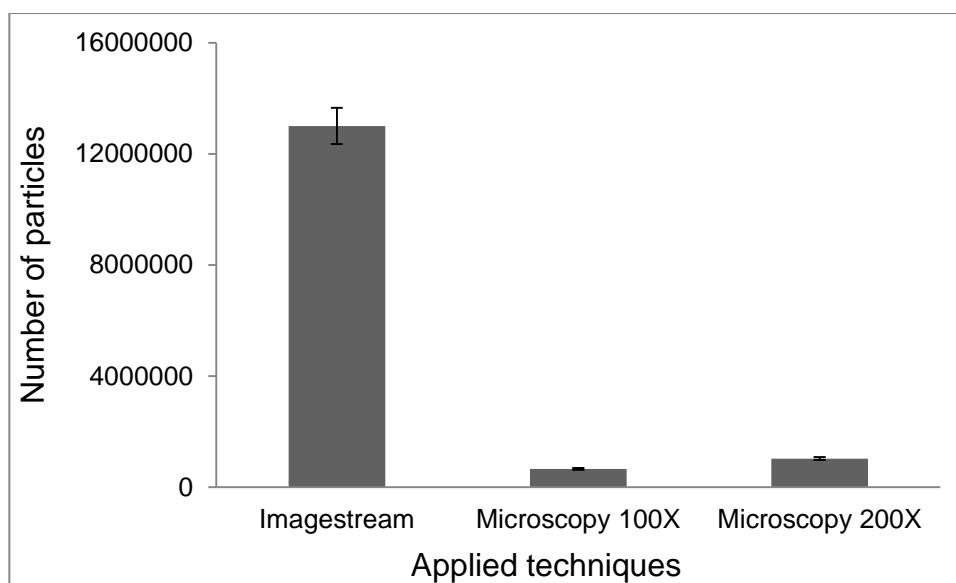


*Figure 4.7.9. Histograms for the number of particles estimated using the imaging flow cytometry technique (Imagestream); and the microscopy technique determined at the magnifications of 100X and 200X.*

The application of imaging flow cytometry demonstrated the ability to estimate the number of particles abraded from kitchen scourers. In addition, the analysis followed the same pattern for particles in FS2 for the personal care products. More particles were abraded from the kitchen scourers but less was separated from personal care products. Furthermore, this was also true for the application of developed templates and for the detection of artefacts of debris which was not possible with microscopy. The results showed that the choice of technique had an influence on the number of particles abraded from the kitchen scourers.

#### 4.8.0. Assessment of the morphology of particles abraded from kitchen scourers as determined by different techniques

In this section, the results for the morphology of the particles abraded from kitchen scourers using different techniques are reported. In particular, the differences in the particle shape between each product and across the techniques used are also presented in this section. Furthermore, the colour of particles is frequently used as an added description of the particle morphology. As such in this section the colour of the particles are reported.

#### *4.8.1. Morphology of particles by Microscopy*

In this section, the morphology of particles abraded from kitchen scourers is presented. The differences in morphology within and between the magnifications used are highlighted and indicated the different colours of the particles. The particles abraded from all five kitchen scourers exhibited a range of shapes and colours. Generally, the shape of the particles ranged from irregular, grain-like and threadlike shapes (Figure 4.8.0). However, for easy shape classification, the particles appeared either as a fragment or particle of fibre (Figure 4.8.0). However, not all products analysed indicated the presence of particles of fibre, as demonstrated by KS2 and KS4 (Figure 4.8.0).

The particles observed at both magnifications demonstrated the occurrence of sharp edges noticeably around some of the particle fragments (Figure 4.8.0). All fragment particles observed exhibited these artefacts and was not unique to any specific product (Figure 4.8.0). The particles abraded from the kitchen scourers were characterised by unique array of shapes. For example at the magnification of 100X, particles in KS1 exhibited shapes ranging from oblong to multi-edged particles. The same was true for particles analysed at the magnification of 200X, where for example particles in KS5, particles were characterised by horse shoe-like shapes (Figure 4.8.0).

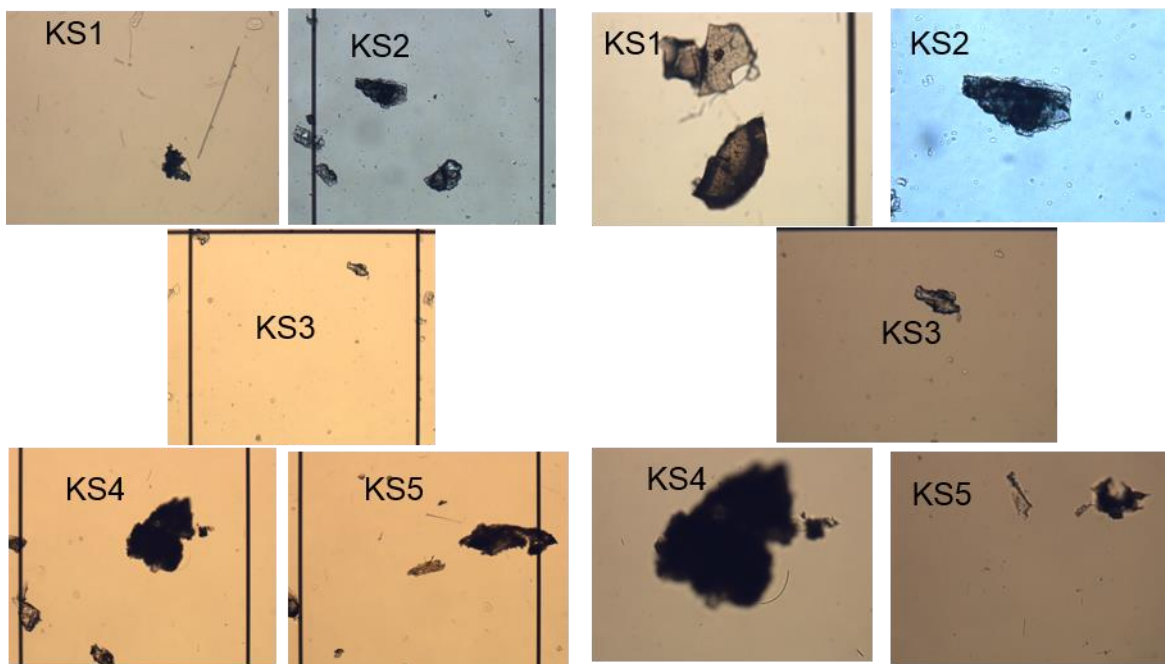


*Figure 4.8.0 Images of particles abraded from five kitchen scourers and analysed at magnifications of 100X (left image) and 200X (right image). The different products showed differences in shape and colour for particles analysed in all five products.*

The results showed the different colours of the particles abraded from kitchen scourers. Therefore, the assessment of colour of particles abraded from kitchen scourers revealed differences between each product. As such, the colours of the particles ranged from black (KS1, KS2, KS5), light brown (KS3) to green (KS4) as was observed.

Microscopy allows for the observation of particles, providing images which aid measurements and observation of differences as demonstrated by the particles abraded from the kitchen scourers. The application of different magnifications had an influence on the resolution of the particles with clear differences between particles from the same product at different magnifications.

#### *4.8.2. Evaluation of particle morphology as determined by Imaging flow cytometry*

The morphology of particles abraded from the kitchen scourers was determined using shape features to show the distinct populations of particles. In addition, the

imaging flow cytometry recorded an image of each particle which facilitated the post analysis of the particle shapes in all the products analysed. The detection of particles was achieved by interrogating the histogram plots in the analysis template, and matching them with corresponding objects in the image display area of the analysis. For example, elongated particles abraded from the kitchen scourers were identified based on interrogations of the histogram and confirmed in the image display area (Figure 4.8.1). Therefore, elongated and circular particles were successfully detected and easily differentiated.

The shape of the particles ranged from elongated, irregular to circular-like shapes. However it was easier to classify the particles into elongated and circular particles, based on the aspect ratio template (Figure 4.8.1).

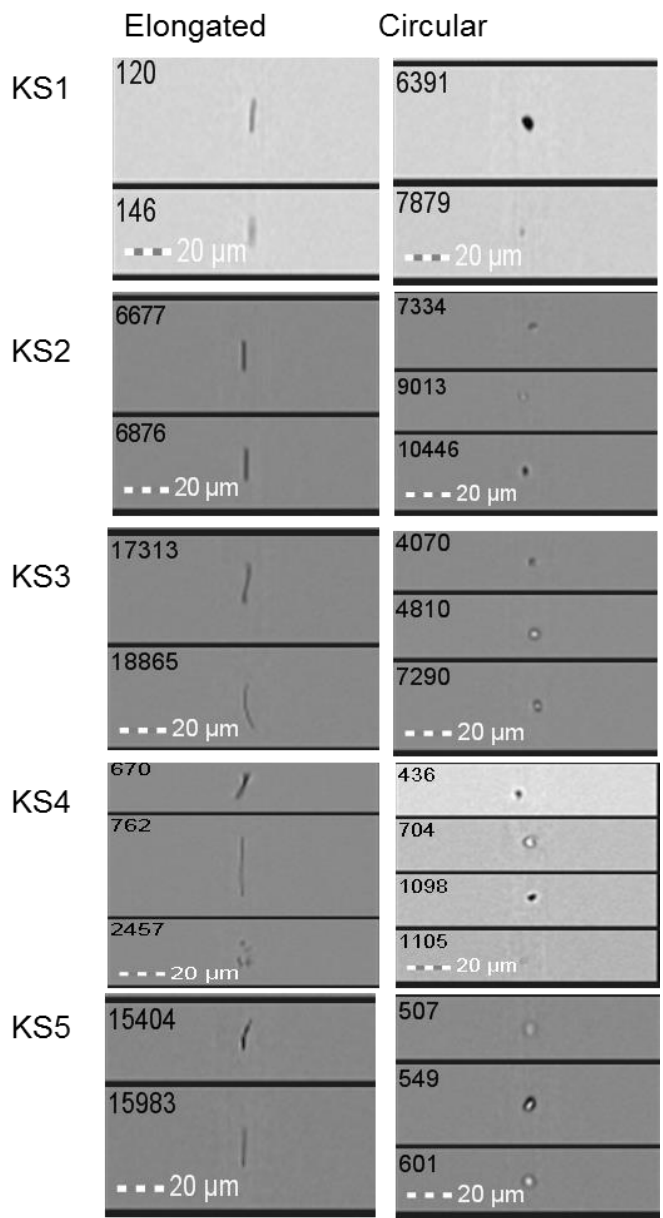


Figure 4.8.1. Types of particles abraded from the five kitchen scourers analysed.

The results indicated that the particles abraded from kitchen scourers were clearly observed in Channel 1, which is the default channel for the display of particles. However only particles abraded from KS1 were visible in all the channels (Figure 4.8.2). As such, based on the channels where particles were detected, the particles in KS1 emitted low light energy absorbed from the light source and were largely granular. Therefore, the abraded particles from KS1 exhibited both fluorescent and side scatter properties.

KS2 and KS5 detected in channel 6, exhibited particles that did not indicate fluorescent properties, but demonstrated side scatter properties (Figure 4.8.2). By contrast however, products KS3 and KS4 had particles that were observed only in channel 1, suggesting that the particles did exhibit only fluorescent properties but not side scatter properties (Figure 4.8.2). The detection of fluorescent and side scatter properties of particles; as is possible with the imaging flow cytometry technique can be applied for the detection of particles that exhibit these characteristics.

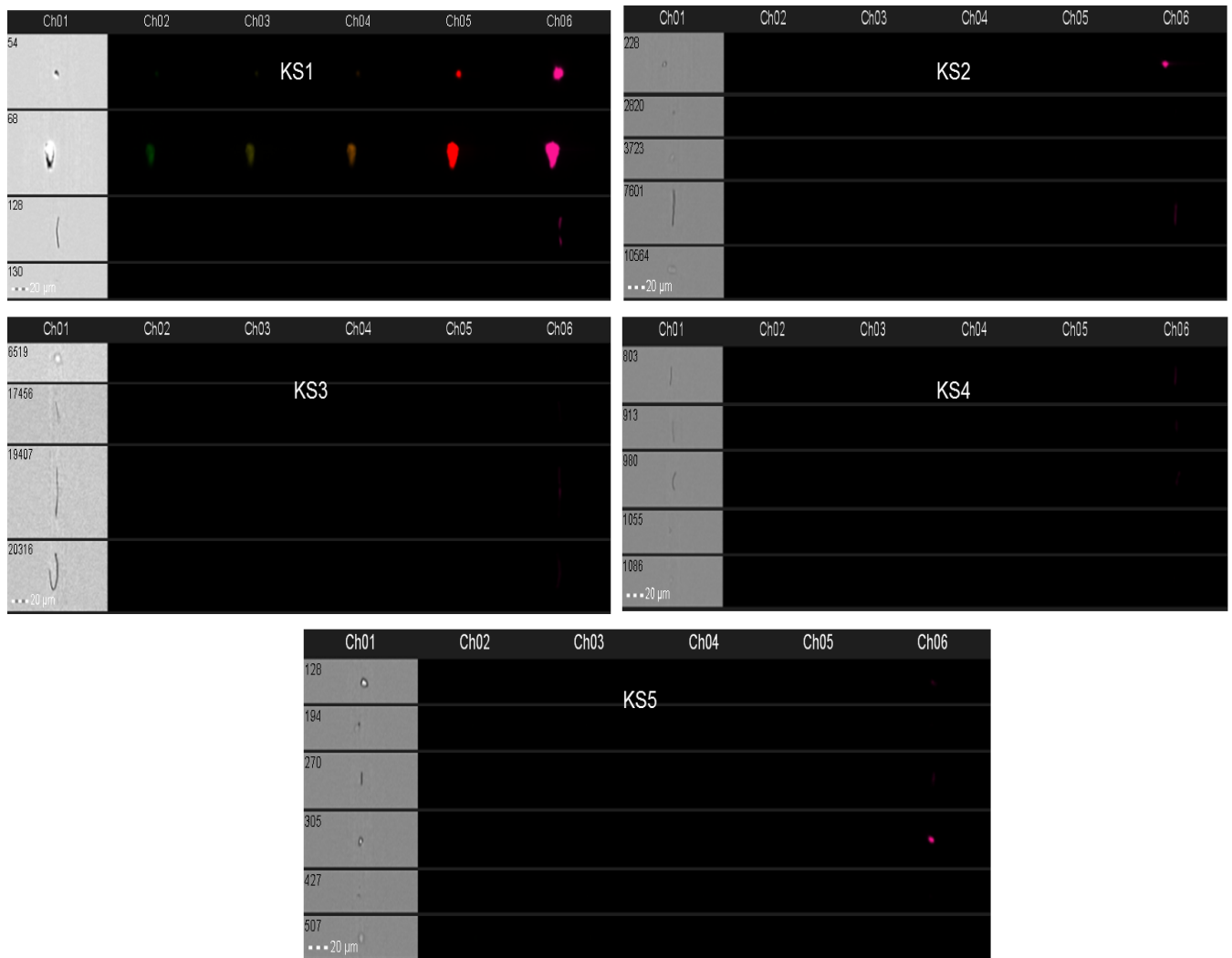


Figure 4.8.2. The elongated and circular particles abraded from five kitchen scourers determined by the imaging flow cytometer. The particles exhibited differences in fluorescence and side scatter properties. KS1 indicated particles demonstrated fluorescence and side scatter properties. Scale bar for all images is 20 μm.

The results indicated that particles abraded from kitchen scourers exhibited a range of colours but were not a true reflection of the actual colours. In particular, the colours



observed were dependent on the channel where the particles were detected. Therefore, in channel 1, the particles were black and white, but in channels 2 to 5, the colours ranged from dark green, light green, light brown, bright red and bright pink. Particles from KS1 exhibited all possible colours because they were detected in all the channels. In addition, KS2 and KS5 were characterised by black and white, and bright pink colours, indicative of their detection in channels 1 and 6 (Figure 4.8.2).

An automated technique like the imaging flow cytometry did not fit with how a manual method like microscopy evaluates particles. Consequently, the application of imaging flow cytometry, a different technique to microscopy, gave a different outcome to microscopy. In particular it was relatively easier to automatically separate particles into distinct populations based on their shape, which was manually determined with microscopy. The ImageStream which combines the power of microscopy and flow cytometry is useful for the multi-spectral imaging of particles in flow.

#### *4.8.3. Assessing particle morphology in products using micro-FT-IR*

The particles abraded from the five kitchen scourers exhibited clear differences in their morphology and colour. For example, particles abraded from KS1 and KS2 exhibited particles that were irregular and circular-like (Figure 4.8.3). As such, the particle shapes ranged from elongated, irregular to circular-like particles. The analysis by micro-FT-IR indicated that KS5 demonstrated a black colour which was true and unique to the product (Figure 4.8.4).

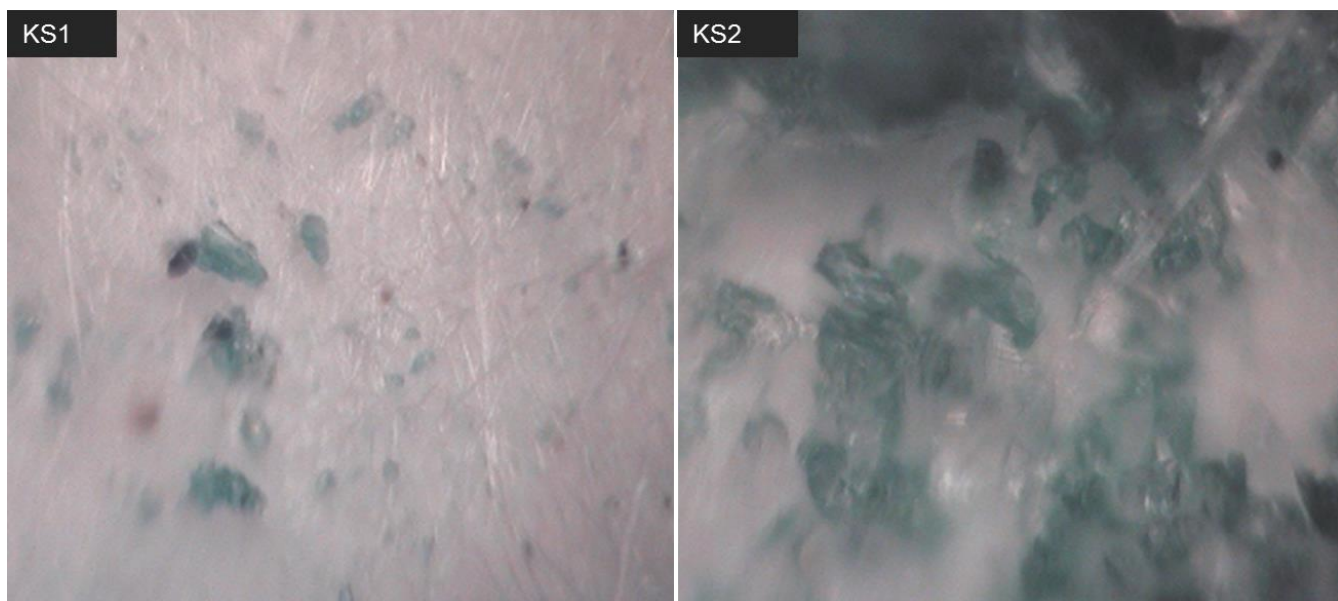


*Figure 4.8.3. Morphology of particles abraded from KS1 and KS2 using the micro-FT-IR technique. The products were characterised by irregular and circular-like particles and a green colour.*



*Figure 4.8.4. Morphology and colour of particles abraded from KS5 using the micro-FT-IR technique. The particles from KS5 exhibited a black colour that was unique to this product. Particles appeared more irregular than elongated or circular-like.*

By contrast, it was a bit of a challenge observing some particles as it was with particles in KS3 which appeared white, the same colour with the surface of the filter paper (Figure 4.8.5). However, this was directly confirmed by interrogation of the samples, as the true colour of the kitchen scourer.

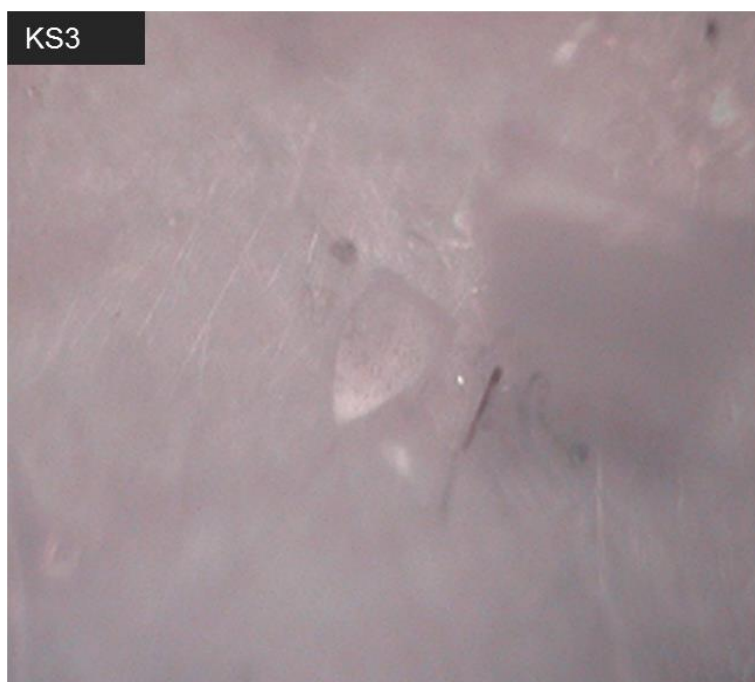


*Figure 4.8.5. Colour of particles abraded from KS3 using the micro-FT-IR technique. The particles abraded from KS3 exhibited a white colour that was the same with the surface of the filter paper.*

It was not clear how the automated micro-FT-IR technique fit with the imaging flow cytometry technique. The images produced by the micro-FT-IR technique appeared larger and demonstrated a more detailed particle morphology than the imaging flow cytometry technique. This was apparent because of the differences in the spatial resolution for both techniques.

Another comparison with imaging flow cytometry was that particles that make up debris were not present or were not detected. However with the imaging flow cytometry, there was debris in the blank water samples. It is possible that there was debris in the blanks, they did not absorb IR light and so were not detected. By comparison the blanks absorbed light energy that was detected by the imaging flow

cytometry. As such, the imaging flow cytometry technique appeared to be more sensitive and could detect debris more readily than the micro-FT-IR technique and microscopy. In addition, it was possible to analyse the shapes of some of the particles by side scatter and fluorescence profile, something that was not possible with the micro-FT-IR technique or the microscopy technique. In addition, it was not possible to apply template to classify particles according to shape features of elongated and circular particles in micro-FT-IR as was possible with the imaging flow cytometry.

#### 4.8.4. Polymer identification of particles abraded from kitchen scourers using micro Fourier transform infrared spectroscopy micro-FT-IR

In this section the results for the polymer identity of the particles are presented. Unless stated otherwise, polymer identification was conducted. The polymer identity of the particles as determined by micro-FT-IR in reflectance mode and ATR-FT-IR in transmission mode is presented. The analysis of the polymer particle identity was not determined based on the shape or colour of the particles abraded.

##### *4.8.4.1. Determining polymer identity using reflectance micro-FT-IR technique*

The polymer identity of all the particles abraded from the kitchen scourers was identified using the absorbance peaks in functional group region of the IR spectrum (Figure 4.8.6). In addition, the absorbance peaks corresponded to the wavenumber regions unique to the different polymers (Figure 4.8.6). To confirm the polymer identity of the particles, the functional groups detected in the regions of absorbance cross referenced with a table showing the FT-IR peaks characteristic for the polymer type, as was done with the PCPs (Table 4.1.9).

The results of the scans showed that the polymer identity of the particles abraded from KS1 and KS4 was polyethylene PE. This was indicated by the more obvious absorbance peaks and illustrated by the bending and stretching of C-H bonds at 1500-1450 and 3000-2770  $\text{cm}^{-1}$ , respectively (Figure 4.8.6). By comparison with the peaks produced by particles from personal care products, the polyethylene peaks from kitchen scourer particles were distorted and characterised by low absorbance. The

FT-IR peaks produced from particles in the personal care products were smooth and indicated a high absorbance. It is possible that particles abraded from the kitchen scourers contained additives from the manufacturing process, (something that was not the focus of this study), that influenced the output of the peaks and absorbance. The polymer identity of the particles abraded from kitchen scourers were confirmed with a table showing the FT-IR peaks and corresponding functional groups that are characteristic of the plastic polymers (Table 4.1.9). In addition, the peaks were matched with FT-IR peaks in the polymer library available at the Experimental techniques centre (ETC), Brunel University.

The polymer identity of particles abraded from KS2, KS3 and KS5 were identified as polyester PET, indicated by high peaks from  $1700\text{ cm}^{-1}$  to  $600\text{ cm}^{-1}$ . The absorbance peaks which slightly overlapped the fingerprint region (region between  $1500\text{ cm}^{-1}$  to  $500\text{ cm}^{-1}$ ) characterised the spectra of the stretching vibrational band of C=O between  $1670\text{ cm}^{-1}$  -  $1820\text{ cm}^{-1}$  (Figure 4.8.6). In addition, there was a stretching vibrational band of C-O-C between  $1000\text{ cm}^{-1}$  -  $1300\text{ cm}^{-1}$  (Figure 4.8.6) As such these bands confirm the presence of an ester linkage in the polymer. Furthermore, in the functional group region (between  $3000\text{ cm}^{-1}$  and  $1500\text{ cm}^{-1}$ ) there were absorbance peaks illustrated by the stretching of C-H bonds at  $2850\text{ cm}^{-1}$  and  $3000\text{ cm}^{-1}$  (Figure 4.8.6). The differences between the spectra of polymers identified in this study allowed for the discrimination between the different particles by visual interrogation. This was useful in determining the difference between spectra of polyethylene and polyester. For example, the stretching of C-H bonds around between  $3000\text{-}2770\text{ cm}^{-1}$ , indicated differences between the differences in ratio of CH<sub>2</sub> and CH<sub>3</sub> groups for polyethylene and polyester (Figure 4.8.6).

Table 4.1.9. IR absorptions of the functional groups for the identification of polymers of polyethylene and polyester.

IR Frequency (cm <sup>-1</sup> )	Functional Group
Polyethylene	
2914, 2846	CH <sub>2</sub> stretch
1474	CH <sub>2</sub> bend
720	CH <sub>2</sub> rock
Polyester	
2969, 2907	C-H stretching
1711	C=O stretching
1504	Aromatic ring C=C stretching
1472, 1405, 1340	C-H bending
1241	Ester's C-O stretching
1093	C-O stretching
871	Aromatic ring C-H bending
718	C-H bending

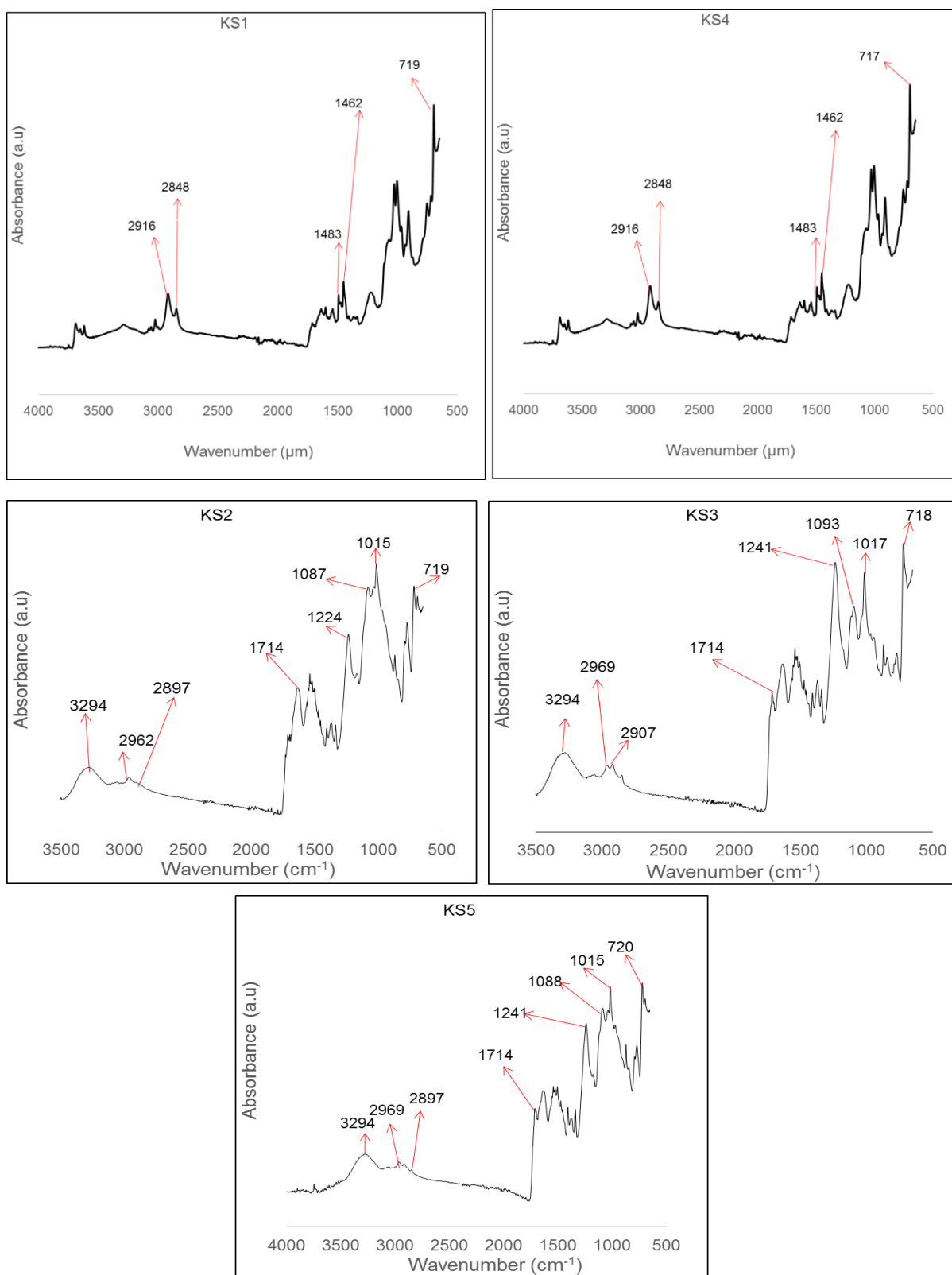


Figure 4.8.6. micro-FT-IR spectra of polyethylene as determined in KS1 and KS4, and the IR spectra for polyester determined in KS2, KS3 and KS5. The red arrows point to the functional groups in the IR spectrum, indicative of polyethylene.

#### *4.8.4.2. Polymer identification of particles abraded from kitchen scourers using attenuated total reflectance infrared spectroscopy ATR-FT-IR*

ATR-FT-IR was applied as an alternative method for the polymer identification of particles abraded from kitchen scourers. This technique allows for the direct analysis of particles without the need to scan the surface of a filter paper, allowing a more rapid approach for the polymer identification of particles. The polymer identity of particles was determined as percentage transmittance.

The polymer identity of all the particles abraded from the kitchen scourers were successfully identified using the absorbance peaks in functional group region of the IR spectrum. Consequently, the results of the scans showed that the identity of particles abraded from KS1 and KS4 was polyethylene PE. Although less pronounced, the absorbance peaks were indicated by the bending and stretching of C-H bonds at 1500-1450 and 3000-2770  $\text{cm}^{-1}$ , respectively (Figure 4.8.7). The qualitative analysis for the identification of particles abraded from kitchen scourers were carried out by using functional groups characteristic of the polymer (Table 4.2.0). In addition, confirmation of the polymer identity of the particles was determined by comparing spectra of the polymer with known reference materials in the data base of the ETC and an IR reference table. These two sources provided reliable results for identifying the microplastics abraded from the kitchen scourers.

By comparison, the absorbance spectra of polyethylene particles identified in personal care products exhibited strong bands that were more pronounced than what was exhibited by particles from the kitchen scourers. The particles abraded from KS2, KS3 and KS5 were identified as polyester PET. In the functional group region; between 3000  $\text{cm}^{-1}$  and 1500  $\text{cm}^{-1}$ , there were absorbance peaks illustrated by the stretching of C-H bonds at 2850-3000  $\text{cm}^{-1}$

However, in the finger print region, the infrared spectra was characterised by the stretching vibrational band of C=O between 1670 - 1820  $\text{cm}^{-1}$  (Figure 4.8.8). In addition, there was a stretching vibrational band of C-O-C between 1000  $\text{cm}^{-1}$  and 1300  $\text{cm}^{-1}$ , confirming the presence of an ester linkage in the polymer (Figure 4.8.8).



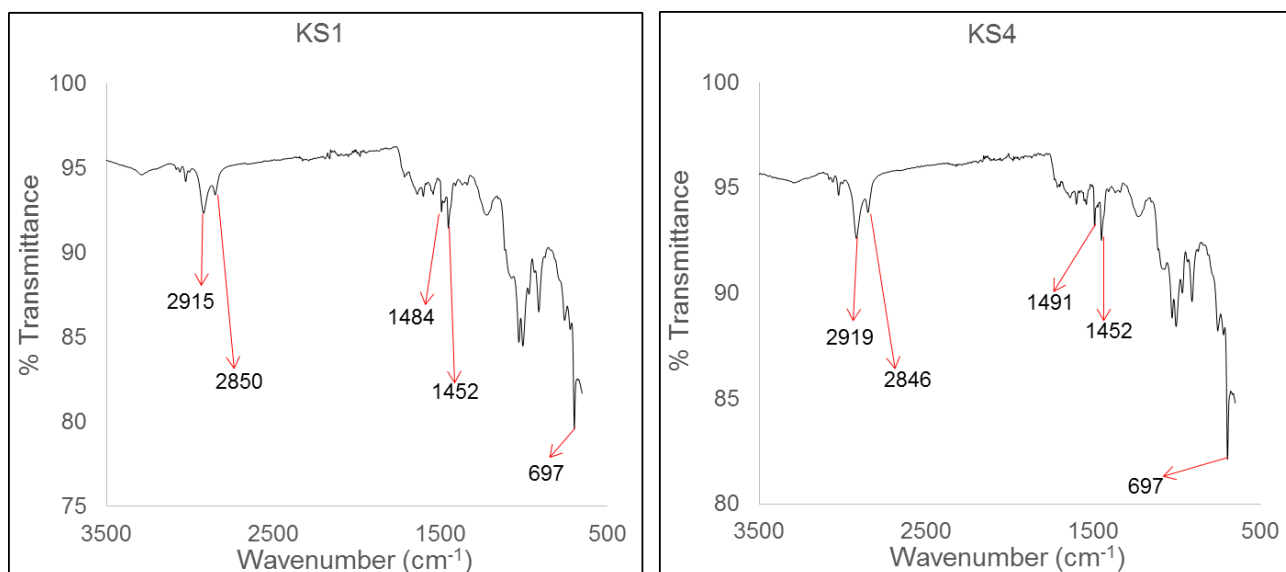


*Figure 4.8.7. ATR-FT-IR spectra of polyethylene as determined in KS1 and KS4. The red arrows point to the functional groups in the IR spectrum, indicative of polyethylene. The spectra are presented as a function of 16 co-added scans carried out for each product at a spectral resolution of 4cm<sup>-1</sup> and a wavenumber ranging from 4000cm<sup>-1</sup> to 500 cm<sup>-1</sup>.*

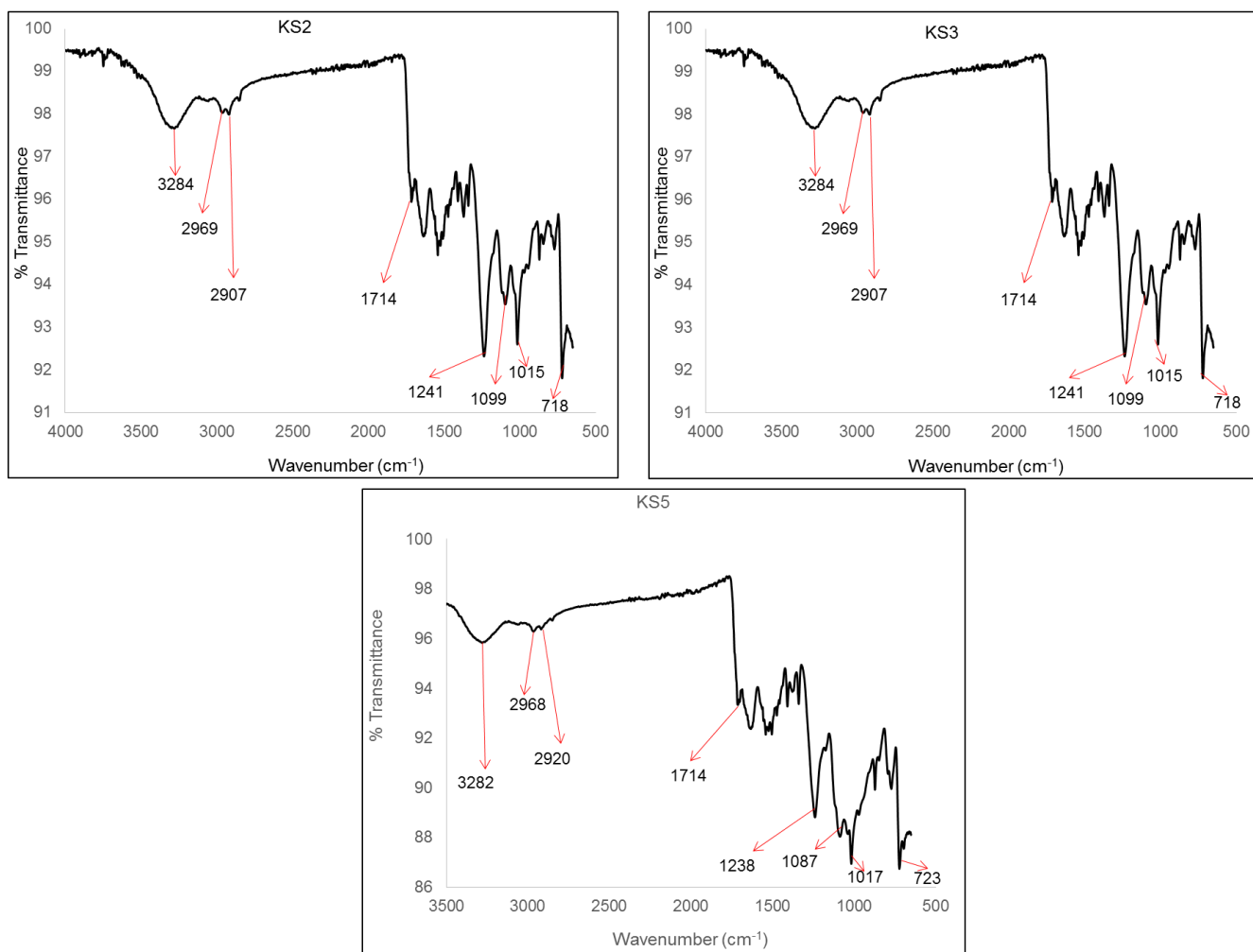


Figure 4.8.8. ATR-FT-IR spectra of polyester as determined in KS2, KS3 and KS5. The functional groups in the IR spectrum that are indicative of polyester are shown with red arrows. The spectra are presented as a function of 16 co-added scans carried out for each product at a spectral resolution of  $4\text{cm}^{-1}$  and a wavenumber ranging from  $4000\text{cm}^{-1}$  to  $500\text{cm}^{-1}$ .

#### 4.9. Multi-technique comparison to characterise particles abraded from kitchen scourers

In the following section a comparison of the results for the characterisation of particles abraded from kitchen scourers is presented. Therefore this section is categorised into a comparison of the results based on analysis conducted on particle size, number and morphology. This section indicates that the application of each technique exhibited differences in the results produced.

#### *4.9.1. Comparison of applied techniques used to determine particle size*

There were differences in the size, number and morphology of the particles analysed. A comparison of the different techniques used revealed differences in results for the characterisation of particles. For example, based on particle size, measurements by laser diffraction, microscopy and imaging flow cytometry demonstrated the largest to the smallest particle size distribution. This is because the laser diffraction measured the widest particle size range (0.04 – 2500m), and imaging flow cytometry determined size of particles  $\leq 70 \mu\text{m}$ . However, the different modes of analysis produced different results even for the same technique. For example, with the microscopy technique, it was possible to measure particles at magnifications of 100X and 200X. Consequently, the results exhibited differences in size based on the magnifications used. Furthermore, the results differed from results of the other techniques used (Figure 4.8.9). The size of particles measured by the laser diffraction technique was larger than measurements conducted with microscopy, at magnifications of 100X and 200X by factors 6 and 1 respectively (Figure 4.8.9). In addition, using the average particle size, the laser diffraction technique demonstrated that particles measured were 13 times larger than the length feature of particles measured by the imaging flow cytometry technique, and 139 times larger than the diameter feature of the particles (Figure 4.8.9).

The different techniques exhibited differences in the way the analysis of particle data was analysed. For example, with the imaging flow cytometry, it was possible to divide particle size into categories, on size measurement features. Typically this technique allowed for the size classifications based on the area, length and diameter features. Furthermore the imaging flow cytometry demonstrated the ability to apply shape features developed in the template, to analyse particle size based on the elongated and circular-like shape features.

The differences exhibited in the size of particles are likely because of the different measurement operating principles of the individual techniques. Particle size results based on the application of the different techniques should be described based on the respective techniques used.

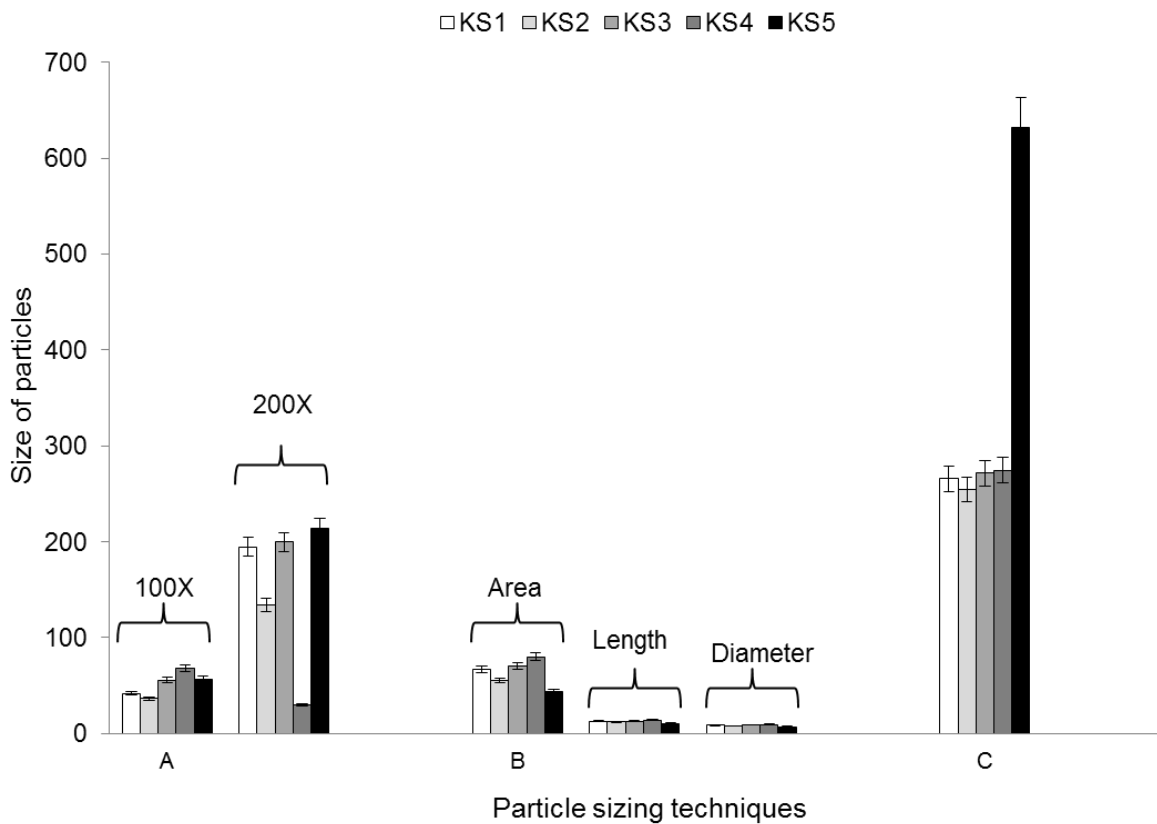


Figure 4.8.9. Bar chart showing the mean size range for particles abraded from kitchen scourers. Mean particle size determined by microscopy at magnifications of 100X and 200X (A), imaging flow cytometry using area, length and diameter (B), and laser diffraction technique (C).

By contrast, the analysis for the number of particles indicated that imaging flow cytometry exhibited the largest number of particles compared to the microscopy analysis. The number of particles was not determined by the laser diffraction technique as the equipment was not able to do so. In addition, the morphology of the particles demonstrated the presence of similar shapes and colours for the techniques applied however there were distinct profiles for the particle shape unique to each technique.

#### *4.9.2. Evaluation of the number of particles using microscopy and imaging flow cytometry techniques*

There was no obvious trend for the number of particles abraded from kitchen scourers. From the microscopy study, counts conducted at both magnifications revealed the smallest to the largest number of particles was indicated as KS4, KS2, KS1, KS3, and KS5 (Figure 4.9.0). By comparison, the imaging flow cytometry technique revealed a difference in the trend of smallest to largest number of particles, indicated by KS1, KS3, KS2, KS4 and KS5. The only similarity of both techniques was that the highest number of particles was indicated by particles in KS5 (Figure 4.9.0).

There were clear differences in the number of particles abraded from kitchen scourers in all five products analysed. The application of the imaging flow cytometry exhibited the highest number of particles by comparison with other techniques applied. The number of particles determined by imaging flow cytometry was larger than counts determined at magnifications of 100X and 200X, by factors of 19 and 14 respectively. Therefore the results demonstrated that the particle number based on a 70 cut-off filter was larger than particle number determined by microscopy.

A comparison of the different shape profiles, used to determine particle number also indicated differences based on the different techniques. Fragment particles, described as circular with the imaging flow cytometry, indicated that microscopy counts at magnifications of 100X and 200X, were less than imaging flow cytometry counts by factors of 36 and 23 respectively. Likewise, the number of fibre particles determined by imaging flow cytometry, was more than results for the microscopy study. Therefore fibre particles determined by imaging flow cytometry was more than that for microscopy at magnifications of 100X and 200X by factors of 5 and 4 respectively.

Generally similar to the assessment of particle size, it is likely that the differences observed for the number of particles was likely because of the different modes of operation of the techniques. Typically, the imaging flow cytometry technique demonstrated the ability to count particles automatically by applying user specific templates, something that is not possible with microscopy technique that is operated manually. In addition, the high sensitivity of the imaging flow cytometry technique indicates that the particles that are not blank corrected will be counted. By comparison,

using the microscopy, it is possible to observe particles in blanks, especially those that are visible to the eye. However, because microscopy is a manual technique, it is prone to bias, time consuming and prone to error. Consequently, the number of particles in the products analysed was largely influenced by the different techniques applied.

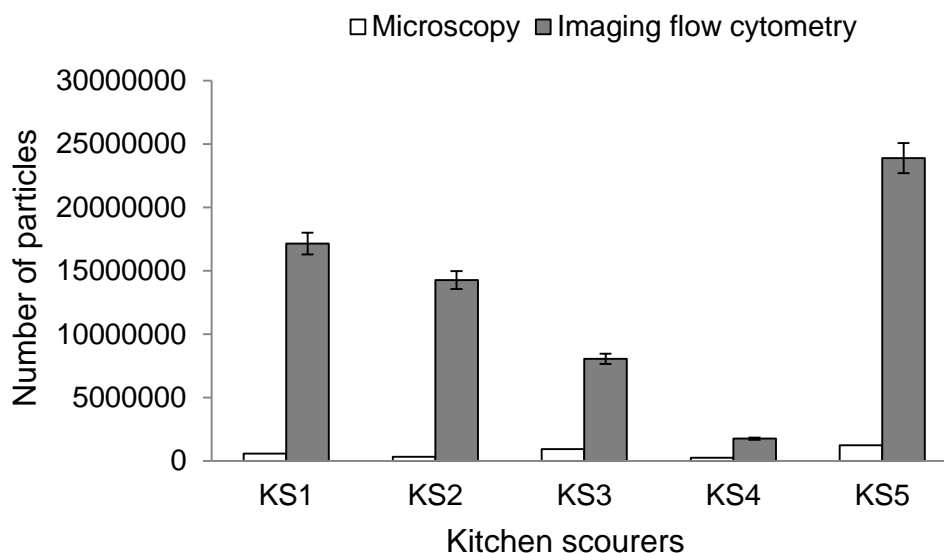


*Figure 4.9.0. Bar chart showing the number of all particles abraded from kitchen scourers and analysed by the different techniques used. The larger number of particles as determined by imaging flow cytometry (bars in grey colour), and the smaller particle number as determined by microscopy (bars in white) are indicated in the chart.*

#### 4.9.3. Comparison of particle morphology applying different techniques

A comparison of the techniques used to determine the morphology and colour of the particles abraded from kitchen scourers revealed a wide range and detail of particle shapes. Therefore the shapes of the particles ranged from irregular, rods to grain-like shapes. Based on observations, the microscopy technique exhibited the most detailed shape description of particles in comparison to the other techniques. As such, the microscopy technique showed that there were irregular, grain-like, elliptical, rods to threadlike shapes (Figure 4.9.1). Similarly, the analysis of particle shape by the FT-IR technique revealed that particle shape ranged from elongated, irregular to circular-like particles and particles appeared more 3-dimensional similar to the particles analysed by the imaging flow cytometry technique. However, the particles analysed by the microscopy technique appeared flat and 2-dimensional (Figure 4.9.2). In addition the application of microscopy and micro-FT-IR techniques highlighted

contours and more sharp edges and more detailed images, compared to the particles analysed by imaging flow cytometry (Figure 4.9.1 and 4.9.2). Although the imaging flow cytometry revealed less detailed particle shape descriptions, it allowed for observations of particles shape based on side scatter and fluorescence properties of the particles. Furthermore, it was possible to classify particle shape automatically into elongated, irregular to circular-like shapes with imaging flow cytometry, something that was not possible with microscopy and micro-FT-IR techniques (Figure 4.9.2).

The techniques also demonstrated differences in the colour of the particles in all products analysed. The micro-FT-IR revealed a true reflection of the colours of the particles abraded from the five kitchen scourers. By comparison, the microscopy and imaging flow cytometry techniques however did not reveal true colours of the particles (Figures 4.9.1 and 4.9.2). Therefore, it is apparent that the difference in the colours of the particles analysed, is based on the different modes of image capture unique to each technique. It is possible that manual and automated techniques will produce differences in the shape and colour of the particles observed. Generally, the different techniques demonstrated the ability to determine particle shape.

---

---

**Microscopy**

---

---

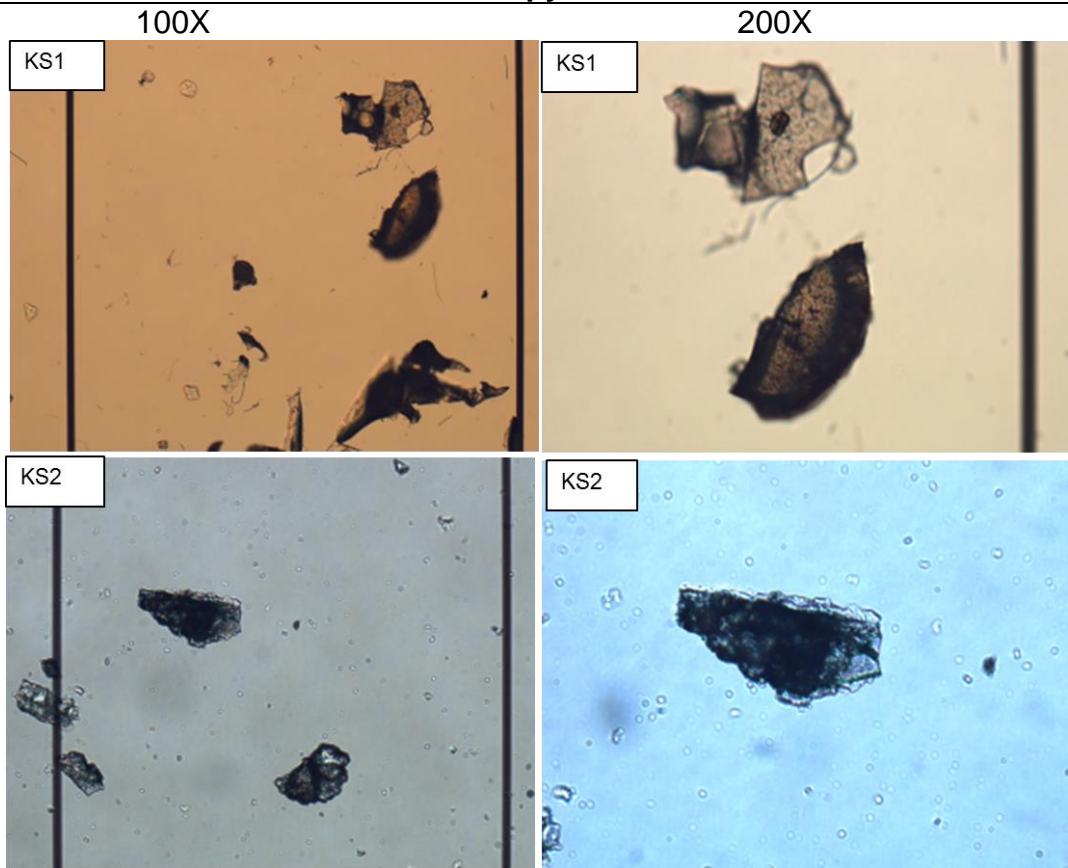


*Figure 4.9.1. Morphology of particles abraded from kitchen scourers and analysed by microscopy. The analysis of particle shape and colour was determined at magnifications of 100X and 200X.*



## Imaging flow cytometry



## FT-IR

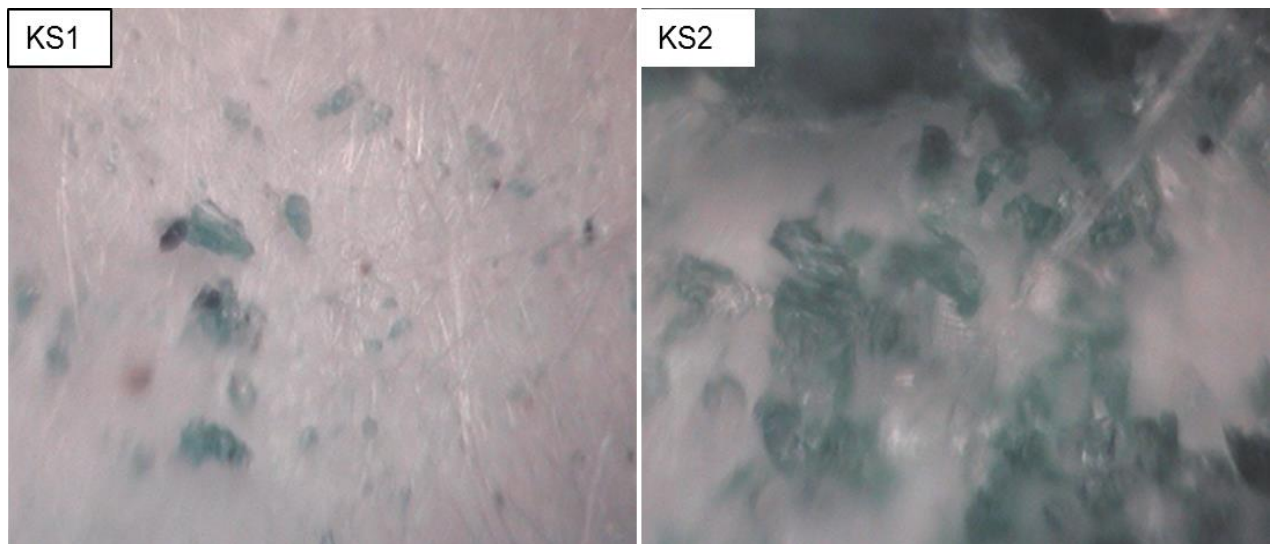


Figure 4.9.2. The images of particles abraded from kitchen scourers using Imaging flow cytometry and FT-IR techniques.

## CHAPTER 5: DISCUSSION

Research on plastic pollution has focused on macroplastics in the aquatic and terrestrial environment, largely because they have clearly impacted living organisms (Imhof et al. 2016; Kanhai et al. 2017). However, there has been a shift in the focus of study to smaller microplastics. This is partly because of the introduction of these particles to the environment from a myriad of sources (Wessel et al. 2016; Bosker et al. 2017b). In particular, the frequent use of personal care products which have microplastic particles as part of their ingredients make up a relatively recent source of contamination to the environment (Bennet 2016; Duis & Coors 2016b; Fendall & Sewell 2009). However, that particle abrasion from kitchen scourers has not been documented as a source of microplastics to the environment.

The characterisation of microplastics is important to understand their likely source, fate and transport in the environment and their impact to living organisms (Andrady 2017; Napper et al. 2015). However there are no universally accepted laboratory protocol and analysis techniques to characterise microplastics (Hidalgo-Ruz & Gutow 2012; Shim et al. 2017). In addition, the current reports on the analysis of particles do not often report on the challenges encountered in sample preparation and the limitations of the techniques used. Furthermore, there has not been a comparison of a multi-technique approach for the characterisation of particles. Therefore this thesis reports on the differences in sample preparation, the application of the different techniques and the different results produced.

### 5.1 Density separation of particles from matrix

In this study it was hypothesised that the application of different sample preparation protocols for the characterisation of particles from PCPs and kitchen scourers would produce similar results. However, the difference in sample preparation indicated substantial differences in the results for the analysis. The sample preparation for microplastic analysis follows a general process of weighing of the sample, density separation and filtration. Particles separated from PCPs were based on the difference in density of the particles and density separation solution. The initial steps taken to

separate particles from PCPs was not successful. During the development of the density separation procedure, particles flooded the membrane filter attached to the syringe and resulted in the loss of samples. The sample preparation of microplastics have been well documented (Maes et al. 2017; Hintersteiner 2015; Hidalgo-Ruz & Gutow 2012). In addition, information on the separation of particles from PCPs have also been reported (Chang 2015; Napper et al. 2015; Fendall & Sewell 2009). However, none of these studies reported using NaCl for the separation of particles from PCPs. These studies report that density separation was conducted using boiling water and distilled water (Chang 2015; Napper et al. 2015). Although the particles were separated, it is not clear whether the differences in density separation methods had an impact on the results produced. The reports did not indicate whether the density separation methods adopted allowed for a complete separation of particles from the products. This is true especially for particles that were characterised by viscosity. It is possible that the boiling water dissolved the viscous solution and allowed for the separation of particles. However, it is not clear whether boiling water had an apparent effect on the integrity of the particles separated. Furthermore, there was no information on the effectiveness of diluted water for density separation of particles from PCPs. Furthermore, the limitations and the advantages of the density separation steps taken were not reported (Chang 2015; Napper et al. 2015).

There are reports on the application of other density separation solutions used for the extraction of particles from complex matrix (sediment samples). These solutions are useful for separating high density particles such as polyethylene terephthalate and polyvinyl chloride from matrix (Mintenig et al. 2017; Brian Quinn, Fionn Murphy 2016). There are reports on the application of zinc chloride and sodium iodide used as density separation solutions, and have been used successfully to separate particles from matrix (Zhao et al. 2017; Nuelle et al. 2014; Liebezeit & Dubaish 2012).

## 5.2 Filtration of particles separated from matrix

During vacuum filtration of particles from the solution, the filter membranes clogged after 10 seconds, a limitation of the method used to separate particles from PCPs. This was more obvious for the particles separated from the toothpastes than facial

scrub particles. The viscous solution that is a part of the products prevented the flow of filtration. Therefore it was necessary to introduce a centrifugation step to aid the separation of particles from the viscous solution. This proved useful and it allowed for particle separation and improved vacuum filtration. After the density separation procedure, the vacuum filtration step allowed for the collection of particles on the surface of the filter paper. This step has been widely documented and has allowed for the collection of particles (Hidalgo-Ruz & Gutow 2012; Karlsson et al. 2017). This thesis reports that particles were filtered using different filters that exhibited differences in pore size. This was because of the differences in the size of particles that could be measured by the different techniques. For example, filter paper (GFC) with a pore size of 1.2  $\mu\text{m}$  was used to filter samples for the FT-IR study, and by contrast, a 70  $\mu\text{m}$  filter was applied to samples for the imaging flow cytometry analysis. (Maes et al. 2017; Hidalgo-Ruz & Gutow 2012). However some studies have reported using non standardised filtration steps while others have not indicated the limitations of the filtration step used (Fendall & Sewell 2009; Chang 2015). It is apparent that the application of different filtration methods will have an impact on the results produced. For example, based on two different density approaches, the size of particles reported ranged from 4.1 to 1240  $\mu\text{m}$  reported in one study, and 60 to 800  $\mu\text{m}$  in another (Chang 2015; Fendall & Sewell 2009).

This difference in the sample preparation indicated that the different approaches produced different outcomes. By contrast, particle separation from kitchen scourers was achieved by abrasion. For this process, it was much easier separating particles from kitchen scourers than it was for particles from PCPs. The process of particle abrasion did not require a density separation solution for the separation of particles. In addition, a centrifugation step was not followed for particles abraded from kitchen scourers because the sample did not demonstrate any viscosity. Furthermore, for the sample preparation of particles from kitchen scourers, washing liquids were not used for this study; this was done to collect only pure particle samples and to prevent contamination of sample from the detergent. Currently, it is not clear if there would be a difference if washing liquid is used for the abrasion of particles from kitchen scourers. A comparison of particle abrasion with and without washing liquid will be useful to determine the differences if any, in the volume of particles separated from kitchen scourers.

This study reports that there were differences in the final volume of samples that were prepared for particle analysis. In particular, this was because of the differences in the final volume of sample prepared for particle analysis and size cut-off for the particles prepared. For example, for the analysis of particles using microscopy, 1 mL of the sample was transferred to the Sedgewick-rafter cell SRC, for the characterisation of particles. Similarly, particle characterisation by the IFC was carried out by transferring 1 mL of the sample to a 1.5 mL microcentrifuge tube for analysis. By comparison, 10 mL of the sample was introduced to the sample holding tank for particle size distribution analysis, using the laser diffraction technique (Table 4.2.1). Therefore more particles were introduced to the CILAS 1180 used for the laser diffraction analysis. Measurements of a larger sample size gives more confidence with the data and reduces the margin of error and therefore is more accurate and increases reliability (Sham & Purcell 2014). This means that the microscopy and IFC techniques used in this research could analyse 10% of what the laser diffraction technique could measure.

*Table 4.2.1. The different final volumes of samples prepared correspond to the different techniques used for the characterisation of particles.*

Technique	Volume of sample	Particle size cut-off
Microscopy	1 mL	No cut-off
Laser diffraction	10 mL	No cut-off
Imaging flow cytometry	1.5 $\mu$ L	70 $\mu$ m
Micro-FT-IR	10 mL	1.2 $\mu$ m
ATR-FT-IR	-	1.2 $\mu$ m

### 5.3. Characterisation of all particles using different techniques

Following sample preparation, characterisation of particles was determined using multiple techniques. It was hypothesised that the application of different techniques for the characterisation of particles separated from PCPs and abraded from kitchen scourers would produce similar results. This was demonstrated by using different

approaches for the analysis of particle size, number and morphology with different techniques. The results for the microscopy, laser diffraction and imaging flow cytometry techniques exhibited differences in particle size for all PCPs and kitchen scourers. As such the results showed that the size of all the particles analysed were < 5 mm.

### *5.3.1. Particle analysis using the microscopy technique*

The microscopy technique indicated differences at both magnifications. Higher magnification allowed for smaller particles to be analysed. In addition, more particles could be observed at the higher magnification. Furthermore, the size measurements and particle count determined in different transects produced different results. Characterisation of particles in more transects of a SRC suggests more particles would be analysed, thus increasing sample size and making data more reliable. However, it is apparent that there is standard protocol for using the SRC to analyse particles and methods currently used are adapted for individual studies (Vassalli et al. 2018; Jauzein et al. 2016; Gollasch et al. 2015). It can be argued that counting more cells of a SRC increases the sample size and provide more raw data for analysis. It is apparent that differences were demonstrated when more cells of the SRC was counted, as reported in this thesis. Therefore it is apparent that the analysis of more particles provides confidence in the results and allows for improved risk assessment for microplastics in the environment. The analysis of particles by microscopy requires long hours of analysis and is labour intensive. For one sample it took about 1.5 hours to measure particles on the SRC. Using microscopy, the size of particles was similar and in some cases at variance with what was reported in other studies (Fendall & Sewell 2009; Desforges et al. 2014; Chang 2015). For example the smallest particle measured using microscopy at the magnification of 200X was 5 microns. However a study reported the smallest particle size determined at the magnification of 40X was 60 microns (Chang 2015). In addition another study reported a minimum particle size of 4.1 microns, determined at the magnifications of 40X or 100X (as reported in the article) (Fendall & Sewell 2009). The largest particle measured in this current study was different from what others have reported. The studies indicated the largest

particles were 800, 1240 and 5810 microns (Fendall & Sewell 2009; Desforges et al. 2014; Chang 2015).

By comparison, the particles abraded from the kitchen scourers exhibited a wider size distribution than particles separated from personal care products. Some of the kitchen scourers were characterised by particles of fibre that were longer than particles separated from personal care products. This implies that larger particles are produced from kitchen scourers than from using personal care products that contain particles of microplastics. The same procedure used for the analysis of particles from PCPs was adopted for the analysis of particles abraded from kitchen scourers. .

Currently, there is no documented evidence reporting on the particles abraded from kitchen scourers. However, there are reports on the release of particles of fibre from laundered garments (Napper & Thompson 2016). Using a Leica light microscope, the study reported that the mean diameter of fibre particles ranged from 11.9 to 17.7  $\mu\text{m}$ , and length ranged from 5.0 to 7.88 mm (Napper & Thompson 2016). This study reported results that were different to that reported in this thesis. In particular, the diameter of particles was not reported in this thesis; however, the length of fibre particles was larger by several orders of magnitude than the length of particles reported in this thesis. The results were different because of the differences in size between the kitchen scourers reported in this thesis and the garments used in the study. Therefore garments would shed relatively larger particles of fibre compared to kitchen scourers. It was not clear what magnification was used for the analysis of particles released from the garments, however image j software was used to determine particle size. Automated software like image j allows for user defined templates for the analysis of particle size and therefore offers a less tedious option for particle analysis. By contrast, this thesis reports that the sizes of particles were determined by direct measurements of observed particles. Particle analysis using an automated software provides more confidence in the output than measurements conducted manually, provided the right templates are developed are applied.

The numbers of particles separated from PCPs have been documented in different studies (Napper et al. 2015; Chang 2015). There is evidence to suggest differences in the number of particles, based on the different approaches adopted for the analysis of particles (Napper et al. 2015; Chang 2015). However it was difficult to make a direct

comparison because results were presented in different formats. In one study, 4594 and 94500 particles were counted, whilst the other study reported particle concentration ranging from 0.08 – 0.1 g/mL. This implies that the different techniques used to quantify particles produced different results.

Currently, there are no reports on the estimation for the number of particles abraded from KS. Reports indicate characterisation of particles of fibre have focused largely on the release of particles of fibre from washed garments (Hernandez et al. 2017; Napper & Thompson 2016). One study indicated that from an average 1 kg wash, about 120,000 particles of acrylic fibre could be released per wash load (Napper & Thompson 2016). Another study reported 0.025 and 0.1 mg/g of fibre particles were released from garments washed with and without detergents respectively (Hernandez et al. 2017). These values are different to the estimates for the number of particles abraded from kitchen scourers. However, a direct comparison between results reported in this thesis and those indicated in both studies was not possible, because the results were reported differently. This is an indication of some of the difficulties encountered in interpreting results produced from different studies that have adopted different methods and produced different results. It can be argued that evaluation of risk assessment for the number of fibre particles will be a challenge because of the differences mentioned.

The particle morphology indicated differences based on the technique that was used. This study shows that using the microscopy technique, the higher magnification demonstrated a more detailed image of the particles. The higher magnification increases the resolution and details of the particle shape. In addition, the higher magnification allowed the observation of particles in the lower size. This implies that using the microscopy technique at a higher magnification demonstrates the ability to detect smaller particles. The study by Chang et al, reported similar morphology of particles, to what was observed in this research, and at a higher magnification (Chang 2015). Although no other study has reported on the morphology of particles abraded from KS, it is clear that there were similarities in the shape of fragments and irregular shaped particles separated from PCPs. In addition the shape of fibre particles show similarities with the morphology of fibre particles reported (Leslie et al. 2017).



### 5.3.2. Laser diffraction analysis of microplastics

The CILAS 1180 laser diffraction instrument used in this study is equipped to measure particle size range from 0.04 – 2500 microns (Latifi et al. 2015; Elliott et al. 2017). The size of particles reported in this thesis indicates a wider size range to that reported in another study that measured particles separated from PCPs (Napper et al. 2015). The study indicated that particle size measurements were conducted by laser diffraction equipment that had a measurement range of 0.015 – 2000  $\mu\text{m}$  (Napper et al. 2015). In addition, the report shows that the mean particle diameter ranged from 164 to 327  $\mu\text{m}$ . The mean particle size reported in this thesis was larger than that documented in another study (Napper et al. 2015). The differences in particle size could be because of the differences in sample preparation and analysis, and the size range that can be measured by both instruments.

The length of particles reported by (Napper & Thompson 2016) indicate particles released from garments were larger than that abraded from kitchen scourers (Table 4.2.2). Thus suggesting that fibre particles from different sources have different sizes. This implies that the larger particles will likely undergo further degradation to produce smaller microplastics in the longterm (Duis & Coors 2016b). On entering the environment, fibre particles are likely to be ingested by organisms and resulting in blocked digestive tracts, injury and mortality (Taylor et al. 2016). By contrast, the smaller fibre particles will readily adsorb toxic chemicals from the environment, due to their large surface area to volume ratio (Taylor et al. 2016). This difference in particle size could be because of the different methods adopted for sample preparation and the differences in the measurement size range of the instruments. .

Table 4.2.2. Comparison of the different results for the size of fibre particles determined using laser diffraction and light microscopy. The results for the thesis are indicated as diameter measurements, and the light microscopy results are based on length measurements. The results from the Napper and Thompson report are based on both length and diameter measurements.

<b>Dimension</b>	<b>Thesis measurements</b>	<b>Napper and Thompson (2016)</b>
	<i>Laser diffraction</i>	<i>Light microscopy</i>
<b>Diameter</b>	254 – 632 $\mu\text{m}$	11.9 – 17.7 $\mu\text{m}$
	<i>Light microscopy</i>	<i>Light microscopy</i>
<b>Length</b>	100X                      200X	Magnification not stated
	36 – 67 $\mu\text{m}$ 29.9–213 $\mu\text{m}$	5 – 7.8 mm

The laser diffraction technique did not allow for the particle differentiation into fibre and fragments as was possible with the microscopy technique. This implies that the microscopy technique will allow for the interrogation of particles to differentiate between fibre particles and fragments, something that is not possible with all laser diffraction techniques. The interrogation of particles is important to determine and understand the differences in size and particle type (fibre or fragment) and the implications for the environment. However, the microscopy technique was not equipped to measure such a wide particle size range, because of the limitations of the magnifications used. A smaller magnification does not allow particles below a certain size to be detected. By contrast the use of higher magnifications limits our ability to observe large particles as was the case in this study. However using the microscopy technique, particles were clearly observed under the Sedgewick-rafter cell SRC, something that was not possible with the laser diffraction technique. This implies that the laser diffraction technique will produce different results to microscopy because they use different fundamental approaches to determine particle size (Rawle et al. 2003; Malvern 2015).

### 5.3.3. Particle analysis using imaging flow cytometry

The imaging flow cytometry technique which is novel in microplastics studies determines the size of particles < 70 microns. Currently, there is no documented evidence for the application of imaging flow cytometry technique in microplastics studies and in particular, for the characterisation of particles separated from PCPs and kitchen scourers. However, this thesis shows proof that using the Imagestream imaging flow cytometer, the size of microplastics separated from PCPs can be determined. Imaging flow cytometry has been used in range of flow cytometry studies to analyse changes to cell structure and the interaction of cells (Beaton-Green et al. 2016; Headland et al. 2014a). The Imagestream characterised by its sensitivity, speed, allows for the analysis of a large population of particles within a very small volume, and ensures a statistically robust results.

The Imagestream is equipped with the IDEAS software which allows templates to be developed for the analysis of particle size. In particular the size features associated with the IDEAS software template allowed for the analysis of particles according to the area, length and diameter. In addition, particles from all PCPs and KS were measured using the shape features of elongated and circular particles. The application of the templates indicated differences based on the size and shape features applied. The application of set templates for the analysis of microplastics is not possible with a manual technique like microscopy or the automated laser diffraction techniques. The manual microscopy technique used in this study did not allow for an automated analysis of particles separated from PCPs and abraded from kitchen scourers. Instead, particles observed were measured directly and categorised based on a general definition of the particle shape. This implies that the imaging flow cytometry technique can allow for a more detailed size analysis of particles based on the differences in shape, because of the templates available in the IDEAS software. Furthermore, because of its sensitivity, this study has shown that the technique is capable of detecting particles as small as 1  $\mu\text{m}$  as indicated in the PCPs and KS. By comparison the laser diffraction technique was able to detect particles as small as 0.2  $\mu\text{m}$ , and the microscopy measured particles as small as 5  $\mu\text{m}$ .

Using the IDEAS software of the imaging flow cytometry technique, particles can be characterised by applying user defined templates as reported in this thesis.

However, it can be challenging separating particles that have similar size and number as reported in this study. This was demonstrated with the difficulty in separating calibration speedbeads from particles separated from PCPs. This study showed that turning off the speed beads allowed for the analysis of the particles alone. However, the particles were detected in the blank water samples analysed by imaging flow cytometry. By contrast, the analysis of blank water samples using the microscopy and laser diffraction techniques did not reveal particles in the blanks. This implies that the imaging flow cytometer characterised by its high sensitivity, was able to detect foreign particles. This implies that it is important to check laboratory grade water commonly used to prepare microplastics samples for analysis, for debris and contaminants.

The proper functioning of the ImageStream<sup>®x</sup> Mark II instrument is assessed using the calibration Speedbeads that constantly run through the machine. It is apparent that Speedbeads do not fluoresce, and exhibit high side scatter and have are characterised by a small area. However during analysis of the particles, it was difficult to distinguish between the calibration Speedbeads and the particles separated from PCPs. This was because of the high number of Speedbeads ( $1.6 \times 10^7$  /mL) and the similarity in size (1  $\mu$ m) to the smallest particles in the samples analysed. This study has shown that some of the particles separated from PCPs and KS exhibited side-scatter and fluorescent properties. However, these properties were not applied to determine the size of particles in all the products analysed. Some of the particle detected in the blanks exhibited similar side-scatter properties to particles from PCPs and KS. This implies that particles demonstrating side-scatter and/or fluorescent properties can be readily detected by the instrument. However, the analysis of particle size based on fluorescent and side-scatter properties was not possible with the microscopy and laser diffraction techniques used for this study.

Because long particles are oriented vertically by flow in the imaging flow cytometer, measurements of maximum particle size is limited by the particle width (Amnis EMD Millipore 2012). Therefore, the largest particle that can be measured is dependent on the objective lens used and its corresponding field of view. This thesis reports that the objective used was 20x and a 120  $\mu$ m field of view (Probst et al. 2017; Amnis EMD Millipore 2012). Therefore particles are filtered through a 70 micron filter, to remove particles that have a width greater than 70 microns and to prevent clogging the instrument (Amnis EMD Millipore 2018). However, because this technique determines

the size of particles in the <70  $\mu\text{m}$  sub-fraction, it is not possible to measure larger particles. By contrast, this implies that this technique can detect particles in the lower size range that have been widely suggested to have environmental implications (Headland et al. 2014a; Lannigan & Erdbruegger 2017; Amnis EMD Millipore 2018). By comparison with the other techniques, the imaging flow cytometer demonstrated the smallest size distribution. Using the imaging flow cytometry technique, the general mean size range of particles abraded from kitchen scourers and separated from personal care products was similar. This implies that for the sub 70  $\mu\text{m}$  fraction, there were similarities in general particle size. However, elongated particles (fibre particles) exhibited larger mean sizes.

The imaging flow cytometry technique estimated the largest number of particles in FS2. This report shows that there were fewer particles abraded from KS. It was difficult successfully applying the templates developed to estimate the number of particles from the other products. The speedbeads demonstrated similarities with particles from all products. Therefore the templates developed could not accurately separate speedbeads from the separated particles. The speedbeads were consequently turned off to allow the quantification of particles separated from the PCPs alone. Therefore, this protocol could be adopted for the estimation of particles abraded from KS. This implies that the sensitivity of the ImageStream and the large numbers it can detect was demonstrated by the detection of debris in the blank water samples.

By comparison, particles of debris were not detected using the microscopy technique. However, with the imaging flow cytometer, the occurrence of debris in the blank water samples increased the particle count well above background levels. Therefore FS2 exhibited the largest number of particles for all the PCPs. However the number of particles in other products could not be determined as they exhibited lower numbers to the blanks. It was observed during operation of the ImageStream that two factors could account for this, firstly in all samples except FS2, the recovered plastics rapidly separated (settled and/or floated in the tube) which, was compounded by a delay in data acquisition by the instrument. Although the instrument was not acquiring, images of larger plastic particles were visible on the real time image display, and the acquired data indicate a decline in both the size and number of particles with time, consistent, with uptake of a non-homogenous sample. The number of particles exceeded the number of particles in the blank water samples. The evidence from FS2

of a high number of small particles in the low micron range is supported by observations reported in facial scrubs of 300 billion particles per gram in the sub-micron size range (Hernandez et al. 2017). Analysis of PCPs using imaging flow cytometry showed 150 times more microplastics than microscopy in one sample.

The occurrence and detection of debris in the blanks indicates the sensitivity of the technique and the possibility of reporting overestimates for the number of particles. There is currently no report on the occurrence of debris in laboratory grade water used as blank water samples. This is because the analysis of blank water samples has not been a focus of Imagestream studies. In addition, the Imagestream analysis is commonly focused on cells which have a defined structure, unlike particles from PCPs that do not. The microscopy technique did not have the sensitivity of the technique to detect the number and size of debris in the blank water samples.

By comparison, this study reports that the morphology of particles determined with the imaging flow cytometer used features available in the developed template. There was a narrow classification of particles using the imaging flow cytometer. Particles were either elongated or circular. However, the morphology of particles determined by microscopy indicated a wider shape classification. The difference produced different outcomes for particle morphology. The IDEAS software of the imaging flow cytometer is automated and can analyse particles in a more defined way. The IDEAS software was useful for the interrogation of bins in the histogram to detect particles in the image display area. It is apparent that this was useful because it allowed for the confirmation of the particle being observed. The imaging flow cytometry technique is useful for the analysis of particles in the lower size range. However, the manual microscopy technique is not equipped with automated software which allows for the rapid and standardised analysis of particle morphology. In addition, this study reports that particles that cannot be detected by the microscopy technique can be analysed by the imaging flow cytometer. However, the microscopy technique revealed a more detailed morphology than the imaging flow cytometer.

#### *5.4. Particle polymer identification using FT-IR*

It has been suggested that the visual inspection of unknown particles does not provide strong evidence for the identification of particles (Hidalgo-Ruz & Gutow 2012). Particle polymer identification was determined by micro-FT-IR, and has recently been used largely in microplastics identification. It is an important technique used for polymer identification because the IR spectra of unknown particles can be cross checked with the known IR spectra available in a library (Tagg et al. 2015; Crichton et al. 2017). To determine whether micro-FT-IR had an apparent impact on the IR spectra of particles, because of the different particle shapes, the results were compared with the ATR-FT-IR. These modes of analysis are largely susceptible to scattering of IR beam because of the morphology of irregularly shaped particles. This report has shown that both modes of analysis had no apparent impact on the IR spectra for particles analysed. However, the particles separated from PCPs exhibited IR spectra with no distortions. But by contrast, although regions of absorbance for the stretching and bending of bonds unique to polyethylene and polyester were present, both modes of analysis demonstrated distorted IR spectra for particles abraded from KS. The presence of additives such as dyes and colourings used for the manufacture of KS interfered with IR beam, resulting in distorted IR spectra. It has been reported that irregularly shaped particles exhibit distorted IR spectra, for micro-FT-IR and ATR-FT-IR (Harrison et al. 2012).

The results in this report implies that particle polymer identification can only be reliably conducted by detecting regions of absorbance that correspond to the stretching and bending of C-H bonds as indicated with reference to the IR spectra (Tagg et al. 2015; Crichton et al. 2017). The combination of the analytical strength of the FT-IR and the optical resolution of a microscope allows for the polymer identification of particles (Hidalgo-Ruz & Gutow 2012; Shim et al. 2017). In addition, the coupling of an FPA detector allows for the analysis of randomly selected parts of a filter paper (Tagg et al. 2015). This is in contrast to the single point analysis of particles on filter paper which limits the sections on the filter paper to be scanned (Nor & Obbard 2014). There is evidence to suggest that particles collected from the environment were thought to be microplastics, until the analysis with the FT-IR confirmed otherwise (Ziajahromi et al. 2017a). Several other methods have been used

to determine particle polymer identity; some include Raman spectroscopy and the pyrolysis-gas chromatography with mass spectrometry (Pyr-GC/MS) (Hidalgo-Ruz & Gutow 2012; T Rocha-Santos & Duarte 2015). The FT-IR technique is useful for the identification of irregularly shaped particle, something that is demonstrated in this study (T Rocha-Santos & Duarte 2015). Therefore, it is a useful technique that demonstrates the ability to distinguish actual microplastics from suspected microplastics.

Although this study reports that the morphology of particles separated from PCPs exhibited some similarities with the shape of particles abraded from KS, there were differences in the output for the morphology of PCPs and KS, using the different techniques. This is because the techniques have different modes for analysing particles. The IDEAS software for the imaging flow cytometry technique allows for the analysis of particle morphology by developing user defined templates. This automated mode of analysis is not available with the microscopy and the micro-FT-IR techniques. However the microscopy and micro-FT-IR techniques provided more detailed images for particle morphology.

It is not clear whether the source of microplastics can be determined based on their morphology. The exposure of these particles in the environment suggests chemical, physical and biological factors will have an impact on the integrity of the particle. Therefore, it is not clear how accurate the predictions of particle origin will be for such particles (Duis & Coors 2016b). This is true for particles collected from the environment that are characterised by fouling with organic matter, than for virgin particles. However, particles exhibiting a distinct morphology and size like resin pellets, can be traced largely to pre-production plastic spills (Duis & Coors 2016b). However, as this report shows, the non-distinct particle shape and morphology exhibited by most particles will make the identification of particle source difficult. However, particles of fibre can be described as originating from a secondary source of microplastics. This is because particles of fibre are suggested to be largely produced shedding from garments, and abrasion from kitchen scourers as reported in this study (Napper & Thompson 2016). It was hypothesised that different techniques will indicate differences in the morphology of the particles.



## 5.5. Assessment of the fate and transport of particles characterised by different techniques

It is acknowledged that the frequent use of PCPs that contain microplastics as part of their ingredients will be routinely washed down drains and will be transported to WWTPs (GESAMP 2015; Chang 2015). The particles abraded from kitchen scourers will also be transported to WWTPs. Microplastics in the environment can originate from aquatic and land-based sources (Duis & Coors 2016d; Nizzetto et al. 2016). Particles from aquatic based sources include fragmented particles produced by physical, chemical and biological action on macroplastics. In addition, land-based sources of microplastics originate largely from urban run-off and discharged effluent from WWTPs (Ziajahromi et al. 2017b; Nizzetto et al. 2016).

Currently, it is not clear how many people use PCPs that contain microplastics, however, there is evidence indicating 99% of households in the UK use kitchen scourers (Mintel 2014). Therefore, kitchen scourers are likely to be more widely used than personal care products that have microplastics as ingredients. This thesis reports larger particles were abraded from kitchen scourers, than particles separated from PCPs. In addition, there were more particles of microplastics separated from PCPs than that abraded from kitchen scourers. This implies that from one use, larger microplastic particles abraded from kitchen scourers during washing of kitchen utensils will be transported down drains to WWTPs and smaller will be released from PCPs. By contrast, more particles will apparently be transported through drains to WWTPs, from a single use of PCPs, than a single use of kitchen scourers. A study reported that microplastics are transported through WWTPs and therefore act as a source of particle entry to the environment (Leslie et al. 2017; Ziajahromi et al. 2017a). Particles > 300  $\mu\text{m}$ , made up of fragments and particles of fibre, have been detected in waters that receive WWTPs effluent. However, the fate of particles < 20  $\mu\text{m}$  is relatively unknown (Kerstin Magnusson et al. 2016).

It is widely acknowledged that the entry of particles to WWTPs is likely to escape capture and enter the environment either directly as effluents or indirectly via run-off from sludge that contains microplastics (Ziajahromi et al. 2017b; Nizzetto et al. 2016). However, it is apparent that identifying and concluding that WWTPs are a source of particle entry to the environment is still challenging (Ziajahromi et al. 2017b; Carr et al.

2016a). The difficulty in understanding the contribution of WWTPs to the microplastics load in the environment is because of a number of reasons.

Firstly, different WWTPs will capture different sizes of particles, based on the technology available at the treatment plant. It is apparent that WWTPs are equipped with different screening methods to capture particles at different stages of the treatment process (Talvitie et al. 2017; Leslie et al. 2017). Some WWTPs have coarse > 6 mm, and others have fine 1.5 – 6 mm screens to separate particles, and others are equipped with membrane bioreactor used for primary effluents (Ziajahromi et al. 2017a; Mason et al. 2016a; Carr et al. 2016). Secondly, the different approaches adopted for particle sampling in WWTPs and the differences in how the outputs are reported does not allow for comparison of data (Talvitie et al. 2017; Leslie et al. 2017; Carr et al. 2016b).

In one report the average size of particles measured in 7 WWTPs with different hydraulic capacities, ranged from 10 – 5000  $\mu\text{m}$ . In addition, influent and effluent concentrations of microplastics in 7 WWTPs ranged from 68 – 910  $\text{L}^{-1}$  and 51 – 81  $\text{L}^{-1}$  respectively (Leslie et al. 2017). However, an average of 510 – 760  $\text{kg}^{-1}$  particles, equivalent to 71%, was retained in sewage sludge (Leslie et al. 2017). This suggests that although the WWTPs were relatively efficient in reducing particles in the effluents, at least 29% of particles would be introduced to the environment. Furthermore, between 1400 and 4900 particles  $\text{Kg}^{-1}\text{dw}$  were detected in surrounding waters that received treated and untreated waste water (Leslie et al. 2017). However, sediment analysis in waters close to urban areas revealed the number of particles ranged from 68 to 10,500 particles  $\text{Kg}^{-1}\text{dw}$  (Leslie et al. 2017). This indicates the distribution of particles from WWTPs into different compartments of the environment. By contrast another study reported a mean of 1.54, 0.48 and 0.28 microplastics  $\text{L}^{-1}$  detected in the primary, secondary and tertiary final effluent of a WWTP (Ziajahromi et al. 2017a). The methods adopted for sample collection, processing and analysis was different for both studies. The study by Leslie et al. 2017 used a 0.7  $\mu\text{m}$  filter to collect particles, while in another report, Ziajahromi et al. 2017b used a combination of filters with size ranging from 25 to 500  $\mu\text{m}$  (Leslie et al. 2017; Ziajahromi et al. 2017b). Furthermore, the particles identified consisted of spheres, coloured fibre particles, fibre particles of polyester and irregularly shaped polyethylene particles (Leslie et al. 2017; Ziajahromi et al. 2017b). Particles not discharged in effluents are frequently applied to farmlands

as sludge, resulting in contamination and entry to water bodies via run-off (Zubris & Richards 2005; Nizzetto et al. 2016; Ziajahromi et al. 2017a). The reports suggest the number of particles removed from effluents and transferred to sludge vary between reports (Talvitie et al. 2017; Mintenig et al. 2017).

It is reported in this thesis that the microscopy, laser diffraction and imaging flow cytometry results indicated that the size of particles separated from the PCPs will be readily transported through the mains to WWTPs (Ziajahromi et al. 2017; Carr et al. 2016a; IOC 2010).

The mean fibre particle size reported in this thesis was many times smaller than mean sizes reported in another study that determined particle size by scanning electron microscopy (Napper & Thompson 2016). The mean fibre particle size was in the micron range compared to the mm size range reported in another study (Napper & Thompson 2016). On the basis of particle size determined from the analysis of kitchen scourers, particles in the lower micron range will either escape capture or be transferred to sludge. The occurrence of particles of fibre in sewage sludge has been reported in studies that measured size of particles of fibre shed from washed garments (Napper & Thompson 2016). Fibres not captured by WWTPs might be added to sewage sludge and used as applications on farmlands (Napper & Thompson 2016; Gallagher et al. 2016). It is possible that during run-off particles of fibre are washed into freshwater environments and eventually into the sea (Ziajahromi et al. 2017a; Carr et al. 2016a). The reports suggested that the particles of fibre were because of abrasion of particles from garments during wash. Therefore, in a similar manner, particles of fibre abraded from kitchen scourers will be transported through sewers into the environment.

The contributions of WWTPs as a significant source of microplastics load to the environment has been widely discussed and in instances not clear. However, it is a potential source of particle entry to the environment with the potential to cause harm to living organisms. (Carr et al. 2016a; Gallagher et al. 2016).

## 5.6. Impact of microplastics on living organisms in the environment

In this thesis it is reported that the particles analysed in toothpastes, facial scrubs, and kitchen scourers will likely be an important primary and secondary source of microplastics to the environment (Duis & Coors 2016b; Chang 2015). At present about 10% of marine debris ingested by living organisms, is made up of microplastics (Napper et al. 2015). In addition, microplastics have been reported in different components in the environment (Van Cauwenberghe, Devriese, et al. 2015b; Kanhai et al. 2017). . The potential for microplastics to cause harm to living organisms has been well documented (Besseling et al. 2017; Rodriguez-Seijo et al. 2017). This implies that frequent use of products like FS2 will contribute to the microplastics load in the environment with potential ecological consequences.

The occurrence of these contaminants in the environment is of special concern because they have the potential to breakdown into smaller sizes and be distributed into different parts of the environment where they become bioavailable to living organisms (Jemec et al. 2016; Ziccardi et al. 2016b). Therefore, particles may be ingested by various living organisms from plankton, to fish, aquatic birds and mammals (Putnam et al. 2017; Oluniyi Solomon & Palanisami 2016). The ingestion of microplastics has been demonstrated in the gastrointestinal tracts of fish on Giglio Island Italy (Avio, Cardelli, et al. 2017). The study reported size of particles ranging from 100 to 1000  $\mu\text{m}$  were found in 77 to 86% of benthic fish species and in all the benthic-pelagic fish analysed (Avio, Cardelli, et al. 2017). Microplastics comprised mainly of fragments of polyethylene, nylon and polystyrene. In another study, mortality in different fish species in the western English Channel was reported after ingesting fragment particles ranging from 50 to 100  $\mu\text{m}$  and longer particles of fibre that ranged from 100 to 1100  $\mu\text{m}$ . Although the source of the particles was not determined, it was suggested that they were likely due to but not restricted to run-off and sewage input (Steer et al. 2017a). With a wide particle size range that organisms exhibiting different feeding methods including filter feeders, detritivores and zooplankton, are constantly exposed to microplastics (Scherer et al. 2017; Van Cauwenberghe et al. 2015). Under laboratory controlled conditions, one study reported on the mortality of freshwater crustaceans *Daphnia magna*, on exposure to different concentrations of polyethylene terephthalate fibre particles (Jemec et al. 2016). Furthermore, other studies have

reported on the uptake of particles of fibre by living organisms in the environment (McGoran et al. 2017; Taylor et al. 2016). This suggests that there is the potential for the accumulation of particles abraded from kitchen scourers to enter and accumulate in the environment, with the potential to cause harm to living organisms (McGoran et al. 2017; Taylor et al. 2016).

This argument of the impact of microplastics is based on the small size and number of particles detected, which enables the ingestion of microplastics by living organisms (Steer et al. 2017b; Oluniyi Solomon & Palanisami 2016). In addition, it is widely discussed that the sorption and transfer of toxic chemicals by particles to living organisms has been the focus for potential harm (Andrady 2017; Batel et al. 2016). However, the extent of the impact is still uncertain, especially at the population level (Ziccardi et al. 2016b; Lusher et al. 2013). The uncertainty is because of the low concentrations of microplastics detected in living organisms from the environment. One study revealed that between 0.2 to 1.2 particles  $g^{-1}$  were detected in two species of marine invertebrates, with no significant impact (Van Cauwenberghe et al. 2015). However, other studies have reported high concentrations of particles in laboratory controlled conditions with no apparent significant impact (McGoran et al. 2017; Karami et al. 2017). It has been argued that the unrealistic and high concentrations of microplastic exposure to living organisms in controlled laboratory conditions do not capture true concentrations in the environment (Burton 2017). In addition, the sorption and transfer of toxic chemicals by ingestion of prey, and smaller nanoparticles may be potential sources of harm to living organisms (Koelmans & Bakir 2016; Burton 2017). Therefore, it is premature to conclude that the occurrence of microplastics alone in the environment is the cause of impact to living organism (Burton 2017). What is certain however is that the characterisations of particles in the environment and laboratory controlled conditions can allow for a better understanding of the impact to living organisms (Sharma & Chatterjee 2017; Auta et al. 2017b).

From the data reported in this work that different techniques for the characterisation of microplastics do provide different results. But it is clear that each technique has its limitations and advantages. Given that the techniques used have fundamentally different principles of measurement, sample introduction and automation this is possibly not an unexpected outcome. Microscopy and laser diffraction gave results that were comparable. However, the novel application of the imaging flow cytometry,

which was more sensitive in detecting lower sized particles, gave results that indicated the presence of significantly higher number of particles in one of the PCP samples. The use of this technique also highlighted the importance of quality control (blanks) and challenges relating to sample handling and introduction to the instrument still remain. This study has focused on off the shelf consumer products with a relatively simple matrix and high numbers of particles per unit mass and different techniques give different results. It is therefore likely that such differences will be seen and possibly magnified if these comparisons were made on environmental samples.

## CHAPTER 6: CONCLUSION

This thesis has shown that different sample preparation protocols and the application of different analytical techniques used for the characterisation of microplastics will produce different results. This study has described the development of laboratory sample preparation protocols and the application of the analytical techniques for the characterisation of particles separated from PCPs. In addition, this report has shown for the first time, evidence of microplastics abraded from KS. There were differences in the size, number, and morphology and polymer identity of particles based on the different techniques used. Furthermore, this study has shown for the first time that sub 70  $\mu\text{m}$  sub fractions of particles can be analysed using the imaging flow cytometry. This is important, because of the significance of microplastics in the low micron size region in the environment.

Although the application of the different methods and analytical techniques allowed for particle characterisation, the imaging flow cytometry did not successfully determine estimates for the number of particles, as demonstrated with the PCPs. This study has highlighted the importance of the analysis of blank water samples to detect particles in debris only when using certain techniques, to prevent over and/or under estimating number of particles. The size of particles reported in this thesis suggests the finer particles will enter the environment through WWTPs that cannot capture them. In addition, the literature states that particles not captured can be incorporated into sludge where they have the potential to enter the environment through run-off.

This study reported that one product FS2 demonstrated the largest estimated number of particles using the microscopy and imaging flow cytometry techniques. In addition, polyethylene is commonly used in the selected products analysed.

With the ban on microplastics in PCPs to take effect from this year, it will be important to look at KS as a source of microplastics entry to the environment. The particles characterised in the KS could act like particles from PCPs with the potential to cause harm to living organisms.

A number of techniques for characterising and quantifying microplastics arising from PCPs and kitchen scourers were developed and outcomes compared. These techniques gave different outcomes in terms of both the characteristics, in terms of size and shape of particles, and in the numbers of particles present.

- Microscopy is a direct imaging technique, a widely used approach, was time consuming although there is evidence that size measurements and counting particles in 6 transects (300 cells) of the Sedgewick-rafter cell can give reproducible results between samples and at fixed magnifications. However, at different magnifications, different results are likely to be obtained. Furthermore, at the higher magnification, smaller particles can be detected.
- Particle size analysis by laser diffraction required the addition of methanol and surfactant to give reproducible results and allow samples to be taken in by the instrument. This technique is not commonly used in studies on microplastics. The widest particle size range was determined by laser diffraction however, with the instrument used in this study; the number and morphology of particles were not determined.
- Flow cytometry was used to analyse particles in the sub 70  $\mu\text{m}$  fraction. The technique is equipped with the IDEAS software that allowed for the development of templates and analysis of particle size, number and morphology. The high sensitivity of the technique was demonstrated by the detection of particles of debris in the blank water samples. This was possible only with this technique. Out of the techniques used in this study, the highest number of particles was determined by the imaging flow cytometry.
- The FT-IR technique is widely used for the confirmation of polymer identity of microplastics. The application of the micro-FT-IR and ATR-FT-IR confirmed the polymer identity of all particles analysed. Particles separated from PCPs were identified as polyethylene, however particles abraded from kitchen scourers were either polyethylene or polyester.

Similarities and differences were observed between techniques used for the characterisation of microplastics. The size of particles indicated that there was no similarity in the results based on the different techniques used. The imaging flow



cytometry technique measured the smallest size range, and by contrast, the laser diffraction technique measured the widest particle size range.

The number of particles was different across the different techniques used. The imaging flow cytometry technique estimated the largest number of particles compared with the microscopy technique. Particle estimates were not determined by the laser diffraction and FT-IR techniques.

However, the microscopy and FT-IR technique indicated similarities in the morphology of particles analysed. The imaging flow cytometry technique analysed particle morphology with a developed template that was unique to this technique. Particle morphology was not determined by the laser diffraction technique.

The facial scrubs were characterised by more circular-like particles than in the toothpastes. The kitchen scourers used in this study were supermarket and top market brands. The particles abraded were characterised by particles of fragments and fibre particles. In addition, the supermarket owned brand abraded more particles than the top market brand kitchen scourer.

## **FUTURE WORK**

Further work will need to explore and understand the differences between the techniques used for the characterisation of microplastics. In addition, there needs to be an evaluation of the different techniques used, to determine which one gives the most accurate measurements. Furthermore, there will be a need to assess the importance and implication of the differences observed using the different techniques.

## Glossary of terms

AIO	Air induced overflow
AR	Aspect ratio
ATR-FTIR	Attenuated total reflectance –Fourier transform infrared spectroscopy
BPA	Bisphenol A
BPF	BRITISH PLASTICS FEDERATION
CILAS	Compagnie Industrielle des LASers
CIS	Commonwealth of independent states
CIR	Circular
DEFRA	The Department for Environment, Food and Rural Affairs
DEHP	Di(2-ethylhexyl)phthalate
ELG	Elongated
EMD	Emmanuel Merck Darmstadt
EPA	Environmental Protection Agency
EU	European Union
FPA	Focal plane array
FS	Facial scrub
FT-IR	Fourier transform infrared spectroscopy
GESAMP	Joint Group of Experts on the Scientific Aspects of Marine Pollution
GFC	Glass fibre grade C
HS	HARD SCOURER
HDPE	High-density polyethylene
IDEAS	Image Data Exploration and Analysis Software
IMO	International monetary organisation
IOC	The Intergovernmental Oceanographic Commission
IR	Infrared radiation
KS	Kitchen scourer
LDPE	Low-density polyethylene
MBR	Membrane bioreactor
MSFD	Marine safety framework directive
MEHP	Mono-(2-ethylhexyl)-phthalate
MSFD	Marine Safety framework directive
OECD	The Organisation for Economic Co-operation and Development
PBDE	Polybrominated diphenyl ethers
PCP	Personal care products
PE	Polyethylene
PET	polyethylene-terephthalate
PP	Polypropylene
PVC	polyvinyl chloride
SRC	Sedgewick-Rafter cell
UV	ultra violet
PAH	Polycyclic aromatic hydrocarbon
PBT	Persistent bio-accumulative and toxic
RMS	Root mean square
SSC	Side scatter
TP	Toothpaste
UK	United Kingdom
US	United States
WWTP	Waste water treatment plant

## REFERENCES

- Acampora, H. et al., 2016. The use of beached bird surveys for marine plastic litter monitoring in Ireland. *Marine Environmental Research*, 120, pp.122–129. Available at: <http://linkinghub.elsevier.com/retrieve/pii/S0141113616301337> [Accessed October 19, 2017].
- Acosta-Coley, I. & Olivero-Verbel, J., 2015. Microplastic resin pellets on an urban tropical beach in Colombia. *Environmental Monitoring and Assessment*, 187(7).
- Amnis, 2018. Amnis - Frequently Asked Questions. Available at: <https://www.amnis.com/index.php/faq.html#Q49> [Accessed January 11, 2018].
- Amnis EMD Millipore, 2018. Amnis - Frequently Asked Questions. Available at: <https://www.amnis.com/index.php/faq.html#Q49> [Accessed January 6, 2018].
- Amnis EMD Millipore, 2012. Amnis® Imaging Flow Cytometers Frequently Asked Questions What are the primary applications for imaging flow cytometry? Available at: [https://www.amnis.com/documents/brochures/FAQ\\_12June2012.pdf](https://www.amnis.com/documents/brochures/FAQ_12June2012.pdf) [Accessed January 15, 2018].
- Andrady, A.L., 2011a. Microplastics in the marine environment. *Marine Pollution Bulletin*, 62(8), pp.1596–1605. Available at: <http://linkinghub.elsevier.com/retrieve/pii/S0025326X11003055> [Accessed February 14, 2017].
- Andrady, A.L., 2011b. Microplastics in the marine environment. *Marine Pollution Bulletin*, 62(8), pp.1596–1605.
- Andrady, A.L., 2015. Persistence of Plastic Litter in the Oceans. In *Marine Anthropogenic Litter*. Cham: Springer International Publishing, pp. 57–72. Available at: [http://link.springer.com/10.1007/978-3-319-16510-3\\_3](http://link.springer.com/10.1007/978-3-319-16510-3_3) [Accessed August 12, 2017].
- Andrady, A.L., 2017. The plastic in microplastics: A review. *Marine Pollution Bulletin*, 119(1), pp.12–22. Available at:

<http://www.sciencedirect.com/science/article/pii/S0025326X1730111X>  
[Accessed June 22, 2017].

Antunes, J.C. et al., 2013. Resin pellets from beaches of the Portuguese coast and adsorbed persistent organic pollutants. *Estuarine, Coastal and Shelf Science*, 130, pp.62–69. Available at:  
<http://linkinghub.elsevier.com/retrieve/pii/S0272771413002941> [Accessed September 30, 2017].

Arnold L. Gordon, 2017. ocean current | Britannica.com. Available at:  
<https://www.britannica.com/science/ocean-current> [Accessed October 3, 2017].

Auta, H.S., Emenike, C.. & Fauziah, S., 2017a. Distribution and importance of microplastics in the marine environment: A review of the sources, fate, effects, and potential solutions. *Environment International*, 102, pp.165–176. Available at: <http://www.sciencedirect.com/science/article/pii/S016041201631011X> [Accessed June 24, 2017].

Auta, H.S., Emenike, C.. & Fauziah, S., 2017b. Distribution and importance of microplastics in the marine environment: A review of the sources, fate, effects, and potential solutions. *Environment International*, 102, pp.165–176. Available at: <http://linkinghub.elsevier.com/retrieve/pii/S016041201631011X> [Accessed August 22, 2017].

Avio, C.G., Cardelli, L.R., et al., 2017. Microplastics pollution after the removal of the Costa Concordia wreck: First evidences from a biomonitoring case study. *Environmental Pollution*, 227, pp.207–214. Available at:  
<http://dx.doi.org/10.1016/j.envpol.2017.04.066>.

Avio, C.G., Gorbi, S. & Regoli, F., 2017. Plastics and microplastics in the oceans: From emerging pollutants to emerged threat. *Marine Environmental Research*, 128, pp.2–11. Available at:  
<http://linkinghub.elsevier.com/retrieve/pii/S0141113616300733> [Accessed October 22, 2017].

Avio, C.G., Gorbi, S. & Regoli, F., 2016. Plastics and microplastics in the oceans: From emerging pollutants to emerged threat. *Marine Environmental Research*.

Available at: <http://linkinghub.elsevier.com/retrieve/pii/S0141113616300733>  
[Accessed July 12, 2016].

Bakir, A., Rowland, S.J. & Thompson, R.C., 2014. Transport of persistent organic pollutants by microplastics in estuarine conditions. *Estuarine, Coastal and Shelf Science*, 140, pp.14–21.

Baosupee, D. et al., 2014. Heteroagglomeration as a mechanism of retaining CaCO<sub>3</sub> particles on the fibrils of cellulosic fines: A study by laser light diffraction and microscopy. *Colloids and Surfaces A: Physicochemical and Engineering Aspects*, 441, pp.525–531. Available at:  
[http://www.sciencedirect.com/science/article/pii/S0927775713007747?\\_rdoc=1&\\_fmt=high&\\_origin=gateway&\\_docanchor=&md5=b8429449ccfc9c30159a5f9aeaa92ffb](http://www.sciencedirect.com/science/article/pii/S0927775713007747?_rdoc=1&_fmt=high&_origin=gateway&_docanchor=&md5=b8429449ccfc9c30159a5f9aeaa92ffb) [Accessed January 20, 2018].

Barnes, D.K. a et al., 2009. Accumulation and fragmentation of plastic debris in global environments. *Philosophical transactions of the Royal Society of London. Series B, Biological sciences*, 364(1526), pp.1985–1998.

Basiji, D., 2016. Principles of Amnis Imaging Flow Cytometry. *Imaging Flow Cytometry: Methods and Protocols*. Available at:  
[http://link.springer.com/protocol/10.1007/978-1-4939-3302-0\\_2](http://link.springer.com/protocol/10.1007/978-1-4939-3302-0_2) [Accessed June 3, 2016].

Batel, A. et al., 2016. Transfer of benzo[a]pyrene from microplastics to *Artemia* nauplii and further to zebrafish via a trophic food web experiment: CYP1A induction and visual tracking of persistent organic pollutants. *Environmental Toxicology and Chemistry*, 35(7), pp.1656–1666.

Beaton-Green, L.A. et al., 2016. Foundations of identifying individual chromosomes by imaging flow cytometry with applications in radiation biodosimetry. *Methods*.

Bennet, O., 2016. *Microbeads and microplastics in cosmetic and personal care products*, Available at:  
<https://researchbriefings.parliament.uk/ResearchBriefing/Summary/CBP-7510#fullreport>.

Besley, A. et al., 2017. A standardized method for sampling and extraction methods

for quantifying microplastics in beach sand. *Marine Pollution Bulletin*, 114(1), pp.77–83. Available at:  
<http://linkinghub.elsevier.com/retrieve/pii/S0025326X16306877> [Accessed October 12, 2017].

Besseling, E. et al., 2017. The effect of microplastic on chemical uptake by the lugworm *Arenicola marina* (L.) under environmentally relevant conditions. *Environmental Science and Technology*.

Bosker, T., Behrens, P. & Vijver, M.G., 2017a. Determining global distribution of microplastics by combining citizen science and in-depth case studies. *Integrated Environmental Assessment and Management*, 13(3), pp.536–541. Available at:  
<http://doi.wiley.com/10.1002/ieam.1908> [Accessed August 18, 2017].

Bosker, T., Behrens, P. & Vijver, M.G., 2017b. Determining global distribution of microplastics by combining citizen science and in-depth case studies. *Integrated Environmental Assessment and Management*, 13(3), pp.536–541. Available at:  
<http://doi.wiley.com/10.1002/ieam.1908> [Accessed June 22, 2017].

BPF, 2018. Plastics Recycling. Available at:  
[http://www.bpf.co.uk/sustainability/plastics\\_recycling.aspx](http://www.bpf.co.uk/sustainability/plastics_recycling.aspx) [Accessed January 6, 2018].

Brian Quinn, Fionn Murphy, C.E., 2016. Validation of density separation for the rapid recovery of microplastics from sediment. *Analytical Methods*.

Browne, M.A. et al., 2011. Accumulation of microplastic on shorelines worldwide: Sources and sinks. *Environmental Science and Technology*, 45(21), pp.9175–9179.

Bryant, J.A. et al., 2016. Diversity and Activity of Communities Inhabiting Plastic Debris in the North Pacific Gyre J. K. Jansson, ed. *mSystems*, 1(3), pp.e00024–16. Available at: <http://msystems.asm.org/lookup/doi/10.1128/mSystems.00024-16> [Accessed January 18, 2018].

Burton, G.A., 2017. Stressor Exposures Determine Risk: So, Why Do Fellow Scientists Continue To Focus on Superficial Microplastics Risk? *Environmental Science & Technology*, 51(23), pp.13515–13516. Available at:

<http://pubs.acs.org/doi/10.1021/acs.est.7b05463>.

Butu, A.W. & Mshelia, S.S., 2014. MUNICIPAL SOLID WASTE DISPOSAL AND ENVIRONMENTAL ISSUES IN KANO METROPOLIS, NIGERIA. *British Journal of Environmental Sciences*, 2(2), pp.10–26. Available at:

[http://nswaienviis.nic.in/Waste\\_Portal/Case\\_Studies/cs\\_dec15/MUNICIPAL SOLID WASTE DISPOSAL AND ENVIRONMENTAL ISSUES IN KANO METROPOLIS, NIGERIA.pdf](http://nswaienviis.nic.in/Waste_Portal/Case_Studies/cs_dec15/MUNICIPAL_SOLID_WASTE DISPOSAL AND ENVIRONMENTAL ISSUES IN KANO METROPOLIS, NIGERIA.pdf) [Accessed January 17, 2018].

Carey, J., 2017. News Feature: On the brink of a recycling revolution? *Proceedings of the National Academy of Sciences of the United States of America*, 114(4), pp.612–616. Available at: <http://www.ncbi.nlm.nih.gov/pubmed/28119494> [Accessed January 16, 2018].

Carpenter, E.J. & Smith, K.L., 1972. Plastics on the Sargasso Sea Surface. *Source: Science, New Series*, 175(4027), pp.1240–1241. Available at: <http://www.jstor.org/stable/1733709> [Accessed January 17, 2018].

Carr, S.A., Liu, J. & Tesoro, A.G., 2016a. Transport and fate of microplastic particles in wastewater treatment plants. *Water Research*, 91, pp.174–182.

Carr, S.A., Liu, J. & Tesoro, A.G., 2016b. Transport and fate of microplastic particles in wastewater treatment plants. *Water Research*, 91, pp.174–182. Available at: <http://linkinghub.elsevier.com/retrieve/pii/S0043135416300021> [Accessed August 18, 2017].

Castillo, A.B., Al-Maslamani, I. & Obbard, J.P., 2016. Prevalence of microplastics in the marine waters of Qatar. *Marine Pollution Bulletin*. Available at: <http://linkinghub.elsevier.com/retrieve/pii/S0025326X16305124> [Accessed July 12, 2016].

Van Cauwenberghe Lisbeth, Wout Van Echelpoel, Kris De Gussem, Greet De Gueldre, M.V. and C.R.J., 2015. Unraveling the sources of marine microplastics: your daily contribution?. BOOK OF ABSTRACTS. Available at: <https://biblio.ugent.be/publication/7053791/file/7053801#page=153> [Accessed July 12, 2016].

Van Cauwenberghe, L., Claessens, M., et al., 2015. Microplastics are taken up by



mussels (*Mytilus edulis*) and lugworms (*Arenicola marina*) living in natural habitats. *Environmental Pollution*, 199, pp.10–17. Available at: <http://linkinghub.elsevier.com/retrieve/pii/S026974911500010X> [Accessed August 19, 2017].

Van Cauwenberghe, L., Devriese, L., et al., 2015a. Microplastics in sediments: A review of techniques, occurrence and effects. *Marine Environmental Research*, 111, pp.5–17. Available at: <http://linkinghub.elsevier.com/retrieve/pii/S0141113615000938> [Accessed June 24, 2017].

Van Cauwenberghe, L., Devriese, L., et al., 2015b. Microplastics in sediments: A review of techniques, occurrence and effects. *Marine Environmental Research*, 111, pp.5–17.

Chang, M., 2015. Reducing microplastics from facial exfoliating cleansers in wastewater through treatment versus consumer product decisions. *Marine Pollution Bulletin*, 101(1), pp.330–333. Available at: <http://linkinghub.elsevier.com/retrieve/pii/S0025326X15301478>.

Chinese ban on plastic waste imports could see UK pollution rise Laville, S., Chinese ban on plastic waste imports could see UK pollution rise | Environment | The Guardian. Available at: <https://www.theguardian.com/environment/2017/dec/07/chinese-ban-on-plastic-waste-imports-could-see-uk-pollution-rise> [Accessed January 6, 2018].

Chris Wilcox et al., 2016, 2016. Using expert elicitation to estimate the impacts of plastic pollution on marine wildlife. *Marine Policy*, 65, pp.107–114. Available at: <http://www.sciencedirect.com/science/article/pii/S0308597X15002985> [Accessed October 18, 2017].

CILAS. Quality, D., 2016. Expertise - Innovation - Solutions. , p.8. Available at: <http://www.cilas.com/brochures/general-brochure-of-cilas-psa.pdf> [Accessed June 15, 2016].

Claessens, M., 2013. New techniques for the detection of microplastics in sediments and field collected organisms. *Marine pollution* .... Available at:

<http://www.sciencedirect.com/science/article/pii/S0025326X13001495>

[Accessed June 3, 2016].

Claessens, M. & Meester, S. De, 2011. Occurrence and distribution of microplastics in marine sediments along the Belgian coast. *Marine Pollution* .... Available at:

<http://www.sciencedirect.com/science/article/pii/S0025326X11003651>

[Accessed June 3, 2016].

Cole, M. et al., 2014. Isolation of microplastics in biota-rich seawater samples and marine organisms. *Scientific reports*, 4, p.4528. Available at:

<http://www.ncbi.nlm.nih.gov/pubmed/24681661> [Accessed January 19, 2018].

Cole, M. et al., 2016. Microplastics Alter the Properties and Sinking Rates of Zooplankton Faecal Pellets. *Environmental Science & Technology*, 50(6), pp.3239–3246. Available at:

<http://pubs.acs.org/doi/abs/10.1021/acs.est.5b05905> [Accessed August 18, 2017].

Cole, M. et al., 2011. Microplastics as contaminants in the marine environment: a review. *Marine pollution bulletin*. Available at:

<http://www.sciencedirect.com/science/article/pii/S0025326X11005133>

[Accessed June 24, 2017].

Cole, M. et al., 2011. Microplastics as contaminants in the marine environment: A review. *Marine Pollution Bulletin*, 62(12), pp.2588–2597.

Cole, M., Lindeque, P. & Fileman, E., 2013. Microplastic ingestion by zooplankton. *science & technology*. Available at:

<http://pubs.acs.org/doi/abs/10.1021/es400663f> [Accessed June 24, 2017].

Courtene-Jones, W. et al., 2017. Microplastic pollution identified in deep-sea water and ingested by benthic invertebrates in the Rockall Trough, North Atlantic Ocean. *Environmental Pollution*, 231, pp.271–280. Available at:

<http://www.sciencedirect.com/science/article/pii/S0269749117312885> [Accessed August 23, 2017].

Cozar, A. et al., 2014. Plastic debris in the open ocean. *Proceedings of the National Academy of Sciences*, 111(28), pp.10239–10244. Available at:

<http://www.pnas.org/cgi/doi/10.1073/pnas.1314705111> [Accessed July 11, 2016].

Crichton, E.M. et al., 2017. A novel, density-independent and FTIR-compatible approach for the rapid extraction of microplastics from aquatic sediments. *Anal. Methods*, 9(9), pp.1419–1428. Available at: <http://xlink.rsc.org/?DOI=C6AY02733D>.

DEFRA(Department for Environment Food and Rural Affairs, 2018. Carrier bags: why there's a charge - GOV.UK. Available at: <https://www.gov.uk/government/publications/single-use-plastic-carrier-bags-why-were-introducing-the-charge/carrier-bags-why-theres-a-5p-charge> [Accessed January 17, 2018].

Desforges, J.P.W. et al., 2014. Widespread distribution of microplastics in subsurface seawater in the NE Pacific Ocean. *Marine Pollution Bulletin*, 79(1-2), pp.94–99. Available at: <http://dx.doi.org/10.1016/j.marpolbul.2013.12.035>.

Doyle, M.J. et al., 2011. Plastic particles in coastal pelagic ecosystems of the Northeast Pacific ocean. *Marine Environmental Research*, 71(1), pp.41–52.

Duis, K. & Coors, A., 2016a. Microplastics in the aquatic and terrestrial environment: sources (with a specific focus on personal care products), fate and effects. *Environmental Sciences Europe*, 28(1), p.2. Available at: <http://www.enveurope.com/content/28/1/2> [Accessed June 22, 2017].

Duis, K. & Coors, A., 2016b. Microplastics in the aquatic and terrestrial environment: sources (with a specific focus on personal care products), fate and effects. *Duis and Coors Environ Sci Eur*, 28(2). Available at: [https://www.ncbi.nlm.nih.gov/pmc/articles/PMC5044952/pdf/12302\\_2015\\_Article\\_69.pdf](https://www.ncbi.nlm.nih.gov/pmc/articles/PMC5044952/pdf/12302_2015_Article_69.pdf) [Accessed October 22, 2017].

Duis, K. & Coors, A., 2016c. Microplastics in the aquatic and terrestrial environment: sources (with a specific focus on personal care products), fate and effects. *Environmental Sciences Europe*, 28(1), p.2. Available at: <http://www.enveurope.com/content/28/1/2> [Accessed June 24, 2017].

Duis, K. & Coors, A., 2016d. Microplastics in the aquatic and terrestrial environment:

sources (with a specific focus on personal care products), fate and effects. *Environmental Sciences Europe*, 28(1), pp.1–25. Available at: <http://link.springer.com/article/10.1186/s12302-015-0069-y>  
<http://link.springer.com/content/pdf/10.1186/s12302-015-0069-y.pdf>.

Duncan Guy, 2017. Shipping company admits to port nurdle accident | Independent on Saturday. Available at: <https://www.iol.co.za/ios/news/shipping-company-admits-to-port-nurdle-accident-11751332> [Accessed January 18, 2018].

Eerkes-Medrano, D., Thompson, R.C. & Aldridge, D.C., 2015a. Microplastics in freshwater systems: A review of the emerging threats, identification of knowledge gaps and prioritisation of research needs. *Water Research*, 75, pp.63–82.

Eerkes-Medrano, D., Thompson, R.C. & Aldridge, D.C., 2015b. Microplastics in freshwater systems: A review of the emerging threats, identification of knowledge gaps and prioritisation of research needs. *Water Research*, 75, pp.63–82. Available at: <http://linkinghub.elsevier.com/retrieve/pii/S0043135415000858> [Accessed October 22, 2017].

Elliott, E.A. et al., 2017. A novel method for sampling the suspended sediment load in the tidal environment using bi-directional time-integrated mass-flux sediment (TIMS) samplers. *Estuarine, Coastal and Shelf Science*, 199, pp.14–24. Available at: <https://www.sciencedirect.com/science/article/pii/S027277141730001X> [Accessed January 6, 2018].

Eriksen, M. et al., 2013. Microplastic pollution in the surface waters of the Laurentian Great Lakes. *Marine Pollution Bulletin*, 77(1-2), pp.177–182. Available at: <http://linkinghub.elsevier.com/retrieve/pii/S0025326X13006097> [Accessed July 13, 2016].

Eriksen, M. et al., 2014a. Plastic Pollution in the World's Oceans: More than 5 Trillion Plastic Pieces Weighing over 250,000 Tons Afloat at Sea H. G. Dam, ed. *PLoS ONE*, 9(12), p.e111913. Available at: <http://dx.plos.org/10.1371/journal.pone.0111913> [Accessed July 12, 2016].

- Eriksen, M. et al., 2014b. Plastic Pollution in the World's Oceans: More than 5 Trillion Plastic Pieces Weighing over 250,000 Tons Afloat at Sea H. G. Dam, ed. *PLoS ONE*, 9(12), p.e111913. Available at: <http://dx.plos.org/10.1371/journal.pone.0111913> [Accessed October 24, 2017].
- Fao, 2017. Microplastics in fisheries and aquaculture Status of knowledge on the[1] Fao, "Microplastics in fisheries and aquaculture Status of knowledge on their occurrence and implications for aquatic organisms and food safety."ir occurrence and implications for aq. Available at: <http://www.fao.org/3/a-i7677e.pdf> [Accessed January 18, 2018].
- Fedotova, N. et al., 2015. Influence of dispersion agents on particle size and concentration determined by laser-induced breakdown detection. *Spectrochimica Acta Part B: ....* Available at: <http://www.sciencedirect.com/science/article/pii/S0584854714003218> [Accessed June 3, 2016].
- Fendall, L. & Sewell, M., 2009. Contributing to marine pollution by washing your face: Microplastics in facial cleansers. *Marine pollution bulletin*. Available at: <http://www.sciencedirect.com/science/article/pii/S0025326X09001799> [Accessed June 3, 2016].
- Fisherscientific, 2017a. Sodium Chloride, Fisher BioReagents :Production:Chemicals And Solvents. Available at: <https://www.fishersci.com/shop/products/sodium-chloride-fisher-bioreagents-3/p-2410158> [Accessed October 6, 2017].
- Fisherscientific, 2017b. Sodium iodide, 99+%, pure, anhydrous, ACROS Organics:Chemicals:Other Inorganic. Available at: <https://www.fishersci.com/shop/products/sodium-iodide-99-pure-anhydrous-acros-organics-5/p-3735065> [Accessed October 6, 2017].
- Fossi, M.C. et al., 2012. Are baleen whales exposed to the threat of microplastics? A case study of the Mediterranean fin whale (*Balaenoptera physalus*). *Marine Pollution Bulletin*, 64(11), pp.2374–2379. Available at: <http://dx.doi.org/10.1016/j.marpolbul.2012.08.013>.
- Galgani, F. et al., 2013. Marine litter within the European Marine Strategy

- Framework Directive. *ICES Journal of Marine Science*, 70(6), pp.1055–1064. Available at: <https://academic.oup.com/icesjms/article-lookup/doi/10.1093/icesjms/fst122> [Accessed January 16, 2018].
- Galgani, F., Pham, C.K. & Reisser, J., 2017. Editorial: Plastic Pollution. *Frontiers in Marine Science*, 4, p.307. Available at: <http://journal.frontiersin.org/article/10.3389/fmars.2017.00307/full> [Accessed October 19, 2017].
- Gall, S.C. & Thompson, R.C., 2015. The impact of debris on marine life. *Marine Pollution Bulletin*, 92(1-2), pp.170–179. Available at: <http://linkinghub.elsevier.com/retrieve/pii/S0025326X14008571> [Accessed July 12, 2016].
- Gallagher, A. et al., 2016. Microplastics in the Solent estuarine complex, UK: An initial assessment. *Marine Pollution Bulletin*, 102(2), pp.243–249. Available at: <http://www.sciencedirect.com/science/article/pii/S0025326X15001903> [Accessed January 6, 2018].
- García-Rivera, S., Lizaso, J.L.S. & Millán, J.M.B., 2017. Composition, spatial distribution and sources of macro-marine litter on the Gulf of Alicante seafloor (Spanish Mediterranean). *Marine Pollution Bulletin*, 121(1-2), pp.249–259. Available at: [http://www.sciencedirect.com/science/article/pii/S0025326X17305027?\\_rdoc=1&\\_fmt=high&\\_origin=gateway&\\_docanchor=&md5=b8429449ccfc9c30159a5f9aeaa92ffb](http://www.sciencedirect.com/science/article/pii/S0025326X17305027?_rdoc=1&_fmt=high&_origin=gateway&_docanchor=&md5=b8429449ccfc9c30159a5f9aeaa92ffb) [Accessed January 16, 2018].
- GESAMP, 2015. Sources, Fate and Effects of Microplastics in the Marine Environment: A Global Assessment. *Reports and Studies GESAMP*, 90(APRIL), p.96.
- GESAMP Joint Group of Experts on the Scientific Aspects of Marine Environmental Protection, 2015. *Sources, fate and effects of microplastics in the marine environment: a global assessment*”, Available at: ISSN: 1020-4873\n[http://ec.europa.eu/environment/marine/good-environmental-status/descriptor-10/pdf/GESAMP\\_microplastics\\_full\\_study.pdf](http://ec.europa.eu/environment/marine/good-environmental-status/descriptor-10/pdf/GESAMP_microplastics_full_study.pdf).

Geyer, R., Jambeck, J.R. & Law, K.L., 2017a. Production, use, and fate of all plastics ever made. *Science Advances*, 3(7), p.e1700782. Available at: <http://advances.sciencemag.org/lookup/doi/10.1126/sciadv.1700782> [Accessed October 23, 2017].

Geyer, R., Jambeck, J.R. & Law, K.L., 2017b. Production, use, and fate of all plastics ever made. *Science Advances*, 3(7). Available at: <http://advances.sciencemag.org/content/3/7/e1700782.full> [Accessed August 19, 2017].

Gil-Delgado, J.A. et al., 2017. Presence of plastic particles in waterbirds faeces collected in Spanish lakes. *Environmental Pollution*, 220, pp.732–736. Available at: <http://linkinghub.elsevier.com/retrieve/pii/S0269749116313306> [Accessed October 22, 2017].

Girard, N. et al., 2106. Microbeads: “Tip of the Toxic Plastic-berg”? Regulation, Alternatives, and Future Implications.

Gollasch, S. et al., 2015. Quantifying indicatively living phytoplankton cells in ballast water samples — recommendations for Port State Control. *Marine Pollution Bulletin*, 101(2), pp.768–775. Available at: <http://www.sciencedirect.com/science/article/pii/S0025326X15300527> [Accessed January 14, 2018].

Graco, 2017. How to Choose the Right Abrasive | Blast Journal. *Blast Journal*. Available at: <http://blastjournal.com/how-to-choose-the-right-abrasive/> [Accessed September 30, 2017].

Gregory, M.R., 1996a. Plastic “scrubbers” in hand cleansers: a further (and minor) source for marine pollution identified. *Marine Pollution Bulletin*, 32(12), pp.867–871. Available at: <http://linkinghub.elsevier.com/retrieve/pii/S0025326X96000471> [Accessed July 15, 2016].

Gregory, M.R., 1996b. Plastic “scrubbers” in hand cleansers: a further (and minor) source for marine pollution identified. *Marine Pollution Bulletin*, 32(12), pp.867–871. Available at:

<http://www.sciencedirect.com/science/article/pii/S0025326X96000471>

[Accessed January 17, 2018].

Grimwade, L.F., Fuller, K.A. & Erber, W.N., 2016. Applications of imaging flow cytometry in the diagnostic assessment of acute leukaemia. *Methods*.

Guerranti, C. et al., 2016. Phthalates and perfluorinated alkylated substances in Atlantic bluefin tuna ( *Thunnus thynnus* ) specimens from Mediterranean Sea (Sardinia, Italy): Levels and risks for human consumption. *Journal of Environmental Science and Health, Part B*, 51(10), pp.661–667. Available at: <https://www.tandfonline.com/doi/full/10.1080/03601234.2016.1191886> [Accessed October 5, 2017].

Hammer, C. & VanBrocklin, H., 2016. Microplastic Bioaccumulation in invertebrates, fish, and cormorants in Lake Champlain. Available at: [http://digitalcommons.plattsburgh.edu/cees\\_student\\_posters/25/](http://digitalcommons.plattsburgh.edu/cees_student_posters/25/) [Accessed June 24, 2017].

Hannes K.Imhof, Natalia P.Ivleva, JohannesSchmid, ReinhardNiessner, C., 2013. Contamination of beach sediments of a subalpine lake with microplastic particles. *Current Biology*, 23(19), pp.R867–R868. Available at: <http://www.sciencedirect.com/science/article/pii/S0960982213011081?via%3Dihub> [Accessed October 22, 2017].

Hansen, L., 2016. Macro and micro plastics in an urbanized and non-urbanized fjord estuary in the Northeast Pacific Ocean. Available at: [https://digital.lib.washington.edu/researchworks/bitstream/handle/1773/36335/hansen\\_lisa\\_ocean\\_senior\\_thesis\\_2016.pdf?sequence=1&isAllowed=y](https://digital.lib.washington.edu/researchworks/bitstream/handle/1773/36335/hansen_lisa_ocean_senior_thesis_2016.pdf?sequence=1&isAllowed=y) [Accessed January 17, 2018].

Harrison, J., Ojeda, J. & Romero-González, M., 2012. The applicability of reflectance micro-Fourier-transform infrared spectroscopy for the detection of synthetic microplastics in marine sediments. *Science of the Total Environment* .... Available at: <http://www.sciencedirect.com/science/article/pii/S0048969711013969> [Accessed June 3, 2016].

Headland, S.E. et al., 2014a. Cutting-edge analysis of extracellular microparticles



using ImageStream(X) imaging flow cytometry. *Scientific reports*, 4, p.5237.  
Available at: <http://www.ncbi.nlm.nih.gov/pubmed/24913598> [Accessed June 3, 2016].

Headland, S.E. et al., 2014b. Cutting-edge analysis of extracellular microparticles using ImageStream(X) imaging flow cytometry. *Scientific reports*, 4, p.5237.  
Available at:  
[http://www.nature.com/srep/2014/140610/srep05237/full/srep05237.html?WT.ec\\_id=SREP-631-20140617](http://www.nature.com/srep/2014/140610/srep05237/full/srep05237.html?WT.ec_id=SREP-631-20140617).

Hennig, H. et al., 2017. An open-source solution for advanced imaging flow cytometry data analysis using machine learning. *Methods*, 112, pp.201–210.  
Available at: <http://linkinghub.elsevier.com/retrieve/pii/S1046202316302912> [Accessed August 23, 2017].

Hernandez, E., Nowack, B. & Mitrano, D.M., 2017. Polyester Textiles as a Source of Microplastics from Households: A Mechanistic Study to Understand Microfiber Release during Washing. *Environmental Science and Technology*, 51(12), pp.7036–7046.

Hernandez, L.M., Yousefi, N. & Tufenkji, N., 2017. Are There Nanoplastics in Your Personal Care Products? *Environmental Science & Technology Letters*, 4(7), pp.280–285. Available at:  
<http://pubs.acs.org/doi/abs/10.1021/acs.estlett.7b00187> [Accessed August 12, 2017].

Hidalgo-Ruz, V. & Gutow, L., 2012. Microplastics in the marine environment: a review of the methods used for identification and quantification. ... *science & technology*. Available at: <http://pubs.acs.org/doi/abs/10.1021/es2031505> [Accessed June 3, 2016].

Hintersteiner, I., 2015. Characterization and quantitation of polyolefin microplastics in personal-care products using high-temperature gel-permeation chromatography. *Analytical and ...*. Available at: <http://link.springer.com/article/10.1007/s00216-014-8318-2> [Accessed June 2, 2016].

Hodgson, D.J., Bréchon, A.L. & Thompson, R.C., 2018. Ingestion and fragmentation

of plastic carrier bags by the amphipod *Orchestia gammarellus*: Effects of plastic type and fouling load. *Marine Pollution Bulletin*, 127, pp.154–159. Available at: <https://www.sciencedirect.com/science/article/pii/S0025326X17310147> [Accessed January 17, 2018].

Hodson, M.E. et al., 2017. Plastic Bag Derived-Microplastics as a Vector for Metal Exposure in Terrestrial Invertebrates. *Environmental Science and Technology*, 51(8), pp.4714–4721.

Horton, A.A. et al., 2017. Microplastics in freshwater and terrestrial environments: Evaluating the current understanding to identify the knowledge gaps and future research priorities. *Science of The Total Environment*, 586, pp.127–141. Available at: <http://linkinghub.elsevier.com/retrieve/pii/S0048969717302073> [Accessed August 19, 2017].

Huang, X. et al., 2017. In-situ cleaning of heavy metal contaminated plastic water pipes using a biomass derived ligand. *Journal of Environmental Chemical Engineering*, 5(4), pp.3622–3631. Available at: <http://linkinghub.elsevier.com/retrieve/pii/S221334371730307X> [Accessed October 18, 2017].

Huerta Lwanga, E. et al., 2017. Incorporation of microplastics from litter into burrows of *Lumbricus terrestris*. *Environmental Pollution*, 220, pp.523–531.

Imhof, H.K. et al., 2016. Pigments and plastic in limnetic ecosystems: A qualitative and quantitative study on microparticles of different size classes. *Water Research*, 98, pp.64–74. Available at: <http://dx.doi.org/10.1016/j.watres.2016.03.015>.

IMO International Maritime Organisation, 2018a. Convention on the Prevention of Marine Pollution by Dumping of Wastes and Other Matter. Available at: <http://www.imo.org/en/OurWork/Environment/LCLP/Pages/default.aspx> [Accessed January 18, 2018].

IMO International Maritime Organisation, 2018b. Garbage. Available at: <http://www.imo.org/en/OurWork/Environment/PollutionPrevention/Garbage/Pages/Default.aspx> [Accessed January 18, 2018].

- Ivar Do Sul, J.A. & Costa, M.F., 2014. The present and future of microplastic pollution in the marine environment. *Environmental Pollution*, 185, pp.352–364.
- Ivleva, N.P., Wiesheu, A.C. & Niessner, R., 2017. Microplastic in Aquatic Ecosystems. *Angewandte Chemie International Edition*, 56(7), pp.1720–1739. Available at: <http://doi.wiley.com/10.1002/anie.201606957> [Accessed October 6, 2017].
- Jauzein, C. et al., 2016. Sampling of *Ostreopsis cf. ovata* using artificial substrates: Optimization of methods for the monitoring of benthic harmful algal blooms. *Marine Pollution Bulletin*, 107(1), pp.300–304. Available at: <http://www.sciencedirect.com/science/article/pii/S0025326X1630176X> [Accessed January 14, 2018].
- Jemec, A. et al., 2016. Uptake and effects of microplastic textile fibers on freshwater crustacean *Daphnia magna*. *Environmental Pollution*, 219, pp.201–209. Available at: <http://www.sciencedirect.com/science/article/pii/S0269749116310533> [Accessed January 9, 2018].
- Jim Walker, 2017. : dumping : Cruise Law News. Available at: <http://www.cruiselawnews.com/tags/dumping/> [Accessed January 18, 2018].
- Kamboj, M., 2016a. Degradation Of Plastics For Clean Environment. *International Journal of Advanced Research in Engineering and Applied Sciences*, 5(3), pp.10–19.
- Kamboj, M., 2016b. DEGRADATION OF PLASTICS FOR CLEAN ENVIRONMENT. *International Journal of Advanced Research in Engineering and Applied Sciences Impact*, 655(3). Available at: <http://www.garph.co.uk/IJAREAS/Mar2016/2.pdf> [Accessed December 16, 2017].
- Kanhai, L.D.K. et al., 2017. Microplastic abundance, distribution and composition along a latitudinal gradient in the Atlantic Ocean. *Marine Pollution Bulletin*, 115(1), pp.307–314. Available at: <http://www.sciencedirect.com/science/article/pii/S0025326X16310116>

[Accessed June 22, 2017].

- Karami, A. et al., 2017. Biomarker responses in zebrafish (*Danio rerio*) larvae exposed to pristine low-density polyethylene fragments. *Environmental Pollution*, 223, pp.466–475. Available at: <http://www.sciencedirect.com/science/article/pii/S0269749116308235> [Accessed January 9, 2018].
- Karl, D.M. & Church, M.J., 2017. Ecosystem Structure and Dynamics in the North Pacific Subtropical Gyre: New Views of an Old Ocean. *Ecosystems*, 20(3), pp.433–457. Available at: <http://link.springer.com/10.1007/s10021-017-0117-0> [Accessed January 18, 2018].
- Karlsson, T.M. et al., 2017. Screening for microplastics in sediment, water, marine invertebrates and fish: Method development and microplastic accumulation. *Marine Pollution Bulletin*, 122(1-2), pp.403–408. Available at: <http://dx.doi.org/10.1016/j.marpolbul.2017.06.081>.
- Koelmans, A. & Bakir, A., 2016. Microplastic as a vector for chemicals in the aquatic environment: critical review and model-supported reinterpretation of empirical studies. *Environmental science* .... Available at: <http://pubs.acs.org/doi/abs/10.1021/acs.est.5b06069> [Accessed June 3, 2016].
- Koelmans, A.A., Besseling, E. & Foekema, E.M., 2014. Leaching of plastic additives to marine organisms. *Environmental Pollution*, 187, pp.49–54. Available at: <http://www.sciencedirect.com/science/article/pii/S0269749113006465> [Accessed January 17, 2018].
- Kole, P.J. et al., 2017. Wear and Tear of Tyres: A Stealthy Source of Microplastics in the Environment. *International journal of environmental research and public health*, 14(10). Available at: <http://www.ncbi.nlm.nih.gov/pubmed/29053641> [Accessed January 20, 2018].
- Koletsis, D. et al., 2016. The effect of rheumatoid arthritis and functional loading on the structure of the mandibular condyle in a transgenic mouse model: An FTIR study. *Archives of Oral Biology*, 61, pp.44–52. Available at: [http://www.sciencedirect.com/science/article/pii/S0003996915300558?\\_rdoc=1&](http://www.sciencedirect.com/science/article/pii/S0003996915300558?_rdoc=1&)

\_fmt=high&\_origin=gateway&\_docanchor=&md5=b8429449ccfc9c30159a5f9aeaa92ffb [Accessed January 20, 2018].

Kowalski, N., Reichardt, A.M. & Waniek, J.J., 2016. Sinking rates of microplastics and potential implications of their alteration by physical, biological, and chemical factors. *Marine Pollution Bulletin*, 109(1), pp.310–319. Available at: <http://dx.doi.org/10.1016/j.marpolbul.2016.05.064>.

Kramm, J. & Völker, C., 2018. Understanding the Risks of Microplastics: A Social-Ecological Risk Perspective. In Springer, Cham, pp. 223–237. Available at: [http://link.springer.com/10.1007/978-3-319-61615-5\\_11](http://link.springer.com/10.1007/978-3-319-61615-5_11) [Accessed January 19, 2018].

Kühn, S., Bravo Rebolledo, E.L. & van Franeker, J.A., 2015. Deleterious Effects of Litter on Marine Life. In *Marine Anthropogenic Litter*. Cham: Springer International Publishing, pp. 75–116. Available at: [http://link.springer.com/10.1007/978-3-319-16510-3\\_4](http://link.springer.com/10.1007/978-3-319-16510-3_4) [Accessed July 12, 2016].

Lannigan, J. & Erdbruegger, U., 2017. Imaging flow cytometry for the characterization of extracellular vesicles. *Methods*, 112, pp.55–67. Available at: <http://www.sciencedirect.com/science/article/pii/S104620231630336X> [Accessed January 6, 2018].

Lasee, S. et al., 2017. Microplastics in a freshwater environment receiving treated wastewater effluent. *Integrated Environmental Assessment and Management*, 13(3), pp.528–532. Available at: <http://doi.wiley.com/10.1002/ieam.1915> [Accessed June 22, 2017].

Latifi, N., Marto, A. & Eisazadeh, A., 2015. Analysis of strength development in non-traditional liquid additive-stabilized laterite soil from macro- and micro-structural considerations. *Environmental Earth Sciences*, 73(3), pp.1133–1141. Available at: <http://link.springer.com/10.1007/s12665-014-3468-2> [Accessed January 6, 2018].

Law, K.L., 2017a. Plastics in the Marine Environment. *Annual Review of Marine Science*, 9(1), pp.205–229. Available at: <http://www.annualreviews.org/doi/10.1146/annurev-marine-010816-060409>

[Accessed June 24, 2017].

Law, K.L., 2017b. Plastics in the Marine Environment. *Annual Review of Marine Science*, 9(1), pp.205–229. Available at:

<http://www.annualreviews.org/doi/10.1146/annurev-marine-010816-060409>

[Accessed June 22, 2017].

Lebreton, L.C.M. et al., 2017. River plastic emissions to the world's oceans. *Nature Communications*, 8, p.15611. Available at:

<http://www.nature.com/doi/10.1038/ncomms15611> [Accessed October 22, 2017].

Lebreton, L.C.M. et al., 2017. River plastic emissions to the world's oceans. *Nature communications*, 8, p.15611. Available at:

<http://www.ncbi.nlm.nih.gov/pubmed/28589961> [Accessed August 22, 2017].

Lee Willimans, 2015. Hundreds of thousands of tiny plastic pellets infest British beaches | The Independent. Available at:

<http://www.independent.co.uk/news/uk/hundreds-of-thousands-of-tiny-plastic-pellets-infest-british-beaches-a6681581.html> [Accessed January 18, 2018].

Leslie, H.A. et al., 2017. Microplastics en route: Field measurements in the Dutch river delta and Amsterdam canals, wastewater treatment plants, North Sea sediments and biota. *Environment International*, 101, pp.133–142. Available at: <http://www.sciencedirect.com/science/article/pii/S0160412017301654> [Accessed January 6, 2018].

Leslie, H.A., Van Velzen, M.J.M. & Vethaak, A.D., 2013. Microplastic survey of the Dutch environment Novel data set of microplastics in North Sea sediments, treated wastewater effluents and marine biota. Available at:

[http://www.ivm.vu.nl/en/Images/IVM\\_report\\_Microplastic\\_in\\_sediment\\_STP\\_Biota\\_2013\\_tcm234-409860.pdf](http://www.ivm.vu.nl/en/Images/IVM_report_Microplastic_in_sediment_STP_Biota_2013_tcm234-409860.pdf) [Accessed January 18, 2018].

LI, W.C., TSE, H.F. & FOK, L., 2016. Plastic waste in the marine environment: A review of sources, occurrence and effects. *Science of The Total Environment*, 566-567, pp.333–349. Available at:

<http://linkinghub.elsevier.com/retrieve/pii/S0048969716310154> [Accessed June

24, 2017].

Liebezeit, G. & Dubaish, F., 2012. Microplastics in Beaches of the East Frisian Islands Spiekeroog and Kachelotplate. *Bulletin of Environmental Contamination and Toxicology*, 89(1), pp.213–217. Available at: <http://link.springer.com/10.1007/s00128-012-0642-7> [Accessed January 6, 2018].

Liu, E.K., He, W.Q. & Yan, C.R., 2014. “White revolution” to “white pollution”— agricultural plastic film mulch in China. *Environmental Research Letters*, 9(9), p.091001. Available at: <http://stacks.iop.org/1748-9326/9/i=9/a=091001?key=crossref.e26b6bac9cc0776b14abf903fe129e64> [Accessed January 17, 2018].

Long, M. et al., 2015. Interactions between microplastics and phytoplankton aggregates: Impact on their respective fates. *Marine Chemistry*, 175, pp.39–46. Available at: [http://www.sciencedirect.com/science/article/pii/S0304420315000766?\\_rdoc=1&\\_fmt=high&\\_origin=gateway&\\_docanchor=&md5=b8429449ccfc9c30159a5f9aea92ffb#bb0380](http://www.sciencedirect.com/science/article/pii/S0304420315000766?_rdoc=1&_fmt=high&_origin=gateway&_docanchor=&md5=b8429449ccfc9c30159a5f9aea92ffb#bb0380) [Accessed January 19, 2018].

Lusher, A., 2015. Microplastics in the Marine Environment: Distribution, Interactions and Effects. In *Marine Anthropogenic Litter*. Cham: Springer International Publishing, pp. 245–307. Available at: [http://link.springer.com/10.1007/978-3-319-16510-3\\_10](http://link.springer.com/10.1007/978-3-319-16510-3_10) [Accessed October 4, 2017].

Lusher, A.L. et al., 2015. Microplastic and macroplastic ingestion by a deep diving, oceanic cetacean: The True’s beaked whale *Mesoplodon mirus*. *Environmental Pollution*, 199, pp.185–191. Available at: [http://www.sciencedirect.com/science/article/pii/S0269749115000421?\\_rdoc=1&\\_fmt=high&\\_origin=gateway&\\_docanchor=&md5=b8429449ccfc9c30159a5f9aea92ffb](http://www.sciencedirect.com/science/article/pii/S0269749115000421?_rdoc=1&_fmt=high&_origin=gateway&_docanchor=&md5=b8429449ccfc9c30159a5f9aea92ffb) [Accessed January 18, 2018].

Lusher, A.L., McHugh, M. & Thompson, R.C., 2013. Occurrence of microplastics in the gastrointestinal tract of pelagic and demersal fish from the English Channel. *Marine Pollution Bulletin*, 67(1-2), pp.94–99. Available at: <http://dx.doi.org/10.1016/j.marpolbul.2012.11.028>.

- MacArthur, E., 2017. Beyond plastic waste. *Science (New York, N. Y.)*, 358(6365), p.843. Available at: <http://www.ncbi.nlm.nih.gov/pubmed/29146782> [Accessed January 16, 2018].
- Maes, T. et al., 2017. A rapid-screening approach to detect and quantify microplastics based on fluorescent tagging with Nile Red. *Scientific Reports*, 7, p.44501. Available at: <http://www.ncbi.nlm.nih.gov/pubmed/28300146> [Accessed October 6, 2017].
- Magnusson, K. et al., 2016. Swedish sources and pathways for microplastics to the marine environment. *A review of existing data*. Available at: [http://www.ivl.se/download/18.7e136029152c7d48c205d8/1457342560947/C183+Sources+of+microplastic\\_160307\\_D.pdf](http://www.ivl.se/download/18.7e136029152c7d48c205d8/1457342560947/C183+Sources+of+microplastic_160307_D.pdf) [Accessed June 24, 2017].
- Magnusson, K. et al., 2016. Swedish sources and pathways for microplastics to the marine environment. A review of existing data. , (C), pp.1–88.
- Malvern, 2015. A basic guide to particle characterization PARTICLE. Available at: [www.malvern.com/contact](http://www.malvern.com/contact) [Accessed January 11, 2018].
- Mason, S.A. et al., 2016. Microplastic pollution is widely detected in US municipal wastewater treatment plant effluent. *Environmental Pollution*, 218, pp.1045–1054. Available at: <https://www.sciencedirect.com/science/article/pii/S0269749116309629#bib34> [Accessed January 9, 2018].
- McGoran, A.R., Clark, P.F. & Morrith, D., 2017. Presence of microplastic in the digestive tracts of European flounder, *Platichthys flesus*, and European smelt, *Osmerus eperlanus*, from the River Thames. *Environmental Pollution*, 220, pp.744–751. Available at: <http://www.sciencedirect.com/science/article/pii/S0269749116314816> [Accessed January 9, 2018].
- Minnes, R. et al., 2017. Using Attenuated Total Reflection–Fourier Transform Infra-Red (ATR-FTIR) spectroscopy to distinguish between melanoma cells with a different metastatic potential. *Scientific Reports*, 7(1), p.4381. Available at: <http://www.nature.com/articles/s41598-017-04678-6> [Accessed January 20,



2018].

Mintel, 2014. Academic mintel kitchen scourers. , p.7.

Mintenig, S.M. et al., 2017. Identification of microplastic in effluents of waste water treatment plants using focal plane array-based micro-Fourier-transform infrared imaging. *Water Research*, 108, pp.365–372. Available at: <http://www.sciencedirect.com/science/article/pii/S0043135416308600> [Accessed January 9, 2018].

Moore, C.J., 2008. Synthetic polymers in the marine environment: A rapidly increasing, long-term threat. *Environmental Research*, 108(2), pp.131–139.

Morden, M., 2106. Indigenizing Parliament: Time to Re-Start a Conversation. Available at: [http://www.revparl.ca/39/2/39n2e\\_16\\_Morden.pdf](http://www.revparl.ca/39/2/39n2e_16_Morden.pdf) [Accessed January 19, 2018].

Napper, I.E. et al., 2015. Characterisation, quantity and sorptive properties of microplastics extracted from cosmetics. *Marine Pollution Bulletin*, 99(1-2), pp.178–185.

Napper, I.E. & Thompson, R.C., 2016. Release of synthetic microplastic plastic fibres from domestic washing machines: Effects of fabric type and washing conditions. *Marine Pollution Bulletin*, 112(1), pp.39–45.

Nizzetto, L., Futter, M. & Langaas, S., 2016. Are Agricultural Soils Dumps for Microplastics of Urban Origin? *Environmental Science and Technology*, 50(20), pp.10777–10779.

Nobre, C.R. et al., 2015. Assessment of microplastic toxicity to embryonic development of the sea urchin *Lytechinus variegatus* (Echinodermata: Echinoidea). *Marine Pollution Bulletin*, 92(1-2), pp.99–104. Available at: <http://dx.doi.org/10.1016/j.marpolbul.2014.12.050>.

Nor, N. & Obbard, J., 2014. Microplastics in Singapore's coastal mangrove ecosystems. *Marine pollution bulletin*. Available at: <http://www.sciencedirect.com/science/article/pii/S0025326X13007261> [Accessed June 3, 2016].

- Nuelle, M.-T. et al., 2014. A new analytical approach for monitoring microplastics in marine sediments. *Environmental Pollution*, 184, pp.161–169. Available at: <http://linkinghub.elsevier.com/retrieve/pii/S0269749113003965> [Accessed June 25, 2017].
- Ojeda, J. et al., 2015. Identification and quantification of microplastics in wastewater using focal plane array-based reflectance micro-FT-IR imaging. Available at: <http://bura.brunel.ac.uk/handle/2438/11030> [Accessed June 3, 2016].
- Ojelowo, S. & Wahab, B., 2017. Journal of Geography and Regional Planning Municipal solid waste and flooding in Lagos metropolis, Nigeria: Deconstructing the evil nexus. , 10(7), pp.174–185. Available at: <http://www.academicjournals.org/JGRP> [Accessed January 16, 2018].
- Oluniyi Solomon, O. & Palanisami, T., 2016. Microplastics in the Marine Environment: Current Status, Assessment Methodologies, Impacts and Solutions. *Journal of Pollution Effects & Control*, 04(02), pp.1–13. Available at: <http://www.esciencecentral.org/journals/microplastics-in-the-marine-environment-current-status-assessment-methodologies-impacts-and-solutions-2375-4397-1000161.php?aid=72325> [Accessed June 22, 2017].
- Patil, B.J. & Raghvendra, C.S., 2017. Extraction of Liquid Fuel from Waste Plastic. *International Journal of Engineering Technology Science and Research IJETSr* [www.ijetsr.com](http://www.ijetsr.com) ISSN, 4, pp.2394–3386. Available at: [http://www.ijetsr.com/images/short\\_pdf/1503857874\\_1081-1087-mccia947\\_ijetsr.pdf](http://www.ijetsr.com/images/short_pdf/1503857874_1081-1087-mccia947_ijetsr.pdf) [Accessed January 18, 2018].
- Peng, J., Wang, J. & Cai, L., 2017. Current understanding of microplastics in the environment: Occurrence, fate, risks, and what we should do. *Integrated Environmental Assessment and Management*, 13(3), pp.476–482. Available at: <http://doi.wiley.com/10.1002/ieam.1912> [Accessed October 4, 2017].
- Peters, C.A. & Bratton, S.P., 2016. Urbanization is a major influence on microplastic ingestion by sunfish in the Brazos River Basin, Central Texas, USA. *Environmental Pollution*, 210, pp.380–387. Available at: <http://linkinghub.elsevier.com/retrieve/pii/S0269749116300185> [Accessed October 22, 2017].

- Pham, C.K. et al., 2017. Plastic ingestion in oceanic-stage loggerhead sea turtles ( *Caretta caretta* ) off the North Atlantic subtropical gyre. *Marine Pollution Bulletin*, 121(1-2), pp.222–229. Available at: <http://linkinghub.elsevier.com/retrieve/pii/S0025326X17304885> [Accessed October 19, 2017].
- Phuong, N.N. et al., 2016. Is there any consistency between the microplastics found in the field and those used in laboratory experiments? *Environmental Pollution*, 211, pp.111–123. Available at: <http://linkinghub.elsevier.com/retrieve/pii/S0269749115302499> [Accessed August 20, 2017].
- PlasticsEurope, 2015. *Plastics – the Facts 2015*. Available at: <http://www.corepla.it/documenti/5f2fa32a-7081-416f-8bac-2efff3ff2fbd/Plastics+TheFacts+2015.pdf> [Accessed January 6, 2018].
- PlasticsEurope, 2016. *Plastics – the Facts 2016*. , p.40.
- PlasticsEurope, 2017. *PlasticsEurope Operation Clean Sweep*®. Available at: [http://www.opcleansweep.eu/wp-content/uploads/2017/09/OCS\\_Report2017.pdf](http://www.opcleansweep.eu/wp-content/uploads/2017/09/OCS_Report2017.pdf) [Accessed January 18, 2018].
- PlasticsEurope, *World Plastics Production 2006 -2015*. Available at: [https://committee.iso.org/files/live/sites/tc61/files/The Plastic Industry Berlin Aug 2016 - Copy.pdf](https://committee.iso.org/files/live/sites/tc61/files/The%20Plastic%20Industry%20Berlin%20Aug%202016%20-%20Copy.pdf) [Accessed October 23, 2017].
- Probst, C., Zeng, Y. & Zhu, R.-R., 2017. Characterization of Protein Particles in Therapeutic Formulations Using Imaging Flow Cytometry. *Journal of pharmaceutical sciences*, 106(8), pp.1952–1960. Available at: <http://www.ncbi.nlm.nih.gov/pubmed/28456724> [Accessed January 11, 2018].
- Provencher, J.F., Bond, A.L. & Mallory, M.L., 2015. Marine birds and plastic debris in Canada: a national synthesis and a way forward. *Environmental Reviews*, 23(1), pp.1–13. Available at: <http://www.nrcresearchpress.com/doi/10.1139/er-2014-0039>.
- Pugsley, H. & Kong, R., 2013. Measuring immunological synapse and actin organization using the FlowSight imaging flow cytometer (P5018). *The Journal*

of .... Available at:

[http://www.jimmunol.org/cgi/content/meeting\\_abstract/190/1\\_MeetingAbstracts/41.10](http://www.jimmunol.org/cgi/content/meeting_abstract/190/1_MeetingAbstracts/41.10) [Accessed June 2, 2016].

Putnam, A. et al., 2017. Microplastic Biomagnification in Invertebrates, Fish, and Cormorants in Lake Champlain. Available at:

[http://digitalcommons.plattsburgh.edu/cees\\_student\\_posters/37/?utm\\_source=digitalcommons.plattsburgh.edu%2Fcees\\_student\\_posters%2F37&utm\\_medium=PDF&utm\\_campaign=PDFCoverPages](http://digitalcommons.plattsburgh.edu/cees_student_posters/37/?utm_source=digitalcommons.plattsburgh.edu%2Fcees_student_posters%2F37&utm_medium=PDF&utm_campaign=PDFCoverPages) [Accessed June 24, 2017].

Qiu, Q. et al., 2016. Extraction, enumeration and identification methods for monitoring microplastics in the environment. *Estuarine, Coastal and Shelf Science*, 176, pp.102–109. Available at:

<http://linkinghub.elsevier.com/retrieve/pii/S0272771416301135> [Accessed June 24, 2017].

Rawle, A. et al., 2003. Basic Principles of Particle. , 44(0).

Rech, S. et al., 2014. Rivers as a source of marine litter – A study from the SE Pacific. *Marine Pollution Bulletin*, 82(1-2), pp.66–75. Available at:

[http://www.sciencedirect.com/science/article/pii/S0025326X14001490?\\_rdoc=1&\\_fmt=high&\\_origin=gateway&\\_docanchor=&md5=b8429449ccfc9c30159a5f9aeaa92ffb](http://www.sciencedirect.com/science/article/pii/S0025326X14001490?_rdoc=1&_fmt=high&_origin=gateway&_docanchor=&md5=b8429449ccfc9c30159a5f9aeaa92ffb) [Accessed January 17, 2018].

Reuters, 2012. Hong Kong government criticized over plastic spill on beaches.

Available at: <https://www.reuters.com/article/us-hongkong-spill/hong-kong-government-criticized-over-plastic-spill-on-beaches-idUSBRE87306J20120805> [Accessed January 18, 2018].

Rillig, M.C., 2012. Microplastic in Terrestrial Ecosystems and the Soil? , 46,

pp.6453–6454. Available at: <http://pubs.acs.org/doi/pdfplus/10.1021/es302011r> [Accessed October 22, 2017].

Rillig, M.C., Ziersch, L. & Hempel, S., 2017. Microplastic transport in soil by earthworms. *Scientific reports*, 7(1), p.1362. Available at:

<http://www.ncbi.nlm.nih.gov/pubmed/28465618> [Accessed October 4, 2017].

Rocha-Santos, T. & Duarte, A., 2015. A critical overview of the analytical approaches

to the occurrence, the fate and the behavior of microplastics in the environment. *TrAC Trends in Analytical Chemistry*. Available at: <http://www.sciencedirect.com/science/article/pii/S0165993614002556> [Accessed June 3, 2016].

Rocha-Santos, T. & Duarte, A.C., 2015. A critical overview of the analytical approaches to the occurrence, the fate and the behavior of microplastics in the environment. *TrAC Trends in Analytical Chemistry*, 65, pp.47–53. Available at: <http://linkinghub.elsevier.com/retrieve/pii/S0165993614002556> [Accessed August 12, 2017].

Rochman, C.M. et al., 2014. Early warning signs of endocrine disruption in adult fish from the ingestion of polyethylene with and without sorbed chemical pollutants from the marine environment. *Science of The Total Environment*, 493, pp.656–661. Available at: <http://linkinghub.elsevier.com/retrieve/pii/S0048969714009073> [Accessed October 22, 2017].

Rochman, C.M. et al., 2013. Plastics and Priority Pollutants: A Multiple Stressor in Aquatic Habitats. *Environmental Science & Technology*, 47(6), pp.2439–2440. Available at: <http://pubs.acs.org/doi/abs/10.1021/es400748b> [Accessed June 24, 2017].

Rochman, C.M. et al., 2015. Scientific Evidence Supports a Ban on Microbeads. *Environmental science & technology*, 49(18), pp.10759–61. Available at: <http://dx.doi.org/10.1021/acs.est.5b03909> [Accessed April 26, 2016].

Rochman, C.M., 2015. The Complex Mixture, Fate and Toxicity of Chemicals Associated with Plastic Debris in the Marine Environment. In *Marine Anthropogenic Litter*. Cham: Springer International Publishing, pp. 117–140. Available at: [http://link.springer.com/10.1007/978-3-319-16510-3\\_5](http://link.springer.com/10.1007/978-3-319-16510-3_5) [Accessed October 22, 2017].

Rochman, C.M., Cook, A.-M. & Koelmans, A.A., 2016. Plastic debris and policy: Using current scientific understanding to invoke positive change. *Environmental Toxicology and Chemistry*, 35(7), pp.1617–1626. Available at: <http://doi.wiley.com/10.1002/etc.3408> [Accessed July 12, 2016].

- Rodriguez-Seijo, A. et al., 2017. Histopathological and molecular effects of microplastics in *Eisenia andrei* Bouché. *Environmental Pollution*, 220, pp.495–503. Available at: <http://linkinghub.elsevier.com/retrieve/pii/S0269749116315500> [Accessed October 22, 2017].
- Romeo, T. et al., 2015. First evidence of presence of plastic debris in stomach of large pelagic fish in the Mediterranean Sea. *Marine Pollution Bulletin*, 95(1), pp.358–361. Available at: <http://linkinghub.elsevier.com/retrieve/pii/S0025326X15002507> [Accessed August 12, 2017].
- Rosenkranz, P. et al., 2009. A COMPARISON OF NANOPARTICLE AND FINE PARTICLE UPTAKE BY DAPHNIA MAGNA. *Environmental Toxicology and Chemistry*, 28(10), p.2142. Available at: <http://doi.wiley.com/10.1897/08-559.1> [Accessed October 22, 2017].
- Rummel, C.D. et al., 2016. Plastic ingestion by pelagic and demersal fish from the North Sea and Baltic Sea. *Marine Pollution Bulletin*, 102(1), pp.134–141. Available at: <http://linkinghub.elsevier.com/retrieve/pii/S0025326X15301922> [Accessed October 19, 2017].
- Ryan, P.G., 2015. A Brief History of Marine Litter Research. In *Marine Anthropogenic Litter*. Cham: Springer International Publishing, pp. 1–25. Available at: [http://link.springer.com/10.1007/978-3-319-16510-3\\_1](http://link.springer.com/10.1007/978-3-319-16510-3_1) [Accessed July 12, 2016].
- Ryan, P.G. et al., 2009. Monitoring the abundance of plastic debris in the marine environment. *Philosophical transactions of the Royal Society of London. Series B, Biological sciences*, 364(1526), pp.1999–2012.
- Saglam, M. et al., 2017. Modeling the effect of biodegradable paper and plastic mulch on soil moisture dynamics. *Agricultural Water Management*, 193, pp.240–250. Available at: [http://www.sciencedirect.com/science/article/pii/S0378377417302676?\\_rdoc=1&\\_fmt=high&\\_origin=gateway&\\_docanchor=&md5=b8429449ccfc9c30159a5f9aeaa92ffb](http://www.sciencedirect.com/science/article/pii/S0378377417302676?_rdoc=1&_fmt=high&_origin=gateway&_docanchor=&md5=b8429449ccfc9c30159a5f9aeaa92ffb) [Accessed January 17, 2018].
- Sanchez W, Bender C, P.J., 2014. Wild gudgeons (*Gobio gobio*) from French rivers

are contaminated by microplastics: Preliminary study and first evidence. *Environmental Research*, 128, pp.98–100. Available at: <http://www.sciencedirect.com/science/article/pii/S0013935113001886?via%3Dihub> [Accessed October 22, 2017].

Saskia Honcoop, 2018. Cosmetic products are full of plastic | Beat the Microbead. Available at: <http://www.beatthemicrobead.org/cosmetic-products-are-full-of-plastic/> [Accessed January 17, 2018].

Scherer, C. et al., 2017. Feeding type and development drive the ingestion of microplastics by freshwater invertebrates. *Scientific Reports*, 7(1), p.17006. Available at: <http://www.nature.com/articles/s41598-017-17191-7> [Accessed January 6, 2018].

Sehly, K. et al., 2015. Stability and ageing behaviour and the formulation of potassium-based drilling muds. *Applied Clay* .... Available at: <http://www.sciencedirect.com/science/article/pii/S016913171400492X> [Accessed June 3, 2016].

Sham, P.C. & Purcell, S.M., 2014. Statistical power and significance testing in large-scale genetic studies. *Nature Reviews Genetics*, 15(5), pp.335–346. Available at: <http://www.nature.com/articles/nrg3706> [Accessed January 12, 2018].

Sharma, S. & Chatterjee, S., 2017. Microplastic pollution, a threat to marine ecosystem and human health: a short review. *Environmental Science and Pollution Research*. Available at: <http://link.springer.com/10.1007/s11356-017-9910-8>.

Shim, W.J., Hong, S.H. & Eo, S.E., 2017. Identification methods in microplastic analysis: a review. *Anal. Methods*, 9(9), pp.1384–1391. Available at: <http://xlink.rsc.org/?DOI=C6AY02558G>.

Silva, J. et al., 2015. Improving clay content measurement in oxidic and volcanic ash soils of Hawaii by increasing dispersant concentration and ultrasonic energy levels. *Geoderma*. Available at: <http://www.sciencedirect.com/science/article/pii/S0016706114003401> [Accessed June 3, 2016].

- Slotwinski, J.A. et al., 2014. Characterization of Metal Powders Used for Additive Manufacturing. *Journal of research of the National Institute of Standards and Technology*, 119, pp.460–93. Available at: <http://www.ncbi.nlm.nih.gov/pubmed/26601040> [Accessed August 21, 2017].
- Song, Y.K. et al., 2015. A comparison of microscopic and spectroscopic identification methods for analysis of microplastics in environmental samples. *Marine Pollution Bulletin*, 93(1-2), pp.202–209. Available at: <http://linkinghub.elsevier.com/retrieve/pii/S0025326X15000314> [Accessed August 22, 2017].
- Sroka-Bartnicka, A. et al., 2015. The biocompatibility of carbon hydroxyapatite/ $\beta$ -glucan composite for bone tissue engineering studied with Raman and FTIR spectroscopic imaging. *Analytical and Bioanalytical Chemistry*, 407(25), pp.7775–7785. Available at: <http://link.springer.com/10.1007/s00216-015-8943-4> [Accessed January 20, 2018].
- Steer, M. et al., 2017a. Microplastic ingestion in fish larvae in the western English Channel. *Environmental Pollution*, 226, pp.250–259. Available at: <http://dx.doi.org/10.1016/j.envpol.2017.03.062>.
- Steer, M. et al., 2017b. Microplastic ingestion in fish larvae in the western English Channel. *Environmental Pollution*, 226, pp.250–259. Available at: <http://www.sciencedirect.com/science/article/pii/S0269749117305031> [Accessed January 6, 2018].
- Steinmetz, Z. et al., 2016. Plastic mulching in agriculture. Trading short-term agronomic benefits for long-term soil degradation? *Science of the Total Environment*, 550, pp.690–705. Available at: <http://dx.doi.org/10.1016/j.scitotenv.2016.01.153>.
- De Stephanis, R. et al., 2013. As main meal for sperm whales: Plastics debris. *Marine Pollution Bulletin*.
- Stolte, A. et al., 2015. Microplastic concentrations in beach sediments along the German Baltic coast. *Marine Pollution Bulletin*, 99(1-2), pp.216–229. Available at: <http://dx.doi.org/10.1016/j.marpolbul.2015.07.022>.



- Sutton, R. et al., 2016. Microplastic contamination in the San Francisco Bay, California, USA. *Marine Pollution Bulletin*. Available at: <http://linkinghub.elsevier.com/retrieve/pii/S0025326X16303976> [Accessed July 12, 2016].
- Syakti, A.D. et al., 2017. Beach macro-litter monitoring and floating microplastic in a coastal area of Indonesia. *Marine Pollution Bulletin*, (May).
- Sympatec GmbH, 2017. Particle Characterisation. Available at: <https://www.sympatec.com/en/particle-measurement/glossary/particle-shape/> [Accessed January 20, 2018].
- Tagg, A. et al., 2015. Identification and Quantification of Microplastics in Wastewater Using Focal Plane Array-Based Reflectance Micro-FT-IR Imaging. *Analytical chemistry*. Available at: <http://pubs.acs.org/doi/abs/10.1021/acs.analchem.5b00495> [Accessed June 3, 2016].
- Talvitie, J. et al., 2017. Solutions to microplastic pollution – Removal of microplastics from wastewater effluent with advanced wastewater treatment technologies. *Water Research*, 123, pp.401–407. Available at: <https://www.sciencedirect.com/science/article/pii/S0043135417305687> [Accessed January 9, 2018].
- Tanaka, K. et al., 2013. Accumulation of plastic-derived chemicals in tissues of seabirds ingesting marine plastics. *Marine Pollution Bulletin*, 69(1-2), pp.219–222. Available at: <http://www.sciencedirect.com/science/article/pii/S0025326X12005942> [Accessed January 17, 2018].
- Taylor, M.L. et al., 2016. Plastic microfibre ingestion by deep-sea organisms. *Scientific reports*, 6, p.33997. Available at: <http://www.ncbi.nlm.nih.gov/pubmed/27687574> [Accessed January 9, 2018].
- Tenzer, R. & Gladkikh, V., 2014. Assessment of density variations of marine sediments with ocean and sediment depths. *TheScientificWorldJournal*, 2014, p.823296. Available at: <http://www.ncbi.nlm.nih.gov/pubmed/24744686>

[Accessed October 24, 2017].

- Thompson, R.C. et al., 2004. Lost at sea: where is all the plastic? *Science (New York, N.Y.)*, 304(5672), p.838.
- Thompson, R.C., 2015a. Microplastics in the Marine Environment: Sources, Consequences and Solutions. In *Marine Anthropogenic Litter*. Cham: Springer International Publishing, pp. 185–200. Available at: [http://link.springer.com/10.1007/978-3-319-16510-3\\_7](http://link.springer.com/10.1007/978-3-319-16510-3_7) [Accessed July 12, 2016].
- Thompson, R.C., 2015b. Microplastics in the Marine Environment: Sources, Consequences and Solutions. In *Marine Anthropogenic Litter*. Cham: Springer International Publishing, pp. 185–200. Available at: [http://link.springer.com/10.1007/978-3-319-16510-3\\_7](http://link.springer.com/10.1007/978-3-319-16510-3_7) [Accessed June 24, 2017].
- Thumanu, K. et al., 2014. Diagnosis of liver cancer from blood sera using FTIR microspectroscopy: A preliminary study. *Journal of Biophotonics*, 7(3-4), pp.222–231.
- Tinke, A., Govoreanu, R. & Weuts, I., 2009. A review of underlying fundamentals in a wet dispersion size analysis of powders. *Powder Technology*. Available at: <http://www.sciencedirect.com/science/article/pii/S0032591009004628> [Accessed June 3, 2016].
- Torres-Mura Juan C; Lemus, Marina L; Hertel, F., 2015. Plastic Material in the Diet of the Turkey Vulture ( *Cathartes aura*) in the...: EBSCOhost. *THE WILSON JOURNAL OF ORNITHOLOGY* , pp.134–138. Available at: <http://web.a.ebscohost.com/ehost/pdfviewer/pdfviewer?vid=1&sid=09565c86-858e-4e79-884f-ee9d916123d4%40sessionmgr4009> [Accessed October 22, 2017].
- Townsend, A.K. & Barker, C.M., 2014. Plastic and the Nest Entanglement of Urban and Agricultural Crows G. Sorci, ed. *PLoS ONE*, 9(1), p.e88006. Available at: <http://dx.plos.org/10.1371/journal.pone.0088006> [Accessed January 17, 2018].
- Vandenberg, L.N., Luthi, D. & Quinerly, D. 'Andr., 2017. Plastic bodies in a plastic world: multi-disciplinary approaches to study endocrine disrupting chemicals.

- Journal of Cleaner Production*, 140, pp.373–385. Available at:  
<http://linkinghub.elsevier.com/retrieve/pii/S095965261500075X> [Accessed October 22, 2017].
- Vassalli, M. et al., 2018. Intercalibration of counting methods for *Ostreopsis* spp. blooms in the Mediterranean Sea. *Ecological Indicators*, 85, pp.1092–1100. Available at:  
<https://www.sciencedirect.com/science/article/pii/S1470160X17304776> [Accessed January 14, 2018].
- Vaughan, A., 2016. Presence of microplastics and nanoplastics in food, with particular focus on seafood. *EFSA Journal*, 14(6). Available at:  
<http://doi.wiley.com/10.2903/j.efsa.2016.4501> [Accessed January 19, 2018].
- Wagner, M. et al., 2014. Microplastics in freshwater ecosystems: what we know and what we need to know. *Environmental Sciences Europe*, 26(1), p.12. Available at: <http://enveurope.springeropen.com/articles/10.1186/s12302-014-0012-7> [Accessed June 24, 2017].
- Weinstein, J.E., Crocker, B.K. & Gray, A.D., 2016. From macroplastic to microplastic: Degradation of high-density polyethylene, polypropylene, and polystyrene in a salt marsh habitat. *Environmental Toxicology and Chemistry*, 35(7), pp.1632–1640. Available at: <http://doi.wiley.com/10.1002/etc.3432> [Accessed July 12, 2016].
- Wessel, C.C. et al., 2016. Abundance and characteristics of microplastics in beach sediments: Insights into microplastic accumulation in northern Gulf of Mexico estuaries. *Marine Pollution Bulletin*. Available at:  
<http://linkinghub.elsevier.com/retrieve/pii/S0025326X16304064> [Accessed July 12, 2016].
- Wilcox, C., Heathcote, G., et al., 2015. Understanding the sources and effects of abandoned, lost, and discarded fishing gear on marine turtles in northern Australia. *Conservation Biology*, 29(1), pp.198–206. Available at:  
<http://doi.wiley.com/10.1111/cobi.12355> [Accessed January 18, 2018].
- Wilcox, C., Van Sebille, E. & Hardesty, B.D., 2015. Threat of plastic pollution to

seabirds is global, pervasive, and increasing. *Proceedings of the National Academy of Sciences of the United States of America*, 112(38), pp.11899–904. Available at: <http://www.ncbi.nlm.nih.gov/pubmed/26324886> [Accessed October 19, 2017].

Woodall, L.C. et al., 2015. Deep-sea litter: a comparison of seamounts, banks and a ridge in the Atlantic and Indian Oceans reveals both environmental and anthropogenic factors impact accumulation and composition. *Frontiers in Marine Science*, 2. Available at: <http://journal.frontiersin.org/Article/10.3389/fmars.2015.00003/abstract> [Accessed July 11, 2016].

Woodall, L.C. et al., 2014. The deep sea is a major sink for microplastic debris. *Royal Society Open Science*, 1(4). Available at: <http://rsos.royalsocietypublishing.org/content/1/4/140317> [Accessed June 24, 2017].

Wrap, 2016. Plastics Market Situation Report. Available at: [http://www.wrap.org.uk/sites/files/wrap/Plastics\\_Market\\_Situation\\_Report.pdf](http://www.wrap.org.uk/sites/files/wrap/Plastics_Market_Situation_Report.pdf) [Accessed January 16, 2018].

Wright, S., Thompson, R. & Galloway, T., 2013a. The physical impacts of microplastics on marine organisms: a review. *Environmental Pollution*. Available at: <http://www.sciencedirect.com/science/article/pii/S0269749113001140> - K%C3%B6rperliche Auswirkungen von Mikroplastik auf marine Organismen (engl.) [Accessed June 24, 2017].

Wright, S., Thompson, R. & Galloway, T., 2013b. The physical impacts of microplastics on marine organisms: a review. *Environmental Pollution*. Available at: <http://www.sciencedirect.com/science/article/pii/S0269749113001140> - K%C3%B6rperliche Auswirkungen von Mikroplastik auf marine Organismen (engl.) [Accessed June 3, 2016].

WVEC, 2017. 9news.com | Navy: Sailor admits to throwing trash disks overboard from ship. *WVEC*. Available at: <http://www.9news.com/article/news/navy-sailor-admits-to-throwing-trash-disks-overboard-from-ship/444851160> [Accessed January 18, 2018].

- Yeo, B.G. et al., 2017. Polycyclic Aromatic Hydrocarbons (PAHs) and Hopanes in Plastic Resin Pellets as Markers of Oil Pollution via International Pellet Watch Monitoring. *Archives of Environmental Contamination and Toxicology*, 73(2), pp.196–206. Available at: <http://link.springer.com/10.1007/s00244-017-0423-8> [Accessed September 30, 2017].
- Zhang, F. et al., 2016. Assembling and Using a Simple, Low-Cost, Vacuum Filtration Apparatus That Operates without Electricity or Running Water. *Journal of Chemical Education*, 93(10), pp.1818–1820. Available at: <http://pubs.acs.org/doi/10.1021/acs.jchemed.5b00997> [Accessed January 19, 2018].
- Zhang, K. et al., 2017. Occurrence and Characteristics of Microplastic Pollution in Xiangxi Bay of Three Gorges Reservoir, China. *Environmental Science & Technology*, 51(7), pp.3794–3801. Available at: <http://pubs.acs.org/doi/abs/10.1021/acs.est.7b00369> [Accessed June 24, 2017].
- Zhao, S. et al., 2017. An approach for extraction, characterization and quantitation of microplastic in natural marine snow using Raman microscopy. *Anal. Methods*, 9(9), pp.1470–1478. Available at: <http://xlink.rsc.org/?DOI=C6AY02302A>.
- Zhilin, D.M. & Kjonaas, R.A., 2013. Simple Apparatus for Vacuum Filtration. *Journal of Chemical Education*, 90(1), pp.142–143. Available at: <http://pubs.acs.org/doi/10.1021/ed3004512> [Accessed January 19, 2018].
- Ziajahromi, S. et al., 2017a. Wastewater treatment plants as a pathway for microplastics: Development of a new approach to sample wastewater-based microplastics. *Water Research*, 112, pp.93–99. Available at: <http://www.sciencedirect.com/science/article/pii/S0043135417300489> [Accessed January 6, 2018].
- Ziajahromi, S. et al., 2017b. Wastewater treatment plants as a pathway for microplastics: Development of a new approach to sample wastewater-based microplastics. *Water Research*, 112, pp.93–99. Available at: <http://www.sciencedirect.com/science/article/pii/S0043135417300489> [Accessed January 9, 2018].

Ziccardi, L.M. et al., 2016a. Microplastics as vectors for bioaccumulation of hydrophobic organic chemicals in the marine environment: A state-of-the-science review. *Environmental Toxicology and Chemistry*, 35(7), pp.1667–1676. Available at: <http://doi.wiley.com/10.1002/etc.3461> [Accessed June 24, 2017].

Ziccardi, L.M. et al., 2016b. Microplastics as vectors for bioaccumulation of hydrophobic organic chemicals in the marine environment: A state-of-the-science review. *Environmental Toxicology and Chemistry*, 35(7), pp.1667–1676.

Zubris, K.A. V. & Richards, B.K., 2005. Synthetic fibers as an indicator of land application of sludge. *Environmental Pollution*, 138(2), pp.201–211. Available at: <http://linkinghub.elsevier.com/retrieve/pii/S0269749105002290> [Accessed October 22, 2017].

## APPENDIX

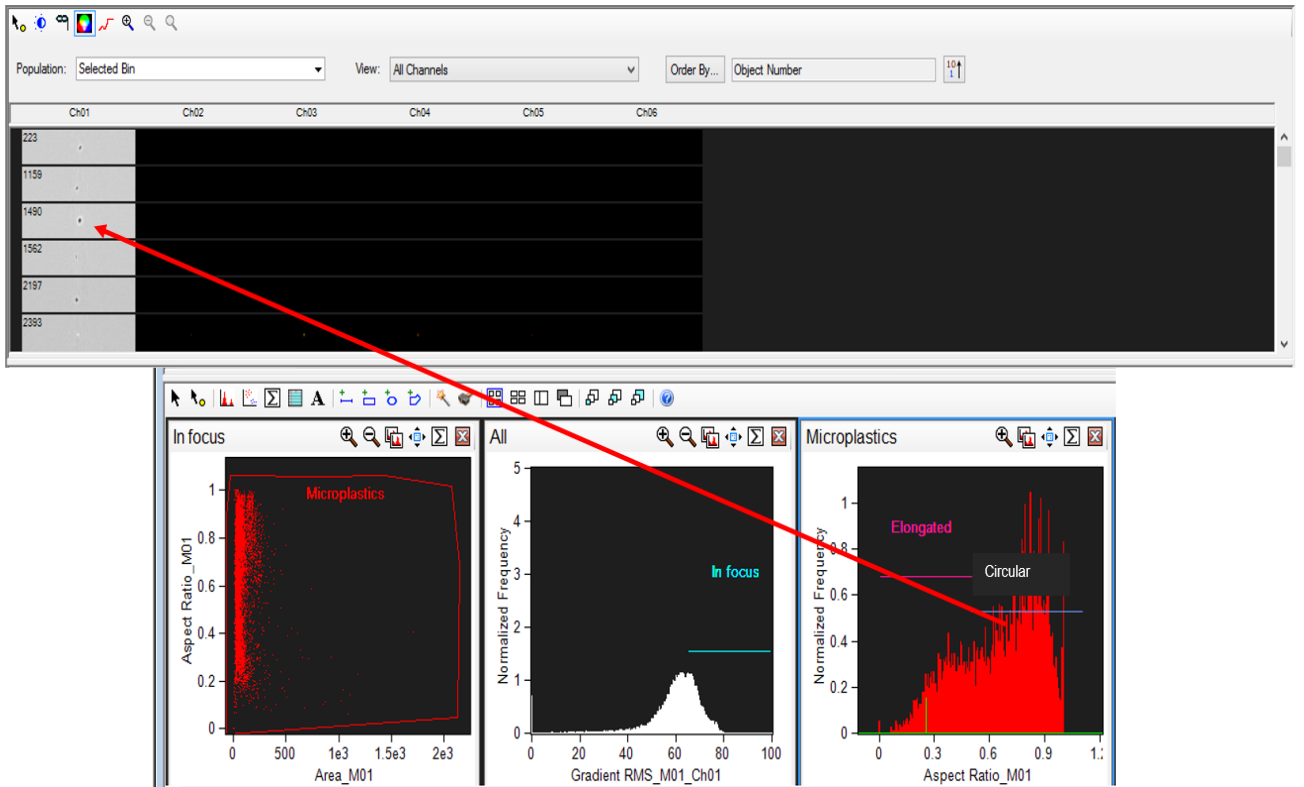


Figure 4.9.6.1. Interrogation of image display gallery to identify circular-like particles separated from PCPs

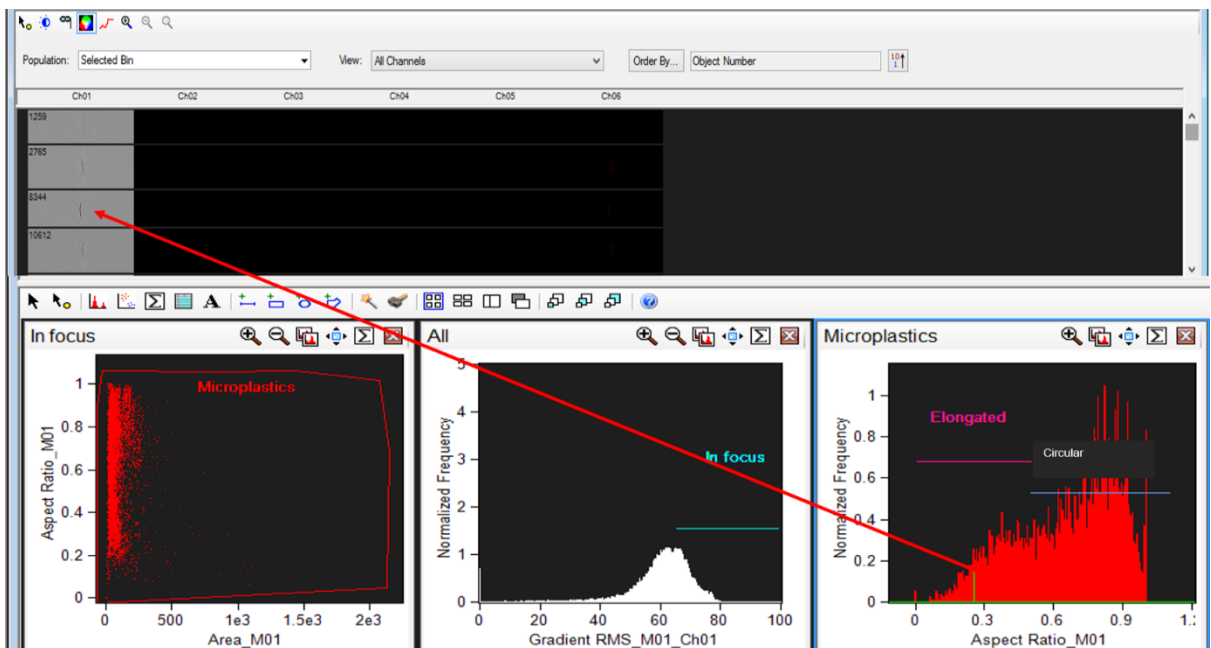


Figure 4.9.6.2. Interrogation of image display gallery to identify elongated particles separated from PCPs

Soil classification table applied to particle size categories.

Feature	Microns	Millimetre
Very coarse sand	2000 - 1000	2.0-1.0 mm
Coarse sand	1000 - 500	1.0-0.5 mm
Medium sand	500 - 250	0.5-0.25 mm
Fine sand	250 - 100	0.25-0.10 mm
Very fine sand	100 - 50	0.10-0.05 mm
Silt	50 - 2	0.05-0.002 mm
Clay	< 2	<0.002 mm

*Table 7.1. Diameter of soil particles in microns and mm*



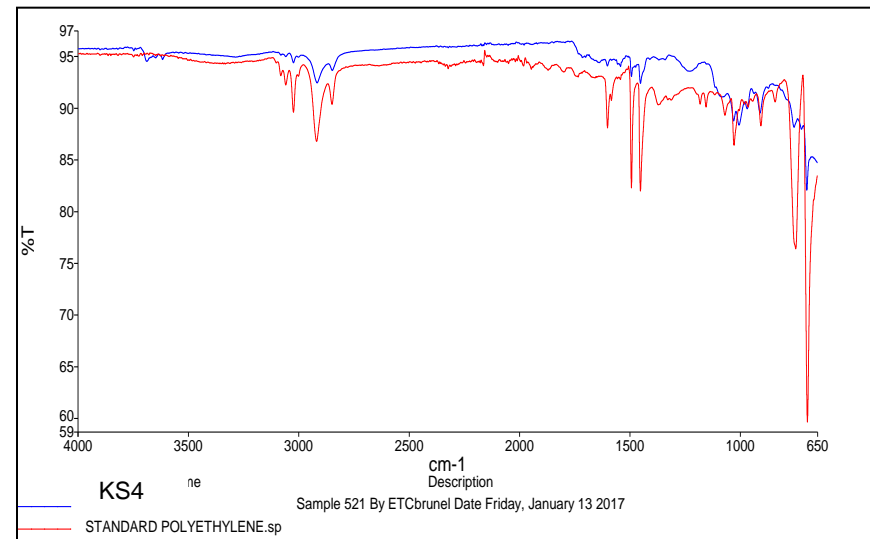
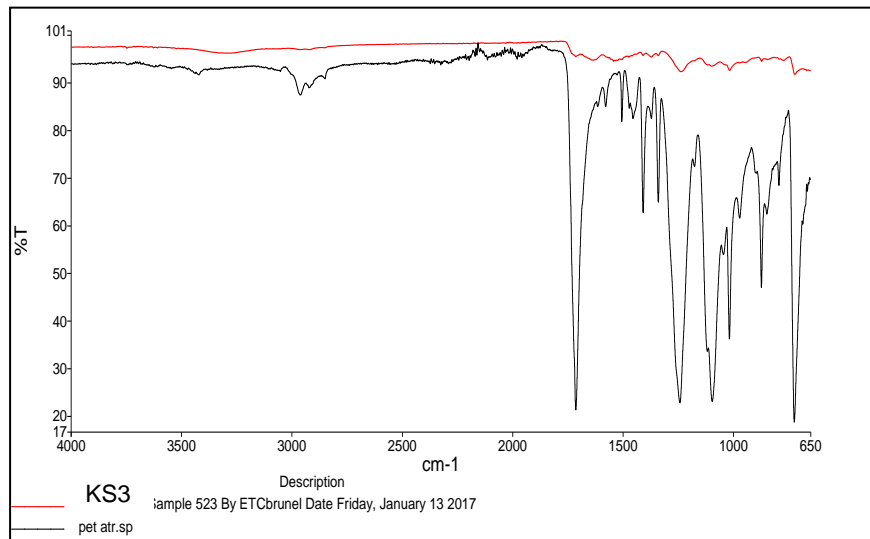
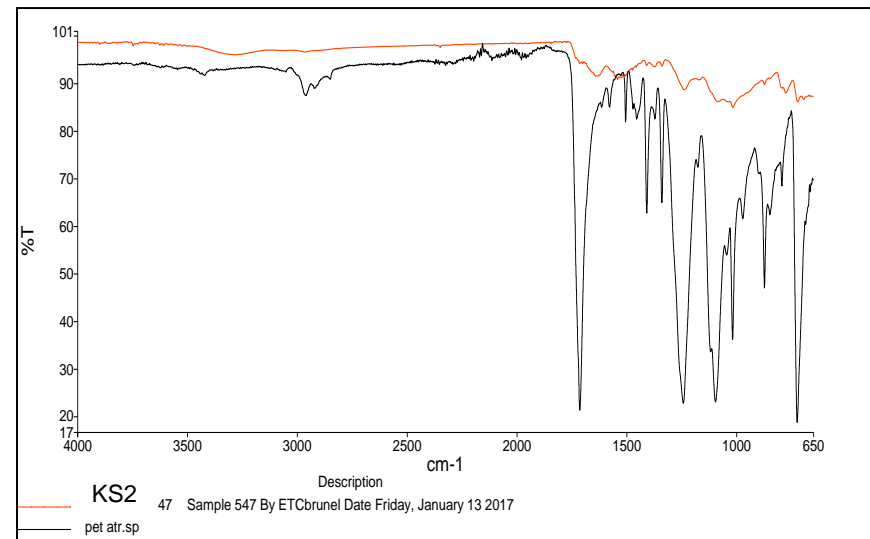
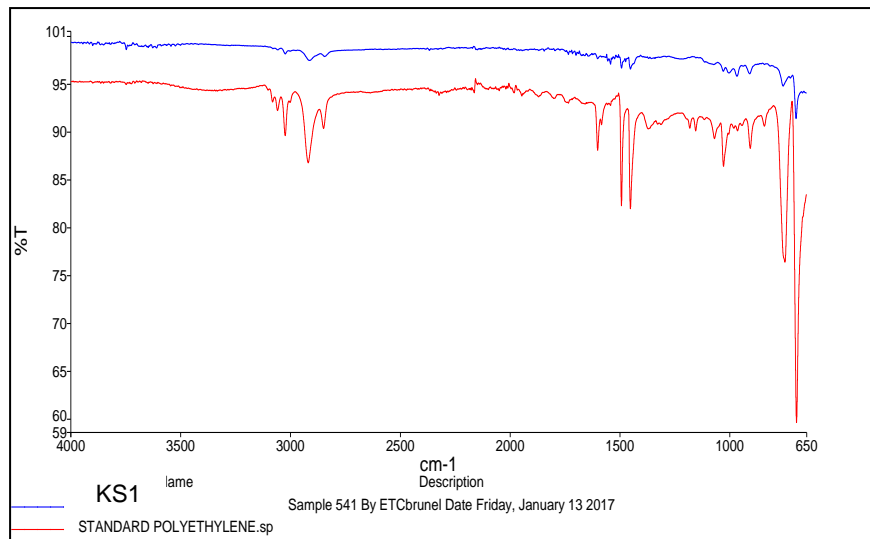
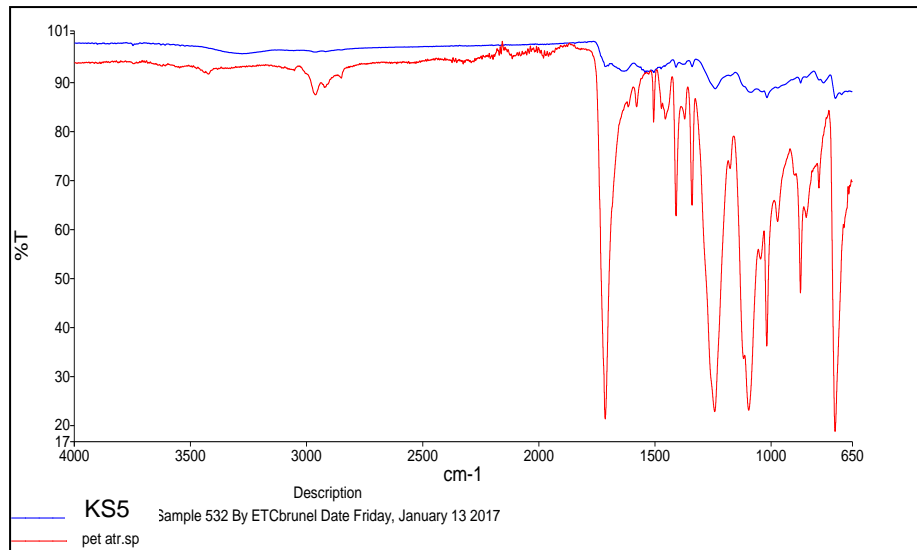


Figure 8.81. FT-IR spectra of particles abraded from KS1 and 4 identified as polyethylene. KS2 and 3 confirmed as polyester with a reference library.



*Figure 8.8.2. FT-IR spectra of particles abraded from KS5. Particles were identified using a reference library, and confirmed as polyester.*



